SIMULTANEOUS REMOVAL OF PHENOL AND CHROMIUM (VI) IN WATER ONTO MODIFIED CHITOSAN BEADS

Pongphun Santiwat[1], Neeranut Kuanchertchoo [2], Somboon Khaewpinthong,[1,*]

[1] *Department of Chemistry, Faculty of Science, Ramkhamhaeng University, Bangkok, 10240 Thailand.*
[2] *Department of Materials, Faculty of Science, Ramkhamhaeng University, Bangkok, 10240 Thailand.*

*E-mail: pongphun_1@hotmail.com, Tel. +66 23191900

Abstract: It is well recognized that the presence of heavy metals and aromatic compounds in wastewater can be detrimental to a variety of living species, including human. Hexavalent chromium (VI) has been found together with a variety of aromatic compounds including phenol, naphthalene, and trichloroethylene (TCE) at high concentrations in a number of contaminated sites. Chromium (VI) and its organic copollutants often originate from industrial sources such as leather tanning, photographic-film making, wood preservation, car manufacturing, petroleum refining, and agricultural activity. A vast number of adsorbents have been synthesized in recent years, including biological compounds, minerals, modified activated carbon, as well as industrial and agricultural wastes. Among adsorbents studied, chitosan and its various forms viz., chitosan membrane, cross-linked chitosan beads, chitosan flakes, sulphated chitin and chitosan, and chitosan derivatives have been studied for adsorption of phenolic compounds as well as chromium (VI) ion in aqueous solution. However, no effort has been directed toward the use of chitosan beads and their modified forms to treat phenol- and chromium (VI)-containing wastewater, simultaneously. Thus, the main objective of this study is to evaluate and compare the performance of chitosan beads and modified chitosan beads for the simultaneous removal of phenol and chromium (VI) in aqueous solution. The maximum sorption capacity of modified chitosan beads was 18.5 mg g^{-1} for phenol and 180.5 mg g^{-1} for chromium(VI) at single ion situation. The concentration of chromium(VI) ions in the effluent was determined spectrophotometrically by using diphenyl carbazide as the complexing agent. The absorbance of the purple colored solution was read at 540 nm after 10 min. The concentration of residual phenol in the effluent was also determined spectrophotometrically. The absorbance of the colored complex of phenol with p-nitroaniline was read at 470 nm. No interference of chromium(VI) ions and phenol on the analysis method of the other pollutant was observed.

1. Introduction

Inorganic and organic environmental contaminants pose a serious problem, because most of them do not undergo degradation. Inorganic elements occurring in various oxidation states are a specific type of impurities, as they often have different degrees of toxicity depending on the particular oxidation state[1].

Chitosan is biodegradable, biocompatatible and non-toxic biopolymer, reported to be an efficient heavy metal scavenger due to the presence of amino group [2] than the chitin. Chitosan is soluble in dilute mineral acids, except in sulphuric acid and it is necessary to reinforce chemical stability using cross-linking agents like glutaraldehyde [3]. Derivatives of chitosan have been applied for the removal of various metal ions and aromatic compound from aqueous solution. Sorption mechanism of mercury was studied on a chitosan derivative by Gavilan et al. [4] and equilibrium and kinetic studies of adsorption of Cu(II) on chitosan/PVA beads were carried out by Wan Nagh et al. [5]. Sorption mechanism of phenol, p-chlorophenol and p-nitrophenol was studied on a chitosan derivative by Mei Li et al.[6].

In the recent years, interest has been focused on simultaneous removal of phenol and chromium(VI) from aqueous solutions using the biosorption method [7-8]. This method, however, poses certain problems associated with the physical characteristics of biomass such as the small size and low density of particles, poor mechanical strength and rigidity, and solid–liquid separation. For this reason, it is worth studying the adsorptive properties of modified chitosan beads, especially that there are no reports concerning mutual adsorption of Cr(VI) and phenol on these adsorbents [9-10].

2. Materials and Methods

2.1 Materials

Chitosan with its deacetylation degree of 92.13% was supplied by Taming Enterprises Laboratory, Samutsakon (Thailand). NaOH, HCl, glacial acetic acid, formaldehyde, cysteine, 1,5-dihenylcarbazide, p-nitroanilene, potassium dichromate, phenol and all other chemicals and reagents were of analytical grade.

2.2 Preparation of modified chitosan beads.

To prepare the chitosan beads, 10.0 g of chitosan powder was dissolved in 300mL of 2% (v/v) acetic acid solution. After dilution to 1 L with deionized water, it was left overnight in stirring condition. It was kept standing for another 6 h to ensure that the chitosan was completely dissolved. The chitosan solution was then added drop-wise into a precipitation bath containing 1 L of alkaline coagulating mixture (H_2O:MeOH:NaOH 4:5:1, w/w) to form chitosan beads [11]. The wet chitosan beads were filtered and extensively washed with deionized water to remove

any NaOH. Before use, the chitosan beads were kept for 30min in the pH adjusted aqueous solution required for different experimental conditions.

After removing the attached surface water, the wet chitosan beads (containing 1 g chitosan on the basis of dry weight) were inserted into a flask containing 500 mL of a 1N NaOH solution [12]. Formaldehyde was added to the chitosan ratio of 0.1:1(formaldehyde : chitosan). After 10 minute the cysteine were added to the chitosan ratio of 0.05:1 (cysteine : chitosan) and the reaction was allowed the process at ambient temperature for 6 h with continuous agitation. The modified chitosan beads were then washed with deionized water to remove any unreacted formaldehyde and cysteine in deionized water for further use.

2.3 Batch sorption studies.

Batch experiments were carried out with synthetic solutions of phenol and Cr(VI) in 50 mL flasks with stopper at 200 rpm of orbital stirring in an incubator shaker, at room temperature and 4 h of contact time with the adsorbent. Samples were then filtered with Whatman No. 42 filter paper, diluted and analyzed for phenol and Cr(VI). Unless otherwise stated the parameters with synthetic water were: sample volume 20 ml, sorbent dose 1 g/l, initial concentration 100 mg/l and 1000 mg/L of phenol and Cr(VI) respectively, equilibration time 4 h. Initial solution pH was maintained at 7 and 4 for phenol and Cr(VI) respectively[14-15]. For equilibrium studies, the initial concentration was prepared from 10 to 200 mg/L and 500 to 5000 mg/L of phenol and Cr(VI) respectively.

2.4 Analysis of chromium(VI) and phenol.

The concentration of chromium(VI) ions in the effluent was determined spectrophotometrically by using diphenyl carbazide as the complexing agent. The absorbance of the purple colored solution was read at 540 nm after 10 min. The concentration of residual phenol in the effluent was also determined spectrophotometrically. The absorbance of the colored complex of phenol with p-nitroaniline was read at 470 nm. No interference of chromium(VI) ions and phenol on the analysis method of the other pollutant was observed[13].

2.5 Characterization

Fourier transform infrared spectroscopy (FTIR) was carried out on PerkinElmer Frontier FT-IR to obtain the structural information of modified chitosan beads. The surface morphology of the sorbent was studied with scanning electron microscope (SEM) with JEOL JSM-S410 LV model.

3. Results and Discussion

3.1 Characterization of the modified chitosan beads.

3.1.1 Scanning electron microscope (SEM)

The field emission scanning electron microscopy was used to observe the surface morphology of Chitosan beads(A) and modified chitosan beads (Fig. 1). The samples were gold coated to improve its conductivity to obtain good images.

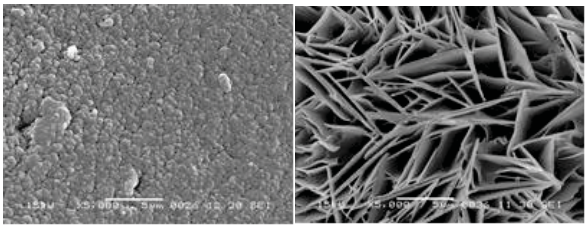

(A) (B)

Figure 1. 5,000x SEM imager of (A) Chitosan beads, (B) Modified Chitosan beads.

3.1.2. FTIR spectra of modified chitosan beads

The spectra of modified chitosan beads is similar to those of the original chitosan beads. The characteristic peaks of chitosan beads are located at 3429 cm^{-1} for the hydroxyl group and 1592 cm^{-1} for the amino group. A peak at 1656 cm^{-1} is due to carbonyl stretching vibration of remaining acetamide group in chitosan, The spectra of modified chitosan beads shows a significant peak at 1566×8 cm^{-1} due to imine bonds (C=N) formed by cross-linking reaction between amino groups in the chitosan and aldehyde group in formaldehyde. This characteristic peak confirms the formation of Schiff base after the reaction of formaldehyde with chitosan. The peak of the ether group becomes stronger and shifted slightly from 1059–1070×5 cm^{-1}, suggesting the formation of a new open chain ether linkage in modified chitosan beads after cross-linking reaction.

3.2. Sorption kinetics

The kinetics of phenol/Cr (VI) removal by modified chitosan beads indicated rapid binding of the sorbate by the sorbent during the first few minutes followed by a slow increase until a state of equilibrium is reached. The necessary time to reach this equilibrium was 4 h for both the metal ions studied and further increase in equilibration time up to 24 h showed no change in the uptake capacity. Hence, the equilibrium time was maintained at 4 h in subsequent analysis. Kinetics of heavy metals adsorption was modeled by the pseudo second order equation[14].

$$t/q_t = 1/(k' q_e^2) + t/q_e \quad (1)$$

where k´ the pseudo second-order rate constant of adsorption (g/mg/min); q_e and q_t are the amounts of metal ion sorbed (mg/g) at equilibrium and at time t, respectively. It is evident from the figure that the prepared adsorbent followed pseudo second order

kinetics for the concentration range studied. The rate constants for phenol and Cr(VI) were found to be 0.0674 and 3.54 g/mg/h respectively.

3.3. Sorption equilibrium

The isotherm studies were conducted at pH 4 for Cr(VI) and pH 7 for phenol. The resulting data were analyzed with the Langmuir and Freundlich isotherms. The results best fitted the Langmuir isotherm, where the adsorbate assumes a monomolecular layer onto the surface of the adsorbent. The linearized form of the Langmuir isotherm equation is[15]:

$$1/q_e = 1/Q_bC_e + 1/Q \quad (2)$$

where q_e is the amount of solute adsorbed (mg/g) at equilibrium and C_e is the equilibrium concentration (mg/l), the values of the empirical constants Q and b, denote the monolayer capacity and energy of adsorption and were calculated from the slope and intercept of plot between $1/C_e$ and $1/q_e$.

The linearized form of Freundlich isotherm is represented below,

$$Ln(X/M) = ln(K_r) + (1/n)ln\ C_e \quad (3)$$

where X is the mass of the adsorbate (mg), M is the mass of the adsorbent (mg), C_e is the equilibrium concentration (mg/l) and K_f and n are constants for a given adsorbent, adsorbate system.

The monolayer adsorption capacity from the Langmuir model for modified chitosan beads was found to be higher for phenol (18.5 mg/g) compared to Cr(VI) (180.5 mg/g). The Freundlich model constant K_f and n for Cr(VI) was found to be 1.02 mg/g and 1.94 respectively. Similarly K_f and n for phenol and Cr(VI) was found to be 6.46 and 1.49 mg/g respectively. The main advantage of the sorbent used in the present study is the ability to remove both phenol and Cr(VI) species.

3.5. Thermodynamic parameters

Mechanism of adsorption was determined by valuating the thermodynamic parameters such as ΔS°, ΔH° and ΔG°. Using Van't Hoff Eq. (4) the value of ΔS and ΔH was determined[16].

$$Log\ K_c = \Delta S^0/2.303 - \Delta H^0/2.303\ RT \quad (4)$$

The value of ΔG° was evaluated using the Eq. (5) given below,

$$\Delta G^\circ = -RT\ ln\ K_c \quad (5)$$

where R is the gas constant, T is the temperature in Kelvin and K_c is the equilibrium constant, determined by Eq. (6) where C_A (mg/l) is the amount of solute adsorbed by the adsorbent at equilibrium and C_e is the equilibrium concentration (g/L).

$$K_c = C_A/C_e \quad (6)$$

For phenol and Cr(VI) systems, log K_c was plotted against 1/T and the plots were found to be linear. Using these plots, ΔS° and ΔH° were determined from intercept and slope respectively. Chemisorption process is indicated by the positive values of ΔS° and ΔH° for both the systems. Positive value of the entropy also indicates the irreversibility and stability of the adsorption process. Negative of value of ΔG° indicates the feasibility and spontaneity of the process.

4. Conclusions

Industrial effluents rarely contain a single component, hence, adsorption systems design must be based on multicomponent systems. It has been demonstrated previously that modified chitosan beads offers interesting possibilities as a metal ion and an organic biosorbent, showing rapid binding. The biosorption of chromium(VI), phenol and phenol–chromium(VI) binary mixtures on the modified chitosan beads was investigated in this study and the mono- and multi-component Langmuir and Freundlich isotherm models were used to predict the equilibrium uptake of components, both singly and in combination.

The applicability of mono-component Langmuir and Freundlic models indicated that the individual biosorption of phenol and chromium(VI) ions could be characterized as a monolayer, single site type phenomenon with no interaction between sorbed components and the microbial surface. The individual Langmuir and Freundlich constants evaluated from the mono-component isotherms were used to compare the biosorptive capacity of the modified chitosan beads for both components and to describe the multi-component adsorption equilibrium. It was concluded that all the adsorption models agreed well with the results found experimentally in the studied concentration ranges except at very high total initial concentrations of both components. It could be said that phenol–chromium(VI) multi-component system could be defined with all the proposed competitive adsorption models.

Acknowledgements

This was supported by Department of Chemistry, Faculty of Science, Ramkhamhaeng University.

References

[1] A. Benhammou, A. Yaacoubi, L. Nibou and B. Tanouti, *J. Hazard. Mater*. **140** (2007) 104-109.
[2] T.C. Yang and R.R.Zall, *Ind. Eng.Chem. prod. Res. Dev.* **23** (1984) 168-172.
[3] T. Y. Hsien and G. L. Rorrer, *Ind. Eng.Chem. Res.* **36** (1997) 3631-3638.
[4] K.C. Gavilan, A.V Pertov, H. Moldonado, Y. Yatlule, J. Rousy and E. Guibal, *J. Hazard. Mater.* **165** (2009) 415-426.
[5] W. S. Wan Nagh, A. Kamari and Y. J. Koay, *Int. J. Biol. Macromol* **36** (1997) 3631-3638.

[6] J. M. Li, X. G. Meng, C. W. Hu and J. Du, *Bioresour. Technol*. **47** (2010) 308-315.
[7] Z. Aksu and D. Akpinar, *Biochem. Eng. J.* **7** (2001) 183-193.
[8] H. Song, Y. Liu, W. Xu, G. Zeng, N. Aibibu, L. Xu and B. Chen, *Bioresour. Technol*. **100** (2009) 5079–5084.
[9] L. Lach, E. Okoniewska, E. Neczaj and M. Kacprzak, *Desalination* **223** (2008) 249–255.
[10] J.Q. Jiang, C. Cooper and S. Ouki, *Chemosphere* **47** (2002) 711–716.
[11] T. Mitani, N. Fukomuro, C. Yoshimoto and H. Ishii, *Agric. Biol. Chem*. **55** (1991) 2419-2425.
[12] S. Chatterjee, D. S. Lee, M. W. Lee and S. H.Woo, *J. Hazard. Mater*. **166** (2009) 508-513.
[13] Z. Aksu and F. Gonen, *Sep. Purif. Technol.* **49** (2006) 205-216.
[14] N. S. Kumar, M. Suguna, M. V. Subbaiah, A. S. Reddy, N. P. Kumar and A. Krishnaiah, *Ind. Eng.Chem. Res* **49** (2010) 9238-9247.
[15] Y. A. Aydin and N. D. Aksoy, *Chem. Eng. J.* **151** (2009) 188-194.
[16] M. R. Gandhi, N. Viswanathan and S. Meenakshi, *Int. J. Biol. Macromol* **47** (2010) 146-154.

METHOD DEVELOPMENT FOR ESTIMATION OF *IN VITRO* BIOACCESSIBILITY OF PHYTOESTROGENS IN SOYBEAN MILK USING HIGH PERFORMANCE LIQUID CHROMATOGRAPHY (HPLC) AFTER DIALYSIS METHOD

Nathanika Butboon, Juwadee Shiowatana, Tinnakorn Tiensing, Atitaya Siripinyanond*

Department of Chemistry and Center of Excellence for Innovation in Chemistry, Faculty of Science, Mahidol University, Bangkok, 10400 Thailand

* Author for correspondence; E-Mail: atitaya.sir@mahidol.ac.th, Tel. +66 22 015129

Abstract: A method for estimation of in vitro bioaccessibility of phytoestrogens in soybean milk using high performance liquid chromatography (HPLC) after dialysis method was developed. Commercial soybean milk samples were extracted by solid-phase extraction (SPE) on C18 SPE cartridge and then the eluted fractions were injected to HPLC system with isocratic elution mobile phase containing acetonitrile : water (40:60 v/v) on a C18 column and quantified by diode array detector at 254 nm. Daidzein and genistein, the two majors isoflavones are separated completely in 5 minute by HPLC and show high signals with SPE pre-concentration factor about 10 times. Bioaccessibility of phytoestrogens in human for phytoestrogens consumption can be estimated by using dialysis system based on a simulation of gastric digestion followed by an intestinal digestion in the optimum volume ratio between gastric digested samples from gastric digestion to $NaHCO_3$ dialyzing solution in intestinal digestion of 1:2. After intestinal digestion, dialyzed phytoestrogens in $NaHCO_3$ were pre-treated by SPE prior to analysis by HPLC.

1. Introduction

Phytoestrogens are members of classes of polyphenolic compounds synthesized by plants which bear structural similarity with estrogenic steroids or human sex hormone, estrogens. The shining similarity of these compounds at the molecular level provides the important role for human health which relates to the menopausal symptom, cardiovascular disease, osteoporosis, and prevention of cancers and in some cases act as an antagonist estrogens [1,2]. Phytoestrogens can be grouped into three main classes: coumestans, lignans, isoflavones. Isoflavones are the most well known phytoestrogens that have both estrogenic activity and antioxidant capacity, related to their structural similarity to 17β-estradiol. They are able to bind to estrogen receptors (ER) and elicit either a weak estrogenic (agonistic) or anti-estrogenic (antagonistic) effect, depending on the levels of endogenous estrogens present and the tissue and ER subtype [3]. Isoflavones are found primarily in Fabaceae family, legumes and soy, especially, soy seeds show high levels of these compounds. Of all isoflavones, genistein and daidzein have received the most attention because of their functionalities are nearly similar to estrogens. The chemical structures of both compounds are illustrated in Figure 1.

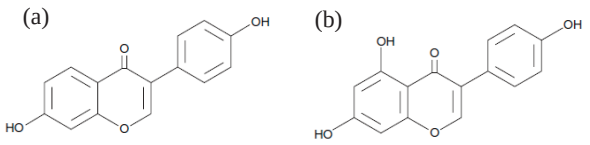

Figure 1. Chemical structures of phytoestrogens: (a) daidzein; and (b) genistein [4]

For many years ago, phytoestrogens consumption has been the topic of widely interest in many women, especially, postmenopausal women, for the possibility of hormone therapy as an alternative and including other side effect by intake of dietary phytoestrogens or phytoestrogens supplement [5]. Phytoestrogens consumption and absorption in human can be estimated in the dialysis system through the simulation of *in vitro* gastrointestinal digestion. For *in vitro* gastrointestinal digestion of phytoestrogens, the investigation of quantitative data can be employed by various analytical methods including high performance liquid chromatography (HPLC).

In this research, the development of HPLC method coupled with solid-phase extraction (SPE) to estimate the bioaccessibility of phytoestrogens in soybean milk after the simulation of *in vitro* gastrointestinal process on dialysis system has been proposed.

2. Materials and Methods

2.1 Chemicals and reagents

Isoflavones standard (daidzein and genistein), all enzymes for digestion (pepsin, pancreatin, bile extract) were purchased from Sigma- Aldrich (St. Louis, United States). Acetonitrile (Fisher Scientific, Leicestershire, United Kingdom) and methanol (Fisher Scientific, Leicestershire, United Kingdom) used were HPLC grade and all chemicals used were analytical reagent grade. Isoflavones standard stock solutions 200 mg L^{-1} were prepared by dissolving 2 mg of each in methanol and adjusted volume to 10 mL and kept for used throughout the experiment. For enzyme solutions: pepsin solution was prepared by dissolving 0.16 g pepsin in 1 mL of 0.1 M HCl (Merck, Germany), and pancreatin bile extract mixture was prepared by weighing 0.004 g of pancreatin and 0.025 g of bile extract into a beaker and dissolved in 5 mL of

0.001 M $NaHCO_3$ (APS FineChem, Australia). In *in vitro* gastrointestinal process, the flat dialysis tubing membrane (MWCO 12-14 kDa) was used for the simulation of intestinal procedure which was prepared by cutting at 35.2 cm length (Spectra/Por® Dialysis membrane). They were boiled for 10 min in 40% ethanol, then soaked in 1 mM EDTA (Fisher Scientific, Leicestershire, United Kingdom) for 30 min, rinsed several times with Milli-Q water, stored in 0.001 M $NaHCO_3$ and rinsed with Milli-Q water before use [7].

2.2 Instrumentation

A high performance liquid chromatography (HPLC) system was 1100 series (Agilent Technology, Santa Clara, United States). The elution system was isocratic elution containing the ratio of mobile phase (acetonitrile : water 40 : 60 v/v) through the analysis. The HPLC instrument consists of a high pressure binary pump at flow rate of 1 mL/min, 50 µL of injection loop, detector as a diode array was set at 254 nm, ZORBAX Eclips XDB-C18 (4.6 ×150 mm, 5 µm) column from Agilent Technology (Santa Clara, United States). The software for control of equipment and data acquisition was Agilent (Hewlett Packard®) ChemStation.

Identification of phytoestrogens was achieved by comparison of retention time of separated compounds with authentic standards and quantification was carried out by integration of the peak area.

2.3 Analytical procedure: the simulation of *in vitro* gastrointestinal process with soybean milk samples

The *in vitro* simulated gastrointestinal digestion method consists of two major parts: gastric digestion and intestinal digestion.

Gastric digestion: The gastric digestion was performed according to the procedure of Miller et al. [6] and Judprasong et al. [7]. Commercial soybean milk samples were weighed, and mixed with 10 g of Milli-Q water. The pH was, adjusted to pH 2 with 6 M HCl and adjusted this sample solution to 12.5 g with Milli-Q water. Then 375 µL of pepsin enzyme was added into the sample and consequently incubate in an incubator shaker at 37 °C for 2 h.

Intestinal digestion: A portion of the mixture after gastric digestion (5.0 g) was added into the flattened dialysis bag and then 1.25 mL of pancreatin bile extract enzyme was added into the sample also. Then these dialysis bags were immersed into the flask containing dialyzing solution with varying volume ratio between gastric digested sample and dialyzing solution from 1:1 to 1:50 (1:1, 1:2, 1:5, 1:10, and 1:50 w/w). The optimum concentration of dialyzing solution ($NaHCO_3$) was determined by titratable acidity method. pH of dialyzing solution became 7 after incubation at 37 °C for 2 h. After incubation, the dialyzed compounds were subjected to HPLC system for analysis.

2.4 Sample pre-concentration by solid-phase extraction

The SPE method was developed for sample pre-concentration from *in vitro* gastrointestinal process. The procedure was performed on the SPE vacuum system with high pressure pump, the SPE cartridge used was C18 (Bond Elute – C18, 500 mg, Varian, California, United States). For the SPE protocol, 10 mL of dialyzed solution were loaded onto the cartridge (10 mL min^{-1}) that has been preconditioned with 10 mL of methanol and 10 mL of water (10 mL min^{-1}). The sample loaded SPE cartridge was further washed with 10 mL of water (at 10 mL min^{-1}), then sample residues in the cartridge were eluted by 1 mL of methanol and collected for HPLC analysis. The optimum conditions of SPE procedure were evaluated and summarized in Table 1.

Table 1: The optimum conditions for SPE procedure

Steps	Optimum conditions
Condition	10 mL of methanol and 10 mL of water (at flow rate of 10 mL min^{-1})
Load	10 mL of dialyzed phytoestrogens (at flow rate of 10 mL min^{-1})
Wash	10 mL of water (at flow rate of 10 mL min^{-1})
Elute	1 mL of methanol (at flow rate of 10 mL min^{-1})

3. Results and discussion

3.1 Dialyzability of phytoestrogens with various volume ratios between gastric digested sample and dialyzing solution $NaHCO_3$ (S: D w/w)

Dialyzability of phytoestrogens is amount of dialyzable phytoestrogens compounds that can diffuse from the inside to the outside of dialysis tube membrane. The measurement of the dialyzed phytoestrogens with various volume ratios between (S: D) was evaluated, as shown in Figure 1.

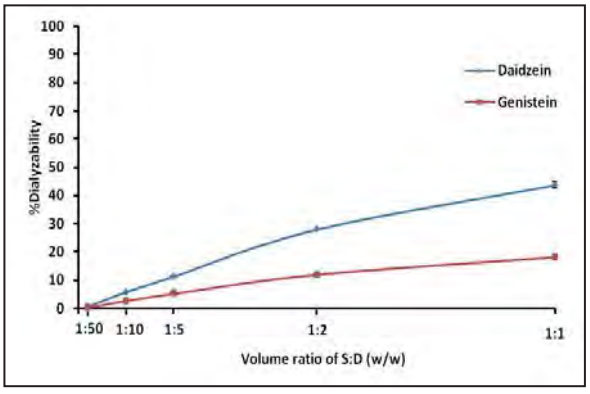

Figure 1. Effect of volume ratio between gastric digested sample and dialyzing solution (S: D) to the dialyzability of phytoestrogens in various volume ratios (1:1, 1:2, 1:5, 1:10, and 1:50 w/w).

The dialyzed amounts obtained from the equilibrium dialysis method were found to be dependent on the volume ratio of the peptic digest and the dialyzing solution. For the volume ratio of 1:1, it can provide %dialyzability as the same trend as volume ratio of 1:2. However, in volume ratio of 1:1, smallest volume of a dialyzing solution limits the contact between dialysis tube and dialyzing solution. Accordingly, to obtain the appropriate contact surface, volume ratio of 1:2 was selected for this experiment.

3.2 *In vitro* bioaccessibility of phytoestrogens based on the dialysis method

Bioaccessibility of phytoestrogens standard: Phytoestrogens bioaccessibility is about a measure of the amount of these compounds that become accessible (*in vitro*) or available (*in vivo*) for tissue distribution where they can exert physiological effects [3,8]. Estimation of bioaccessibility of phytoestrogens, phytoestrogens standard was performed for the first time. Figure 2 shows the chromatograms of dialyzed phytoestrogens standard which were clearly dialyzed into two peaks and separated completely in 5 min. However, the signals from dialyzed phytoestrogens standard were quite low, which was difficult to be clearly identified (Figure 2A). This limitation can be improved by one of commonly used pre-concentration technique that is SPE (Figure 2B).

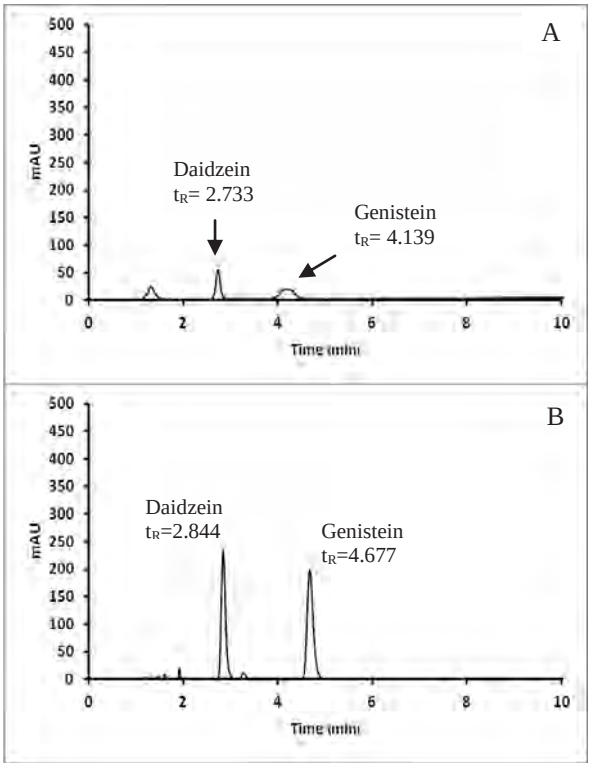

Figure 2. Chromatograms of dialyzed phytoestrogens standard without SPE pre-concentration (A) and with SPE pre-concentration (B).

With the use of SPE technique to the original dialyzed phytoestrogens from dialysis system, the dialyzed phytoestrogens signals were obviously increased and the retention time was slightly shifted which may be caused by the different of solvent composition in dialysis system and SPE system.

Bioaccessibility of phytoestrogens in real sample soybean milk: After the dialyzability of phytoestrogens standard was evaluated, the real samples (soybean milk) was also evaluted. Soybean milk has widely gained attention to consumption in all humans, as it is convenient to buy and gives a good taste, consists of the most major isoflavones phytoestrogens. For the estimation of bioaccessibility of phytoestrogens in soybean milk samples, the results are shown in Figure 3.

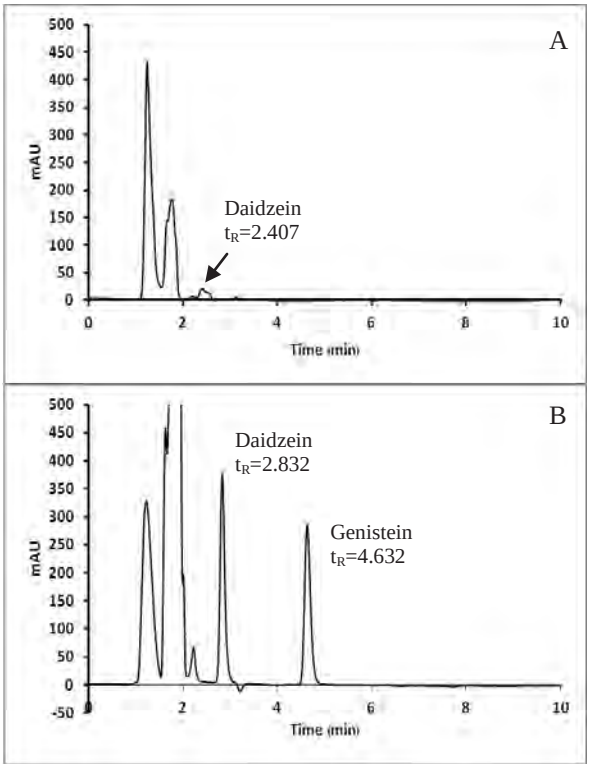

Figure 3. Chromatograms of dialyzed phytoestrogens in soybean milk *without* SPE pre-concentration (A) and *with* SPE pre-concentration (B).

Similarly to the dialyzed phytoestrogens standard, the original dialyzed phytoestrogens from the dialysis system are very low (Figure 3A). In addition, in a chromatogram of dialyzed phytoestrogens in soybean milk, genistein peak disappeared from the observation, indicating that, the estimation of bioaccessibility of phytoestrogens in real samples directly analysed by HPLC was difficult. Therefore, SPE pre-concentration technique is neccessary for analysis of these compounds (Figure 3B) and provides the pre-concentration factors about 10 times for real sample in this research.

4. Conclusions

In this work, the estimation of bioaccessibility of phytoestrogens based on the dialysis system for simulation of *in vitro* gastrointestinal process was investigated. Phytoestrogens in soybean milk can be dialyzed from the inside to the outside of dialysis tubing membrane after the *in vitro* gastrointestinal digestion and showed a higher signal than the original dialyzed phytoestrogens signal with SPE pre-concentration factors of about 10 times.

5. Acknowledgment

The authors would like to acknowledge the Center of Excellence for Innovation in Chemistry (PERCH-CIC) and the Thailand Research Fund (TRF) for instrument and financial support.

6. References

[1] B. D. Oomah, F. S. Hosseinian, *Method of Analysis for Functional Foods and Nutraceuticals. CRC Press LLC, UK*, (2002), pp. 1-83.
[2] A. L. Ososki, E. J. Kennelly, *Phytother. Res.* **17** (2003) 845-869.
[3] T. A. Larkin, W. E. Price, L. Astheimer, *Crit. Rev. Food Sci.* **48** (2008) 538-552.
[4] Y. Y. Peng, J. N. Ye, *Fitoterapia.* **77** (2006) 171-178.
[5] L. Markiewicz et al, *J. Steroid Biochem. Mol. Biol.* **45** (1993) 399-405.
[6] D. D. Miller, B. R. Schricker, B. S. Rasmussen and D. Van Campen, *Am. J. Cin. Nutr.* **34** (1981) 2248-2556.
[7] K. Judprasong et al, *J. Anal. At. Spectrom.* **20** (2005) 1191-1196.
[8] J. Shiowatan et al, *J. Agric. Food Chem.* **54** (2006) 9010-9016.
[9] M. A. Rostagno, M. Palma, C. G. Barroso, *J. Chromatogr. A.* **1076** (2005) 110-117.

SYNTHESIS AND CHARACTERIZATION OF CdS QUANTUM DOTS AND ITS APPLICATION TO SPECTROFLUOROMETRIC DETERMINATION OF MERCURY (II)

Aurachat Lert-itthiporn [1,2*] and Nathawut Choengchan [1,2]

[1]Flow Innovation-Research for Science and Technology Laboratories (FIRST Labs),
[2]Applied Analytical Chemistry Research Unit, Department of Chemistry, Faculty of Science,
King Mongkut's Institute of Technology Ladkrabang, Bangkok 10520 Thailand

[*] Author for correspondence; E-Mail: Aurachat.lert@gmail.com

Abstract: This work presents a simple method for synthesis of cadmium sulfide quantum dots (CdS QDs) under mild condition at ambient temperature. The dots were prepared from cadmium nitrate and sodium sulfide dissolved in pure methanol and polyvinyl pyrrolidone was used as stabilizing agent. The CdS QDs were optically characterized by spectrophotometer and spectrofluorometer. The excitation wavelength (λ_{ex}) was located at 300 nm while maximum emission wavelength was obtained at 700 nm. Application of the dots to determination of mercury (Hg (II)) was carried out. Detection principle is based on quenching of fluorescence intensity of CdS QDs by Hg (II). Calibration was plotted accordingly to the Stern-Volmer's relationship. It was observed that linear calibration was found up to 50 mg/l Hg (II) with good linearity ($I_0/I = 0.997 + 0.011$[Hg (II)], $r^2 = 0.994$). RSD of 1.20 % (50 mg/l Hg (II)) was obtained. LOD and LOQ were of 9.8 and 32.7 mg/l, respectively. Applications to spiked water samples (tap, drinking and river water) were studied. Recoveries were found from 97 to 115 %.

1. Introduction

Mercury (Hg (II)) is one of the most toxic heavy metals which strongly harmful to living things. It can be contaminated to water resources through industrial waste effluent. Its effect is well known as *'Minamata'* syndrome where central nervous system, DNA and mitosis are damaged [1]. Because of its seriously hazardous effect, monitoring of Hg (II) is very important.

Several analytical methods have been developed for determination of Hg (II) in various kinds of samples. The methods including atomic absorption spectrometry (AAS) [2-3], inductively coupled plasma mass spectrometry (ICP-MS) [4], colorimetry [5-6] and so on. Among the methods, spectrofluorometric method, using fluorescence sensors (organic dyes) has several advantages such as more simplicity and less time consuming [7]. However, most sensors are based on organic molecules [8] that usually function in non polar media while Hg (II) ion is existed in aqueous sample. Use of additional organic solvent is necessary for preventing immiscibility [9]. Furthermore, the organic dyes typically suffer from some limitations which are photo bleaching and most of them trend to have narrow excitation spectra and often exhibit broad emission band with red tailing [10].

In recent years, quantum dots (QDs) based researches have been received great attention due to their attractive optical properties comparison to organic fluorophores [11] such as broad excitation spectra, narrow emission spectra (which can be tuned by varying particle size and surrounding), negligible photo-bleaching and excellent chemical stability [12]. Some groups have employed QDs as chemical sensors for metal ions determination [13-15]. However, many QDs-based sensors require complicated conditions for synthesis whatever reflux under inert gas flow for very long time (10 hr) [13, 15] or using high temperature (100 °C) [14]. For this reason, in this work, we are aimed to synthesize CdS QDs with simple procedure under mild conditions. After synthesis, the particles were optically characterized by means of spectrophoto- and spectrofluorometry. Application of the dots to spectrofluorometric determination of Hg (II) in water samples was also investigated for demonstration of its real uses. Detection principle is based on quenching effect of the dots in the presence of Hg (II) ion. Quantitation approach is accordingly to the Stern-Volmer's relation [16] where the emission intensity is in diverse proportion to concentration of the quencher.

2. Materials and Methods

2.1 Reagents and water sample preparation

All chemicals were of analytical reagent grade and deionized-distilled water was used throughout. The CdS QDs were prepared from cadmium nitrate ($Cd(NO_3)_2 \cdot 4H_2O$, UNILAB) and sodium sulfide ($Na_2S \cdot 9H_2O$, PANREAC) in polyvinyl pyrrolidone (SIGMA-ALDRICH) dissolved with pure methanol. Standard Hg (II) ($HgCl_2$, from CARLO ERBA) was prepared in water. Working standard solutions were appropriate diluted from this stock solution.

Water samples were tap, drinking and river water. Tap and drinking waters were analysed directly without any pretreatment. For river water, after collection from the rivers near Ladkrabang industrial estate and King Mongkut's Institute of Technology Ladkrabang, they were filtered through a 0.22 μm Nylon membrane filter prior to analysis.

2.2 Procedure for synthesis of CdS QDs and their optical characterization

Cadmium nitrate and sodium sulfide were used as precursors and polyvinyl pyrrolidone (PVP) as stabilizer. Firstly, 50 ml of 3.2 mM $Cd(NO_3)_2$ was taken into an erlenmeyer flask, followed by adding 20 ml of 0.5 % (w/v) PVP. The solution was continuously stirred at ambient temperature. Then, 30 ml of 3.2 mM Na_2S was gradually added. A yellow solution, composing of CdS QDs was observed. The colloidal QDs solution was optically characterized by using spectrophotometer (SHIMADZU UV-1800PC) and spectrofluorometer (JASCO FP-6300).

2.3 Procedure for Hg (II) determination

The determination procedure for Hg (II) was as follows: into a test tube, 4.0 ml of CdS QDs solution and 1.0 ml of either mercury standard (with different concentrations) or water sample was sequentially added. The solution was homogeneously mixed by vortex for exactly one minute. The fluorescence intensity was measured at $\lambda_{ex}/\lambda_{em}$ = 300/700 nm. Reference solution was carried out with similar procedure unless mercury was not included. The amount of Hg (II) was quantitated through the linear plot of the Stern-Volmer's relationship.

3. Results and Discussion

3.1 Optical characterization of CdS QDs

Optical characterization of CdS QDs was carried out by monitoring their absorption and emission spectra. Results in Fig. 1 reveal that absorption and emission peaks are appeared in UV and visible region, respectively. Maximum absorption wavelength is not observed while maximum emission wavelength is located at 700 nm. Results in Fig. 2 are photographs of synthesized QDs in methanol. Under irradiation with UV lamp, the bright yellow color is obviously observed (Fig. 2 (b)).

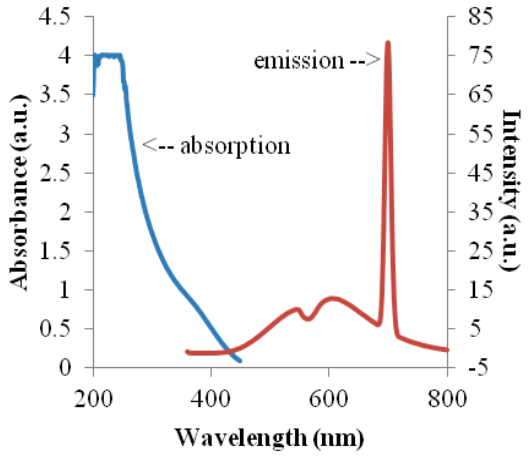

Fig. 1. Absorption and emission spectra of 3.2 mM CdS QDs.

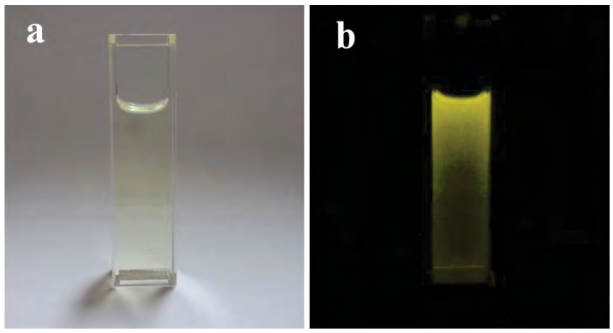

Fig. 2. Photographs of 3.2 mM CdS QDs: (a) without and (b) with UV irradiation.

3.2 Effect of excitation wavelength

Effect of excitation wavelength (λ_{ex}) was investigated. Results in Fig. 3 demonstrate that the emission intensities are not difference when 300 to 350 nm was studied. At higher than 350 nm the intensity was dramatically decreased because the energy is relatively low and not sufficient to stimulate all particles to excitation state. Therefore, we selected 300 nm as appropriate excitation wavelength.

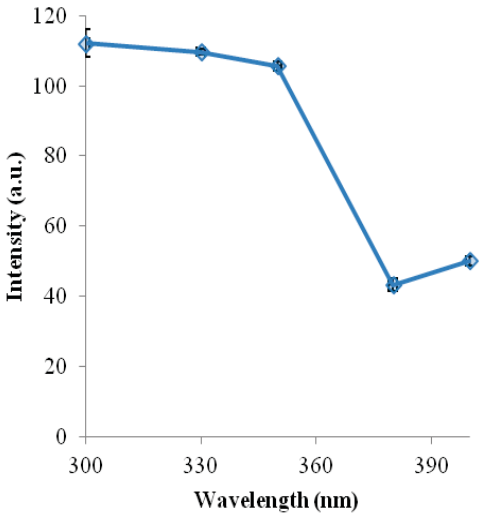

Fig. 3. Effect of different excitation wavelength on emission intensity.

3.3 Effect of stirring time

Effect of stirring time was studied from 5 to 30 min. When stirring time is increased, the fluorescence intensity was also increased (Fig. 4.). It was due to the CdS colloidals were cumulative formed. In this work, we chose a stirring time at 30 min for further studies.

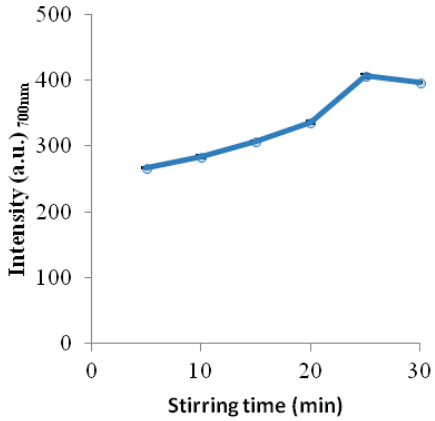

Fig. 4. Effect of stirring time on emission intensity.

3.4 Stability of CdS QDs

The fluorescence intensity of CdS QDs was measured at 700 nm at different time periods. Results are presented in Fig. 5.

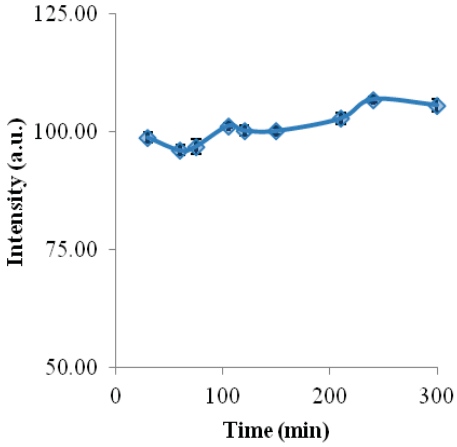

Fig. 5. Emission intensity (at 700 nm) of CdS QDs at different time periods.

This result implies that the CdS colloidals can be dispersed in solution for very long time (at least 5 hr) without any aggregation. Only minor change in intensity is observed.

3.5 Characteristics of the quenching reaction of CdS QDs by Hg (II) ion

Emission spectra of CdS QDs without and with addition of standard Hg (II) are shown in Fig. 6. Spectrum (a) is corresponded to blank solution of CdS QDs. Spectra (b) to (d) are obtained from CdS QDs in the presence of the quencher at different concentrations (5, 10, 25 and 50 mg/l Hg (II)). From the spectra, the intensity was decreased with increasing the concentration of Hg (II).

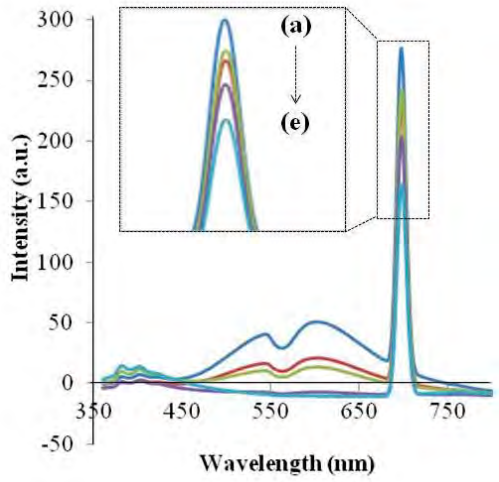

Fig. 6. Emission spectra of CdS QDs without and with addition of standard Hg (II).

Results in Fig. 6 indicate that fluorescence intensity of the CdS QDs are deactivated by Hg (II) ion. This kind of deactivation process can be represented by the Stern-Volmer's equation [16] as the following:

$$I_0/I = 1 + Kq\tau_0[Q] \quad \text{..... (1)}$$

where I_0 and I are fluorescence intensity in the absence and presence of quencher, respectively, Kq is the quencher rate coefficient, τ_0 is the fluorescence lifetime in the absence of quencher and [Q] is the concentration of quencher. Under this assumption, linear plot of the intensity ratio against the quencher concentration can be achieved.

We have found that the correlation between fluorescence intensity of CdS and concentration of Hg (II) ion (I_0/I = 0.997 + 0.011[Hg (II)]) was complied with the Stern-Volmer's equation and was in good linearity up to 50 mg/l (r^2 = 0.994) (Fig. 7.).

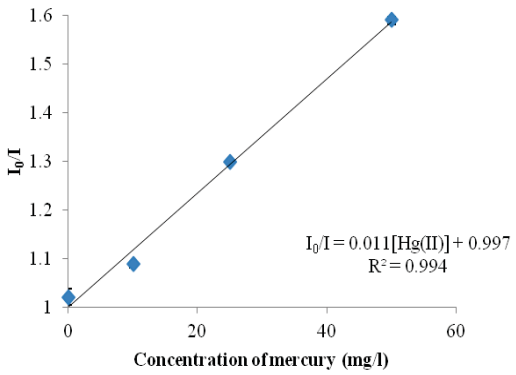

Fig. 7. The modified Stern-Volmer plot against the concentration of mercury. The intensity was corrected against baseline.

3.6 Application of the quenching reaction to determination of Hg (II)

The quenching reaction was applied as detection principle of the method for spectrofluorometric determination of Hg (II) in water samples. However, we have studied analytical performances of the method prior to determine the Hg (II) content in samples. Limit of detection, LOD (y_b+3S_b) and limit of quantitation, LOQ (y_b+10S_b) were evaluated accordingly to [17]. It was observed that LOD and LOQ were of 9.8 and 32.7 mg/l, respectively. The method gave high precision (RSD = 1.20 % at 50 mg/l Hg (II)). In term of accuracy, spiked water samples in different matrices, *i.e.*, tap, drinking and river water, were analyzed. Results, as analytical recovery, are summarized in Table 1.

Table 1. Analytical recovery of spiked water samples.

No.	Hg (II) original (mg/l)	Hg (II) added (mg/l)	Hg (II) found** (mg/l)	Recovery (%)
S 1	n.d.*	10	9.8 ± 1.9	98.0
S 2	n.d.	25	25.3 ± 3.2	101.2
S 3	n.d.	25	24.3 ± 4.1	97.2
S 4	n.d.	30	34.7 ± 3.6	115.6
S 5	n.d.	50	50.1 ± 0.3	100.2
S 6	n.d.	50	49.3 ± 1.6	98.6
S 7	n.d.	50	51.7 ± 5.8	103.4

Note * n.d. = non detectable
** mean ± SD (n = 3)

The recoveries are nearly to 100% in any kind of water samples. This implies that the method provides high accuracy. Therefore, the developed method can be used for mercury determination.

4. Conclusions

A simple procedure for synthesis of CdS QDs under mild condition at room temperature was developed. After irradiation at 300 nm, the QDs provided its highest fluorescence intensity at 700 nm. In the presence of Hg (II) ion, the intensity was decreased due to quenching reaction. This effect can be exploited as the method for determination of Hg (II). Based on the Stern – Volmer's ralationship, the developed method acquires a good linearity ranging from 0 to 50 mg/l [Hg (II)]. LOD of 9.8 mg/l and LOQ of 32.7 mg/l were obtained. The method gave high precision with high accuracy. In addition, it was applicable for determination of Hg (II) in spiked water samples.

Acknowledgements

Applied Analytical Chemistry Research Unit, Department of Chemistry, Faculty of Science, King Mongkut's Institute of Technology Ladkrabang is grateful acknowledged for equipments and financial support.

References

[1] K. V. Gopal, *Neurotoxicology and Teratology*. **25** (2003) 69-76.
[2] H. Matusiewicz and E. Stanisz, *Microchemical Journal*. **95** (2010) 268–273.
[3] J.V. Cizdziel and S. Gerstenberger, *Talanta*, **64** (2004) 918–921.
[4] E. Curdová, L. Vavrušková, M. Suchánek, P. Baldrian and J. Gabriel, *Talanta*, **62** (2004) 483–487.
[5] Y. Wang, , F. Yang and X. Yang, *ACS Appl. Mater. Interfaces*, **2 (2)** (2010) 339-342.
[6] T. Lou, , Z. Chen, Y. Wang and L. Chen, *ACS Appl. Mater. Interfaces***3 (5)** (2011) 1568–1573.
[7] L. Prodi, F. Bolletta, M. Montalti and N. Zaccheroni, *Coordination Chemistry Reviews* **205** (2000) 59–83.
[8] A. G. Lista, M. E. Palomeque and B.S. Fernandez Band, *Talanta* **50** (1999) 881–885.
[9] Y. S. Xia and C. Q. Zhu, *Talanta* **75** (2008) 215–221.
[10] M. Jr. Bruchez, M. Moronne, P. Gin, S. Weiss and A. P. Alivisatos, *Science* **281 (5835)** (1998) 2013-2016.
[11] W. CW. Chana, D. J. Maxwellb, X. Gaob, R. E. Baileyb, M. Hanc and S. Nie, *Current Opinion in Biotechnology* **13 (1)** (2002) 40–46.
[12] K. S. Lee and M. A. El-Sayed, *J. Phys. Chem. B* **110 (39)** (2006) 19220–1922..
[13] M. Koneswaran and R. Narayanaswamy, *Sensors and Actuators B* **139** (2009) 104–109.
[14] X. Liu, L. Guo, L. Cheng and H. Ju, *Talanta* **78** (2009) 691–694.
[15] Z. X. Cai, H. Yang, Y. Zhang and X. P. Yan, *Analytica Chimica Acta* **559** (2006) 234–239.
[16]http://en.wikipedia.org/wiki/Stern%E2%80%93Volmer_ relationship
[17] J. N. Miller and J. C. Miller, *Statistics and Chemometrics for Analytical Chemistry*, fourth ed., Pearson Education, Essex, 1993.

SEPARATION OF PHENOLIC COMPOUNDS IN WOOD VINEGAR USING SEQUENTIAL INJECTION CHROMATOGRAPHY

Arjnarong Mathaweesansurn[1,2 *], Suwannee Janyapoon[2], Nathawut Choengchan[1,2]

[1]Flow Innovation-Research for Science and Technology Laboratories (FIRST Labs),
[2]Applied Analytical Chemistry Research Unit, Department of Chemistry, Faculty of Science,
King Mongkut's Institute of Technology Ladkrabang, Bangkok 10520 Thailand

*E-mail: a.mathawee@live.com

Abstract: In this work, sequential injection chromatography (SIC) with monolithic column (Chromolith® flash RP-18e column) and UV detection was developed for separation of major phenolic compounds existed in wood vinegar, *i.e.*, syringol, vanillic acid and gallic acid. Optimal conditions of SIC were listed as the following: injected volume; 10 µL, mobile phase composition; methanol (10 %) in 0.1 M acetate buffer (pH 4.0), flow rate; 25.0 µL s^{-1} and detection wavelength; 264 nm. Gallic acid was firstly eluted, followed by vanillic and syringol, respectively. Separation was complete within 10 min. Retention times were highly precise (RSD = 1.14 to 2.70 %). Good linearity ranges of all analytes were also achieved (linear regression coefficients (r^2) were range from 0.997 to 0.999). The system was then applied to a wood vinegar sample from eucalyptus. Analytical recoveries were observed from 97 to 114 %.

1. Introduction

'Wood vinegar' or *'Pyroligneous acid'* is a by-product in charcoal production. It is condensate of smoke which is occurred during wood burning. One interesting component in wood vinegar is phenolic groups due to their high radical scavenging activity [1]. P. Rungruang *et al.* [2] found that major phenolic compounds, existed in wood vinegar from eucalyptus, are syringol, vanillic acid and gallic acid. Syringol and vanillic acid can be exploited as food flavoured additives. Gallic acid is useful by taking into account of its anti-wrinkle property, thus it is widely used as supplement in many cosmetic products. However, it is necessary to separate and purify the mentioned phenolic compounds from wood vinegar matrix prior further applications.

There are many analytical methods developed for separation of phenolic compounds. Those methods are based on gas chromatography (GC) [2, 3] and liquid chromatography (LC) [4-9]. Although GC, especially with mass detection (MS), is appropriate to identify kinds of phenolic compounds in wood vinegar, the separated fractions are damaged during detection. LC is more applicable since the liquid fractions can be individually collected for advanced uses without any destruction. Most of LC methods [4-9] employed conventional packed columns for separation of phenolic compounds in various kinds of samples. Despite the fact that all LC methods mentioned above provided high separation efficiency, some drawbacks such as long retention time and use of high pressure pump were not negligible. These can be solved by exploiting more porosity column, namely *'monolithic column'* [10]. M. Castellar *et al.* [11] demonstrated advantages of monolithic column by coupling with HPLC for determination of phenolic groups in wines. Even though the results gave short analysis time with good separation under low pressure, samples were manually injected which is not suitable for routine works.

Recently, a sequential injection chromatography or *'SIC'* was reported for the sake of fast separation under low pressure and fully automated manipulation [12, 13]. Those publications were involved in development of SIC methods for separation with subsequent detection of pesticides [12] and sulfonated-azo dyes [13]. To our knowledge, application of the SIC to phenolic compounds in wood vinegar has not been reported so far.

In this work, we therefore aimed to develop a monolithic-based SIC method for separation and determination of phenolic compounds, *i.e.*, syringol, vanillic acid and gallic acid in wood vinegar from eucalyptus. Separation conditions were optimized in order to obtained high resolution with short retention time. Validation by evaluation of the method performances was also carried out.

2. Materials and Methods

2.1 Reagents and samples preparation

All solvents were of HPLC grade and were purchased from Carlo Erba. Deionized-distilled water was used throughout. Exactly 0.1 g of standard syringol, vanillic acid and gallic acid (all from Sigma-Aldrich) were weighed and dissolved in mobile phase (100.00 mL). Mixed working standard solutions were prepared by diluted from the stock solutions to give final concentration ranges of 50 to 200 mg L^{-1}. The mobile phase consisted of 10 % methanol in acetate buffer pH 4.0 was prepared by mixing 0.1 M acetic acid and 0.1 M sodium acetate. All solutions were filtered through 0.45 µm Nylon membrane prior to analysis unless commercial wood vinegar samples (from eucalyptus wood, similar sample to [2]) were filtered through 0.22 µm Nylon syringe filter after centrifugation for 15 min.

2.2 Chromatographic system and operating conditions

The SIC system consisted of syringe drive module equipped with 2.5 mL Gastight® syringe and an 8-port multi-selection valve (All devices were purchased from Hamilton, USA). The system was automatically manipulated by Auto-pret® software (MKG Company, Japan). Separation was done on a Chromolith® Flash RP-18e silica based monolithic column (25 x 4.6 mm, Merck, Germany) with flow rate of 25 µL s^{-1}. The injection volume was kept constant at 10 µL for all injections. Detection was carried out on Jasco v-630 UV-visible spectrophotometer (USA) at 264 nm.

3. Results and Discussion

3.1 Choices for monitored wavelength

Since maximum absorption wavelengths (λ_{max}) for syringol, vanillic acid and gallic acid are different (Fig. 1) and the available spectrophotometer for SIC system is not diode array detector, it is necessary to investigate the compromised wavelength for appropriate detection of all analytes.

It is clearly noticed from Fig. 1 that syringol is very less absorption than vanillic acid and gallic acid. However, from our previous results [2], syringol content was much greater than the other two phenolic substances in wood vinegar. A wavelength at 264 nm was therefore selected as a monitored wavelength in order to enhance sensitivity for determination of vanillic acid and gallic acid in real sample.

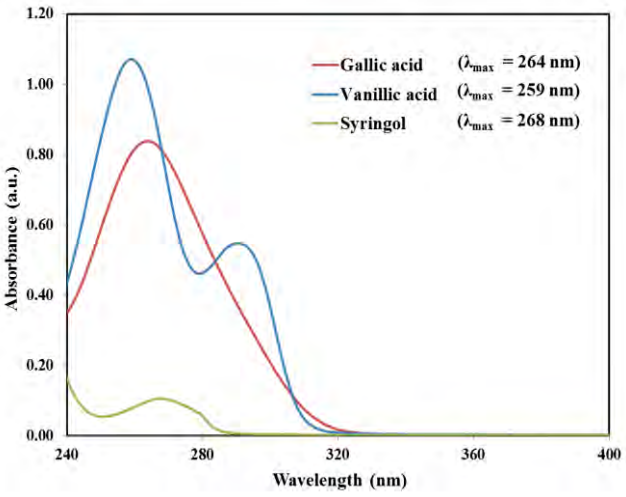

Fig. 1. UV spectra of the interested phenolic compounds at equivalence concentrations of 10^{-4} M.

3.2 Optimization of SIC system

Optimization of the SIC system was performed using standard solution of syringol, vanillic acid and gallic acid (at 100 mg L^{-1} for all standards). Mobile phase composition was primarily studied. Results in Fig. 2 illustrate the influence of mobile phase composition on resolution and retention time. Although decreasing in the methanol (MeOH) concentration in mobile phase from pure to 5 % can improve resolution of the separation, analysis time is prolonged. This reduces throughput of the method. Therefore, we selected 10 % for further study.

From literature [5], addition of acetic acid into the mobile phase can enhance separation efficiency of the phenolic compounds. In this work, effect of acetic acid concentration was also investigated. As expected when the acid (2 %) is added into 10 % MeOH, resolution is improved (Fig. 2). However, this concentration led to the mobile phase's pH of 2.0 which reach tolerance pH for the exploited monolithic column. This can damage the column in case of long usage term. We, therefore, changed to prepare the mobile phase in acetate buffer solution (pH 4.0) instead. This mobile phase composition gave satisfied resolution and analysis time.

Besides of the mobile phase component, the other parameters, including flow rate and injection volume, were also examined. Higher flow rate and injection volume resulted in worse separation. A flow rate of 25 µL s^{-1} and an aliquot of 10 µL were regarded as appropriate flow rate and injection volume, respectively, by compromising between resolution and analysis time.

Optimal conditions for the proposed SIC system were summarized in Table 1.

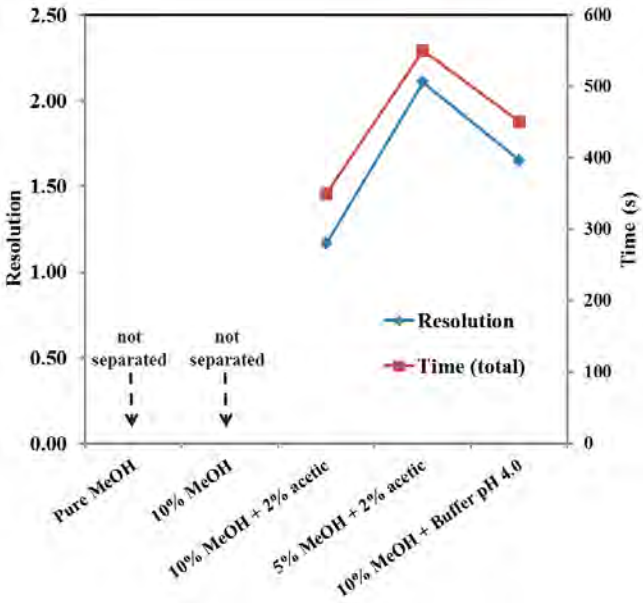

Fig. 2. Effect of the mobile phase composition on resolution of the separation and analysis time.

Table 1. Optimal conditions of the SIC system.

Parameter	Optimal value
Sample volume (µL)	10
Flow rate (µL s^{-1})	25
Mobile phase composition (isocratic elution)	10% methanol in acetate buffer pH 4.0
Detection wavelength (nm)	264
Sample volume (µL)	10
Flow rate (µL s^{-1})	25

3.3 Analytical performances

An example of chromatograms obtained from the optimal conditions is shown in Fig. 3. Under isocratic elution, gallic acid is initially eluted, followed by vanillic acid and syringol. Results in Fig. 3 indicate that all the phenolics can be completely separated within 10 min.

Although satisfied separation efficiency was achieved under isocratic elution, we are now studying on gradient elution system for the aim of shortening the retention time for syringol.

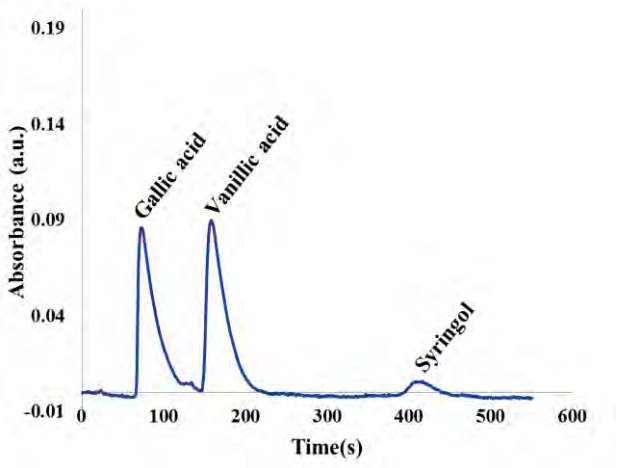

Fig. 3. Example of chromatograms of mixed standard phenolic compounds at 100 mg L^{-1}.

Table 2. Analytical performances of the SIC method

Performances	Phenolic compounds		
	Gallic	Vanillic	Syringol
Retention time (min)	1	3	7
Linearity range (mg L^{-1})	50-200	50-200	50-200
Calibration equation	y = 0.0012x + 0.007	y = 0.0013x + 0.004	y = 0.0001x - 0.0003
Linear regression coefficients (r^2)	0.992	0.997	0.996
RSD (%) of retention time	1.86	1.14	2.70
Recovery (%)	114.3	103.3	97.2
LOD [a] (mg L^{-1})	0.063	0.034	0.007
LOQ [b] (mg L^{-1})	0.182	0.098	0.023

Note [a]; $LOD = y_b + 3S_B$
[b]; $LOQ = y_b + 10S_B$

The other analytical performances were also examined and the results are concluded in Table 2. Linearity ranges of 50 to 200 mg L^{-1} were achieved with good linearity for all analytes. The SIC system also gave high precision of retention time with high accuracy (by regarding analytical recovery). Limit of detection (LOD) and limit of quantitation (LOQ) were evaluated accordingly to [14]. In accordance with our previous results [2], the calculated limits are adequate to be applied the developed method to determine the interested phenolic substances existed in wood vinegar from eucalyptus wood.

3.4 Application to wood vinegar sample

The SIC method was applied to determination of syringol, vanillic acid and gallic acid in wood vinegar sample, from eucalyptus. Concentrations of the phenolic compounds are presented in Table 3.

Table 3. Concentrations of the phenolic compounds in wood vinegar samples, determined by the SIC method.

Sample	Concentration (mg L^{-1}, mean ± SD)		
	Gallic	Vanillic	Syringol
1	113 (± 2.5)	127 (± 0.7)	453 (± 1.2)
2	76.4 (± 0.5)	90.2 (± 1.9)	310 (± 1.7)
3	60.1 (± 1.3)	64.5 (± 0.7)	251 (± 0.5)
4	51.3 (± 0.9)	46.1 (± 0.2)	238 (± 0.4)

The phenolic concentration trends are similar to our previous results by GC-MS [2] where the most abundance phenolic compound in this kind of wood is syringol.

Nevertheless, in order to verify the developed method, further validation of the method with LC is required and the process is now going on. We selected LC with UV detection as the validating method instead of GC-MS because any derivatization procedure is not required.

4. Conclusions

The monolithic SIC method was developed for determination of syringol, vanillic acid and gallic acid in wood vinegar. The method provides fast separation (< 10 min/sample) under low pressure with fully automated manipulation. High analytical performances (such as precision and accuracy) were also achieved. However, further validation by statistical comparison of the results with LC-UV technique is necessary.

Acknowledgements

Applied Analytical Chemistry Research Unit, Department of Chemistry, Faculty of Science, King Mongkut's Institute of Technology Ladkrabang is grateful acknowledged for equipments and financial support.

References

[1] A.Y. Loo, K. Jain and I. Darah, *Food Chem.* **107** (2008) 1151-1160.

[2] P. RungRuang, *Antioxidation activity of phenolic compounds in pyroligneous acid produced from bamboo wood, eucalyptus wood and teak slab*, Master's Thesis, KMITL, (2011).
[3] A.Y. Loo, K. Jain and I. Darah, *Food Chem.* **104** (2007) 300-307.
[4] B. Abad-Garcia, L.A. Berrueta, D.M. Lopez-Marquez, I. Crespo-Ferrer, B. Gallo and F. Vicente, *J. Chrom. A.* **1154** (2007) 87-96.
[5] M. Tarnawski, K. Depta, D. Grejciun and B. Szelepin, *J. Pharm. Biomd. Anal.* **41** (2006) 182-188.
[6] H. Kelebek, S. Selli, A. Canbas and T. Cabaroglu, *Microchem. J.* **91** (2009) 187-192.
[7] M.A. Rodriguez-Delgado, S. Malovana, J.P. Perez, T. Borges and F.J. G. Montelongo, *J. Chrom. A.* **912** (2001) 249-257.
[8] D. Blanco Gomis, N. Fraga Palomini and J. J. Mangas Alonso, *Anal. Chem. Acta.* **426** (2001) 111-117.
[9] A. Schieber, P. Keller and R. Carle, *J. Chrom. A.* **910** (2001) 265-273.
[10] G. Guiochon, *J. Chrom. A.* **1168** (2007) 101-168.
[11] M. Castellari, E. Sartini, A. Fabiani, G. Arfelli and A. Amati, *J. Chrom. A.* **973** (2002) 221-227.
[12] P. Chocholous, D. Satinsky, R. Sladkovsky, M. Pospisilova and P. Solich, *Talanta*. **77** (2008) 566-570.
[13] C. Fernandez, M. Soledad Larrechi, R. Forteza, V. Cerda and M. Pilar Callao, *Talanta*. **82** (2010) 137-142.
[14] J. N. Miller and J. C. Miller, *Statistics and Chemometrics for Analytical Chemistry*, fourth ed., Pearson Education, Essex, 1993.

DETERMINATION OF HEAVY METALS AND PARTICLE SIZE DISTRIBUTION OF MARINE SEDIMENT AT THA CHIN ESTUARY, THAILAND

Passorn Pongsaeve[1], Waret Veerasai[1], Nongnuch Tantidanai-Sungayuth[1, 2*]

[1] Department of Chemistry, Faculty of Science, Mahidol University, Ratchathewee, Bangkok, 10400, Thailand
[2] Office of Interdisciplinary, Mahidol University at Kanchanaburi Campus, 199, Lumsum, Saiyok, Kanchanaburi, 71150, Thailand

*E-Mail: scntt@mahidol.ac.th, Tel. (662) 2015124

ABSTRACT: The lower Tha Chin River along Samut Sakorn Province, Thailand is an area where risks of metal contamination because there are many activities of aquaculture fishery, industry, and household. The environmental assessment is very important to qualify the lower Tha Chin River. Many works reported that the smaller sediment grain size was, the more adsorption capacity and the easier distribution of metals took place. In this work, the metal distributions of marine sediments in Tha Chin Estuary were investigated. Their particle size distributions (PSDs) and heavy metal contents (As, Cd, Co, Cr, Cu, Fe, Mn, Ni, Pb, and Zn) were determined. Thirteen sites (S1-S13) were studied far from the coastline approximately 2 km from east to west direction. Their PSDs were divided into four patterns based on Wentworth grain-size scale. The first (S1, S2, S3, S4, S5, S8, and S9) and the second (S6, S12, S13) patterns mainly consisted of silt and very fine sand, respectively. The third pattern (S10 and S11) was composed of silt and very fine sand. The fourth pattern (S7) was mainly formed of fine sand. The metal contents were determined by using ICP-OES and compared with the sediment quality guideline standard by the effects range low (ERL) and effects range median (ERM) level from Pollution Control Department of Thailand. For all sites, the concentrations of Cd were higher than the ERM level. Therefore, the Cd risk assessment should be aware and the Cd treatment may be required along the lower Tha Chin River. Although the concentrations of As, Cu, Ni, and Pb presented higher than the ERL level, the concentrations of those elements should be attended and monitored because their concentrations closed to the ERM level. The concentrations of other elements (Co, Cr, Fe, Mn, and Zn) were lower than the ERL level.

1. Introduction

The lower Tha Chin River is the important local economic development area because of its high population density and human activities such as aquaculture fishery, livestock, industries, transportation, water supply and household [1-3]. These activities are the major sources of the release and accumulation of harmful pollutants, especially heavy metals that provide high toxicity and directly affect the aquatic environmental quality [4, 5]. In aquatic ecosystem, there are only less than 0.1% of heavy metals dissolved in the water system and more than 99.9% of those stored in the bottom sediment [6]. The accumulation of heavy metals in marine system is also resembled to aquatic system. However, the release of heavy metals back to the aquatic and marine system through Bio-Geo-Physico-Chemical processes is still at a risky situation and should be concerned [7]. Therefore, monitoring heavy metals in sediment is necessary.

Many studies [8-11] mentioned that sediment particle size distributions (PSDs) is one of the major parameters that can indicate the effect of accumulation of heavy metals because the smaller particle size has presented the higher adsorption capacity and the easier dispersion to the water column leading to the dissolution back into the water system or contamination in plant or aquatic animal tissue [12].

In this work, the PSDs and heavy metal contents (As, Cd, Co, Cr, Cu, Fe, Mn, Ni, Pb, and Zn) in contaminated marine sediment from the Tha Chin estuary, Thailand were determined. The PSDs of marine sediment were classified by Wentworth grain-size scale [13]. The heavy metal concentrations were detected by ICP-OES. Moreover, the metal concentrations of marine sediments were compared with the sediment quality guideline standard (SQG) of the declaration of Pollution Controlled Department (PCD) Thailand which is defined as the limit value of eight heavy metals (As, Cd, Cr, Cu, Hg, Ni, Pb, and Zn) in sediment [14]. SQG is divided into two levels, effects range low (ERL) and effects range median (ERM), by quantity of metal polluting in sediment. The ERL and ERM are proposed guideline values to define total contaminant concentration ranges in sediment that are rarely (below ERL), occasionally (above ERL and below ERM), and frequently (above ERM) associated with adverse biological effects in order to evaluate the risk of heavy metal contamination levels in marine sediment samples.

2. Materials and Methods

2.1 Reagents

All reagents were of analytical grade. The concentrated 65% (w/v) HNO_3 and 30% (w/v) H_2O_2 were purchased from Merck (Darmstadt, Germany). The standard solutions for As, Cd, Co, Cr, Cu, Fe, Mn, Ni, Pb, and Zn were prepared by using Perkin Mayer (Shelton Connecticut, USA) standard solutions.

2.2 Sample collection

Surface marine sediment samples were collected in 20 February 2012 from the different locations named

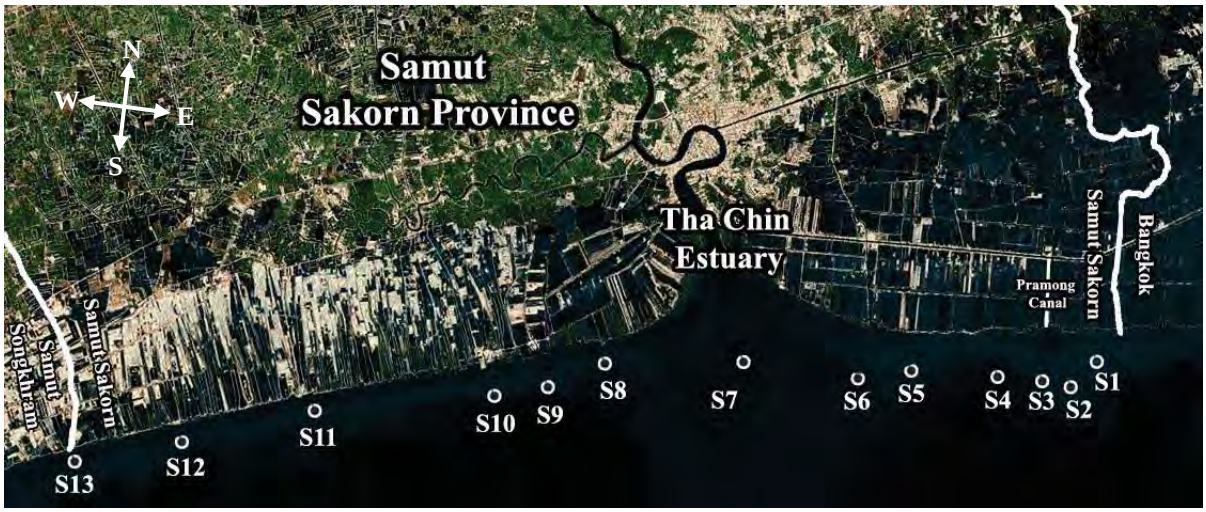

Figure 1. Location map of the study area and sample site locations (S1-S13).

S1 - S13 of Tha Chin Estuary as shown in Figure 1. The locations of sampling were far from the coastline of Samut Sakorn Province about 2 km and sample collected in the direction from east to west and the distance between each site was 1 km. The surface marine sediment samples were collected by using the stainless Birge-Ekman grab sampler. A portion of each sediment sample was kept in tightly closed plastic black bags (2 layers). Then, they were transferred to High Density Polyethylene (HDPE) bottles and stored at 4°C in a refrigerator.

2.3 Particle size distribution

The particle size distribution of marine sediments was determined by Master Sizer 2000 Instrument (Malvern, Worcestershire WR14 1XZ, United Kingdom) in Wet mode by using pump speed of 2000 revolutions/min and sediment reflective index of 1.52. The sludge sediments were stirred in DI water for 5 minutes and ultrasonicated for 1 minute before the particle size distribution was measured. Types of marine sediments in aspects of particle size distributions (PSDs) are divided based on the Wentworth scale (Table 1.).

Table 1: Wentworth grain-size scale of sediment [13].

Sediment	Type	Diameter (µm)
Sand	Coarse	500 - 1000
	Medium	250 - 500
	Fine	125 - 250
	Very fine	62.5 - 125
Mud	Silt	3.9 - 62.5
	Clay	0.2 - 3.9

2.4 Microwave-assisted acid digestion

The homogeneous freeze-dried marine sediment was weighed for 0.25xx g to performed in microwave PTFE vessel. Mixture solution HNO_3:H_2O_2 (21:3 v/v) of 24 ml was added into a microwave vessel. The vessel was then tightly sealed and placed into a Milestone Ethos 1 microwave system (Milestone Inc., Shelton Connecticut, USA). The heating program consists of two steps. First, the temperature was slowly increased to 180 ºC within 10 minute. After that, the temperature was suddenly increased to 200 ºC and constantly held at 200 ºC for 20 minutes. Since the organic content (C_{org}) of sediment samples was more than 1 wt% C_{org}, each sample was repeatedly digested with the same condition again for completed digestion.

2.5 Determination of heavy metals

The heavy metal concentrations (As, Cd, Co, Cr, Cu, Fe, Mn, Ni, Pb, and Zn) in sediment samples were detected by ICP-OES (Spectro Ciros CCD, Kleve, Germany equipped with a 27.12 MHz RF generator with a standard torch and controlled with SMART analyzer software). The analytical wavelengths and method detection limit (MDL) for these elements were summarized in Table 2. The MDL was defined as three times the standard deviation of ten measurements of the blank divided by the slope of the calibration curve.

Table 2: The emission wavelengths for analytical elements and MDL ($mg.kg^{-1}$) obtained using the ICP-OES.

Element	Wavelength (nm)	MDL ($mg.kg^{-1}$)
As	189.042	0.52
Cd	226.502	0.01
Co	228.615	0.03
Cr	267.716	0.26
Cu	324.754	0.08
Fe	238.204	0.25
Mn	257.610	0.06
Ni	231.604	0.04
Pb	220.351	0.16
Zn	213.856	0.04

3. Results and Discussion

3.1 Particle size distribution (PSDs)

PSDs of marine sediments from thirteen sample sites (S1-S13) were examined and divided into four

patterns (Table 3, Figure 2.). The first pattern (S1, S2, S3, S4, S5, S8, and S9) was the sediment grain size which mainly consisted of silt (74.5 – 95.2% volume). The second pattern (S6, S12, and S13) was mainly consisted of very fine sand (45.1– 55.0% volume). The third pattern (S10 and S11) was composed of silt (55.8 – 67.4 % volume) and very fine sand (31.4 – 35.5% volume). The fourth pattern (S7) was major formed of fine sand (74.4% volume). When the particle size of marine sediment decreased, the adsorption of heavy metals tended to increase. Additionally, the sediment in first pattern was likely to disperse more easily than other patterns.

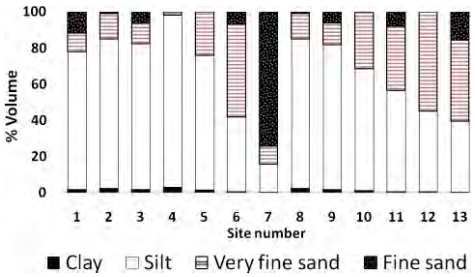

Figure 2. Percentage of grain size of marine sediment from Tha Chin Estuary, Thailand.

Table 3: Grain size distribution of marine sediment in %volume

Pattern*	Site	% Grain size composition				
		Clay	Silt	Mud	Very fine sand	Fine sand
1	S1	1.8	76.1	77.9	10.2	11.8
	S2	2.4	82.6	85.0	14.0	1.1
	S3	2.0	80.2	82.2	11.7	6.1
	S4	3.1	95.2	98.3	1.7	0.0
	S5	1.5	74.5	76.0	24.0	0.0
	S8	2.4	82.6	85.0	14.0	1.1
	S9	2.0	79.9	81.9	12.0	6.1
2	S6	0.5	41.4	41.9	51.2	6.9
	S12	0.6	44.5	45.1	55.0	0.0
	S13	0.4	39.0	39.4	45.1	15.5
3	S10	1.2	67.4	68.6	31.4	0.0
	S11	0.7	55.8	56.5	35.5	8.1
4	S7	0.3	15.5	15.8	9.9	74.4

* Pattern 1 and 2 were the sediment grain size which mainly consisted of silt and very fine sand, respectively. Pattern 3 was the sediment grain size which mainly consisted of silt and very fine sand and Pattern 4 was majorly formed of fine sand.

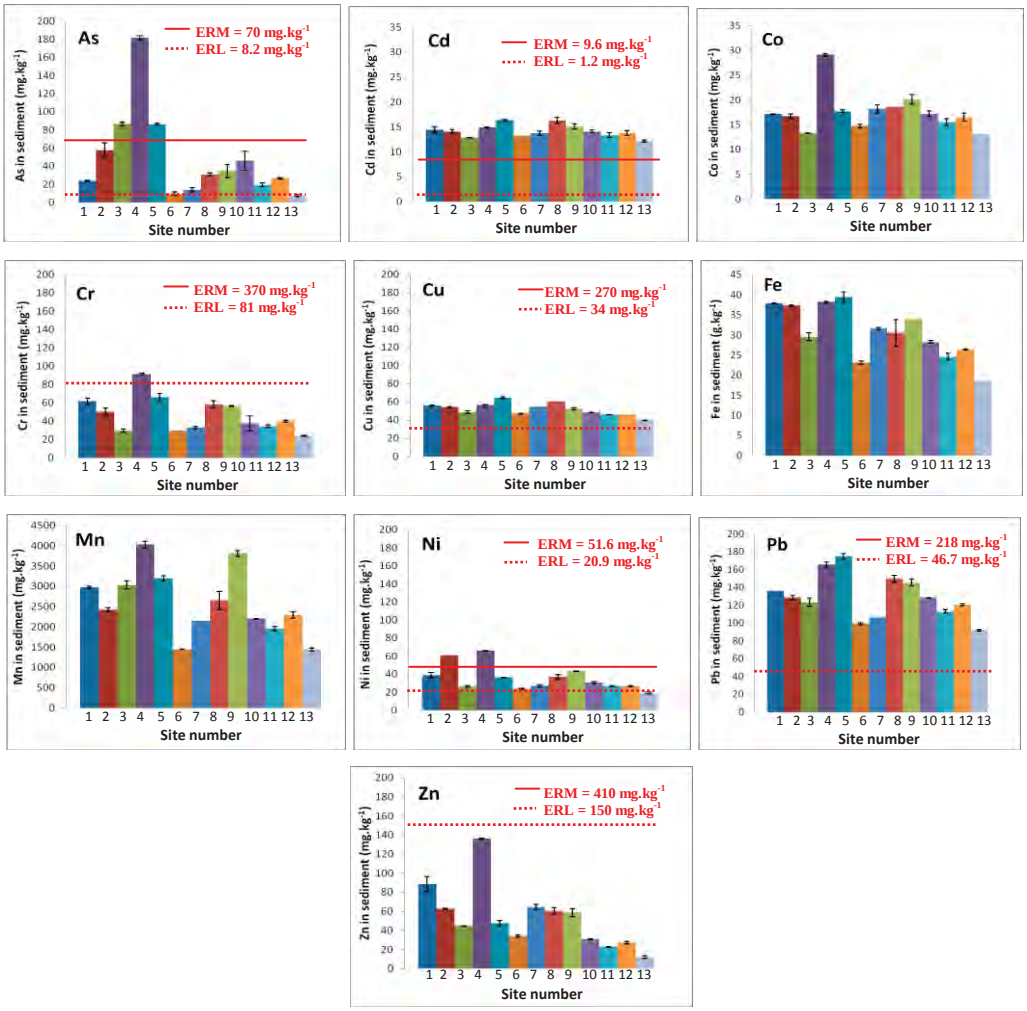

Figure 3. Concentrations of As, Cd, Co, Cr, Cu, Fe, Mn, Ni, Pb, and Zn in mg.kg^{-1} dry of marine sediments at Tha Chin estuary, Thailand.

3.2 Determination of heavy metals

The concentrations of heavy metals in marine sediments from 13 sampling sites which were known their PSDs were determined and compared with the ERL and ERM value to evaluate the risk of heavy metal contamination in marine sediment samples. The results are presented in Figure 3.The concentrations of As, Cu, Ni, and Pb were found within ERL - ERM levels while the concentrations of Cd (12.2 – 16.3 mg.kg-1) found were higher than ERM level (9.6 mg.kg-1) for all sediment sample sites. As the results, the concentrations of As, Cd, and Ni in marine sediment from sample of site 4 (Pramong Canal region) were higher than ERL level while those of Cd and Cr were higher than ERM levels. This phenomenon was happened from this area because of the congestion of industrial factories and other activities. Therefore, the risk assessment should be aware and the treatment is required along the Pramong Canal. Though the concentration levels of Co, Fe, and Mn were undefined by SQG from PCD, Thailand, the determination of those elements is necessary since it is important to the heavy metals absorption and desorption processes in marine sediment.

This study presented that the particle size of sediment and the activities around the sample collection areas were influential on the amount of heavy metals adsorbed in this area. According to the results from the fourth site, the percentage of mud composed of silt and clay having small size, (98.3%) is the highest. Therefore, this site will cause metal accumulation at high level if the metal ions are released from activities over the area. Over the forth site, there is dense aquaculture fishery, especially, mussel and cockle farming along the area [15, 16] which corresponds to the results.

4. Conclusions

The heavy metal concentrations and PSDs in marine sediment obtained along Tha Chin Estuary, Thailand indicated that the sediments at this area have been at high risk of contamination of the heavy metals. Especially, the concentrations of Cd from all sites were higher than the ERM level and the around Pramong Canal. The concentrations of As, Cu, Ni, and Pb were also higher than the ERM level. The activities over the sampling sites and the PSDs of marine sediment, especially mud portion may be the major parameters that affect to the accumulation of the heavy metals. Therefore, the monitoring and treatment of the heavy metals in Tha Chin Estuary should be aware, especially around the Pramong Canal. The activities over the Tha Chin Estuary should be paid attentions.

Acknowledgements

We would like to thank the Department of Chemistry, Faculty of Science, Mahidol University for the financial support and also thank the Flow Innovation-Research for Science and Technology Laboratories (FIRST Labs) for sample collection support.

References

[1] M. Schaffner, and I. Wittmer, *Eawag News*. **62** (2007) 18-20.

[2] S. Ilhan, and et al. *Turkish Electronic Journal of Biotechnology*, **2** (2004) 50-57.

[3] N. Brown, S. Eddy, S. Plaud, *Aquaculture*, **322-323** (2011) 177-183.

[4] M. A. Ashraf, M. J. Maah, I. Yusoff, *Int. J. Environ. Res.* **6** (2012) 209-218.

[5] I. Sen, A. Shandil, V. S. Shrivastava, *Advances in Applied Science Research*, **2** (2011), 161-166.

[6] S. Pradit, and et al. *Water Air and Soil Pollution*, **206** (2010) 155-174.

[7] X. Wen, and H. E. Allen, *The Science of the Total Environment*, **227** (1999) 101-108.

[8] S. Buajan, and N. Pumijumnong, *J. Environ. Res.* **32(2)** (2010) 61-77.

[9] J.C. Klamer, W.J.M. Hegeman, and F. Smedes, *Hydrobiologia*, **208** (1990) 213-220.

[10] KH. M. EL-Moselhy, and H. ABD EL-AZIM, *Egyptian Journal of Aquatic Research*, **31(2)** (2005) 224-238.

[11] H. Zhao, X. Li, X. Wang, and D. Tian, *Journal of Hazardous Materials*, **183** (2010) 203–210.

[12] M. A. Ashraf, M. J. Maah, and I. Yusoff, *Int. J. Environ. Res.* **6(1)** (2012) 209-218.

[13] Proposed Marine and Coastal Sediment Quality Guidelines, Pollution Controlled Department, Thailand (2006).

[14] C. K. Wentworth, *Journal of Geology*, **30** (1922), 377–392.

[15] http://www.samutsakhon.go.th

[16] P. Sukasem, and M.S. Tabucano, *The Science of the Total Environment*, **139/140** (1993) 297-3.

SYNTHESIS OF GRAPHENE/Co_3O_4 AND APPLICATIONS FOR GAS SENSING AT ROOM TEMPERATURE

Nittaya Sa-ard[1*], Suwan Chaiyasith[2], Winadda Wongwiriyapan[3], and Worawut Muangrat[4]

[1*, 2] Department of Analytical Chemistry, Faculty of Science, King Mongkut's Institute Technology Ladkrabang , Chalongkrong Road, Bangkok, 10520 Thailand
[3, 4] College of Nanotechnology, King Mongkut's Institute of Technology Ladkrabang,Chalongkrung Road, Bangkok 10520, Thailand

[*] Nittaya Sa-ard; E-Mail: nitnoi_31@hotmail.com, Tel. +66 908060835

Abstract: We have developed a candidate material for high performance gas sensors. In this work, Co_3O_4 and graphene materials were prepared by reduction in water with phenol hydrazine. The reduced materials were characterized by X-ray diffractometry (XRD), scanning electron microscopy (SEM), and Fourier transform infrared spectroscopy (FT-IR). Graphene/Co_3O_4 was used as gas sensing active layer and its sensing performance to NH_3 was compared with other three materials; graphene, carbon nanotube (CNT), and CNT/Co_3O_4 at room temperature. The sensitivity increased from CNT/Co_3O_4, CNT, graphene, and graphene/Co_3O_4. The advantages of graphene/Co_3O_4 sensor are fast response time, short recovery time, low power consumption, showing promising potential for using as NH_3 sensors.

1. Introduction

Ammonia (NH_3) is one of the most important chemical toxic substances met in everyday life. NH_3 is a widely used chemical that can be found in a variety of common industrial environments. It is a colorless gas with a pungent suffocating odor. It is characterized as flammable although it is very difficult to ignite. When exposed to heat, NH_3 solution will decompose to form ammonia gas and oxides of nitrogen, (NO_x). NH_3 is an irritant and will become extremely irritating as concentrations increase.

There are many kinds of gas-sensing devices based on various materials. Since the development of the first metal oxide gas sensors [1], several other research groups have been attempting to make improvements to gas sensors. And after that, metal oxide gas sensors have been marketed in the last 50 years. However, these sensors show low performance with respect to sensitivity and selectivity, and the metal oxide gas sensors are usually operated at a high temperature [2-5], generally working at a temperature between 200 and 400 ^{0}C. Subsequently, polymer was brought to build gas-sensing devices with the aim of enhancing the sensing performance, such as polypyrrole (PPy), polyaniline (PANI), and metaphthalocyanines, etc. Gas-sensing devices had high gas sensitivity at room temperature, whereas their responded long time due to the orderly structure hinders their usage [6, 7]. For the past several years, carbon nanotubes (CNT) have been considered for sensing materials that can detect gases such as NH_3, NO_2, H_2, O_2, CO, and CO_2 [8–15]. After that, graphene have been interested for gas-sensing devices because graphene has very high electron mobility at room temperature, and hence, its sensitivity is very high and important advantage is high surface area [16]. In this study, we have developed high-performance materials as gas sensors. Co_3O_4 and graphene materials were prepared by reduction in water with phenol hydrazine. The reduced materials were characterized by X-ray diffractometer (XRD), scanning electron Microscope (SEM), and Fourier transform Infrared Spectroscope (FT-IR). This present work compares graphene/Co_3O_4 with other three materials such as graphene, CNT, and CNT/Co_3O_4 used as gas sensing active layer. The sensitivity of four different materials was explored by detection of NH_3 at room temperature. The advantages of graphene/Co_3O_4 sensor are fast response time, short recovery time, low power consumption showing promising potential for using as NH_3 sensors.

2. Materials and Methods

2.1 Preparation of graphene

All chemical reagents were of analytical grade and used as received without further purification. 20 ml of graphene oxide aqueous dispersion (20 mg graphene oxide in 20 ml of distilled water) was then obtained by ultrasonication with an ultrasonic probe for 30 minutes. The graphene oxide dispersion was diluted to 80 ml with deionized water under magnetic stirring for 30 minutes. Next, 20 ml of phenol hydrazine was added to the above solution and the mixed solution was refluxed at 100 ^{0}C for 5 h. During this process, graphene oxide was reduced to graphene sheets. The resultant black precipitate was isolated by filtration, washed with deionized water and ethanol, and finally dried in an oven for 15 h.

2.2 Preparation of Co_3O_4

Co_3O_4 was prepared as follows: 100 mg of $CoCl_2 \cdot 6H_2O$ was mixed with a suspension of 0.2 g 1,10-phenanthroline (phen) in 20 mL of deionized water under magnetic stirring for 30 minutes. During this process, the coordination compound (phen) Co^{2+} was formed. After that, 20 mL of phenol hydrazine aqueous solution was

quickly added. The mixture turned black, indicating the reduction of (phen) Co^{2+} into phen-capped Co particles. The suspension was further stirred for 3 h before the Co particles were spun down in a centrifuge. The resultant black precipitate was mixed with NaCl (2 g) and KCl (3 g), heated at 700 °C for 1 h, cooled gradually to room temperature in air, washed several times with distilled water to remove the NaCl and KCl, filtered, and finally dried in an oven at 100 °C for 5 h.

2.3 Preparation of graphene/Co_3O_4 and CNT/Co_3O_4

Graphene/Co_3O_4 was prepared as follows: 20 mg of Graphene was mixed with 20 mg Co_3O_4. Then, the mixtures were crushed thoroughly. CNT/Co_3O_4 was prepared by the same method of graphene/Co_3O_4

2.4 Sensor fabrication

Sensor devices were fabricated by using a dispersion 10 mg of materials (graphene, graphene/Co_3O_4, CNT, CNT/ Co_3O_4) in 20 ml of dimethylformamide (DMF).The materials dispersion were prepared by sonicating in DMF for 1 h and were dropcasted onto PCB substrate. PCB substrate consists of interdigitated copper electrodes with a gap of 250 μm as shown in Figure 1. The initial resistance of sensor was adjusted to be 100 kΩ. After dropcasting, all sensor devices were heated at 120ºC for 1 min to remove the solvent.

2.5 Gas sensing measurement

NH_3 Sensing performance was evaluated in a sealed stainless chamber at room temperature. Two probe electrical conductivity measurements were performed. N_2 at a flow rate of 2.5 L/min was introduced into the chamber for purging and cleaning for 5 min. To expose NH_3 to sensor, N_2 with a flow rate of 1.5 L/min was used to carry NH_3 vapor.

3. Results and Discussion

3.1 Structure characterization

Figure 2. shows XRD pattern of the prepared Co_3O_4, graphene, and graphene/Co_3O_4. Well-defined diffraction peaks at around 19° (111) peak, 31° (220) peak, 37° (311) peak, 39° (222) peak, 45° (400) peak, 59° (511), peak and 64° (440) peak are indicative to sized Co_3O_4, which is in good agreement with the Joint Committee on Power Diffraction Standards (JCPDS) card 76-1802. Graphene material at around 27° (002) peak, and 42° (100) peak, as indicated in the XRD patterns.

Figure 3. shows SEM images of Co_3O_4, graphene, and Co_3O_4/graphene, respectively. As seen that the average grain sizes of Co_3O_4, graphene, and Co_3O_4/graphene were 1 μm, 1 μm, and 10 μm, respectively.

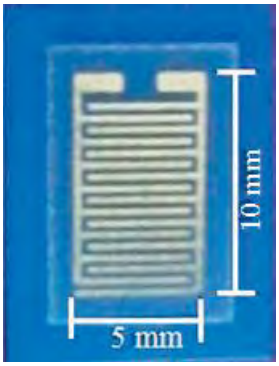

Figure 1. A photograph of interdigitated copper electrode-patterned substrate

3.2 Gas sensors performance

Figure 4. shows a photograph of interdigitated copper electrode-patterned substrate coating with sensing materials. Figure 5. shows NH_3 sensor response of CNT/Co_3O_4, CNT, graphene, and graphene/Co_3O_4 at room temperature with 35% NH_3 exposure, respectively. All sensors were sensitive to NH_3. The resistance of sensor increased after expose to NH_3 and reached to the saturated value in 360 s. The resistance suddenly decreased after switching to N_2 gas. The sensitivity increased from CNT/Co_3O_4, CNT, graphene, and graphene/Co_3O_4, respectively. The increase of resistance of the sensors when exposed to NH_3 may be due to the electron donating from NH_3 molecules on sensing, resulting the increase in resistance for p-type materials.

For CNT, the sensor recovered to the initial resistance within 5 min. However, graphene, and graphene/Co_3O_4, the recovery time was longer than 5 mins. This may due to the higher bonding energy between sensing materials with NH_3. Such results were also observed in previous publications [17, 18]

Next, the dependence of gas concentration of graphene and graphene/Co_3O_4 gas sensors was investigated. Figure 6 shows the relation of NH_3 concentration and resistance response. The resistance response linearly increased with an increase in the concentration range of 1–50 ppm NH_3 for graphene,

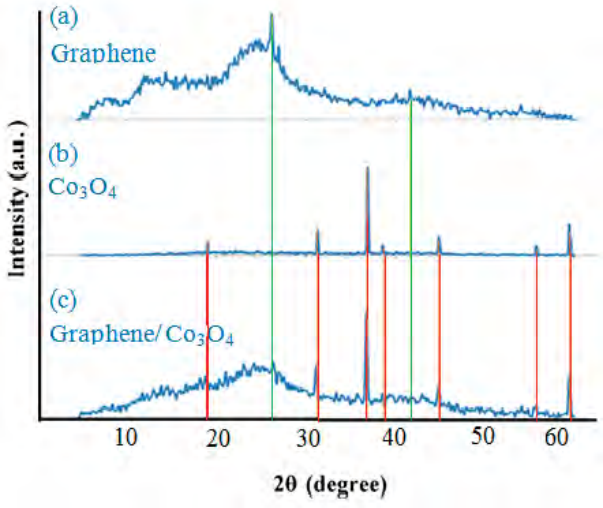

Figure 2. X-ray diffraction pattern of, (a) graphene, (b) Co_3O_4 and (c) graphene / Co_3O_4

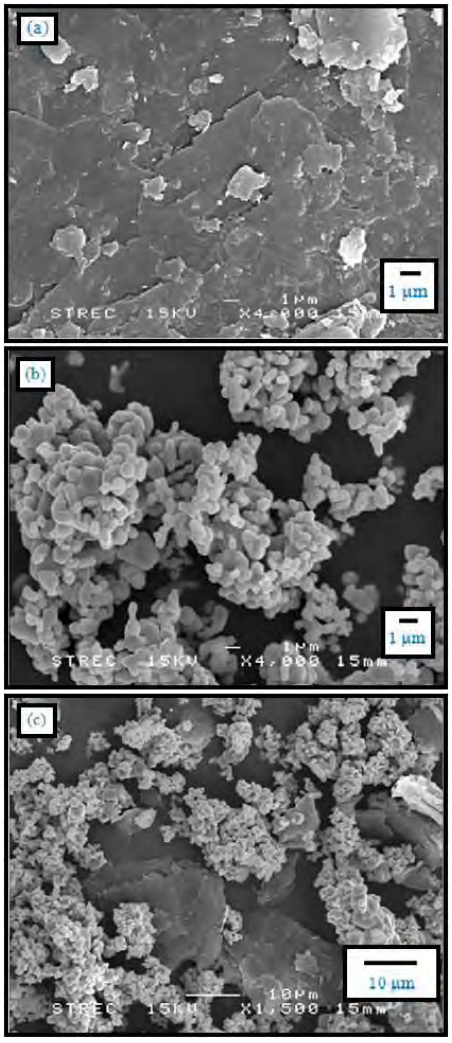

Figure 3. SEM images of (a) graphene, (b) cobalt oxide (Co_3O_4), and (C) graphene / Co_3O_4

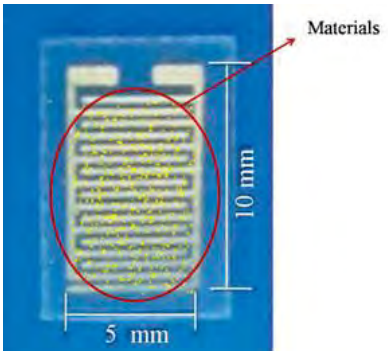

Figure 4. A photograph of interdigitated copper electrode-patterned substrate coating with sensing materials (graphene, graphene/Co_3O_4, CNT, CNT/ Co_3O_4)

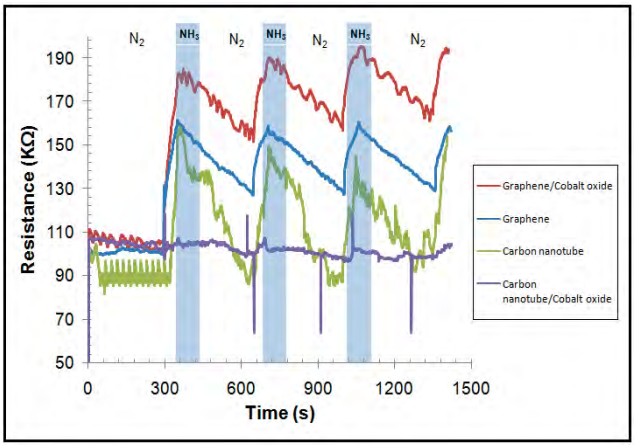

Figure 5. Sensor response of carbon nanotube/cobalt oxide (CNT/Co_3O_4), carbon nanotube (CNT), graphene, and graphene/Co_3O_4 gas sensors

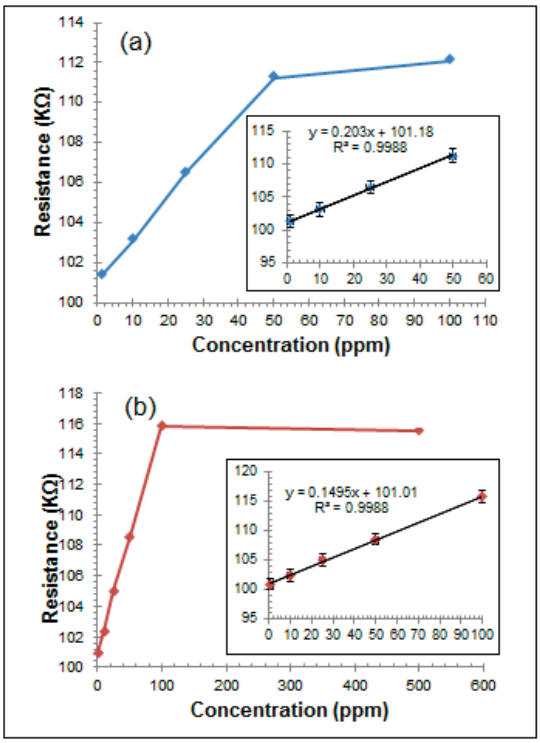

Figure 6. Relationship between sensor response and NH_3 concentration. (a) graphene and (b) graphene/Co_3O_4

and 1–100 ppm NH_3 for graphene/Co_3O_4, respectively. From above preliminary sensing responses to NH_3, graphene/Co_3O_4 afford the quantitative NH_3 detection. For a practical application, study on cross-sensitivity and interfering gases properties has been stringently required in the future.

4. Conclusions

In this study, with the purpose of developing high performance materials as gas sensors, report on a Co_3O_4 and graphene materials were prepared by reduction in water with phenol hydrazine. Co_3O_4 gas sensors are usually operated at a high temperature while graphene gas sensors are usually operated at a room temperature because very high electron mobility at room temperature, and hence, its sensitivity is very high and important advantage is high surface area. When graphene mixed with Co_3O_4 its sensitivity is very high and NH_3 can be detected at room temperature. This present work compares graphene/Co_3O_4 with other three materials such as graphene, CNT, and CNT/Co_3O_4. The sensitivity increased from CNT/Co_3O_4, CNT, graphene, and graphene/Co_3O_4. The graphene/Co_3O_4 shows significant resistance changes when exposed to various concentrations of NH_3 in air. The graphene/Co_3O_4 sensor has fast response time, and low power consumption.

Acknowledgements

This work was supported by Department of Analytical Chemistry, Faculty of Science, King Mongkut's Institute Technology Ladkrabang, Thailand and College of Nanotechnology, King Mongkut's Institute of Technology Ladkrabang, Thailand.

References

[1] T. Seiyama, A. Kato, K. Fujiishi, M. Nagatani, *Anal. Chem*. **34** (1962) 1502–103.

[2] C. Grimes, *Journal of Materials Chemistry* **17** (2007) 1451–1457.

[3] J. Tamaki, Y. Okochi, S. Konishi, *Electrochemistry (Tokyo, Jpn.)* **74** (2006)159–162.

[4] V.V.Plashnitsaa, V.Guptab, N.Miurac, *Electrochim. Acta* **55** (2010) 6941–6945.

[5] P.C. Xua, Z.X. Cheng, Q.Y. Pan, J.Q. Xu, Q. Xiang, W.J. Yu, Y.L. Chu, *Sens. Actuators B: Chem*. **130** (2008) 802–808.

[6] A.Z. Sadek, W. Wlodarski, K. Shin, R. Bkaner and K.K. Zadeh, *Nanotechnology* **17** (2006) 4488.

[7] S.S. Joshi, C.D. Lokhande and S.H. Han, *Sens. Actuators B*, **123** (2007) 240.

[8] P.G. Collins, K. Bradley, M. Ishigami, A. Zettl, Science **287** (2000) 1801–1804.

[9] J. Kong, M.G. Chapline, H. Dai, *Adv. Mater*. **13** (2001) 1384–1386.

[10] K.G. Ong, K.Zeng, C.A.Grimes, *IEEE Sens. J.* **2** (2002) 82–88.

[11] C. Cantalini, L. Valentini, L. Lozzi, I. Armentano, J.M. Kenny, S. Santucci, *Sens. Actuators B* **93** (2003) 333–337.

[12] S. Chopra, K. McGuire, N. Gothard, A.M. Rao, *Appl. Phys. Lett*. *83* (2003) 2280–2282.

[13] S.G. Wang, Q.Z. Zhang, D.J. Yang, P.J. Sellin, G.F. Zhong, *Mater.***13** (2004) 1327–1332.

[14] J. Suehiro, G. Zhou, H. Imakiire, W. Ding, M. Hara, *Sens. Actuators B* **108** (2005) 398–403.

[15] W. Wongwiiryapan, S. Honda, H. Konishi, T. Mizuta, T. Ikuno, T. Ito, T. Maekawa, K. Suzuki, H. Ishikawa, K. Oura and M. Katayama, *Jpn. J. Appl. Phys*. **44** (2005) L 482–L 484.

[16] F. Schedin, A.K. Geim, S.V. Morozov, D. Jiang, E.H. Hill, P. Blake, K.S. Novoselov, *Nat. Mater*. **6** (2007) 652–655.

[17] J. Li, Y. Lu, Q. Ye, M. Cinke, J. Han, M. Meyyappan, *Nano Lett*. **3** (2003) 929–933.

[18] E. Bekyarova, M. Davis, T. Burch, M.E. Itkis, B. Zhao, S. Sunshine, R.C. Haddon, *J. Phys. Chem. B* **108** (2004) 19717–19720.

HPLC ANALYSIS OF SECONDARY METABOLITES IN THE LICHEN *PARMOTREMA TINCTORUM* FROM DIFFERENT SUBSTRATES

Phiphatphong Thepnuan[1*], Chutima Sriviboon[1], Thitima Rukachaisirikul[1], Kansri Boonpragob[2]

[1] *Department of Chemistry, Faculty of Science, Ramkhamhaeng University, Bangkabi, Bangkok, 10240 Thailand.*

[2] *Department of Biology, Faculty of Science, Ramkhamhaeng University, Bangkapi, Bangkok, 10240 Thailand.*

[*] *E-mail: tungkhai2007@hotmail.com*

Abstract: The main secondary metabolites of the lichen *Parmotrema tinctorum* are orsellinic acid, methyl orsellinate, lecanoric acid and atranorin. These lichen substances could vary among habitats because different environmental stress. The purpose of this study was to develop an analytical technique to determine quantities of the lichen substances grew in different substrates. The lichen *Parmotrema tinctorum* were collected from rocks, barks of trees and nylons mesh, of which the latest was the transplanted lichens, from Khao Yai National Park. Pure substances were prepared by extracting lichen with acetone and purified by column chromatography to be used as standard substances for quantitative analysis. The chemical structures were confirmed by spectroscopic method. The analysis was performed by HPLC system of HP1100 binary pump and using hypersil C18 column (250 x 4.0 mm, 5 µm). The chromatographic conditions were investigated for analyzing each substance. It was found that the optimum HPLC condition for the analysis of oresllinic acid, methyl orsellinate and lecanoric acid consisted of gradient elution using methanol as solvent A, and 1% phosphoric acid as solvent B with UV detection at wavelength 265 nm. The optimum HPLC condition for the analysis of atranorin included isocratic elution using 82:18 of methanol: 1% phosphoric acid as mobile phase and UV detection at wavelength 254 nm. Analysis samples were prepared by extracting lichen with suitable solvent overnight at room temperature followed by filtration and evaporation to dryness. The residues were then dissolved by methanol in exact volume using benzoic acid as an internal standard. The solution samples were filtered through 0.45 µm syringe membrane before injection to HPLC. The amount of orsellinic acid, methyl orsellinate, lecanoric acid and atranorin in lichen samples collected from rocks, barks of host tree and nylons mesh were evaluated and compared.

1. Introduction

Lichens received special attention in recent years because of their ability to use as bioindicator of air pollution and production of secondary metabolites[1,2] which have potential to be used commercially. Lichen produces secondary metabolic products for auto-protection against adverse environment which vary among habitats. Some of the main compounds were produced for survival in extreme environments for example lecanoric acid, parietin, emodin, atranorin, gyrophoric acid, fumarprotocetraric acid, rhizocarpic acid, pulvinic dilactone and usnic acid, etc.[1,3]. The technique of high performance liquid chromatography (HPLC) is widely used for quantitative determination of secondary metabolites in lichen. Precise determination of lichen products is essential to enhance our understanding on production and roles of lichen novel products, which have extensive implication on sustainable utilization in several aspects.

The objective of this study were to prepare standard substances of orsellinic acid, methyl orsellinate, lecanoric acid and atranorin (Figure 1) by isolation and purification from lichen *Parmotrema tinctorum* and then quantify them from different substrates at Khao Yia National Park, which were rocks, barks of trees and nylons mesh. In order to evaluate and compare their substances on different substrate

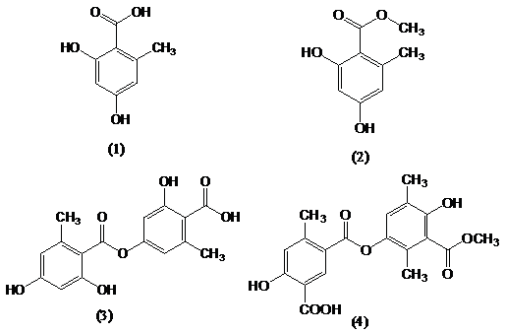

Figure 1. Chemical structures of lichen substances from *Parmotrema tinctorum*. Orsellinic acid (**1**), methyl orsellinate(**2**), lecanoric acid(**3**) and atranorin(**4**).

2. Materials and Methods

2.1 Chemicals and reagents

Methanol and acetone were HPLC grade, ortho-phosphoric acid, hexane, ethyl acetate, silica gel 60 (less than 0.063 mm) were analytical reagent grade and $CDCl_3$ and acetone-d_6 for NMR. All of them were bought from Merck.

2.2 Preparation of standard lichen substances

Standard lichen substances, orsellinic acid, methyl orsellinate, lecanoric acid and atranorin were prepared by extracting from lichen *Parmotrema tinctorum*. The crude extract was isolated and purified by column chromatography. The lichen substances were identified by spectroscopic technique. ^{1}H and ^{13}C NMR spectra of orsellinic acid methylorsellinate, lecanoric acid and atranorin were recorded in $CDCl_3$ or acetone-d_6 on a Bruker 400 UltraShield^{TM} (^{1}H:400 MHz,^{13}C:100MHz) then compared to those reported earlier[7,8].

Exactly 10.0 mg of each pure lichen substances, orsellinic acid, methyl orsellinate, lecanoric acid and atranorin were dissolved in 10 ml of methanol, They were used as stock standard solution for preparing standard calibration curve.

2.3 Samples preparation

Thalli of the lichen *Parmotrema tinctorum* were collected from different substrates which were rocks, barks of trees and nylons mesh in the same area at Khao Yia National Park. Five samples were collected each substrate. They were transferred to the analytical laboratory at the Chemistry Deparment, Ramkhamheang University. The samples were kept in air dried condition at room temperature and foreign debris on thallis were manually removed. Samples were ground into powder with liquid nitrogen using a ceramic mortar and pestle, and were then sieved through a 500 µm filter. The fine powder samples were kept frozen in refrigerator until analysis. A 10.0 mg of grounded samples were exactly weighted and extracted with 7 ml of pure methanol by soaking over night. The extract was then made to exact volume of 10 ml by DI water for analyzing orsellinic acid, methyl orsellinate and lecanoric acid. Another 10.0 mg of grounded samples were precisely weighed and extracted with acetone: dichloromethane (50:50) the extracted samples were filtered and evaporated to dryness. The residues were then dissolved by 70:30 of methanol: water in 10 ml, this solution was used to analyse atranorin. The solution samples were filtered through 0.45 µm syringe membrane before injection to HPLC. The analyses were three replicate and the results were average from three readings.

2.4 HPLC analysis

Lichen extracts were analyzed on a HP 1100 series consisting of HP G1312A binary pump, HP G1314A UV variable wavelength detector. Separation was achieved on an ODS Hypersil 250 x 4 mm I.D., 5 µm column. The analysis of orsellinic acid, methylorsellinate and lecanoric acid were used by gradient elution. The solvent A consisting of 1% phosphoric acid in water (pH = 2.3 - 2.7) and solvent B was 100% methanol. The run start with 35% B at flow rate 1.0 ml/min solvent B was increased to 100% within 20 min and hold for 5 min. At the end of run time, the post time was set to 10 min before a new run was started. The compounds were detected at wavelength 265 nm. The analysis of atranorin was used by isocratic elution with 82:18 (methanol: 1% phosphoric acid) at flow rate 1.0 ml/min using wavelength 254 nm. The identification of compounds was based on retention times and quantified by using external standard calibration curve.

2.5 Method validation

Linearity

Linearity of compounds were determination by using mixture of standard lichen substances in the following range: orsellinic acid and methyl orsellinate were in 1-16 µg/ml, lecanoric acid was in 100-500 µg/ml and atranorin was in 5-25 µg/ml. The calibration curves were obtained by plotting the peak area versus the concentration of the standard solutions. The linearity of calibration curve is defined in term correlation coefficient (r^2) as shown in Table1.

Limit of detection (LOD) and limit of quantification (LOQ)

The LOD of each lichen substances were calculated from equations:

$$\mathrm{LOD} = \frac{3S_{y/x}}{b}$$

Whereas b is slope and $S_{y/x}$ is standard deviation of calibration curve calculated from

$$S_{y/x} = \left\{ \frac{\sum_i (y_i - \hat{y}_i)^2}{n-2} \right\}^{\frac{1}{2}}$$

The LOQ of each lichen substances were calculated by 10 time of $S_{y/x}$. The results of LOD and LOQ of orsellinic acid, methyl orsellinate, lecanoric acid and atranorin are shown in Table 1.

Precision

The precision was determined by seven replicates of analyses of lichen extract solution. The precision was expressed in percentage of relative standard deviation (%RSD) as shown in Table 2.

Accuracy

The accuracy of the method was tested by added (spiked) a known amount of standard lichen substances into lichen sample. Three different concentration of the standard solution of orsellinic acid (2, 4 and 6 µg/ml), methyl orsellinate (2, 4 and 6 µg/ml) lecanoric acid (5, 10 and 15 µg/ml), and atranorin (5, 10 and 15µg/ml) were added to the lichen extract solution and analyzed by the proposed HPLC method. The recovery was determined by subtraction the concentration of lichen sample from spiked lichen sample. The results are shown in Table 3.

Table1. Linearity (r^2), limit of detection (LOD) and limit of quantification (LOQ) of secondary metabolites of the lichen *Parmotrema tinctorum*

Compounds	Concentration range (µg/ml)	Linearity (r^2)	LOD (µg/ml)	LOQ (µg/ml)
orsellinic acid	1 - 16	0.9995	0.23	0.77
methyl orsellinate	1 - 16	0.9996	0.19	0.65
lecanoric acid	100 - 500	0.9992	0.68	2.28
atranorin	5 - 25	0.9993	0.14	0.47

Table 2. Precision data of amount and retention time of secondary metabolites of the lichen *Parmotrema tinctorum* (N=7)

Compounds	Amount of substances (mg/g)		Retention time	
	$\bar{x}$ ± SD	%RSD	$\bar{x}$ ± SD	%RSD
orsellinic acid	10.36 ± 0.02	0.19	6.33 ± 0.07	1.11
methyl orsellinate	15.71 ± 0.01	0.06	10.74 ± 0.07	0.65
lecanoric acid	330.24 ± 0.26	0.08	12.74 ±0.07	0.55
atranorin	13.14 ± 0.03	0.23	5.31 ± 0.02	0.38

Table 3. Accuracy/recovery data of secondary metabolites of the lichen *Parmotrema tinctorum*

Level	% Recovery ± SD			
	Orsellinic acid	Methyl orsellinate	Lecanoric acid	Atranorin
1	99.03 ± 2.92	100.35 ± 0.53	99.10 ± 1.60	102.68 ± 1.41
2	99.03 ± 2.41	99.61 ± 2.61	98.97 ± 2.67	102.26 ± 0.93
3	98.49 ± 0.65	99.84 ± 1.15	98.38 ± 1.14	99.39 ± 0.21

3. Results and Discussion

The suitable solvent for complete extraction of orsellinic acid, methyl orsellinate and lecanoric acid from *lichen Parmotrema tinctorum* is methanol whereas acetone:dichloromethane (50:50) is suitable for atranorin. Quantitative analysis was achieved by using reversed-phase high-performance liquid chromatography, gradient elution was used for separation and quantify of orsellinic acid, methyl orsellinate and lecanoric acid where as isocratic elution was used for quantify of atranorin. The chromatograms of secondary metabolites of lichen *Parmotrema tinctorum* are shown in Figure 2.

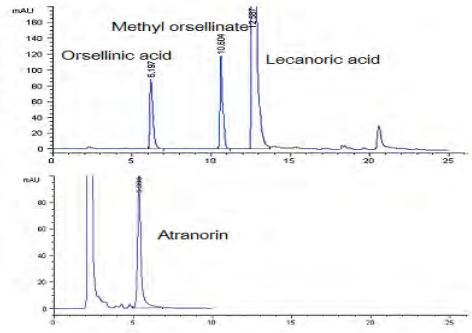

Figure 2. The HPLC chromatogram of orsellinic acid, methyl orsellinate, lecanoric acid and atranorin.

Method validation in terms of detection limit, linearity, accuracy/recovery and precision are shown in tables 1-3. It shows that the HPLC methods are efficient analytical techniques for determination secondary metabolites in the lichen *Parmotrema tinctorum*.

The amount of secondary metabolites of the lichen *Parmotrema tinctorum* from different substrates are shown in Table 4. The average amount from five sites of orsellinic acid, methyl orsellinate, lecanoric acid and atranorin in lichen on the nylon mesh were 6.3 ± 0.7, 2.5 ± 0.3, 394.6 ± 31.1 and 17.2 ± 8.0 mg/g, respectively. Those on bark of host tree were 6.7 ± 1.9, 1.9 ± 0.1, 376.9 ± 13.5 and 11.8 ± 1.8 mg/g, respectively. On rock were 7.0 ± 1.3, 2.5 ± 0.5, 387.4 ± 75.9 and 9.8 ± 2.1 mg/g, respectively. Figure 3 showed the comparison of the average amounts of these lichen substances from three substrates. The results show that atranorin has higher variation among substrate where as the other substances were not significantly differences. Sunlight could affect the amounts of atranorin [9]. Lichens grown on nylon mesh at different aspect orientation had the highest variation of atranorin, because they received different light intensity. By contrast those grew on tree and rock had less variations of this substance.

Table 4. Amount of orsellinic acid, methyl orsellinate, lecanoric acid and atranorin of the lichen *Parmotrema tinctorum* from different substrate

	Amount of orsellinic acid (mg/g)on substrate			Amount of methylorsellinate (mg /g) on substrate		
Site	Nylon	Tree	Rock	Nylon	Tree	Rock
1	6.9	5.9	5.9	2.1	2.0	2.6
2	6.8	8.0	5.8	2.6	1.8	2.5
3	5.2	5.2	8.3	2.2	1.9	2.8
4	6.5	9.4	6.5	2.6	2.1	2.9
5	6.3	4.9	8.4	2.9	1.9	1.6
mean	6.3	6.7	7.0	2.5	1.9	2.5
SD	0.7	1.9	1.3	0.3	0.1	0.5
CV	10.7	29.1	18.3	13.2	5.9	20.8

	Amount of lecanoric acid (mg /g) on substrate			Amount of atranorin (mg /g) on substrate		
Site	Nylon	Tree	Rock	Nylon	Tree	Rock
1	352.0	379.7	424.9	7.9	9.9	11.1
2	413.5	357.6	411.9	16.5	11.9	12.3
3	373.8	381.9	403.0	15.0	12.2	6.8
4	405.3	393.9	442.8	16.7	14.5	9.6
5	428.5	371.2	254.2	30.0	10.7	9.1
mean	394.6	376.9	387.4	17.2	11.8	9.8
SD	31.1	13.5	75.9	8.0	1.8	2.1
CV	7.9	3.6	19.6	46.4	14.8	21.4

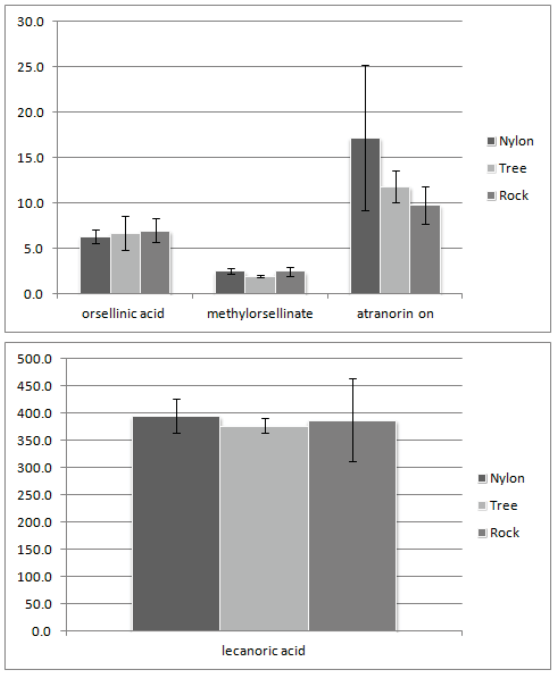

Figure 3. Comparing the amounts of orsellinic acid, methyl orsellinate, lecanoric acid and atranorin from different substrates.

4. Conclusions

The amount of four secondary metabolites, orsellinic acid, methyl orsellinate, lecanoric acid and atranorin were quantified by using external standard calibration curve of HPLC technique. The standard substances were prepared by extracting and purifying from the lichen *Parmotrema tinctorum*. The results showed that the amounts of secondary metabolites from Nylon mesh, bark of host tree and rock from the same locality did not significantly differences. It can be concluded that lichens inhabited different substrates of the same locality, exposed to similar environmental factors, produced comparable amounts of secondary metabolites.

Acknowledgements

Thank to Lichen Research Unit, Department of Biology and Department of Chemistry Ramkhamhaeng University, Bangkok, Thailand for supporting lichen samples , instrument and chemical reagents. Spectial gratitude goes to Khao Yai National Park under the department of National Parks, Wildlife and Plant Conservation, Ministry of Natural Resources and Environment of Thailand.

References

[1] C. Plinio Cesar Pinto, P. Marcelo Marcelli, F. Hello Dos Santos and G.M. Howell Edwards. *Journal of Molecular Structure*. (2009) 128-133.
[2] D.Bialonska and F.E. Dayan. *Journal of Chemical Ecology*. **31** (2005) 2975-2991.
[3] H.G.M. Edwards, E.M. Newton, D.D. Wynn-Williams and S.R. Combes. *Journal of Molecular Structure*. **648** (2003) 49.
[4] H.G.M. Edwards, E.M. Newton, D.D. Wynn-Williams and S.R. Combes. *Journal of Molecular Structure*. **36** (2003) 27.
[5] G.K. Jayaprakasha, L. Jaganmohan Rao, R.P. Singh and K.K. Sakariah, *Journal of Chromatographic Science*, **36** (1998)
[6] J.L. Ramaut, M. Brouers, E. Serusiaux and M. Corvisier, *Journal of Chromatography*, **155** (1978) 450-453.
[7] I. B. L.Thiago, G. C. Roberta, C. Y. Nídia and K. H. Neli *Chemical & Pharmaceutical Bulletin Instructions for Authors*. **56(11)** (2008) 1551-1554.
[8] T. L. P. P.Marize, M. M.Ana, F.Odival, T.G. Alcir and K. H. Neli, *Brazilian Archives of Biology and Technology*, **52** (2009) 1019-1026.
[9] M.D. Begora and D. Fahselt, *The Bryologist*, **104(1)** (2001) 134-140.

DISCRIMINATION OF THE GEOGRAPHICAL ORIGIN OF THAI CHILI PEPPERS (*CAPSICUM ANNUUM L.*) USING CHROMATOGRAPHIC AND SPECTROSCOPIC PROFILES COMBINED WITH CHEMOMETRIC TECHNIQUES

Worraluck Meemak[1], Kanet Wongravee[2], Soparat Yudthavorasit[1], Natchanun Leepipatpiboon[1*]

[1] Chromatography and Separation Research Unit, Department of Chemistry, Faculty of Science, Chulalongkorn University, Patumwan, Bangkok10330, Thailand
[2] Sensor Research Unit, Department of Chemistry, Faculty of Science, Chulalongkorn University, Patumwan, Bangkok, 10330, Thailand

*E-mail: natchanun.l@chula.ac.th

Abstract: In Thailand, chili peppers (*Capsicum annuum L.*) are commonly well-grown in almost every region of the country. It is also regarded as a high-value commodity in Thailand. Due to a large diversity of variety and region of origin, traceability of chili peppers has been a challenge. Food traceability is important for the protection of consumer rights and to prevent fraudulent and deceptive practices. In this research, the total composition of chili peppers, capsaicinoids, volatile compounds and total phenolic content (TPC) which is a potent part of antioxidants agents were all qualitatively and quantitatively analyzed using HPLC-DAD, GC-MS and UV-visible spectroscopy, respectively. Three chemometric methods principal component analysis (PCA), cluster analysis (CA), and linear discriminant analysis (LDA) were used in the discrimination of ripe chili peppers fromSrisaket, Prachuapkhirikhan, Nakhonsawan, Chiangmai, Ubonratchathani, and Kamphaengphet. The contents of capsaicin and dihydrocapsaicin arethe main source of spicy heat ranged from 1.35 – 3.10g/kg and 0.52 - 1.06 g/kg dry weight, respectively. Nineteen chemical compounds were determined as the major volatile compounds of chilli peppers and the amount of TPC varied between 2.07 and 2.75 mg gallic acid/100 g FW. The combination of PCA, CA, and LDA were subsequently utilized. CA can be clearly differentiated the origins of chili at distance 0.3. In PC score plot, the six groups of chilli peppers were established and strongly clustered according to their origins.Original group of samples can be predicted with 100% correction by cross-validated LDA. We were successful in the identification of unique characteristic patterns of chili peppers from different regions.

1. Introduction

Chili peppers (*Capsicum annuum L.*) are a popular and important ingredient of Thai and worldwide cooking because of their unique aroma and spiciness [1]. Chili pepers are commonly used for cooking in households, and as a feedstock in industry, because they are an excellent source of vitamin A, B, C, E and contain a range of essential minerals. Furthermore, chili peppers have extensive application in disease prevention and health promotion; the pharmaceuticals industries use them for their anti-bacterial, anti-carcinogenic, analgesic and anti-diabetic properties.The unique aroma of the chili pepper arises from its volatile components, and its characteristic pungency is mainly a result of its capsaicinoid content, of which capsaicin and dihydrocapsaicin are the major components. The total phenolic content (TPC) represents a group of potent antioxidants that are present in chili pepper.

Only a few reports of the characterization of various commodities [2-4] have described the combination of analytical techniques with chemometric methods, such as principal component analysis (PCA), cluster analysis (CA), and linear discriminant analysis (LDA) to statistically classify the sources of large amount quantities of samples. The commodities investigated by these studies are all economically important crops to their countries of origin.

In Thailand, where large quantities of a diverse range of peppers are consumed, chili is a commercially important spice. For food traceability and authenticity issues, it is necessary to characterize chili products to confirm their original source. This is important for ensuring food safety, and for protecting consumers from food fraud. Thus, the objective of this studywas to discriminate the geographical origin of chili peppers by using chromatography and spectroscopic methods to separate and analyze capsaicinoids, volatile compounds, and TPC components of chili pepers. Multivariate techniques such as PCA, CA, and LDA were applied to the analytical data to monitor chili pepper profiles and construct a mathematical model to aid the identification of the origins of chili peper samples.

2. Materials and Methods

2.1 Samples and chemicals

Sample: fresh mature chilli peppers from six provinces (Sisaket, Prachuapkhirikhan, Nakhonsawan, Chiangmai, Ubonratchathani, and Kamphaengphet) were purchased fromTaladthai market in Thailand. After purchase, samples were stored in polyethylene bags at 4°c until required for analysis.

Chemical: Natural capsaicinoids standard, Folin &Ciocalteu's phenol reagent, and gallic acid were purchased from Sigma-Aldrich (St. Louis, MO, USA). High pure water (Milli Q gradient) and Methanol (HPLC-grade) was purchased from Merck (Darmstadt,

Germany). Anhydrous sodium carbonate (Na_2CO_3) was purchased Riedel-de Haën (Hanover, Germany).

2.2 Analysis of capsaicin and dihydrocapsaicin

Fresh chilli peppers were dried in an oven at 60°c for 2 d, and then homogenized to fine powder using a blender. For extraction, samples (0.5 g) were weighed accurately into test tubes and then extracted by sonication with methanol (10 ml) for 1 h at room temperature. Each sample solution was then filtered through a 0.45 µm PTFE membrane filter before HPLC analysis. HPLC analyses of chili peppers extract were performed using an Agilent series 1100 HPLC system equipped with an Eclipse plus C18 column (4.6×100 mm, 3.5 µm). The mobile phase (isocratic system) was a 30:70 water:methanol mix, at a flow rate of 1 ml/min. Absorbances were recorded at 280 nm. The injection volume was 5µl, and the total run time was30 min.

2.3 Volatile compounds analysis

Homogenized fresh chilli pepper samples (3.0 g) were placed into a headspace vial for headspace-GC-MS analysis. Determination of volatile compounds was performed on a headspace-GC-MS system (Agilent HP 6890 Series gas chromatography (GC) system with 5973 Mass selective Detector). Volatile compound analysis was performed using a headspace autosampler, at an oven temperature of 60°Cand transferline temperatureof110°C.Volatile compound were separated using a GC capillary column (DB-624, 25m × 0.2 mm id × 1.12 µm, J&W Scientific, Folsom,CA, USA).The oven temperature was held at 40°C for 3 min, then increased to 240°C at a rate of 4°C min^{-1} and held at 240°C for 15 min. The carrier gas was helium at a flow rate of 1 mL/min. The detector was operated in electron impact mode (70 eV) at 230 °C. Chemical constituents were identified by comparison of their mass spectra with the NIST library database.

2.4 Total phenolic content analysis

Fresh chilli peppers were homogenized using a blender. Samples (1 g) were extracted with methanol (10 ml) and then centrifuged at 5000 rpm for 15 min. The methanolic extract (125 µl) was diluted with Milli Q water (375 µl) in a test tube, and 10 % Folin-Ciocalteu reagent (2.5 ml) was then added. After 6 min mixing using a vortex, 2 ml of 7.5% $Na_2CO_3$was added, and the mixture stood for 90 min at room temperature in darkness. Absorbance was measured at 760 nm using a Spectrophotometer (HP/Agilent 8453 UV-Vis spectrophotometer). Gallic acid was used the references tandard. The results are expressed as milligrams of gallic acid equivalent / 100 g FW (GAE/100 g FW).

2.5 Chemometric technique

Principal component analysis (PCA) is a useful exploratory analysis when the data were obtained from a large number of variables. The data matrices should be reduced by transform the multivariate profiles into a a new coordinate system called "Principal Components" (PCs). PCs are calculatedas linear combinations of the variables that account for most of variance in the data. Cluster analysis (CA) is another unsupervised pattern recognition method that rearrangesthe data intoclusters.The distance, which represents the dissimilarity, between all pairs of objects are calculated. To be illustrated, the catagory of samples is visualized by dendrogram plot. The objects with smaller distances are clustered in the same group, whereas objects with larger distance are clusterd in another group. Linear discriminant analysis (LDA) is a supervised pattern recognition that constructs the classification model to predict the origin of an unknown sample. LDA performs dimensionality reduction while preserving as much of the class discriminatory information as possible.Group of the sample is determined by seeking the classes with the smallest distance. In the study, the leave-one-out cross validation is performed to validate the model performance. This technique is very useful when many samples and several groups are involved [5].

3. Resultsand Discussion

3.1 Determination of chili peppers

Capsaicin and dihydrocapsaicin are effectively separated by HPLC, with retention times of 3.45 and 6.79 min, respectively. (Fig. 1). Among the various chili pepper samples, the Ubonratchathani sample has the greatest capsaicin and dihydrocapsaicin content, followed in order of decreasing concentration by samples from Kamphaengphet,Sisaket, Nakhonsawan, Prachuapkhirikhan, and Chiangmai. Table 1 shows the quantitative HPLC data.

The volatile compounds (VOCs) in chili peppers were analyzed using HS-GC-MS. VOCs were identified by comparing the MS spectrum with the NIST library database.We identified 16 VOCs as the main volatile components of the chili pepper samples were determined. Table 1 shows that the Chiangmai sample has the greatest total phenolic content, followed in order of decreasing content by Ubonratchathani, Sisaket, Nakhonsawan, Kamphaengphet, and Prachuapkhirikhan.

The measured total phenolic contents are shown in Table 1. The data presented in Table 1 are further discriminated by geographical origin using chemometric methods (PCA, CA andLDA).

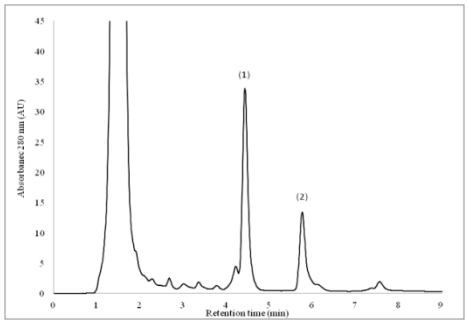

Figure 1. Representative chromatogram of (1) capsaicin and dihydrocapsaicin (2) in chilli pepper.

3.2 Discrimination of the geographical origin of Thai chili peppers

The raw data presented in Table 1was normalized to present numerical data from many experiments on the same scale, and thus facilitate comparisons. In Fig. 2, Pre-processing stage outputs are grouped by chemometric technique; the PCA results in Fig. 2 are shown as score and loading plots. The score plot (Fig. 2a) emphasises relationships between samples, while the loading plot shows the relationship among variables. Two principle components were sufficient to account for 72.16% of the total variance for score and loading plot. PC1 and PC2 have a variance of 47.84% in the X-axis and 24.32%in the Y-axis, respectively. Score plot (Fig 2a) shows the clear differentiation of 6 origins by forming 6 groups of samples from Srisaket, Prachuapkhirikhan, Nakhonsawan, Chiangmai, Ubonratchathani, and Kamphaengphet. The loading plot (Fig. 2b) expresses the relationships between nineteen variables. The association between variables and the chilli samples could be visualized by relating the data score and loading plot for each location. For example, Fig. 2(b) shows how the Prachuapkhirikhanchili sample was effectively characterized by its high hexanal and (E)-hex-2enal contents, indicating that these compounds could be used as marker to identify Prachuapkhirikhan chili peppers among samples from other regions.

Moreover, the Kamphaengphetchilli samples exhibit characteristically high level of ethanol and 3-pentanonethat allowed their identification from the panel of six samples. The Ubonratchathanichili samples are characterized by high ethene, pentanal, 2-propenyl ester, 4-Methyl-1-pentanol, Hexyl 2-methylpropanoate, Hexyl 2-methylbutanoate, Hexyl 3-methylbutanoate and dihydrocapsaicin. The analyte concentrations of chili peppers from Sisaket, Nakhonsawan and Chiangmai showed moderate associations to the samples' regions of origin. The CA results show similarities in the data in the form of a dendrogram (Fig.3). In the figure, the X-axis represents the number of samples, while the Y-axis represents the Euclidean distance. The dendrogram illustrate that the samples could be categorized into 6 groups of origin at the distance of 0.3 which are in agreement with the result of PCA.

LDA constructed a classification model for predicting the origin of chilli peppersfrom raw data and leave-one-out cross validation was performed in order to validate the generated model. It was found that chili peppers from six origins were 100 %correctly classified. This indicates a prediction abilityof the model for determining geographical origin of an unknown.

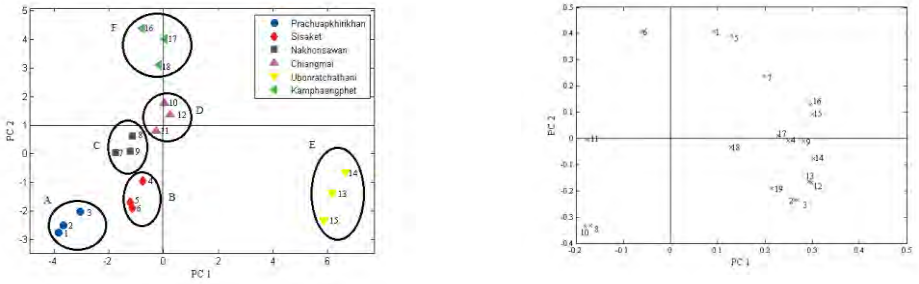

(1) (2)

Figure 2. Principal component analysis (1) score plot and for chili peppers and (2) loading plot for variables

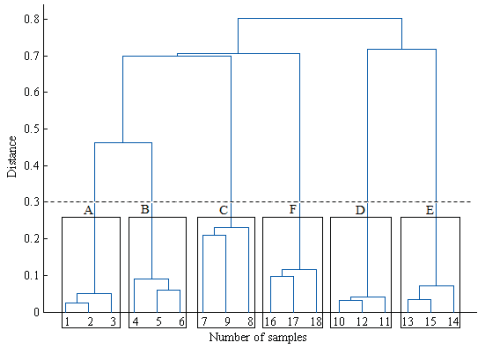

(3)

Figure 3. Dendrogram of cluster analysis of chilli peppers of six origins. (A: Prachuapkririkhan, B: Sisaket, C: Nakhonsawan, D: Chaingmai, E: Ubonratchathani, F: Kamphaengphet)

Table 1: The amount of volatile compounds, capsaicin, dihydrocapsaicin and total phenolic content in chilli pepper of different origins.

No.	Compounds	Prachuapkhirikhan	Sisaket	Nakhonsawan	Chiangmai	Ubonratchathani	Kamphaengphet
1	Ethanol	675018.70	1394509.00	2305220.00	2007400.00	2005598.00	3450797.00
2	Ethene	42923.33	60426.67	50033.00	55954.33	102612.00	24759.33
3	Pentanal	49744.00	69472.67	59609.67	56255.67	102754.00	37559.33
4	Formic acid (2-propenyl ester)	19980.67	0	26423.00	29814.00	51930.33	19359.67
5	Prop-2-yn-1-ol	30119.67	43308.00	43777.00	50700.33	46842.00	58202.33
6	Pentan-3-one	49308.67	48805.00	56503.67	53222.33	44029.00	86952.00
7	2-Methyl-3-vinyl-oxirane	18300.33	21853.67	16484.00	25038.00	66067.67	80158.33
8	Hexanal	182740.00	168801.70	53466.67	19740.33	46388.00	29749.00
9	4-Methyl-1-pentanol	61680.33	48257.00	27754.33	73080.33	135822.30	78821.67
10	(E)-hex-2-enal	1104601.00	729596.70	311634.30	121520.00	260183.00	167407.70
11	(E)-hex-2-en -1-ol	475138.30	234308.70	217341.70	224949.00	213016.00	375675.30
12	Hexyl 2-methylpropanoate	21852.67	33274.33	20512.33	11057.67	167359.30	16101.67
13	Hexyl 2-methylbutanoate	73142.67	125456.30	72860.67	31493.00	378456.00	85826.33
14	Hexyl 3-methylbutanoate	22375.33	34408.67	22258.33	65524.00	104310.00	25873.33
15	6-ethyl-2-methyldecane	29510.33	40760.33	29823.00	44719.67	64513.67	50061.33
16	1-(6-nitro-1,3-benzodioxol-5-yl)-N-phenethylmethanimine	0	39552.33	25595.00	37342.67	71330.33	48706.67
17	Total Phenolic content (GAE/100 g FW).	2.25	2.36	2.32	2.75	2.69	2.32
18	Capsaicin (mg/kg dry weight)	2251.40	2785.06	2621.02	1357.39	3099.23	2916.17
19	Dihydrocapsaicin (mg/kg dry weight)	699.02	852.43	821.86	527.36	1057.48	722.67

4. Conclusions

The capsaicin, dihydrocapsaicin, volatile compounds, and total phenolic content of chili peppers vary according a growing plant's location. Thus, PCA, CA, and LDA chemometric techniques can be used to assign a chili sample's profile for these compounds to a particular geographical origin.The proposed methods is highly efficient ,and produces reliable data.

Acknowledgements

This work was partially supported by the Higher Education Research Promotion and National Research University Project of Thailand, Office of the Higher Education Commission (FW 0648I)

References

[1] L. Liu, X. chen, J. Liu, X. Deng, W. Duan and S. Tan, *Food Chem.* **119** (2010) 1228-1232.
[2] I.J. Misiak, A. Poliwoda, M. Deren and P. Kafarski, *Food Chem.* **131** (2012) 1149-1156.
[3] C. Karadas and D. Kara, *Food Chem.* **130** (2012) 196-202.
[4] O. Youssef, F. Guido, I. Manel, N.B. Youssef, C.P. Luigi, H. Mohamed, D.Daoud and Z. Mokhtar, *Food Chem.* **124** (2011) 1770-1776.
[5] A. Patras, N.P. Brunton, G. Drowney, A. Rawson, K. Warriner and G. Gernigon, *J. Food Compos. Anal.* **24** (2011) 250-256

QUANTITIES OF SECONDARY METABOLITES FROM THE LICHEN *PARMOTREMA TINCTORUM* BEFORE AND AFTER TRANSPLANTED TO POLLUTED AREAS IN BANGKOK, THAILAND

Chutima Sriviboon[1]*, Tawatchai Sriviboon[1], Chaiwat Boonpeng[2], Prichukorn Khongsatra[1] and Kansri Boonpragob[2]

[1]*Department of Chemistry, Faculty of science, Ramkhamhaeng University, Bangkok, 1024 Thailand*
[2]*Department of Biology, Faculty of Science, Ramkhamhaeng University, ,Bangkok ,10240 Thailand*

*E-mail: s_chutima@ru.ac.th, Tel. +66 23108403, Fax +66 23108401

Abstract: The amounts of secondary metabolic products from the lichen *Parmotrema tinctorum* before and after transplanted from Khao Yai National Park to nine public parks in Bangkok, Thailand, were analyzed by using HPLC method. Lichen substances were isolated through Hypersil C18 column (250 mm x 4.0 mm, 5 μm) under gradient elution and UV detection at λ 254 nm using methanol and 1% phosphoric acid as mobile phases. Lichen samples before and after transplantation were ground in liquid nitrogen and extracted by acetone. Benzoic acid was used as internal standards to control HPLC system. The lichen compounds including orsellinic acid, methyl orsellinate, lecanoric acid, atranorin and chloroatranorin were quantified by using peak area for comparing the amount before and after transplantation. Transplantation period was 7 months lasted from 19 September 2010 to 20 April 2011. The average peak area of orsellinic acid, methyl orsellinate, lecanoric acid, atranorin and chloroatranorin before transplantation were 657.6±179.5, 47.6±17.5, 17140.7±1219.0, 1465.8±101.9, and 266.6±39.2, respectively. After transplantation these amounts were 753.3±265.1, 34.8±22.7, 11066.5±1679.9, 1502.5±161.0 and 271.0±43.5, respectively. By using Paired Samples T-Test, the amounts of lichen substances before and after transplanted to polluted sites are compared. The results revealed that lecanoric acid was significantly decreased after transplanted (P < 0.05), whereas the other substances were not different statistically.

1. Introduction

Lichens contain a great number of organic compounds including primary and secondary metabolites [1,2]. Secondary metabolic products were produced from biochemical pathways known as lichen substances [3]. They provide protective roles against adverse environment and vary as a result of environmental stress [4]. Many hypotheses concerning their biological role have been proposed [5-7]. The lichen *Parmotrema tinctorum* is a widely distributed species globally. It produces polyphenolic lichen acid such as orsellinic acid, methyl orsellinate, lecanoric acid, and atranorin which commonly occurs with chloroatranorin [8,9]. Their structure are shown in figure 1. Lecanoric acid is the main–product of the lichen *Parmotrema tinctorum* which has an important role in modern medicine. It has inhibitory function of histamine decarboxylase, potential agent against allergy, microcirculatory hemostasis, gastric secretion, inflammation and some neutral functions [10]

The objective of this study was to compare the amount of secondary metabolic products of lichen *Parmotrema tinctorum* before and after transplantation from Khao Yai National Park to nine public parks in Bangkok, Thailand.

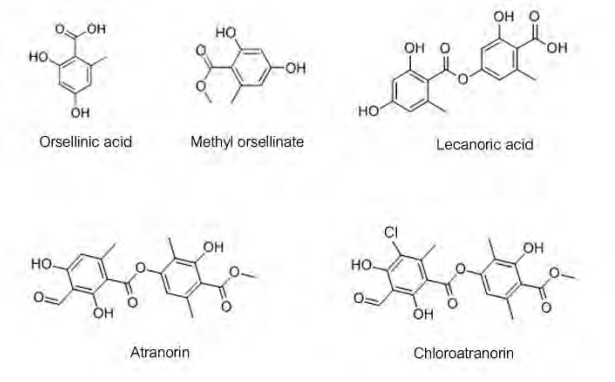

Figure 1. The structures of five secondary metabolic products from lichen *Parmotrema tinctorum*

2. Materials and Methods

2.1 Chemicals and reagents

All chemicals are analytical grade except methanol is HPLC grade from Merck. Deionized water (DI) with specific resistance > 18.0 MΩ-cm was prepared by an Easy Pure RF Compact ultrapure water system from Barnstead, was used for preparation 1% phosphoric acid as mobile phase A.

2.2 Lichen samples

This experiment quantified the amount of secondary metabolites in the lichen *Parmotrema tinctorum* before and after transplanted to public parks in Bangkok known as polluted areas. The thalli of *Parmotrema tinctorum* were collected and then exposed to ambient air at the lichen's camp at KaoYai National Park before fixing on 40 x 50 cm plastic nets Five nets were left at KhaoYai National Park as control lichen (CL). The others were brought to nine public parks in Bangkok and attached on trees as show in figure 2. Five plastic nets, with fixed lichens, were placed in each public parks. The nine public parks

were described by Polyium, et al., 2009 [11] which included: (1) Thawiwanarom (TW), (2) Thonburirom (TR), (3) Lumphini (LN), (4) Suanluang Rama IX (R9), (5) Nong Chok (NC), (6) Phra Nakhon (PK), (7) Santiphap (SP), (8) Seri Thai (ST), (9) Rommani Thongsikan (RT). The transplanted period lasted for 7 months from 19/9/2010 to 20/4/2011. The lichen samples were brought to analysis at the laboratory of Chemistry Department, Ramkhamhaeng University.

Figure 2. The lichen *Parmotrema tinctorum* on plastic nets were transplanted to public parks in Bangkok.

2.3 Samples preparation

Lichen samples were air-dry at room temperature for two days. Foreign debris on thalli were manually removed. Samples were ground into powder with liquid nitrogen using a ceramic mortar and pestle, and were then sieved through a 500 µm filter. The fine powder samples were kept frozen in refrigerator before analysis. A 10 mg of grounded lichen samples was accurately weighed and extracted with acetone by soaking overnight. The extracted samples were filtered and evaporated to dryness. The residues were then dissolved by small amount of methanol and diluted to exact volume by 70:30 of methanol : water using benzoic acid as an internal standard. The sample solutions were filtered through 0.45 µm syringe membrane before injection to HPLC. The analysis include three replicate and the average was taken from two or three readings that had similar values. Quality control of the analytical procedure was carried out by analyzing the same procedure.

2.4 HPLC analysis

Lichen extracts were analyzed by a HP 1100 series consisting of HP G1312A binary pump, HP G1314A UV variable wavelength detector. Separation was achieved on an ODS Hypersil 250 x 4 mm I.D., 5 µm column. The solvent A consisted of 1% phosphoric acid in water (pH = 2.3-2.7) and solvent (B) was 100 % methanol. The run start with 30% B at flow rate 0.7 ml/min solvent B was increased to 70% within 14 min, then up to 100 % in 30 min. The programmed run was modified from G.B. Feige [12]. At the end of the run time, the post time was set to 10 min before a new run was started. The compounds were detected at wavelength 254 nm and the identification of compounds were based on retention times. .

3. Results and Discussion

The chromatogram of the lichen *P. tinctorum* was shown in figure 3. The order of retention times were orsellinic acid, benzoic acid, methyl orsellinate, lecanoric acid, atranorin and chloroatranorin. The precision values of retention times and peak areas of compounds were analyzed from seven replicates as shown in table 1. The results showed that %RSD were less than 5%. Since peak area was a direct proportion of concentration, therefore they represented the amount of lichen substances and can be used to compare quantities of lichen substances before and after transplantation.

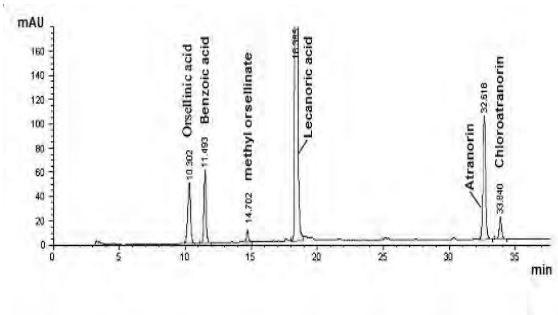

Figure 3. The HPLC chromatogram of lichen *Parmotrema tinctorum*

Table 1. Precision data of retention time and peak area of lichen substances in seven replicate of analyses

Compound	Retention time		Peak area	
	$\bar{X}$ ± SD	%RSD	$\bar{X}$ ± SD	%RSD
Orsellinic acid	10.28 ± 0.05	0.5	687.2 ± 13.6	2.0
Benzoic acid	11.48 ± 0.04	0.4	677.6 ± 8.6	1.3
Methyl orsellinate	14.69 ± 0.04	0.3	37.7 ± 1.1	2.9
Lecanoric acid	18.35 ± 0.05	0.3	19953.6 ± 138.8	0.7
Atranorin	32.55 ± 0.11	0.3	1427.7 ± 36.7	2.6
Chloroatranorin	33.77 ± 0.12	0.4	236.8 ± 5.8	2.4

The amount of secondary metabolites before and after transplantation to nine public parks are shown in Table 2. The average amounts of orsellinic acid, methyl orsellinate, lecanoric acid, atranorin and chloroatranorin from the nine public parks before transplantation were 657.6±179.5, 47.6±17.5, 17140.7±1219.0, 1465.8±101.9, and 266.6±39.2 respectively. After transplantation these amounts were 753.3±265.1, 34.8±22.7, 11066.5±1679.9, 1502.5±161.0 and 271.0±43.5 respectively. The average amount of lichen substances from the nine sites before and after transplantation were compared by Paired Samples T-Test using SPSS 17.0 for window. The results revealed that lecanoric acid in the lichens after transplantation was significantly lower ($P < 0.05$) than those before transferring to Bangkok. Other substances were not different significantly.

Table 2. The amount (peak area) of lichen substances at nine public parks in Bangkok city before and after transplantation (the value are the average of three replicate analyses)

site	Orsellinic acid		methyl orsellinate		Lecanoric acid		Atranorin		Chloroatranorin	
	before	after	before	after	before	after	before	after	before	after
(1)TW	456.8	726.7	36.7	36.2	16852.6	8699.0	1536.9	1568.3	237.3	288.4
(2) TR	796.0	750.1	64.0	56.8	14993.2	12130.5	1349.5	1584.4	201.2	308.2
(3) LN	1008.1	576.5	78.9	47.5	17970.3	12273.2	1590.5	1734.9	279.7	322.7
(4) R9	580.8	614.4	32.2	46.0	17935.4	12472.2	1583.2	1447.8	316.1	273.0
(5) NC	785.4	1290.7	41.6	64.7	18418.2	13467.1	1420.5	1656.3	272.7	309.3
(6) PK	568.0	307.4	63.5	ND	15572.9	9366.6	1464.5	1184.0	240.1	182.0
(7) SP	570.1	805.7	37.1	ND	17793.5	9218.6	1406.8	1393.5	286.7	240.7
(8) ST	466.2	867.4	26.4	33.4	16572.3	11389.7	1307.4	1500.5	245.0	251.5
(9) RT	686.6	840.4	48.1	29.1	18157.8	10581.9	1533.0	1452.8	320.6	263.3
$\overline{X}$	657.6	753.3	47.6	44.8	17140.7	11066.5	1465.8	1502.5	266.6	271.0
SD	179.5	265.1	17.5	12.9	1219.0	1679.9	101.9	161.0	39.2	43.5
CV	27.3	35.2	36.8	28.8	7.1	15.2	7.0	10.7	14.7	16.0

Seven months after transplantation lichen at Khao Yai National Park, the control samples, were also corrected and determined the amount of secondary substances. The results show that the amounts of all substances from these lichens increased as showed in table 3.

Table 3. The amount of control lichens at control sites (Khao Yai National Park)
A = starting time before transplantation
B = after time past to 7 months

Lichen substances	A	B
Orsellinic acid	546.0	739.9
Methyl orsellinate	61.5	67.3
Lecanoric acid	14853.6	20154.2
Atranolin	1619.5	1757.4
Chloroatranorin	288.7	332.9

It was reported that concentration of the secondary metabolites is higher in older thalli, larger size, than the younger ones [7]. However, this study choose lichens which had similar thallus sizes. Pangpet and Boonpragob, 2005 [13] revealed that growth rate of the lichen *P. tinctorum* varied among ecosystems. Lichens produced secondary metabolites to protected them against adverse environment, which different among ecosystems. *P. tinctorum* transplanted to nine public parks in Bangkok accumulated atmospheric pollutants and heavy metals about 0.3- 19.5 folds higher than those before transplantation reported by Boonpeng et al. [14]. These pollutants affected lichen primary metabolism such as photosynthesis [15,16], and thus lichen secondary metabolites were declined.

4. Conclusions

Lichen substances including orsellinic acid methyl orsellinate, lecanoric acid, atranorin and chloroatranorin, from the lichen *P. tinctorun* were quantified before and after transplanted to nine public parks in Bangkok. Lecanoric was the main substance with concentration of over 10 folds higher amount than the other substances. This substance had declined amounts in all parks after transplantation, whereas the other three substances, of small quantities, had lower amounts in some parks. It is reasonable to conclude that air pollutants in public parks caused the decline of the major lichen substance, lecanoric acid. Whilst declining and increasing of the other three minor substances might be the effects of human, methodological and instrumental errors due to very small quantities of these substances.

Acknowledgements: This work was supported by the National Research Council of Thailand (NRCT). Spectial gratitude goes to Khao Yai National Park under the department of National Parks, Wildlife and Plant Conservation, Ministry of Natural Resources and Environment of Thailand.

References

[1] S. Huneck and I. Yoshimura, *Springer*. (1996), 493p.
[2] http://www.anbg.gov.au/lichen/chemistry-1.html (Retrieved May 15, 2012)
[3] J.A. Elix, & E. Stocker-Wörgötter, Biochemistry and secondary metabolites by Nash, TH (ed.) *Lichen Biology 2nd. ed.* Cambridge University Press. (2008).
[4] D. Bialonska and F.E. Dayan, *Journal of Chemical Ecology*. **31** December (2005).
[5] S. Huneck, *Naturwissenschaften*. **86** (1999) 559-570 Review article.
[6] J.D. Lawrey, *Bryologist*. **89:1** (1986) 1-122.
[7] J. ASPLUND and Y. GAUSLAA, *The lichenologist*. **39(3)** (2007) 273-278.
[8] G.K. Jayaprasha, L. Jaganmohan Rao, R.P. Singh and K.K. Sakariah, *Journal of Chromatographic Science*. 36 (1998).

[9] J.L. Ramaut, M. Brouers. E. Serusiaux and M. Corvisier, *Journal of Chromatography*. **155** (1978) 450-453.
[10] H. Umezawa, N. Shibamoto, H. Naganawa, S. Ayukawa, M. Matsuzaki and Takeuchi, *J. Antibiot*, **27** (1974) p 587.
[11] W. Polyium, R. Thanomchit, C. Boonpeng, S. Meesom and K. Boonpragob, *Lichens in the public parks in Bangkok and their indication of environmental quality*. In Proceedings of Ramkhamhaeng University Research Conference, Bangkok, Thailand (2009) 51-63.
[12] G.B.Feige, H.T. Lumbsch, S. Huneck and J.A. Elix, *Journal of Chromatography*. **646** (1993) 417-427.
[13] M. Pangpet and K.Boonpragob, *Preliminary observation on the growth of transplanted lichens Parmotrema tinctorum in four ecosystems at Khao Yai National Park*. 31 st Congress on Science and Technology of Thailand, Suranaree University of Technology, 18-20 october (2005).
[14] Boonpragob K. (ed.). *Molecular genetics, biodiversity and ecology of lichens in Thailand*, Research report presented to the National Research Council of Thailand (NRCT). Lichen research unit, Faculty of science, Ramkhamhaeng University, Bangkok, (2012).
[15] C. Boonpeg and K. Boonpragob, *Assessing air quality of public parks in Bangkok, Thailand from photosynthesis and chlorophyll fluorescence of the transplanted lichen Parmotrema tinctorum (Nyl.) Hale*. In The XVIII International Botanical Congress Melbourne: University of Melbourne (2011) p. 366.
[16] M.E. Conti and G. Cecchetti, *Environmental Pollution*. **114:3** (2001) 471 – 492. Review article.

ONLINE REDUCTION AND USING pH GRADIENTS IN FLOW INJECTION SYSTEM FOR THE DETERMINATION OF Fe(II) AND Fe(III) WITH PAR

Monnapat Vongboot[1]* Thattaboon Janrung[1] and Jariyaporn Wongsa[1]

[1] Department of Chemistry, Faculty of Science, King Mongkut's University of Technology Thonburi, Bangkok, Thailand

* Author for correspondence; E-Mail: sumalee.tan@kmutt.ac.th, Tel. +66 24708869, Fax. +66 24708843

Abstract: Reduction of Fe(III) to Fe(II) with ascorbic acid, following the pH gradient method for the $Fe(PAR)_2$ formations in flow injection (FI) system was developed. The pH gradients in the FI system were generated by injecting the acidic solution of Fe(II) form to the basic solution of 4-(2-pyridylazo) resorcinol (PAR) and the different pH values were established. The formations of $Fe(PAR)_2$ complexes were, at the optimum pH, detected at the wavelength of 710 nm. The effects of ascorbic acid concentrations, the initial pH of solutions, flow rate and the length of mixing coil were investigated. The performance of reduction in different ratios of Fe(III) and Fe(II) was closely to 100%. The relative standard deviation was within 3% (n=10) and the percent recovery was 99 %. The calibration graph between absorbance and the concentration of Fe(II) or Fe(III) was found to be linear in the range of 0.1-24.0 ppm ($y=0.0234x+0.0118$, $r^2=0.9996$) within 0.03 ppm detection limit. The proposed method was used to determination of Fe(II) and Fe(III) in tap water.

1. Introduction

Flow injection analysis (FIA) has gained an interest for the development of analytical method because of its simplicity, feasibility, rapidity and reproducibility [1-3]. A chemical reactions can be implemented and automated in flow system which has advantages of exhausting little reagent and sample.

A pH gradient technique in flow injection system was first reported by Betteridge and Fields [4] by injecting acid into base or base into acid. The formation of complexes can be performed at optimum pH during gradient of pH [5-11].

The reagent PAR, 4-(2-pyridylazo) resorcinol, is a phenolic compound with a pyridine ring in its structure which reacts with Fe(II), then producing the intense coloured complex showing advantageous high solubility in water. The determination of the Fe(II) and Fe(III) in water samples has been generally achieved by complexation with specific chelating agents followed by spectrophotometric measurement [12].

For this paper, the proposed method was described for determination of Fe(II) and Fe(III) in water samples. This method is based upon a two steps in FI system. First, Fe(III) is reduced to Fe(II) by ascorbic acid and later reacts with PAR using pH gradient method to form a coloured complexes which is monitored spectrophotometrically.

2. Materials and Methods

2.1 Chemicals

All reagents were of analytical reagent grade and deionized water was used throughout for preparation of solutions. The stock solutions of Fe(II) and Fe(III), using from ferrous ammonium sulfate (AJEX) and ferric ammonium sulfate (AJEX), respectively, were prepared from their sulfate salts diluting with 0.01 M HNO_3 (J.T. Baker). The series of the standard solutions of Fe(II) and Fe(III) were prepared daily prior to use from their stock solutions. The 0.01 % w/v solution of PAR reagent at pH 10.0 was prepared by dissolving an accurately weighed amount of 4-(2-pyridylazo) resorcinol (New Jersey) in 1.0×10^{-4} M NaOH (Merck). The different concentrations of ascorbic acid (J.T. Baker) solutions were prepared and diluted with deionized water.

2.2 Apparatus

The flow injection system consisted of peristaltic pump (Masterflex, Cole-Parmer, USA), Rheodyne (model 7725i) injection valve with 100 µl loop and 50 cm mixing coil connected to flow through cell in UV-visible spectrophotometer (SECOMAM, France).

2.3 Procedures

The flow injection system with spectrophotometer was shown in Figure 1. The acid (pH 2.0) standard solution of Fe(II) or Fe(III) was mixed with ascorbic acid in the mixing coil 1 (MC1) in which Fe(III) was reduced completely to Fe(II) and injected (100 µl) subsequently into the basic (pH 10.0) solution of the PAR reagent to form the $Fe(PAR)_2$ complexes in the mixing coil 2 (MC2). Afterward, the $Fe(PAR)_2$ complexes were flown continuously through the cell in the UV-visible spectrophotometer. The maximum absorbance of this complexes showed clearly a peak at 710 nm and the height of peak relied on proportion of the concentration of Fe(II) or Fe(III).

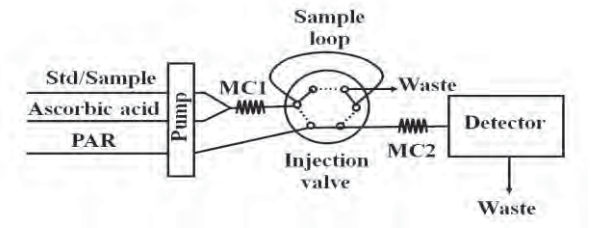

Figure 1 Schematic diagram of FIA-UV-visible Spectrophotometer for online reduction of Fe(III) to Fe(II) and pH gradient method for $Fe(PAR)_2$ complexes.

3. Results and Discussion

3.1 Measurement wavelength

The absorption spectrum of $Fe(PAR)_2$ complexes was scanned in the range 200 nm to 1100 nm by using the pH gradient technique in flow injection system as shown in Figure 2. The result was shown that the maximum absorption of the complexes was at the wavelength of 710 nm to be used in this study.

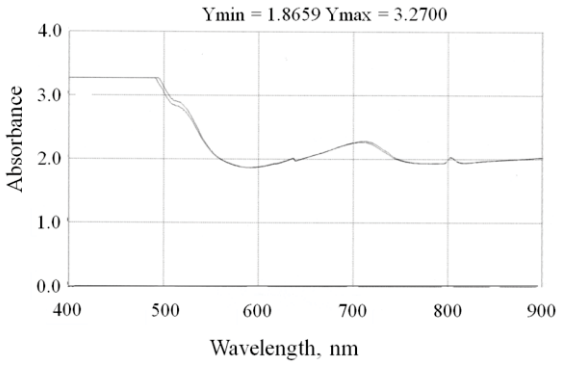

Figure 2 Absorption spectrum of $Fe(PAR)_2$ complex.

3.2 Effect of Parameters in FIA

Concentration of ascorbic acid: Ascorbic acid was used to reduce Fe(III) to Fe(II). The experiment was studied by mixing each of Fe(II) and Fe(III) in the different concentrations, 2.0-25.0 ppm Fe(II) and 2.0-25.0 ppm Fe(III), with ascorbic acid. The concentrations of ascorbic acid were studied in the range of 0.01-0.02 M. The results were found that the absorbance of $Fe(PAR)_2$ was not significant in different concentration between Fe(II) and Fe(III) and displayed a graph as a linearity at concentration of 0.0127 M ascorbic acid as shown in Figure 3. Thus, in this study, the concentration of 0.0127 M ascorbic acid was selected.

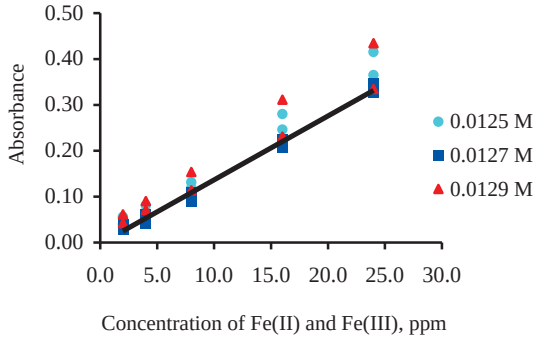

Figure 3 Concentrations of ascorbic acid to reduce Fe(III) to Fe(II).

Initial pH of solutions: In order to obtain pH gradient by injecting the acid standard into the basic reagent, the range of pH was varied from the initial pH of the standard solution and the PAR solution. The initial pH values of Fe(II) or Fe(III) and the PAR reagent were studied in the ranges of 2.0 to 10.0, 3.0 to 9.0 and 4.0 to 8.0, respectively. The result was shown in Figure 4 that the pH range from 2.0 to 10.0 gave the high sensitivity. For this reason, the pH value of 2.0 to 10.0 was the optimal initial pH of the standard solution and the PAR reagent.

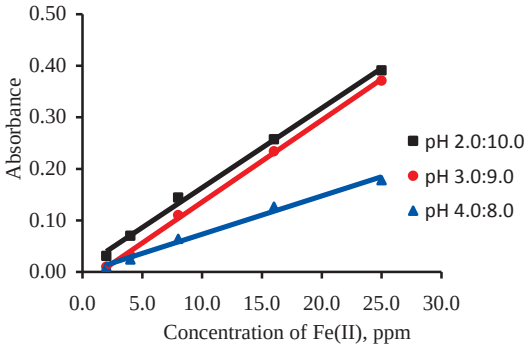

Figure 4 Effect of the initial pH of the standard solution and the PAR solution.

Effect of flow rate: The flow rate of FI system for reduction and the complex formation were studied at 1.3 and 0.9 ml/min, 1.0 and 1.0 ml/min and 1.7 and 1.7 ml/min. The pH gradient depends upon the flow rate of reagent and the distance traveled from injection valve to sample cell in the FI system. The flow rate of the system is an important due to its influences to the dispersion of the gradient zone. A high flow rate leads to uncompleted pH gradient and a low flow rate can be large dispersion because they can reduce the sensitivity. The flow rate of 1.3 and 0.9 ml/min was completely to reduce Fe(III) to Fe(II), checked by comparison of the absorbance between Fe(II) and Fe(III). The result was found that the absorbance at the same concentration of Fe(II) and Fe(III) obtained nearly value and gave overlap linearity graphs as shown in Figure 5.

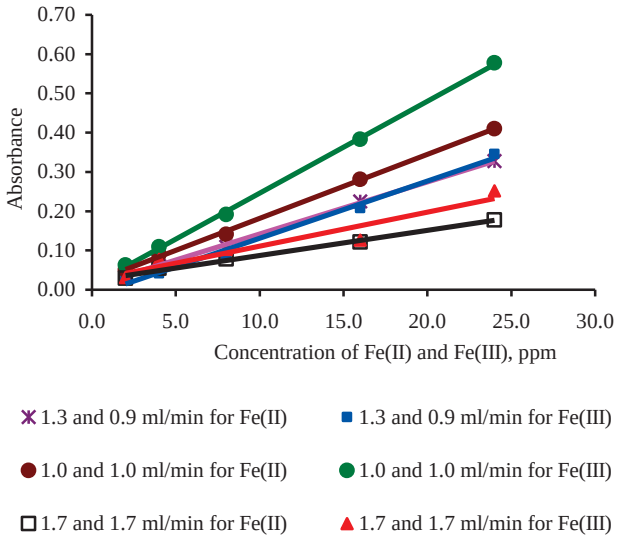

Figure 5 Effect of flow rates of FI system.

Length of mixing coil: The mixing coil 1 (MC1) and the mixing coil 2 (MC 2) were used to complete the reduction of Fe(II) and to form entirely the $Fe(PAR)_2$ complexes in the FI system, respectively. The MC 1 was studied in the length of 100 and 200 cm. A 200 cm of the MC 1 gave completely reductive of Fe (III) to Fe(II). The MC 2 was studied the lengths of 50, 100 and 200 cm. According to the pH gradient also depends upon the distance traveled in the system. The result was found that the absorbance was decreased by increasing the length of mixing coil because it increased dispersion of gradient zone. Therefore, the length of 50 cm was used for the optimum length. The results were shown in Figure 6.

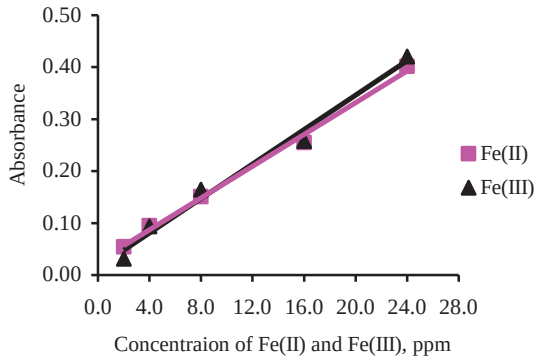

Figure 6 The lengths of the mixing coil 1 (MC 1) 200 cm and the mixing coil 2 (MC 2) 50 cm.

3.3 The performance of reduction

Table 1 presents the online reduction of Fe(III) to Fe(II) at different ratios of Fe(II):Fe(III). The outcomes of reduction were obtained by comparing the slopes of the analytical curves of which obtained from the accurate concentration of Fe(II) solutions and from total Fe at vary ratios between Fe(II) and Fe(III) mixtures. The analytical curves of both were obtained to be a good linearity in the same slope value as displayed in Figure 7. The performance of reduction was 104.3 % which indicated the accuracy of the proposed method.

Table 1: The performance of reduction of Fe(II): Fe(III) ratios.

Std Fe(II) ppm	Total Fe from Fe(II):Fe(III) ratios, ppm	Absorbance	Performance of reduction, % each of ratios	average
2.0		0.0165		
	3.0 (1:2)	0.0888	118.3	
4.0		0.0904		
	4.0 (3:1)	0.1081	117.3	
	6.0 (1:5)	0.1236	93.5	104.3
	7.0 (5:2)	0.1506	103.0	
8.0		0.1538		
	10.0 (9:1)	0.1892	94.9	
	15.0 (12:3)	0.2780	98.3	
16.0		0.3115		
24.0		0.4346		

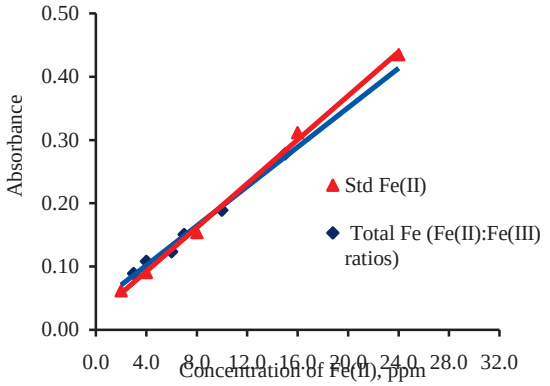

Figure 7 The performance of reduction of Fe(II): Fe(III) ratios.

3.4 The optimum of the proposed method

Thus, the proposed condition, as illustrated in Table 2, of the online reduction in FI system and the pH gradient for the formation of the $Fe(PAR)_2$ complexes was the optimal condition.

Table 2: The proposed condition of reduction and the complexes formation.

Parameters	**Value**
pH of standard/sample	2.0
pH of PAR	10.0
Flow rate of PAR	1.0 ml/min
Flow rate of ascorbic	1.3 ml/min
Flow rate of standard/sample	1.3 ml/min
Concentration of PAR	0.01 %w/v
Concentration of ascorbic acid	0.0127 M
Injection loop	100 µl
Mixing coil 1	200 cm
Mixing coil 2	50 cm
Wavelength	710 nm

The calibration graph for the determination of Fe(II) and Fe(III) was obtained under the optimum condition in Table 2. The results showed that a good linear relationship was observed over the range 0.10-24.00 ppm with the regression equation y=0.0234x-0.0118 (r^2=0.9996) as shown in Figure 9, where y is the absorbance and x is the concentration of Fe(II) or Fe(III) solution. The detection limit estimated (S/N=3) was 0.03 ppm Fe(II). The reproducibility of the proposed method was calculated as the relative standard deviation (RSD) of the maximum peak and its height was computed from ten replicates. The result obtained from this proposed method was good agreement with the precise value within 3%.

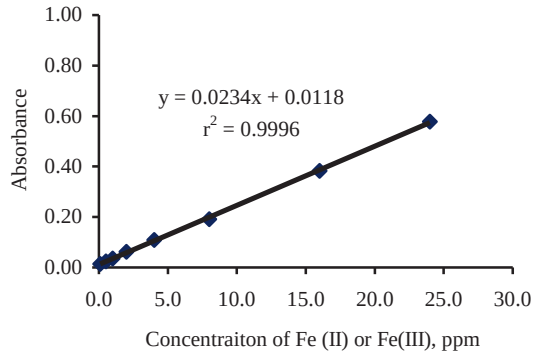

Figure 9 The calibration graph of the optimum condition.

3.5 The percent recovery of analysis

The reliability of the proposed method was evaluated by reporting in term of the percent recovery of Fe(II) and Fe(III). Thence, the recoveries studied were carried out by analyzing the water samples. Accordingly, this proposed method was used to determine Fe(II) and Fe(III) in both of the water samples and the water samples which spiked the standard solutions of Fe(II) and Fe(III), respectively. The results were found that the average percent recovery was 99 %.

3.6 Analysis of water samples

The proposed method the described above was used to analyze iron ions in water samples. The analyses were performed for applying to the determination of Fe(II) and Fe(III) in tap water samples collecting from Chemistry building in KMUTT. These water samples were treated by adding the concentrate nitric acid before analysis. The results obtained were illustrated in Table 3. It can be seen that the concentrations of Fe(II) and Fe(III) in tap water samples were in the range 0.58-0.70 ppm and in the range 0.31-0.44 ppm, respectively. The quality of tap water is allowed total Fe contaminated at least 0.3 ppm (WHO for tap water). Possibly, the high amount of Fe(II) in tap water results from corrosion of pipelines. In corrosion process, iron reacts with soluble oxygen in water and convert to Fe(II). In excess oxygen and high temperature, Fe(II) is some converted to iron(III) [12].

Table 3: The determination of Fe(II) and Fe(III) in water samples.

Sample waters	Fe(II) ppm	Fe(III) ppm
S1	0.65	0.34
S2	0.60	0.42
S3	0.61	0.39
S4	0.62	0.44
S5	0.58	0.41
S6	0.70	0.31
S7	0.68	0.35

4. Conclusions

The proposed method can be advantage for the online reduction and perform the pH gradient for the complexes formation without using the buffer solution for adjusment. This method demonstrates high accuracy and precision and has great potential to be automated management. The speciation of Fe(II) and Fe(III) in tap water samples could be determined successfully by this proposed method.

Acknowledgement

The Author wishes to thank the research funding source of Chemistry Department for support.

References

[1] J. Ruzicka and E.H. Hansen, *Flow Injection Analysis*, 2nd Edition, Wiley, NY (1998).
[2] Z.L. Fang, *Flow Injection Separation and Preconcentration*, VCH Publishers, Inc., NY (1993).
[3] M. Trojanowicz, *Flow Injection Analysis Instrumentation and Applications*, World Scientific, River Edge, NJ (1999).
[4] D. Betteridge and B. Fieldas, *Anal. Chim. Acta* **132** (1981), pp. 139–155.
[5] N. Porter, B.T. Hart and R. Morrison, *Anal. Chim. Acta* **281** (1993), pp. 229–242.
[6] N. Porter, B.T. Hart, R. Morrison and I.C. Hamilton, *Anal. Chim. Acta* **308** (1995), pp. 313–328.
[7] C. Pasquini, J. Lu and C.D. Tran, *Anal. Chim. Acta* **319** (1996), pp. 315–324.
[8] S. Zhao, X. Xia, G. Yu and B. Yang, *Talanta* **46** (1998), pp. 845–850.
[9] J. Saurina, S. H. Cassou, R. Tauler and A.I. Ridorsa, *Anal. Chim. Acta* **408** (2000), pp. 135–143.
[10] J. Saurina and S. H. Cassou, *Anal. Chim. Acta* **438** (2001), pp. 335–352.
[11] A. Pheca, R. Oliver, S. Hernandez-Cassou and J. Saurina, *Anal. Chim. Acta* **592** (2007), pp. 173–180.
[12] H. Baghero, A. Gholami and A. Najafi, *Anal. Chim. Acta* **424** (2000) 233–242.

PEPTIDE NUCLEIC ACID PROBE FOR ELECTROCHEMICAL DETECTION OF HUMAN PAPILLOMA VIRUS DNA TYPE 16

Sakda Jampasa[1], Wanida Wonsawat[2], Tirayut Vilaivan[3], Orawon Chailapakul[1, 4, 5,*]

[1] Program in Petrochemicals and Polymer Science, Faculty of Science, Chulalongkorn University, Patumwan, Bangkok, Thailand

[2] Department of Chemistry, Faculty of Science and Technology, Suan Sunandha Rajabhat University, 1 U-Thong Nok Road, Dusit, Bangkok, Thailand

[3] Organic Synthesis Research Unit, Faculty of Science, Chulalongkorn University, Patumwan, Bangkok, Thailand

[4] Electrochemistry and Optical Spectroscopy Research Unit, Department of Chemistry, Faculty of Science, Chulalongkorn University, Bangkok, Thailand

[5] National Center of Excellence for Petroleum, Petrochemicals, and Advanced Materials, Chulalongkorn University, Patumwan, Bangkok, Thailand

[*]Author for correspondence; E-Mail:corawon@chula.ac.th, orawon.c@chula.ac.th, Tel. +66 022187615, Fax. +66 022187615

Abstract: A novel electrochemical biosensor for the detection of high-risk human papilloma virus (HPV) DNA type 16 based on pyrrolidinyl peptide nucleic acid (acpcPNA) as a sensor probe was proposed. A 14-mer PNA probe was designed to specifically target the DNA sequence of HPV type 16. The probe was modified at the N-terminus via N-acylation with anthraquinone (AQ) as a redox-active label. The success of the synthesis of the AQ labeled PNA (PNA-AQ) was confirmed by MALDI-TOF mass spectrometry and by thermal denaturation study with a complementary synthetic DNA target with a sequence corresponding to the HPV DNA (T_m= 69.9 ^oC). An inexpensive screen print carbon electrode (SPCE) was used in this study. Ink compositions containing graphite powder, carbon ink and binder solution were mixed together with the ratio of 0.2 g: 1 g: 1 mL, respectively. The PNA-AQ probe (20 μM) was covalently immobilized onto the electrode surface using 1-ethyl-3-(3-dimethylaminopropyl) carbodiimide) (EDC) as a coupling agent after the electrochemical pretreatment of electrode. Hybridization between the PNA-AQ probes and the synthetic DNA target was studied by measuring the peak current of AQ using a square-wave voltammetric (SWV) method. The results showed that the redox signal response decreased by three folds after addition of the DNA. This is explained by the rigidity of PNA-DNA duplexes, which affected the accessibility and electron transfer between the AQ label and the electrode surface. It is hoped that this method will be applicable in screening for the HPV-DNA type 16 in the primary stage of cervical cancer in the developing country.

1. Introduction

Peptide Nucleic Acid (PNA) is an important synthetic polymer which has an analogous structure to DNA. PNA was discovered by Nielsen's group almost twenty years ago [1-4]. PNA consists of a peptide-like backbone replacing the sugar-phosphate in natural DNA or RNA. PNA was widely used in biochemical sensing applications due to its excellent characteristics, such as sequence-specific binding to DNA or RNA, resistance to nuclease and protease enzyme, and strong binding to the target DNA. Because of these advantages, PNA was therefore applied as biomolecular probe, such as for disease diagnostic. Recently, a new pyrrolidinyl PNA system was developed by Vilaivan's group [5,6]. The newly developed PNA system (known as acpcPNA) possesses an α,β-peptide backbone deriving from D-proline/2-aminocyclopentanecarboxylic acid. The acpcPNA showed a stronger binding affinity and higher specificity toward complementary DNA target than Nielsen's PNA. AcpcPNA has been used as a probe to detect the target DNA in combination with suitable detection techniques such as MALDI-TOF mass spectrometry, fluorescence microscopy, surface plasmon resonance (SPR), and electrochemical detection [7-12].

Electrochemical DNA biosensor that is simple to use, inexpensive and can provide high throughput diagnosis is in great demand and rapidly developed. Electrochemical detection is highly sensitive, rapid, cheap, portable and requires only a small volume of sample. Therefore, electrochemical detection is an attractive technique for high throughput screening. The general working principle of DNA electrochemical biosensor involves immobilization of the probe (usually a DNA or PNA) onto the electrode surface. Subsequent hybridization with the correct target DNA causes a change in the electrochemical signal (increase or decrease) [13-17]. Different types of electrode were applied as electrochemical transducers for the DNA detection, such as gold electrode, hanging mercury drop electrode (HMDE) and various carbon-based electrodes, have been widely used [13-17].

There are many of electroactive species that have been used as PNA/DNA labels/indicators for electrochemical detection of the PNA/DNA

hybridization [13-17]. Organometallics and organic compounds are widely used as indicators. These labels may be covalently attached to the probe or with other methods [13-19].

Anthraquinone (AQ) is one of electroactive species which provides high sensitivity, reversible redox peak and high stability [15]. Thus, AQ is an attractive organic compound for the labeling of probe. In this work, AQ was applied as the redox-active label in acpcPNA probe for the electrochemical detection of the PNA/DNA hybridization. The HPV DNA type 16 has been chosen as the target DNA. This virus causes cervical cancer that leads to deaths of woman populations around the world, particularly in developing countries having limited resources for public healthcare. These countries are in need of a well-developed technology to solve this problem. We hoped that the developed method would be applicable in screening for the HPV-DNA type 16 in the primary stage of cervical cancer, which can save the life or reduce the death rate of these people.

2. Materials and Methods

2.1. Apparatus

All electrochemical measurements were performed with a PGSTAT 30 potentiostat, and controlled with the general purpose electrochemical system (GPES) software.

2.2. Synthesis of the PNA probe

A 14-mer PNA probe with a sequence N-terminus-CGACCTCCACATAC-terminus-C was designed to specifically target the DNA sequence of HPV type 16. The probe was synthesized by solid-phase peptide synthesis using Fmoc chemistry. The synthesis procedure consists of deprotection, coupling and capping steps (Figure 1).

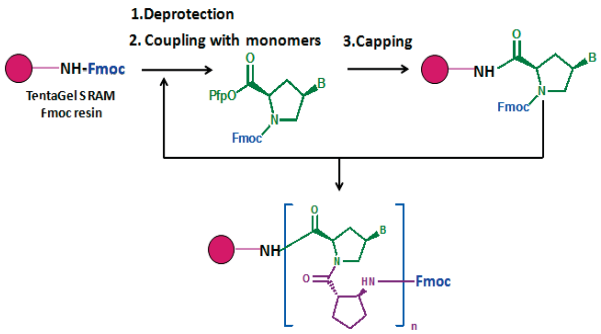

Figure 1. Schematic illustration of the synthetic procedures of the PNA probe

2.3. Labeling of the PNA probe

The acpcPNA probe was labeled with AQ at the N-terminus by acylation reaction (Figure 2). The N-Fmoc-deperotected PNA (0.5 µmol) on the solid support was treated with 1-carboxymethoxyanthraquinone 4 eq**,** HATU 4 eq, and N, N diisopropylethylamine (DIEA) in dimethylformamide (DMF). The reaction was left overnight at room temperature. The labeled PNA probe was then cleaved from the solid support with trifluoroacetic acid, followed by ether precipitation and HPLC purification.

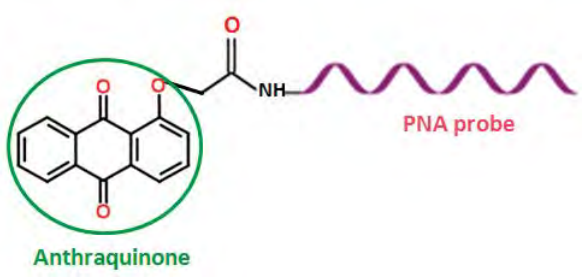

Figure 2. Labeling of the PNA probe with AQ

2.4. Preparation of screen-printed carbon electrode (SPCE)

The SPCE was consisted of the three-electrode system. The pattern was designed by adobe illustrator. Ink compositions contained graphite powder, carbon ink and binders solution. All compositions were mixed together with the ratio of 0.2 g: 1 g: 1 mL, respectively. The screen print procedures are described. First of all, Silver/Silver chloride ink was screen-printed onto polyvinyl chloride **(**PVC**)** substrate as base layer which was used for the reference electrode and the connecting pads. Then, the screening of the carbon ink for the working and counter electrode was performed as the second layer. After that, the insulator was screened as the last layer. In the final step, the complete electrode was baked at 55 ^{o}C to evaporate the organic binder solvent and to dry the electrode. The SPCE is shown in the figure 3.

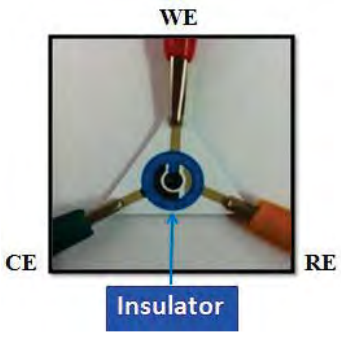

Figure 3. The design of three electrodes system of SPCE used in this study.

2.3 Preparation of PNA solutions

All solutions were prepared in daily fresh deionized (DI) water. The PNA stock solution was prepared with DI water and was kept frozen when not in use. The stock PNA and DNA solutions were diluted with phosphate buffer (PBS) solution pH 7.4. PBS buffer, pH 7.4 contained 140 mM NaCl, 2 mM KH_2PO_4, 10 mM Na_2HPO_4, 2 mM KCl diluted in 1000 mL deionized water.

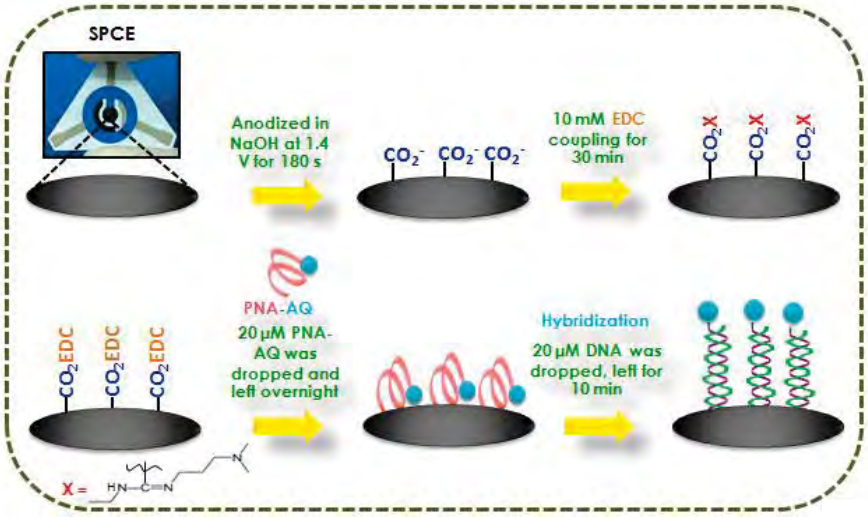

Figure 4. Schematic illustration of the immobilization and hybridization of PNA-AQ probe

2.4 Immobilization and hybridization of PNA probe

PNA-AQ probe was covalently immobilized onto the electrode surface. The procedures were as follows: Step I, the SPCEs were pretreated in 0.5 M NaOH at 1.4 V for 180 s, and then the electrode was rinsed with DI water. Step II, after electrochemical treatment, 15 µL 1-ethyl-3-(3-dimethylaminopropyl) carbodiimide) (EDC) (10 mM) coupling agent was dropped onto the electrode, and left at room temperature for 30 minutes. After that the washing step was performed. Step IV, 10 µL PNA-AQ probe solution (20 µM) was pipetted onto the electrode surface and the reaction was left overnight at room temperature. After the immobilization of PNA-AQ probe, the electrode was washed with PBS pH 7.4 twice to remove the excess and nonspecifically adsorbed PNA-AQ probe on the electrode surface. Step V, the modified electrode was hybridized with the target DNA for 10 minutes by dropping the target DNA (20µL) solution onto the electrode surface and after 10 minutes, the electrode was rinsed with PBS pH 7.4 again. The immobilization and hybridization procedures are illustrated as in Figure 4.

3. Results and Discussion

3.1 Characterization of PNA -labeled probe

The unlabeled and labeled PNA probes were characterized by MALDI-TOF mass spectrometry which confirmed the successful labeling and the stability of the AQ moiety. As shown in Figure 5, the 14-mer unlabeled PNA showed a mass peak at 4644 m/z. After labeling, the mass increased to 4909 m/z. The increment of 265 m/z coincides with the AQ-label. Therefore, successful labeling of the PNA probe with the electroactive species had been achieved.

For the stability of PNA hybridization, it was studied by thermal denaturation with a complementary synthetic DNA corresponding to the HPV DNA type 16. The results revealed that the hybridization form is stable with melting temperature (T_m) of 69.9 ^oC.

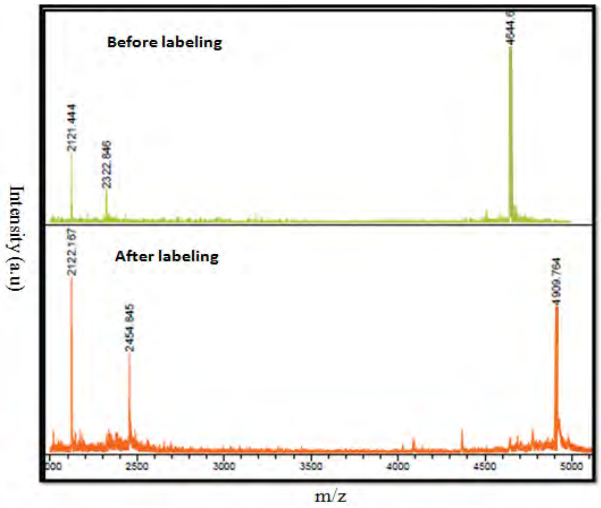

Figure 5. MALDI-TOF mass spectra of crude PNA before and after labeling with AQ.

3.2. Characterization of electrode

Prior to each experiment, the SPCE was characterized by1.0 mM $[Fe(CN)_6]^{3-/4-}$ in 0.5 M KCl solution to characterize the electrode that was ready to use (figure 6).

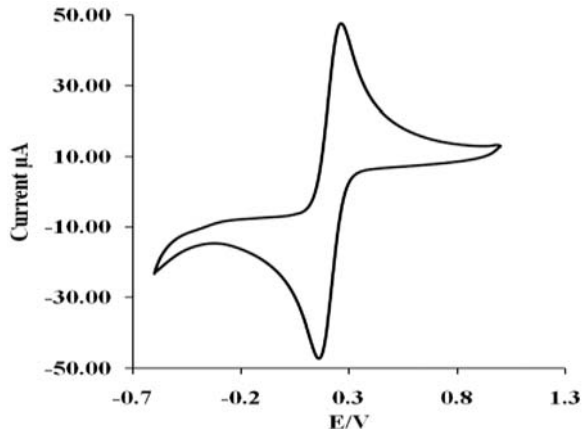

Figure 6. Cyclic voltammograms of 1mM $[Fe)CN(_6]^{3-/4-}$ in 0.5 M KCl at scan rate :100 mV/s

3.3. Immobilization and hybridization of PNA probe

The successful immobilization of PNA probe was followed by the redox-label peak of AQ after the immobilizing steps were performed. The hybridization occurred between the 20 μM PNA-AQ probes and the 20 μM synthetic DNA target which was studied by measuring the peak current of AQ using a square-wave voltammetric (SWV) method. The results showed that (Figure 7) the redox signal response decreased by three folds after addition of the DNA. This is explained by the rigidity of PNA-DNA duplexes, which affected the accessibility and electron transfer between the AQ label and the electrode surface.

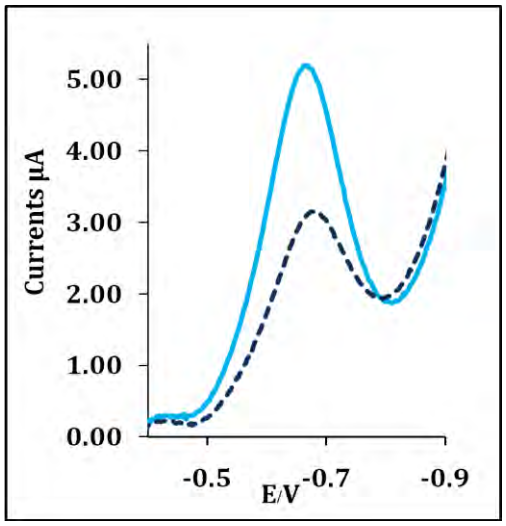

Figure 7. SWV of the peak currents of PNA-AQ probe before and after hybridization with target DNA. Parameters are frequency of 25 Hz, amplitude of 50 mV and step potential of 30 mV in PBS pH 7.4. — Before hybridization, ---- After hybridization.

3. Conclusion

A novel electrochemical biosensor for the detection of high-risk human papilloma virus (HPV) DNA type 16 based on pyrrolidinyl peptide nucleic acid (acpcPNA) as a sensor probe was successfully applied to detect the HPV DNA types 16 sequence. The result showed that the signals response was clearly decreased with the presence of the target DNA. Therefore, we hoped that this method will be applicable as an inexpensive tool for screening HPV type 16 DNA in the primary stage of cervical cancer in the developing countries.

Acknowledgments

The authors would like to thank the partial financial support from Center of Innovative Nanotechnology (CIN), Electrochemistry and Optical Spectroscopy Research Unit and Program in Petrochemical & Polymer Science, Chulalongkorn University.

References

[1] P.E. Nielsen, M. Egholm, R.H. Berg and O. Buchardt, *Science.* **254** (1991) 1497–1500.
[2] M. Egholm, O. Buchardt, P.E. Nielsen and R.H. Berg, *J. Am. Chem. Soc*. **114** (1992) 1895–1897.
[3] M. Egholm, O. Buchardt, P.E. Nielsen and R.H. Berg, *J. Am. Chem. Soc*. **114** (1992) 9677–9678.
[4] M. Egholm, O. Buchardt, L. Christensen, C. Behrens, S. M. Freier, D.A. Driver, R.H. Berg, S.K. Kim, B. Norden and P.E. Nielsen, *Nature*, **365** (1993) 566-568.
[5] T. Vilaivan and C. Srisuwannaket, *Org. Lett.* **8** (1993) 1897-1900.
[6] C. Vilaivan, C. Srisuwannaket, C. Ananthanawat, C. Suparpprom, J. Kawakami, Y. Yamaguchi, Y. Tanaka and T. Vilaivan, *Artificial DNA:PNA & XNA.* **2** (2011) 50-59.
[7] B. Boontha, J. Nakkuntod, N. Hirankarm, P. Chaumpluk and T. Vilaivan, *Anal. Chem.* **80** (2008) 8178-8186.
[8] P. Boontha, J. Nakkuntod, N. Hirankarm, P. Chaumpluk and T. Vilaivan, *Anal. Chem.* **80** (2008) 8178-8186.
[9] B. Korkeaw and T. Vilaivan, *Nucleic Acids Symposium Series*, **52** (2008) 251-252.
[10] C. Ananthanawat, T. Vilaivan, W. Mekboonsonglarp and V.P. Hoven, *Biosens. Bioelectron.* **24** (2009) 3544-3549.
[11] C. Ananthanawat, T. Vilaivan, V.P. Hoven and X. Su, *Biosens. Bioelectron*. **25** (2010) 1064-1069.
[12] A. Macanovic, C. Marquette, C. Polychronakos and M.F. Lawrence, *Nucleic Acids Res.* **32** (2004) 2-20.
[13] L.Civit, A. Fragoso and C.K. O'Sullivan, *Biosens. Bioelectron*. **26** (2010) 1684-1687.
[14] R.E.Sabzi, B. Sehatnia, M.H. Pournaghi-Azar and M.S Hejazi, *J. Iran. Chem. Soc.* **5** (2008) 476-483.
[15] D. kang, R.J. White, F. Xia, X. Zuo, A. Valle'e-Be'lisle and K.W. Plaxco, *NPG Asia Materials*, **4** (2012) xx-xx
[16] C. Xu, H. Cai, Q. Xu, P. He and Y. Fang, *Fresen. Anal. Chem.* **369** (2001) 428-432.
[17] D. Ozkan, P. Kara, K. Kerman, B. Meric, A. Erdem, F. Jelen, P.E. Nielsen and M. Ozsoz, *Bioelectrochemistry*, **58** (2002) 119-126.
[18] C. fang, H. Ji, W.Y. Karen and S.R.M. Rafei, *Biosens. Bioelectron*. **26** (2011) 2670-2674.
[19] E. Palec'ek, M. Trefulka and M. Fojta, *Electrochem. Commun*. **11** (2009) 359-362.

ANTIMONY-FILM ELECTRODE FOR THE SIMULTANEOUS DETERMINATION OF ZINC AND CADMIUM BY POTENTIOMETRIC STRIPPING ANALYSIS

Saowapa Saen-inkoon, Winai Oungpipat *

Division of Chemistry, Department of Science, Rajamangala University of Technology Krungthep, 2 Nang Linchi Road, Sathron, Bangkok 10120, Thailand

*Author for correspondence; E-mail: winai_o@rmutk.ac.th, Tel. +66 22879600 Fax. +66 22863596

Abstract: In this research, a potentiometric stripping analysis method for quantitative determination of zinc and cadmium by using antimony-film modified glassy carbon electrode as working electrode was developed. The antimony-film was deposited in situ by adding 500 µg/L antimony(III) directly to the sample solution using 0.03 M hydrochloric acid as supporting electrolyte and simultaneously depositing the antimony and target metals on the glassy-carbon. Zinc and cadmium was potentiometrically deposited at -1.2 V (vs. Ag/AgCl) for 550 seconds. The electrode exhibited highly linear behaviour in the examination range from 10-100 µg/L for Zn(II) and Cd(II), with limits of detection (3σ) of 0.517 and 0.675 µg/L Zn(II) and Cd(II), respectively. Good repeatability of 2.46% and 3.06% relative standard deviation for 100 µg/L Zn(II) and Cd(II) (n = 10) was achieved, respectively. Likewise, good reproducibility of 7.48% and 7.54% for 100 µg/L Zn(II) and Cd(II) (n = 10) was obtained, respectively. The percentage recovery of 70-125 for Zn(II) and Cd(II) was achieved. The results obtained reveal that antimony film electrode has been shown an attractive stripping voltammetric performance for zinc and cadmium which compares favourably with that of inductively couple plasma spectrometry.

1. Introduction

Heavy metals such as zinc and cadmium are used mainly in metal processing industries. They are found naturally in small quantities in water and soil. However, heavy metals nowadays, increasingly contribute to the pollution of the environment, playing an important role in the development of human illnesses and toxic effect. Intake of zinc in a high amount can cause a deficiency of copper in the liver, the serum and the heart [1]. Acute exposure to cadmium fumes may cause flu like symptoms including chills, fever, and muscle ache sometimes referred to as "the cadmium blues"[2]. Although they can be detected by various analytical techniques such atomic absorption spectrophotometry (AAS) [3], inductively coupled plasma-optical emission spectroscopy (ICP-OES) [4], inductively coupled plasma-mass spectrometry (ICP-MS) [5], and electroanalytical techniques such as potentiometric stripping analysis (PSA) [6]. PSA can be considered as the most powerful technique for in-field analysis due to its excellent detection limit, high sensitivity, high speed, simplicity and relatively low cost. Mercury electrode provides a wide cathodic potential limit for reduction of several metals and allows the formation of amalgams for accumulative preconcentration of the metals leading to very high sensitivity and reproducibility for PSA determination. However, due to toxicity of the mercury [7-9], mercury electrode is recently limited use for voltammetric analysis and other alternative electrodes are being developed. This includes bismuth film electrode (BiFE) [10] and antimony film electrode (SbFE) [11]. BiFE on various substrate materials have been successfully used for anodic stripping voltammetry and determination of metals at trace levels [12]. SbFE has recently been proposed as an alternative to mercury film electrode [11]. However, the use of this film electrode is still incipient and few papers have been dedicated.

The aim of this paper is to describe the application of antimony film electrode (SbFE) for determination of zinc and cadmium in water samples by PSA.

2. Materials and Methods

2.1 Chemicals

All chemicals used were of analytical grade. All standard and reagent solutions were prepared with ultrapure water (Milli Q water, resistivity of 18.2 MOhm cm^{-1}).

Atomic absorption standard solutions of antimony, cadmium and zinc were purchased from Merck (Germany). 0.03 M solution of hydrochloric acid (HCl) served as the supporting electrolyte.

2.2 Apparatus

All electrochemical experiments were performed using a potentiostat/galvanostat Autolab® PGSTAT-12 (Eco Chemie B.V., The Netherlands). A three-electrode cell configuration was employed for the voltammetric measurements. SbFE was used as working electrode, with a Ag/AgCl reference electrode and a platinum counter electrode.

2.3 Analytical Procedure

Aliquots of stock solution of zinc and cadmium were added into the electrochemical cell containing 0.03 M HCl and 500 µg/L antimony. A constant accumulation potential of -1.2 V (vs. Ag/AgCl) was then applied for an accumulation duration of 550 s at stirred solution. At the end of the accumulation period, the stirring was stopped and a 10 s rest period was allowed for the solution to become quiescent. The PSA signal was then recorded by scanning the electrode potential towards the positive direction from -1.2 to -0.3 V. Stripping potentiograms were recorded as d*t*/d*E* (s/V) vs. *E* (V). All experiments were carried out without removal oxygen.

3. Results and Discussion

3.1 Optimization of the Parameters

The parameters affecting analytical performance, including deposition potential, antimony concentration, type of supporting electrolytes, hydrochloric concentration and deposition time upon the PSA signals of zinc and cadmium were investigated.

Figure 1 shows the effect of deposition potential in the range of -1.0 -1.6 V upon the PSA signals of zinc and cadmium. As can be seen from Figure 1, the PSA signals of both metals increased with increasing deposition potential and provided the highest response at -1.2 V. Increasing potential higher than this value resulted in the decrease in the PSA signals. Therefore the potential -1.2 V was used as the deposition potential.

The effect of antimony concentration in the range from 0.0 - 1000 mg/L on PSA signals of zinc and cadmium are shown in Figure 2. The PSA signal of both metals increased with increasing antimony concentration and reached the maximum at antimony concentration of 500 mg/L. Slightly decrease in the current response was observed at the antimony concentration higher than 500 mg/L. This may be ascribed to the saturation of antimony in the film formed on the PE. Consequently, the antimony concentration of 500 mg/L was selected as the optimum value.

The effect of type of supporting electrolytes on PSA signals of zinc and cadmium was studied. Five solutions including HCl, KSCN, acetate buffer, ammonia buffer and phosphate buffer were chosen for this purpose. The result revealed that HCl resulted in the best PSA signal obtained. Therefore, the effect of HCl concentration was then studied. It can be seen from Figure 3 that 0.01 M of HCl was the best supporting electrolyte for plating solution. It is most likely due to the stability of SbFE at 0.01 M HCl.

The effect of concentration of HCl in the range from 0.01- 0.2 M on PSA signals of zinc and cadmium is shown in Figure 4. As can be seen from Figure 4, the best PSA signal for zinc and cadmium was observed at 0.03 M HCl .

Deposition time also has the profound effect on the current response. Figure 5 shows the optimization of the deposition time. The PSA signals of zinc and cadmium increased rapidly with the deposition time at first and then decreased after 550 s. The rapid and highly accumulation was attributed to the strong interaction between SbFE and zinc and cadmium. Thus, 550 s of deposition time was employed.

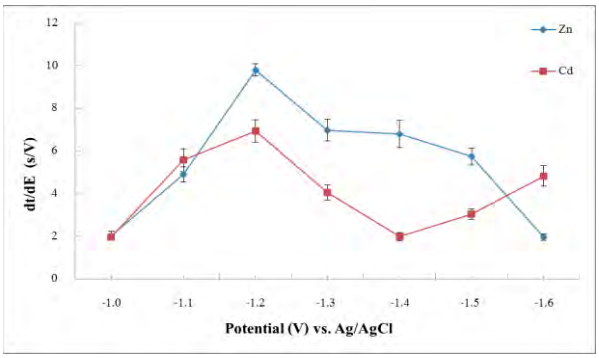

Figure 1. Influence of deposition potential on the potentiometric response for zinc and cadmium at seven different deposition potentials. The experiment was performed in a medium containing 0.1 M HCl in the presence of 100 µg/L Sb (III) ions with deposition time of 350 s.The concentration of each analyte was 100 µg/L.

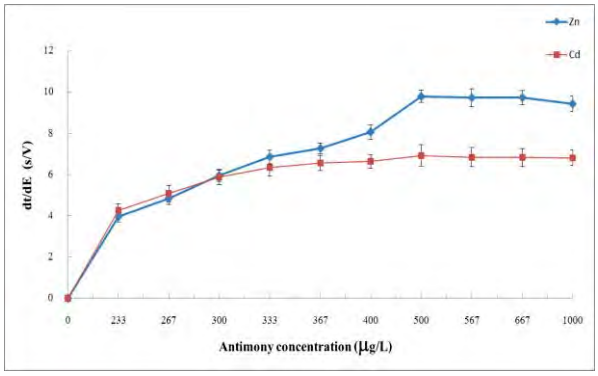

Figure 2. Influence of antimony concentration on the potentiometric response for zinc and cadmium at different antimony concentrations. The experiment was performed in a medium containing 0.1 M HCl with deposition time of 350 s.The concentration of each analyte was 100 µg/L and the deposition potential was −1.2 V.

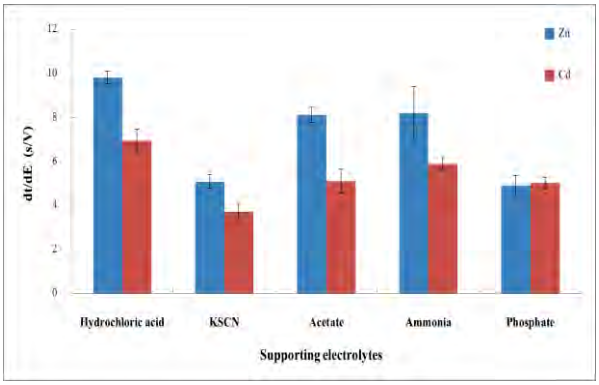

Figure 3. Influence of type of supporting electrolytes on the potentiometric response for zinc and cadmium at different supporting electrolytes.The experiment

was performed in the presence of 500 µg/L Sb (III) ions with deposition time of 350 s.The concentration of each analyte was 100 µg/L and the deposition potential was −1.2 V.

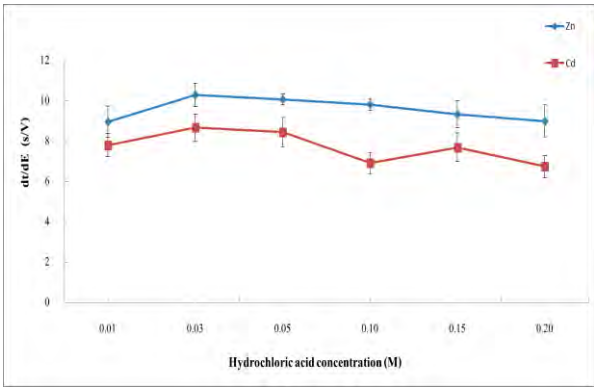

Figure 4. Influence of hydrochloric concentration on the potentiometric response for zinc and cadmium at different hydrochloric concentrations.The experiment was performed in the presence of 500 µg/L Sb (III) ions with deposition time of 350 s.The concentration of each analyte was 100 µg/L and the deposition potential was −1.2 V.

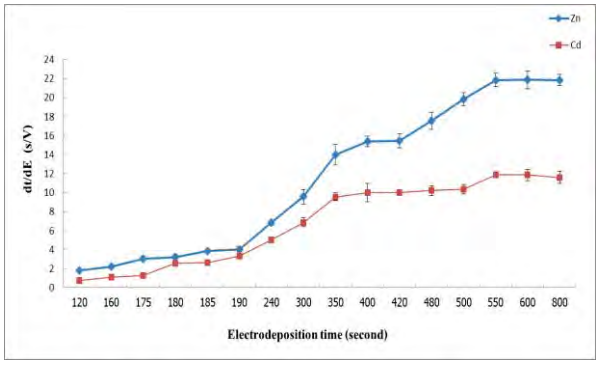

Figure 5. Influence of electrodeposition time on the potentiometric response for zinc and cadmium at different electrodeposition times.The experiment was performed in a medium containing 0.03 M HCl in the presence of 500 µg/L Sb (III) ions with deposition time of 550 s.The concentration of each analyte was 100 µg/L and the deposition potential was −1.2 V.

3.2 Validation of analytical procedure

Under the optimal experimental conditions, the validation data including, calibration curve, detection limit, precision and accracy were examined. The typical records of PSA for increasing concentration of Zn(II) and Cd(II) are displayed in Figure 6 (a). Calibration curves for Zn(II) and Cd(II) illustrated in Figure 6(B) were linear in the range 10 to 100 µg/L with good correlation coefficient of 0.9955 for Zn(II) and 0.9962 for Cd(II). Detection limit was calculated basing on 3 times the standard deviation of 10 measurements of the blank solution. The results obtained for detection limit were found to be 0.517 and 0.675 µg/L for Zn(II) and Cd(II), respectively.

The analytical precision of the developed method was verified from the relative standard deviation (RSD) in terms of repeatability and reproducibility for 10 replicate determinations of 100 µg/L Zn(II) and Cd(II). Good repeatability for Zn(II) and Cd(II) with respective RSD of 2.46 and 3.06% was achieved. Likewise, good reproducibility with RSD of 7.48% for Zn(II) and 7.54% for Cd(II) was obtained.

The accuracy of the proposed method was assessed as percentage recoveries for the determinations of spiked water samples with known amounts of target analytes. The recovery of 70.5-114.5% for Zn(II) and 80.5-114.5% for Cd(II) at the spiked concentration of Zn(II) and Cd(II) ranging from 10–50 µg/L was obtained. According to AOAC guidelines [13], the acceptable recovery for the analyte concentration at 10 µg/kg (ppb) level is 70-125% . Thus the percentage recovery for Zn(II) and Cd(II) obtained from the proposed method was accepted.

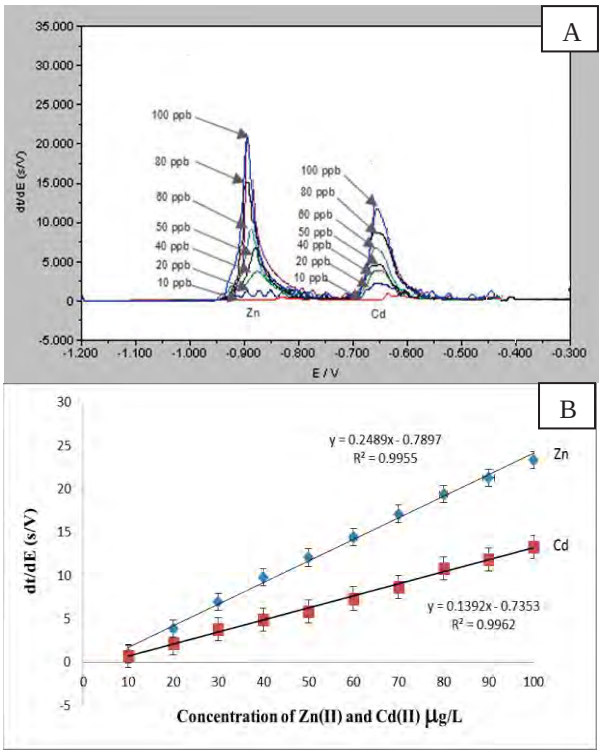

Figure 6. Potentiometric stripping obtained from SbFE system of solution containing Zn(II) and Cd(II) of increasing concentration, from 10-100 µg/L (A) and calibration graphs of Zn(II) and Cd(II) (B).

3.3 Application to real samples

The developed method was successfully applied to the simultaneous determination of Zn(II) and Cd(II) in water samples. The calibration graph was used for quantification of each metal. The accracy of the method was checked by means of comparison with those data obtained from ICP-OES. The results obtained for 4 water samples are summarized in Table 1 and Table 2. It was found that the results from the

proposed method were in good correlation with those of ICP-OES method.

Table 1: Determination of zinc in water samples

Sample	Concentration of zinc (μg/L)	
	ICP-OES	PSA-SbFE
1	7.93±0.43	7.53±0.63
2	17.97±0.74	16.35±0.74
3	27.50±0.93	28.37±0.94
4	47.74±2.47	48.51±0.79

Table 2: Determination of cadmium in water samples

Sample	Concentration of cadmium (μg/L)	
	ICP-OES	PSA-SbFE
1	8.50±0.66	8.02±0.91
2	17.78±0.93	16.15±1.04
3	26.45±1.14	27.06±1.84
4	43.90±1.36	42.80±1.61

4. Conclusions

In the present study preparation of in situ antimony film on glassy carbon electrode was employed for simultaneous determination of zinc and cadmium for anodic potentiometric stripping voltammetric. The proposed method provided high sensitivity and convenient operation for the determination of zinc and cadmium at trace level. The environmentally friendly SbFE can be used with a good reproducibility. Application for analysis of real water was demonstrated.

Acknowledgement

This project was financial supported by the Division of Chemistry, Department of Science, Faculty of Science and Technology, Rajamangala University of Technology, Bangkok, Thailand.

References

[1] M.R. L'Abbé and Peter W.F. Fischer, *Clinical Biochemistry* **19** (1986), 175-178.
[2] http://en.wikipedia.org/wiki/Cadmium_poisoning/ (Retrieved November 2012).
[3] N. Manutsewee, W. Aeungmaitrepirom, P. Varanusupakul and A. Imyim, *Food Chemistry* **101** (2007) 817-824.
[4] D. Atanassova, V. Stefanova and E. Russeva, *Talanta* **47** (1998) 1237-1243.
[5] D.V. Biller and K. W. Bruland, *Marine Chemistry* **130–131** (2012) 12-20.
[6] C.R.T. Tarley, V.S. Santos, B.E.L. Baeta and A. C. Pereira, *Journal of Hazardous Material* **169** (2009) 256-262.
[7] E. Fischer and M.G. van den Berg, *Analytica Chimica Acta* **385** (1999) 273-280.
[8] S. Stankovica, D. Cb icbkariia and J. Markoviib *Desalination* **213** (2007) 282–287.
[9] J.M.Estela, C.Tomás, A.Cladera and V.Cerdà, *Critical Reviews in Analytical Chemistry* **25** (1995) 91–141.
[10] E. Tesařová and K. Vytřas, *Electroanalysis* **21** (2009) 1075–1080.
[11] V. Urbanová, K. Vytřas and A. Kuhn, *Electrochemistry Communications* **12** (2010) 114-117.
[12] E.A. Hutton, S.B. Hočevar, L. Mauko and B. Ogorevc, *Analytica Chimica Acta* **580** (2006) 244-250.
[13] http://www.aoac.org/Official_Methods/slv_ Guidelines/ (Retrieved November 2012).

ELECTROGENERATED CHEMILUMINESCENCE OF CdTe QUANTUM DOTS CAPPED WITH THIOGLYCOLIC ACID FOR DETERMINATION OF THIOL COMPOUNDS

Triyaporn Kittisarakul[1, 2], Numpon Insin[1], Orawon Chailapakul[1, 2, 3], Suchada Chuanuwatanakul[1, 2,3*]

[1] Department of Chemistry, Faculty of Science, Chulalongkorn University, Pathumwan, Bangkok 10330, Thailand
[2] Electrochemistry and Optical Spectroscopy Research Unit, Department of Chemistry, Faculty of Science, Chulalongkorn University, Bangkok 10330, Thailand
[3] Center of Excellent for Petroleum, Petrochemicals and Advanced Materials, Chulalongkorn University, Bangkok 10330, Thailand

[*] E-Mail: suchada.c@chula.ac.th, Tel. +66 22187614, Fax. +66 22 187598

Abstract: Quantum dots (QDs) have attracted massive interest due to their excellent properties, such as, narrow and symmetric emission spectra, broad excitation spectra, better photostability than traditional fluorescent materials, as well as unique optical and electrochemical properties. For their promising advantages, QDs are widely used in various kinds of study, including determination and quantification of various compounds of interests. In this study, we applied electrochemical process to generate the luminescence signal of QDs and used these electrogenerated chemiluminescence (ECL) signals for the detection and measurement of thiol compounds in water-based samples. In our research, water-soluble thioglycolic acid (TGA)-capped CdTe QDs (TGA-CdTe QDs) were synthesized in aqueous medium. The structures and optical properties of TGA-CdTe QDs were characterized and studied by transmission electron microscopy (TEM) and optical spectroscopy, respectively. Then, the modified electrode was used in order to amplify ECL signal of TGA-CdTe QDs, resulting in efficiently high sensing for thiol compounds determination. The developed ECL sensor can be used to determine thiol compounds with simple operating processes while achieving better detection performance.

1. Introduction

Semiconductor nanocrystals (NCs) with excellent luminescent properties have been extensively attracted much interest due to their promising applications in many fundamental areas and technical importance in recent years [1-3]. With several advantages compared with conventional luminescence materials, quantum dots (QDs) provide a high photoluminescence (PL) quantum yield (QY), tunable emission wavelength because of the quantum size effect, multiplexing capabilities, and long-term photostability against photo-bleaching [4-6]. Especially, semiconductor QDs in Group II-VI including CdS, CdSe, and CdTe have been extremely studied because their emission in the visible range can be simply tuned by changing their diameter and the advances in their preparation methods.

Electrogenerated Chemiluminescence (ECL), a phenomenon that a chemiluminescence reaction is initiated and controlled by the application of an electrochemical potential, making luminophore species generated at the electrode undergo high-energy electron-transfer reaction to form excited states, and emission of light is then presented [7-9]. ECL is well-known as an alternative method for detection of various analytes since it combines the advantages of luminescence and electrochemical techniques providing the added selectivity. For instance, the timing and spatial location of the luminescent reaction can be selectively controlled. In addition to rapidity and simplicity of this method, high sensitivity can be achieved due to its low background intensity. ECL has been widely used in a large number of analytical chemistry in recent years [10-12]. The publications about ECL involving quantum dots (QDs) has increased significantly due to their optical, electrical, electrochemical and luminescent properties. The beginning of ECL study using QDs was started by Bard and his coworkers [13], who firstly reported ECL coupled with the use of Si QDs in an organic solvent with various types of coreactant. Since then, the ECL analytical techniques coupled with QDs have been rapidly developed; however, the effective methods to enhance QDs ECL performance are still in need for ECL application's further development in analytical field.

Carbon nanotubes (CNTs) have been exploited as electrode materials due to their outstanding electronic, chemical, and mechanical properties. CNTs-modified electrodes can exhibit excellent abilities compared with bare electrodes [14] and have been widely used in conventional electrochemistry [15] and ECL systems [16]. Hence, from the advantages of both CNTs-modified electrode and QDs, We were encouraged to study the CdTe QDs of ECL using CNTs-modified electrode. We expect that the enhanced QDs ECL, by reducing the injection barrier of electrons to the QDs, could be benefit for both studying of QDs ECL and accelerating the application of QDs ECL in analytical field.

In this research, for the first time, we propose a novel strategy for ECL sensor using TGA-capped CdTe QDs ECL sensor based on the CNTs-modified screen-printed electrodes (SPCNTEs) that are inexpensive, flexible to design, and easy to fabricate and modify. ECL procedures with cyclic voltammetry were conducted in 0.10 M phosphate buffer solution containing potassium peroxydisulfate ($K_2S_2O_8$) as a

co-reactant. The possible ECL mechanism was also proposed in this research. Furthermore, a novel method for the determination of homocysteine, a thiol-containing amino acid, was developed.

2. Materials and Methods

2.1 Chemicals and materials

Multi-walled CNTs were obtained from Nanomaterials Research Unit (Chiangmai University, Thailand). Prior to use, the CNTs were treated in a mixture of concentrated sulfuric acid (analytical grade, 95–97%, 1.84 g mL^{-1}, Merck, Germany) and concentrated nitric acid (analytical grade, 65 %, 1.39 g mL^{-1}, Merck, Germany). Cadmium chloride ($CdCl_2$), sodium tellurite (Na_2TeO_3), sodium borohydride ($NaBH_4$), tri-sodium citrate and thioglycolic acid (TGA) were purchased from Sigma-Aldrich (USA, ACS quality). All standard and reagent solutions were prepared from standard and analytical grade reagents using ultrapure water from a Milli-Q Ultrapure Water Purification System (Millipore, USA). The 0.1 M phosphate buffer (PBS, pH 8) containing 0.005M $K_2S_2O_8$ was used as the electrolyte throughout the experiment.

2.2 Instruments

We measured the ECL emission by using potentiostat (Autolab, The Netherland) and Electron Tubes (model 98285B) photomultiplier tube (PMT, model 98285B, Electron Tubes, UK). The operational potential for the PMT was provided by a stable power supply (Thorn-EMI model PM20D, Electron Tubes, UK). The sample cell, PMT, and voltage divider were encased in a custom-built light tight, while the detector output was recorded on a PC (Pentium IV) via a USB/RS-232 interfaced to the detector. The multimeter (UNI-T, UT60F, Hong Kong) was used to determine the peak.

The conventional three-electrode system used SPCNTEs as the working electrode, a platinum wire as the auxiliary electrode, and an Ag/AgCl (saturated KCl) electrode as the reference electrode. The ultraviolet-visible (UV-Vis) spectra were acquired on the UV-Vis spectrometer (8453E UV-Vis, Agilent, USA) using a 1.0 cm quartz cell. The photoluminescence (PL) spectra were measured with luminescence spectrometer (LS 45, Perkin Elmer, USA) and the excitation wavelength was fixed at 390 nm. Transmission electron microscopy (TEM) images were performed on transmission electron microscope (JEM-2100, JEOL, Japan).

2.3 Preparation of TGA-capped CdTe QDs

The thiol-capped CdTe QDs were synthesized using TGA as stabilizing agent according to the method reported previously [17] with slight modifications. Briefly, 38 mL of Milli-Q water and 10 mL of 0.01M $CdCl_2$ were transferred to a two-necked round bottom flask. Then, N_2 gas was purged in the flask for 10 min. 10 µL of TGA was added quickly at N_2 atmosphere. The pH of this solution was adjusted to 11.0 with 1 M NaOH. After the color of solution became clear, 55.5 mg tri-sodium citrate and 2 mL of 0.01 M Na_2TeO_3 were respectively added into this solution. 3.0 mg $NaBH_4$ was also added, and the solution was de-aerated by highly pure N_2 bubbling for 10 min. Finally, about 25 mL of this mixture was transferred to a reaction kettle, heated at 180 °C and refluxed for 60 min. As a result, thiol-capped CdTe QDs could be obtained. Afterward, the resulted products were precipitated by acetone. The superfluous Cd^{2+} and TGA were removed by centrifugation at 3000 rpm for 10 min. Then, the resultant precipitate was re-dispersed in water and then re-precipitated for more than two times by a copious amount of acetone. The products were kept in the dark for further use.

2.4 Fabrication of SPCNTEs

Before modifying the electrode, CNTs were functionalized by dispersing 1.0 g of CNTs in 50 mL of a 3:2 (v/v) of concentrated H_2SO_4 and HNO_3. The mixture was then agitated by ultrasonic wave for 12 h. After that, the CNT suspension was washed with Milli-Q water until the pH of the mixture approached 7, filtered and dried at 80 °C [18-19].

SPCNTEs were prepared in house by using silver ink (Electrodag 7019, Acheson, USA) as a conductive pad, which was printed onto the polyvinyl chloride (PVC) substrate and dried in an oven at 55 ± 0.2 °C for 1 h. The 5 % w/w CNTs was mixed with carbon ink (Electrodag PF-407C, Acheson, USA) to form the homogenized ink, which was then screen-printed onto the silver conducting part and dried in an oven at 55 ± 0.2 °C for 1 h.

2.5 Procedure for ECL detection

QDs ECL assay was achieved in 0.1 M PBS (pH 8) containing 0.005 M $K_2S_2O_8$ and 5.0×10^{-7} M CdTe QDs, scanning from 0 V to -1.8 V with scan rate of 0.1 Vs^{-1}. QDs ECL intensity was recorded at the PMT, which operated at a voltage of 800 V. According to the result, PMT gave the proportional output with ECL intensity, while the analytical signal of the ECL was at the maximal output potential corresponding to peak maximum. Certain volume of various concentrations of homocysteine standard solutions or sample solutions were added into the ELC cell and the quenched ECL intensities were recorded correnspoding to the concentration of homocysteine.

3. Results and Discussion

3.1 Characterization of TGA-capped CdTe QDs

TGA-capped CdTe QDs were characterized by UV–Vis and PL spectroscopy to confirm their particle size. As shown in Fig. 1, the UV–Vis spectra and PL spectra of CdTe QDs appeared at 505 nm and 587 nm, respectively. The estimated particle size of TGA-capped CdTe QDs was 2.47 nm as calculated in virtue of the following empirical equation [20].

$D = (9.8127 \times 10^{-7})\,\lambda^3 - (1.7147 \times 10^{-3})\,\lambda^2 + 1.0064\,\lambda - 194.84$

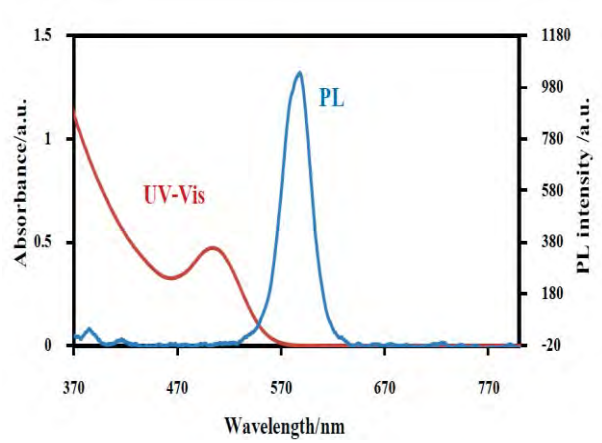

Figure 1. PL and UV–Vis absorption spectra of TGA-capped CdTe QDs.

where D is the average diameter (nm) of a given TGA-capped CdTe QDs and λ is the wavelength (nm) of the first excitonic absorption peak of the UV–Vis spectra. Moreover, morphology and particle size of TGA-capped CdTe QDs were also observed clearly by TEM image (Fig. 2). These results show that the average size of TGA-capped CdTe QDs was approximately 2.53 nm, and considered close to the value of 2.47 nm resulting from the empirical formula which seems to be convenient to calculate the size of CdTe QDs.

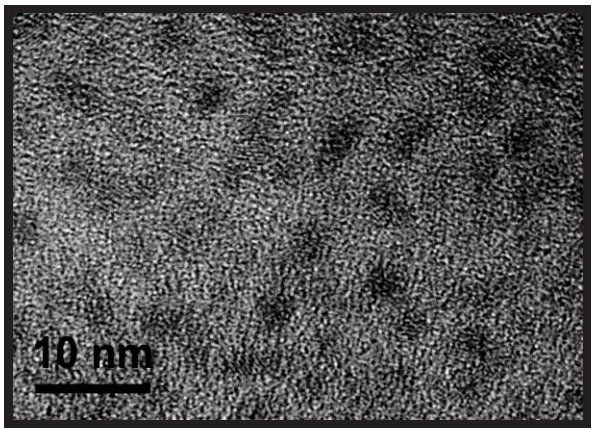

Figure 2. TEM image of TGA-capped CdTe QDs.

3.2 ECL behaviors of TGA-capped CdTe QDs at SPCNTEs

Fig. 3 shows the ECL behaviors of TGA-capped CdTe QDs using SPCNTEs, of which the cathodic current shifted positively comparing to TGA-capped CdTe QDs at bare screen-printed carbon electrodes (SPCEs). These results indicate that CNTs eased the CdTe QDs reduction and decreased the potential barriers on the SPCEs. Because ECL is light emission that arises from the electron-transfer reaction between electrogenerated species, a significant ECL signal of CdTe QDs at SPCNTEs (curves b) were observed as shown in Figure 4. The ECL signal showed that SPCNTEs greatly facilitated the ECL of CdTe QDs. In contrast, it can be seen that the ECL intensity of CdTe QDs at bare SPCEs (curves a) was much lower than that observed at SPCNTEs. These phenomena indicated that the effective surface area of the CNTs-modified electrode was much larger than that of the bare SPCEs. It explained that CNTs performed as nanowires connection between CdTe QDs and co-reactant with electrode surface, which introduced many electrocatalytic sites onto the electrode surface and encouraged the electron transfer through the conducting tunnels of CNTs. Consequently, electron transfer in the ECL process at SPCNTEs was accelerated as compared with that at bare SPCEs, and the efficiency of producing excited-state QDs was enhanced.

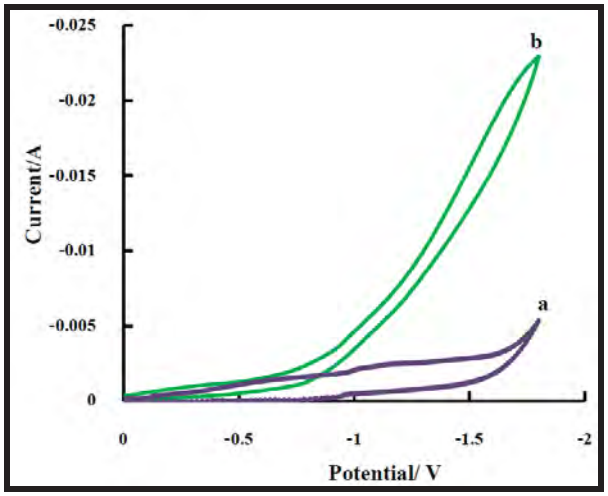

Figure 3. CV curves of TGA-capped CdTe QDs at (a) bare SPCEs and at (b) SPCNTEs in 0.1 PBS (pH 8) containing 0.005 M $K_2S_2O_8$.

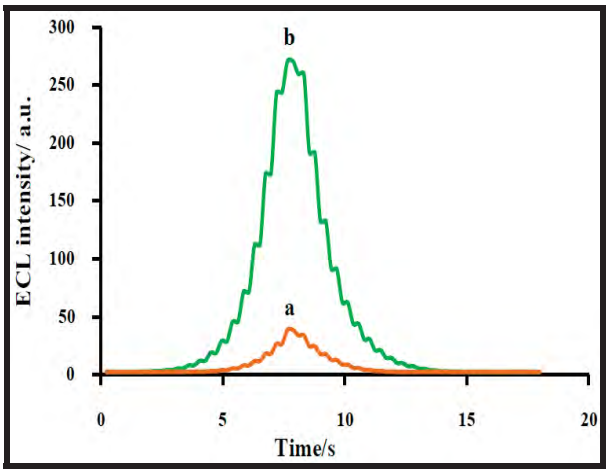

Figure 4. ECL-time curves of TGA-capped CdTe QDs at (a) bare SPCEs and at (b) SPCNTEs in 0.1 M PBS (pH 8) containing 0.005 M $K_2S_2O_8$.

3.3 Effect of coreactant

In ECL studies, there are two main mechanisms: one is ion annihilation ECL and another is co-reactant ECL. Thus, we propose that potassium peroxydisulfate ($K_2S_2O_8$) can accelerate the radical species generation, acts as the media in emission section, and then amplifies the QDs ECL intensity. Peroxydisulfate ion ($S_2O_8^{2-}$) is reduced to produce a strong oxidizing agent ($SO_4^{-\bullet}$), which quickly injects a hole into the valence band of reduced QDs to produce excited QDs. We suppose the reaction mechanism as the following equations:

$$CdTe + e^- \rightarrow CdTe^{-\bullet} \quad (1)$$

$$S_2O_8^{2-} + e^- \rightarrow SO_4^{2-} + SO_4^{-\bullet} \quad (2)$$

$$CdTe^{-\bullet} + SO_4^{-\bullet} \rightarrow CdTe^{*} + SO_4^{2-} \quad (3)$$

$$CdTe^{*} \rightarrow CdTe + h\nu \quad (4)$$

As theoretically predicted, the increased ECL intensity was observed when 0.005 M $S_2O_8^{2-}$ was added in the CdTe QD solution. The ECL spectrum shown in Fig. 5 indicate time-resolved ECL intensity from the solution of CdTe QDs and $S_2O_8^{2-}$, showing that the emission intensity increased 9–10 folds upon adding $S_2O_8^{2-}$.

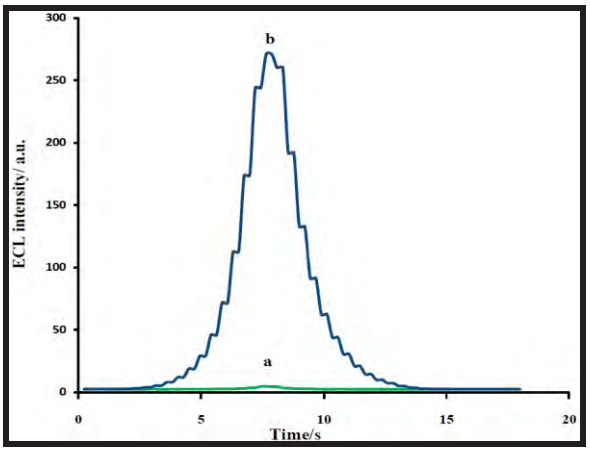

Figure 5. ECL-time curves of TGA-capped CdTe QDs at SPCNTEs in 0.1 M PBS (pH 8). (a) in the absence of $S_2O_8^{2-}$ and (b) in the presence of 0.005 M $S_2O_8^{2-}$.

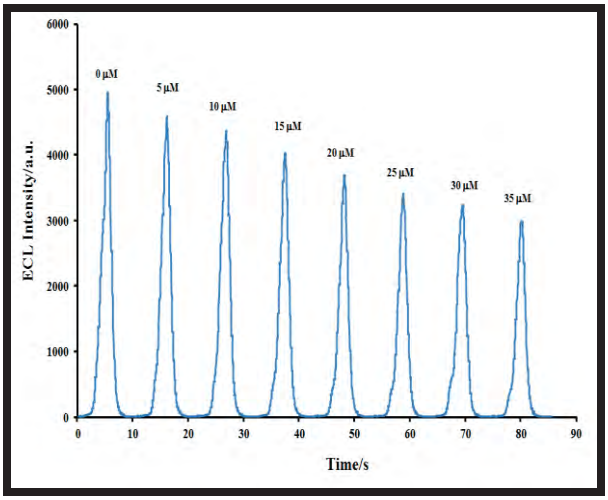

Figure 6. ECL-time curves of TGA-capped CdTe QDs at SPCNTEs in 0.1 M PBS (pH 8) containing 0.005 M $K_2S_2O_8$ in the presence of homocysteine at the concentration of 5, 10, 15, 20, 25, 30 and 35 μM.

3.4 Determination of homocysteine based on the quenching effect

Fig. 6 shows that, the CdTe QDs ECL intensity greatly decreased with the increase in homocysteine concentration from 5 μM to 35 μM. The relationship between ECL emission of TGA-capped CdTe QDs at SPCNTEs and homocysteine concentration revealed that the detection mechanism was based on the quenching effect of homocysteine. The responsible for quenching effect of homocysteine could be explained that a reactive sulfhydryl group (-SH) of homocysteine (RSH) react with dissolved oxygen, $S_2O_8^{2-}$ or their intermediate species produced in the processes of CdTe QDs ECL to form disulfide (RSSR) and resulted in the lowering of ECL intensity. For this reason, the homocysteine concentration dependence of the ECL intensity of CdTe QDs could be used for homocysteine quantification. Other thiol compounds could have similar effects to the ECL and will be furthur studied.

4. Conclusions

The cathodic ECL of TGA-capped CdTe QDs at SPCNTEs was studied for the first time. It was found that SPCNTEs could greatly enhance ECL intensity of CdTe QDs, decrease their ECL onset potential and ECL peak potential, which avoided the interferences resulted from high potential in TGA-cappd CdTe QDs solution. Furthermore, a novel approach for determination of homocysteine was developed based on the quenching effect of homocysteine in the CdTe QDs ECL sensor. Therefore, the simplicity, low-cost, excellent sensitivity and easy modification of SPCNTEs would allow their wide application in analytical field.

Acknowledgments

We gratefully acknowledge financial support from the National Research University Project of CHE and the Ratchadaphiseksomphot Endowment Fund (AM1009I-56) and Electrochemistry and Optical Spectroscopy Research Unit, Chulalongkorn University. We also grateful to the Department of Chemistry, Faculty of Science, Chulalongkorn University for providing chemicals and laboratory facilities. Special thanks are extended to Dr. Sakchai Satienperakul, Department of Chemistry, Faculty of Science, Maejo University for his advice and providing the PMT instrument for this research.

References

[1] X. L. Su and Y. Li, *Anal. Chem.* **76** (2004) 4806.
[2] Q. Lu, J. M. Moore, G. Huang, A. S. Mount, A. M. Rao, L. L. Larcom and P. C. Ke, *Nano Letters* **4** (2004) 2473.
[3] A. M. Smith and S. Nie, *Acc. Chem. Res*. **43** (2010) 190–200.
[4] Y. D. Yin and A. P. Alivisatos, *Nature* **437** (2005) 664.
[5] A. P. Alivisatos, *Science*. **271** (1996) 933.
[6] C. Burda, X. B. Chen, R. Narayanan and M. A.El-Sayed, *Chem. Rev*. **105** (2005) 1025.
[7] M. Richter, *Chem. Rev*. **104** (2004) 3003-3036.
[8] R. Pyati and M. M. Richter, *Annu. Rep. Prog. Chem., Sect. C: Phys. Chem.* **103** (2007) 12-78.
[9] R. J. Forster, P. Bertoncello and T. E. Keyes, *Annu. Rev. Anal. Chem.* **2** (2009) 359-385.
[10] V. R. Rivera, F. J. Gamez, W. K. Keener and M. A. Poli, *Anal. Biochem*. **353** (2006) 248.
[11] Y. Chi, J. Duan, S. Lin and G. Chen, *Anal. Chem.* **78** (2006) 1568.
[12] J. Wang, Z. Yang, X. Wang and N. Yang, *Talanta* **76** (2008) 85.
[13] Z. Ding, B. M. Quinn, S. K. Haram, L. E. Pell, B. A. Korgel and A. J. Bard, *Science* **296** (2002) 1293.
[14] Z. Y. Lin, J. J. Sun, J. H. Chen, L. Guo and G. N. Chen, *Electrochem. Commun*. **9** (2007) 269.
[15] X. Chu, D. X. Duan, G. L. Shen and R. Q. Yu, *Talanta* **71** (2007) 2040.
[16] Z. Y. Lin, J. H. Chen and G. N. Chen, *Electrochim. Acta* **53** (2008) 2396.
[17] N. Gaponik, D. V. Talapin, A. L. Rogach, K. Hoppe, E. V. Shevchenko, A. Kowski, A. Eychmu1ller and H. Weller**,** *J. Phys. Chem. B*. **106** (2002) 7177-7185.
[18] S. Chuanuwatanakul, W. Dungchai, O. Chailapakul and S. Motomizu, *Anal. Sci*. **24** (2008) 589–594.
[19] A. Kuznetsova, D. B. Mawhinney, V. Naumenko, J. T. Yates Jr., J. Liu and R.E. Smalley, *Chem. Phys. Letter* **321** (2000) 292–296.
[20] W. W. Yu, L. H. Qu, W. Z. Guo and X. G. Peng, *Chem. Mater*. **15** (2003) 2854.

INVESTIGATION OF KINETIC LEACHING FOR NUTRIENTS IN SOILS USING MEMBRANE HOLDER EXTRACTION CELL

Sirinart Preecha[1], Duangjai Nacapricha[1], Kanchana Uraisin[1], Wanpen Wiriyakitnateekul[3], Nongnuch Tantidanai-Sungayuth[1,2*]

[1] Department of Chemistry, Faculty of Science, Mahidol University, Ratchathewee, Bangkok, 10400,Thailand.
[2] Mahidol University, Kanchanaburi Campus, 199 Lumsum, Saiyok, Kanchanaburi, 71150, Thailand.
[3] Land Development Department, Phaholyothin Rd., Chatuchak, Bangkok, 10900,Thailand.

[*] E-Mail: scntt@mahidol.ac.th, Tel. +66 22015124

Abstract: Batch extraction procedures with a single extractant are widely used in soil science. However, only element concentration can be obtained. The aim of this study is to investigate kinetic leaching of some nutrients such as Ca, Cu, Fe, K, Mg, Mn, Mo, P, and Zn in soil by flow-through extraction approach. In the extraction procedure, Mehlich 1 solution was continuously pumped through the membrane holder extraction cell. The soil extracts were collected as subfractions for element concentration measurements by ICP-OES. The results of each element were shown as the extractograms. It was found that amounts of Ca, K, Mg, Mn and Zn were completely leached in the first subfraction, while Fe was gradually leached and became steady from the fourth to the last subfraction. For Cu, Mo and P, these elements were constantly available until the last subfraction.

1. Introduction

Single extractions are widely used in soil science. These extractions are commonly applied in many studies such as the quality of fertilizers and crops, the prediction of the uptake of essential elements, the diagnosis of deficiency and excess of one element in a soil, etc. [1].

The Mehlich 1 extraction method, also known as dilute double acid, was proposed by Adolf Mehlich in 1953. It is one of the single extractions that has been employed in several laboratories because it is simultaneous multi-element extraction. This method is available not only to macronutrients (Ca, K, Mg and P) but also to micronutrients (Cu, Fe, Mn and Zn) [2]. The Mehlich 1 method is more interesting with the development of the inductively coupled plasma - optical emission spectrometer (ICP-OES) since it can measure the element concentrations in the soil extracts at the same time [3-4]. The extraction procedure is performed in a batchwise fashion by mixing between the entire sample and the Mehlich1 solution at a defined solution/sample ratio for 5 minutes at room temperature. After that, the soil extract is separated from the solid phase by filtration and then analyzed. Therefore, the batch extraction method provides only the element concentrations.

Tantidanai-sungayuth et.al. (2010) proposed the flow-through extraction approach using membrane holder extraction cell [5]. In the extraction procedure, the extracting solution was continuously pumped through the extraction cell at constant flow rate and the soil extracts were collected in the order of subfractions. The extraction profile, that is referred as extractogram, is obtained by plotting the concentration of element versus the subfraction number. Therefore, the kinetic mobility and chemical associations of elements can be estimated. The extraction system offers other advantages such as the reduction of contamination from experimental environment, personal errors and also the manual separation step between solid and soil extract.

In this work, the flow-through extraction using membrane extraction holder with Mehlich 1 solution was employed to investigate kinetic leaching of macronutrients (Ca, K, Mg and P) and micronutrients (Cu, Fe, Mn, Mo, and Zn) by ICP-OES.

2. Materials and Methods

The continuous-flow extraction system

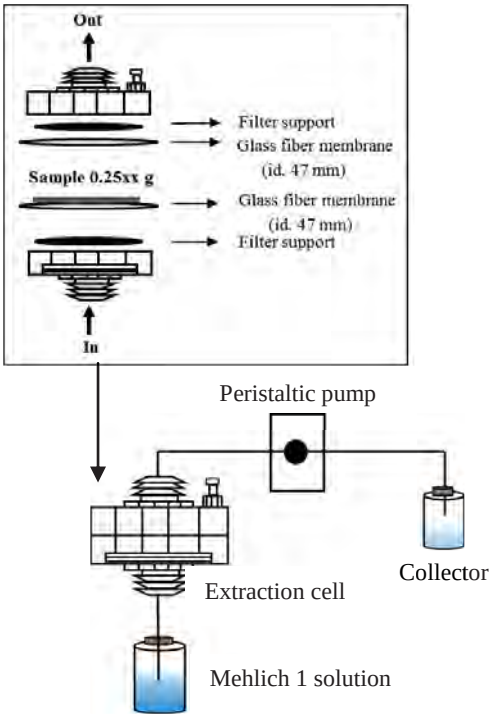

Figure 1. The continuous-flow extraction system setup and the composition of the membrane holder extraction cell.

The commercial membrane holder extraction cell (PALL) was fabricated from polycarbonate. A weighed soil sample 0.25xx g was placed in between two glass filter membranes (Whatman glass microfiber filter GF/B 1821 with 1-µm particle retention). The Mehlich 1 solution, that is a mixture of 0.05 N HCl and 0.025 N H_2SO_4, was flowed through the extraction cell at constant flow rate 5 ml min^{-1}. The soil extracts were collected in 10 polyethylene bottles at 30 ml volume intervals. The nutrient concentrations were measured by ICP-OES (Spectro Ciros CCD, Germany). The operating condition and wavelengths of these elements were shown in Table 2.

Table 2: The ICP-OES instrumental parameters.

ICP parameters	
2.1 Operating condition	
RF generator	27.12 MHz
RF incident power	1350 W
Nebulizer argon gas flow rate	0.6 L min^{-1}
Auxiliary gas flow rate	1.0 L min^{-1}
Coolant gas flow rate	12 L min^{-1}
Sample uptake flow rate	1.0 ml min^{-1}
2.2 Wavelength of emission line	
Element	**Wavelength (nm)**
Ca	422.673
Cu	324.754
Fe	238.204
K	766.490
Mg	279.553
Mn	257.610
Mo	202.030
P	214.914
Zn	213.865

Soil samples

Soil samples were provided by Land Development Department. Three soil samples were dried at 60 ° C and ground to pass through 2 mm sieve. The properties of each soil sample were presented in Table 3.

Table 3: The properties of soils.

Soil sample	%OM	%Clay	pH
S1	5.97	38	5.1
S2	6.04	37	5.0
S3	6.08	37	5.3

OM = organic matter (%)

3. Results and Discussion

The kinetic leaching patterns of three soil samples can be classified into 3 groups as shown in Figure 2 (a,b and c).

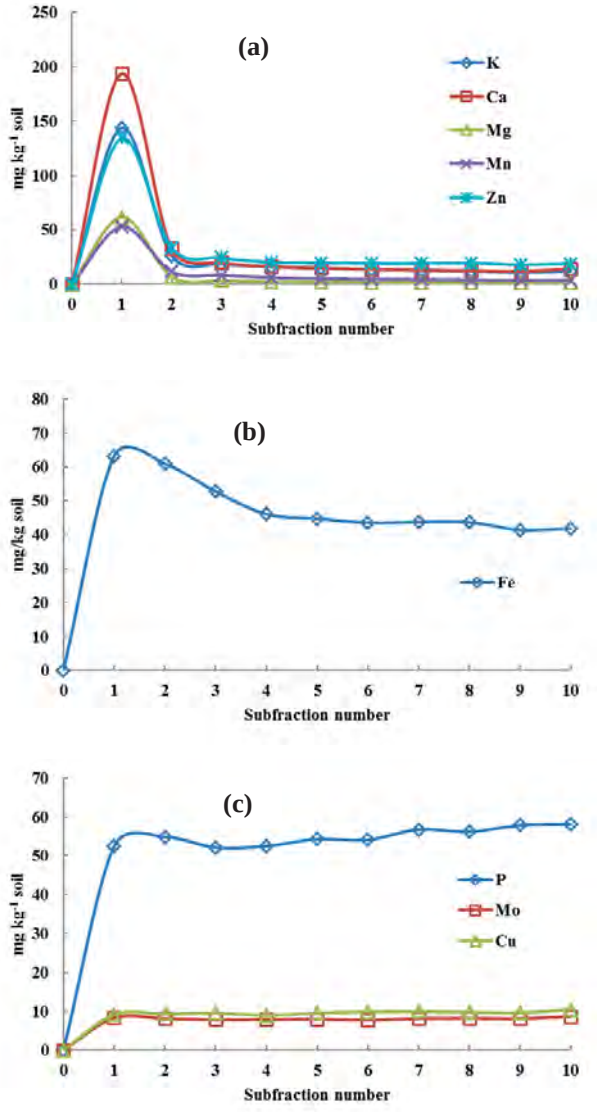

Figure 2. The extractograms of flow extraction with ICP-OES detection of (a) Ca, K, Mg, Mn and Zn, (b) Fe and (c) Cu, Mo and P in the soil sample S1.

The first group consisted of K, Ca, Mg, Mn and Zn as shown in Figure 2a. The extractograms indicated that all elements in this group were mostly leached out in the first subfraction number and rapidly decreased. Fe was also leached out at the highest amount in the first subfraction but it gradually decreased and became steady at the fourth subfraction number as shown in Figure 2b. The last group containing Cu, Mo and P as shown in Figure 2c was different from the others,the amounts of Cu, Mo and P were continuously leached out until the last subfractions of the observation. The extracted concentrations of all elements were derived

from the summation of peak area (subfraction number1-10) and presented in Table 4.

Table 4: The amounts of nutrients in the soils extracted by using the continuous-flow extraction system

Element	Extracted amount (mg kg^{-1} soil) mean±SD.		
	S1	S2	S3
Ca	341.05 (9.95)*	1004.03 (41.29)	1081.19 (9.32)
Cu	96.15 (25.07)	102.52 (27.07)	137.52 (47.12)
Fe	481.90 (15.10)	250.61 (30.94)	244.65 (57.43)
K	280.32 (25.01)	319.00 (6.77)	316.44 (23.09)
Mg	83.93 (4.56)	216.83 (6.08)	192.48 (1.85)
Mn	104.34 (7.73)	75.10 (6.85)	60.12 (4.95)
Mo	81.03 (27.92)	82.30 (20.65)	108.86 (34.65)
P	549.34 (138.74)	553.12 (125.31)	717.84 (209.82)
Zn	325.92 (32.17)	313.46 (8.00)	369.59 (30.42)

* The number in parenthesis denoted the standard deviation

The kinetic leaching via the exchange reaction may possibly be controlled by the clay and organic matter (humus) contents in soils. Humus substances (humin, humic acid and fulvic acid) that are predominate organic matters in soils have a very high cation exchange capacity when compared to clays. The stability of humic acids and fulvic acids with nutrient cations was expressed by the stability constant (K_{st}) as shown in Table 5.

Table 5: The stability constants of humic acids and fulvic acids with nutrient cations at pH 5.0 [6].

Nutrient	Stability constant (K_{st})	
	Humic acid (log K_{st})	Fulvic acid (K_{st})
Ca^{2+}	-	2.92
Cu^{2+}	12.60	8.69
Fe^{2+}	6.41	5.77
Fe^{3+}	8.46	-
Mg^{2+}	-	2.09
Mn^{2+}	-	2.78
Zn^{2+}	7.15	2.34

According to the stability constants of fulvic acids and humic acids as shown in table5, it was mentioned that Ca, Mg, Mn and Zn are loosely adsorbed on organic matter surfaces. For K, the attraction between K ions and organic matters is relatively weak [7]. Therefore, these elements were almost completely leached in the first subfraction number as shown in Figure 2a.

Due to the high stability constants of complexes of humic acids with Fe, the leaching of Fe is influenced from the fulvic acid complexes more than the humic acid complexes. The complexes of fulvic acids with Fe^{2+} and Fe^{3+} are assumed to be the cause of the gradual leaching in the first four subfraction numbers, as only the fulvic acid complex with Fe^{2+} may affect the constant leaching of the remaining subfraction numbers.

The last group of kinetic leaching consisted of Cu, Mo and P. Because of the very high stability constants of the complexes of fulvic acids and humic acids with Cu, the binding of Cu with these acids is extremely strong. The leaching of Cu occurs slowly and continuously throughout the extraction as shown in Figure 2c. Since Mo and P are negatively charged in soils, the kinetic leaching of Mo and P is associated with positively charged hydrous oxides of iron and aluminum, some type of 1:1-type clays and amorphous materials [7], instead of the humic and fulvic acids. Their leaching is more complex than nutrient cations because of the specific reactions between the anions and soil constituents although Mo and P provided the same kinetic leaching patterns as Cu.

4. Conclusions

The results illustrated that the flow-through extraction using membrane holder extraction cell can be used to investigate the kinetic leaching of plant nutrients, such as Ca, Cu, Fe, K, Mg, Mn, Mo, P, and Zn in the soils that indicated the strength of the attraction between plant nutrients and soil particles. Therefore, this extraction system can be used to estimate the dynamic conditions and the chemical associations of elements in the environment.

Acknowledgements

The author would like to thank the Center of Excellence for Innovation in Chemistry (PERCH-CIC) for financial support and Department of Chemistry, Faculty of Science, Mahidol University. And also thanks to Land Development Department for providing the soil samples.

References

[1] G. Rauret, *Talanta* **46** (1998) 449-455.
[2] J.T. Sims, in: G.M. Pierzynski (ed.), *Methods for Phosphorus analysis for Soils, Sediments, Residuals and Waters*. Southern Cooperative Series Bulletin No. 396, North Carolina State University, Raleigh, North Carolina, (2000), pp. 15.
[3] R.E. Franklin, L. Duis and B.R. Smith, *Comm Soil Sci Plant Anal* **37** (2006) 679-691.
[4] L. Bortolon and C. Gianello, *Comm Soil Sci Plant Anal*

43 (2012) 1615-1624.
[5] B. Chunpen, *Use of a continuous-flow sequential extraction method for speciation of phosphorus and cadmium in soil amended with phosphate rock and citric acid*, Master's Thesis, Mahidol University, (2010).
[6] D.S. Orlov, *Soil Chemistry*, A.A. Balkema Publishers, Vermont, USA (1992).
[7] N.C. Brady and R.R. Weil, *The Nature and Properties of Soils*, Prentice-Hall, Inc., New Jersey ,USA (1996).

SULFONIC ACID-FUNCTIONALIZED MCM-41-COATED MAGNETIC NANOPARTICLES FOR EXTRACTION OF CREATININE

Sakkarin Boontham[1*], Fuangfa Unob[1]

[1] Environmental Analysis Research Unit, Department of Chemistry, Faculty of Science, Chulalongkorn University, Pathumwan, Bangkok 10330, Thailand

[*]E-Mail: kintaro5104@hotmail.com (S. Boontham), Fuangfa.u@chula.ac.th (F.Unob)

Abstract: Jaffé method, a well-known procedure for determination of creatinine in biological samples, is based on the reaction of creatinine and picric acid in basic condition to give orange-red complex which can be analysed by UV-visible spectrometer. However, the method is known to have interference and the separation of creatinine from sample matrix is recommended. In this research, sulfonic acid functionalized MCM-41-coated Fe_3O_4 nanoparticles (Fe_3O_4/MCM-41/SO_3H) which have magnetic properties for easy separation from media and high surface area was synthesized and used to extract creatinine. The process begins with Fe_3O_4 preparation via co-precipitation of ferric and ferrous ions and then MCM-41 was coated on Fe_3O_4 surface. The results from X-ray Diffractometer (XRD) and Fourier transform infrared spectrometer (FTIR) showed the successful synthesis. After that Fe_3O_4/MCM-41 was functionalized with 3-mercaptopropyltrimethoxysilane and subsequently oxidized using H_2O_2 to convert thiol group to sulfonic acid group. Fe_3O_4/MCM-41/SO_3H was treated with 1 M NaCl solution before further use. The parameters affecting creatinine extraction were optimized including pH, amount of adsorbent, sample volume and eluent concentration. Under optimum condition, creatinine could be extracted from solution of pH 3 with 50 mg adsorbent using 0.5 mL sample and 0.5 M NaCl as eluent. The percent extraction of 90.6±1.1%, the percent elution of 96.0±1.3% and the percent recovery of 86.9±1.8% were achieved (n=3). Percent Fe leaching from the adsorbent was determined by inductively coupled plasma atomic emission spectrometer (ICP-AES) and it was found to be 0.05%. The adsorbent Fe_3O_4/MCM-41/SO_3H has good potential for the use in creatinine extraction from human urine samples.

1. Introduction

Creatinine is a waste product from metabolic process of creatine and phosphocreatine. It is generated and spread into the bloodstream [1]. Elimination of creatinine in plasma is mainly achieved by glomerular filtration and excretion with urine [2]. Amounts of creatinine in the 24-hour urine samples are useful information for the use as an indicator of the glomerular filtration rate (GFR) which is roughly constant for an individual person [3]. Therefore, alteration of urinary creatinine content can indicate renal problems [4]. Moreover, urinary creatinine concentration can be used as indicator of urine dilution, so it was often used as a normalization factor in the determination of other substances in urine samples [4].

At present, there are numbers of method for determination of creatinine such as enzymatic methods [5-6] and chromatographic methods [7-8]. However, Jaffé method [9] is commonly used method in clinical laboratory because it is simple, rapid and low operating cost method, compared to other methods. This colorimetric method based on the reaction of creatinine and picric acid in an alkaline solution. The orange-red complex formed can be analysed by UV-visible spectrometer. Nevertheless, sample matrix in biological specimens such as glucose [10], cycloketone [11] and albumin [12] would interfere the method sensitivity and accuracy and sample preparation is required.

In this research, sulfonic acid functionalized MCM-41-coated magnetic nanoparticles (Fe_3O_4/MCM-41/SO_3H) which have magnetic properties for easy separation from sample media and high surface area was synthesized. The obtained adsorbent was used for extraction and isolation of creatinine from sample matrix before the determination by Jaffé method. The parameters affecting extraction efficiency were optimized and application for creatinine determination in human urine sample was also investigated.

2. Materials and methods

2.1 Apparatus

UV-visible spectrometer (HP 8453) was employed for the determination of creatinine by Jaffé method. Inductively coupled plasma atomic emission spectrometer (Thermo iCAP 6000 Series) was employed to determine Fe leached from adsorbent during the extraction. Fourier transform infrared spectrometer (Nicolet 6700) and X-ray Diffractometer (Rigaku 1200+) were used for characterization of Fe_3O_4 and Fe_3O_4/MCM-41.

2.2 Material

Tetraethyl orthosilicate (TEOS, 98%), 3-mercaptopropyl trimethoxysilane (MPTS, 95%), ethylenediaminetetraacetic acid disodium salt dihydrate, hexadecyltrimethylammonium bromide (CTAB) and creatinine anhydrous of reagent grade were purchased from Sigma-Aldrich. 30% H_2O_2

solution (AR grade) was purchased from Merck. All chemicals were used without further purification.

2.3 Preparation of MCM41-coated magnetic nanoparticles (Fe_3O_4/MCM-41)

Fe_3O_4 magnetic nanoparticles (MNPs) were synthesized via co-precipitation method as previously described [13]. Five grams of the obtained MNPs were dispersed in a mixture of 10.5 g of CTAB, 261 mL of deionized water and 121.5 mL of 25% NH_3 solution and then 50 mL of TEOS was added dropwise. The mixture was stirred at 35 ºC for 3 hours and then left at room temperature for 24 hours. The solid was filtered and washed with deionized water until neutral pH of the washing solution (using pH papers) was observed. The resultant solid was dried in an oven at 120 ºC overnight and then calcined at 550 ºC for 8 hours. The obtained Fe_3O_4/MCM-41 was characterized by Fourier transform infrared spectrometer (FTIR) and X-ray diffractometer (XRD).

2.4 Surface modification of Fe_3O_4/MCM-41

Four grams of the obtained Fe_3O_4/MCM-41 was dispersed into a mixture of 15.9 mL of 3-mercaptopropyl trimethoxysilane in 160 mL of deionized water and 160 mL of ethanol. The mixture was sonicated using sonication bath and then refluxed under nitrogen atmosphere for 5 hours. The solid was filtered and washed with deionized water. The exiting thiol groups on Fe_3O_4/MCM-41 surface were oxidized to sulfonic acid group by dispersion of the resultant solid into a solution containing 160 mL of H_2O_2, 160 mL of deionized water and 160 mL of ethanol. The mixture was stirred at room temperature for 24 hours. After that the solid was filtered and washed with plenty of deionized water. It was further treated with 160 mL of 1 M NaCl, washed again with deionized water and then dried at 120 ºC overnight.

2.5 Parameters optimization

The extraction efficiency was observed under various experimental conditions such as different amount of adsorbent, sample pH, sample volume and eluent concentration to find optimum condition of the extraction process. Moreover, Fe leaching from adsorbent at various pH was also studied.

Extraction procedure: 50 and 100 mg of adsorbent were added into polyethylene test tubes. They were washed twice with 5 mL of 1 M NaCl and once again with 5 mL of deionized water. After that 0.50, 0.75 and 1.00 mL of creatinine standard solution were added and HNO_3 solution was added subsequently to adjust final volume to 5.00 mL. The solution pH was adjusted to the value of 3, 4 and 5 with HNO_3 solution. The mixtures were stirred for an hour and then the solids were separated by external magnetic force or centrifugation. Supernatants were kept for the analysis of residual creatinine. After that 5.00 mL of NaCl of various concentrations (0.1, 0.5 or 1.0 M) were added as eluent. The mixtures were stirred for an hour. The solids were separated and supernatants were kept for the analysis of eluted creatinine.

Creatinine analysis procedure: 3 mL of creatinine sample was added into a test tube. After that 1 mL of 0.01 M picric acid and 1 mL of 0.75 M NaOH were added subsequently. The solution was stirred at 25 ºC for 15 minutes and its absorbance was measured at 500 nm by UV-visible spectrometer.

Fe leaching determination: the amount of Fe leaching from the adsorbent into the extracted and eluted solutions were determined by inductively coupled plasma atomic emission spectrometer (ICP-OES) and percent Fe leaching at various extraction pH was calculated.

3. Results and Discussion

3.1 FTIR and XRD characterization of Fe_3O_4 and Fe_3O_4/MCM-41

IR spectra of Fe_3O_4 and Fe_3O_4/MCM-41 (Figure 1) show broad peaks at about 3300 cm^{-1} and intense peaks at about 550 cm^{-1} corresponding to OH-stretching and Fe-O stretching, respectively. These results indicate the presence of hydroxyl group and Fe-O bond of Fe_3O_4. However, only Fe_3O_4/MCM-41 spectra show Si-O-Si stretching at 1042 cm^{-1}. This implies that the obtained Fe_3O_4/MCM-41 also has Si-O-Si bond of MCM-41. Moreover, XRD diffractograms of both materials (Figure 2) show characteristic peaks of Fe_3O_4 at 2theta about 30.5º, 36.0º, 43.0º, 53.7º, 57.0º and 62.8º but only diffractograms of Fe_3O_4/MCM-41 (Figure 3) display signal at 2theta about 2.3º, 4.0º and 4.7º which are characteristic peaks of MCM-41. The described information confirms that the synthesized Fe_3O_4 and Fe_3O_4/MCM41 composite were obtained.

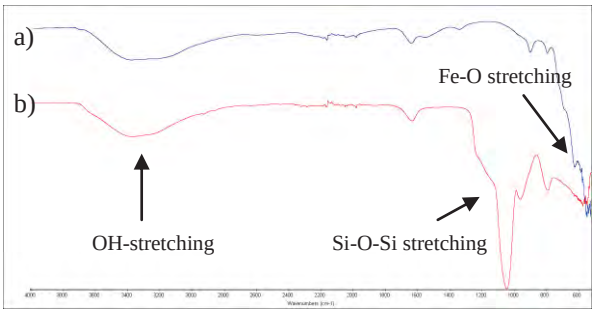

Figure 1. FTIR spectra of Fe_3O_4 (a) and Fe_3O_4/MCM-41 (b).

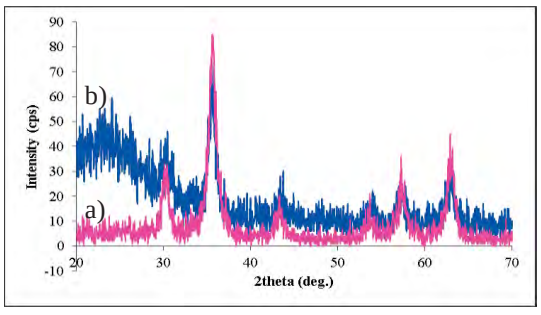

Figure 2. XRD diffractogram of Fe_3O_4 (a) and Fe_3O_4/MCM-41 (b) at 2theta in a range of 20º to 70º.

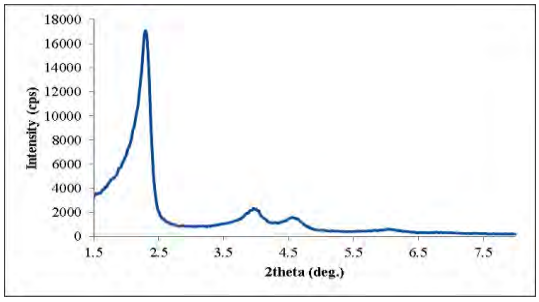

Figure 3. XRD diffractogram of Fe_3O_4/MCM-41 at 2theta in a range of 1.5º to 8.0º

3.2 Parameters optimization

Sample pH: in acidic solution, creatinine is protonated and can be extracted by ion-exchange mechanism. However, extraction of creatinine at pH 1-2 using Fe_3O_4/MCM-41/SO_3H can cause the leaching of Fe into extracted and eluted solution, so the effect of sample pH on the extraction efficiency was studied over the range of 3-5. A solution of 60 mg/L creatinine was used in this study. The results show that higher extraction efficiency could be achieved by lowering solution pH. It could be explained by an increase in the content of protonated creatinine ions when the acidity of solution increases. The highest percent extraction was achieved at pH 3 with an acceptable value of percent Fe leaching (Table 1). Therefore, it was selected as optimum pH.

Table 1. Effect of sample pH on extraction efficiency and percent Fe leaching from the adsorbent (n=3).

pH	%Extraction	%Fe leaching
3	92.4±0.2	0.05±0.01
4	86.7±1.0	0.05±0.01
5	83.5±1.1	0.03±0.01

Amount of adsorbent: The effect of adsorbent amount on the extraction efficiency was investigated. The obtained results (Figure 4) show that an increase of adsorbent amount from 50 to 100 mg was not beneficial. Therefore, 50 mg of adsorbent was selected as optimum value.

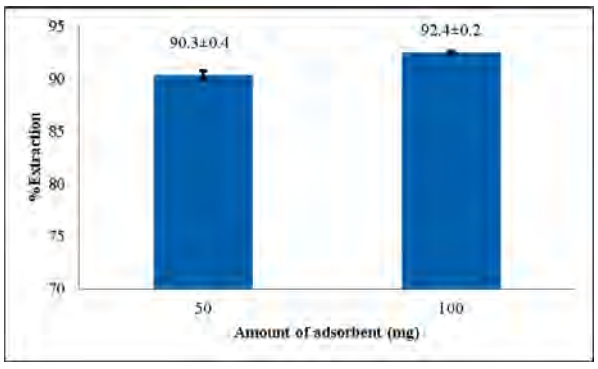

Figure 4. Effect of adsorbent amount on extraction efficiency (n=3); extraction condition: 1 mL of creatinine standard solution (60 mg/L, pH 3) and an hour of extraction time.

Sample volume: The effect of sample volume on the extraction efficiency was studied over the range of 0.50-1.00 mL. Alteration of sample volume using in extraction process did not affect the extraction efficiency (Figure 5). However, incomplete elution and poor recoveries were observed when samples volume was higher than 0.5 mL. Thus, 0.5 mL of sample volume was selected.

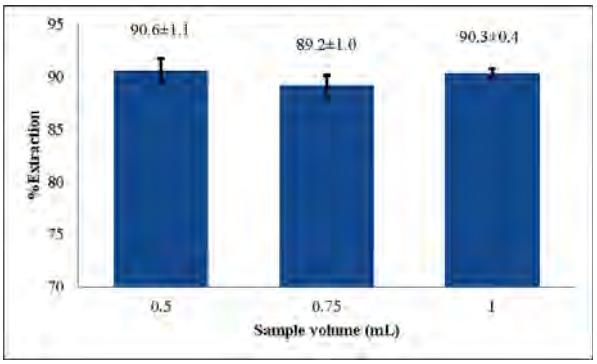

Figure 5. Effect of sample volume on extraction efficiency (n=3); extraction condition: 60 mg/L creatinine standard solution (pH 3), 50 mg of adsorbent and an hour of extraction time.

Eluent concentration: The effect of sodium chloride concentration within the range of 0.1-1.0 M on the elution efficiency was investigated to find suitable concentration of NaCl for creatinine elution. Using unnecessary high concentration of NaCl solution is a waste of chemicals. Furthermore, the higher alkali ions concentration in analysed solution, the lower sensitivity of the Jaffé method could be observed. The results show that elution efficiency is increased when higher concentration of NaCl is employed (Figure 6). However, increasing NaCl concentration from 0.5 to 1.0 M did not increase percent elution, so 0.5 M of NaCl was selected as optimum eluent.

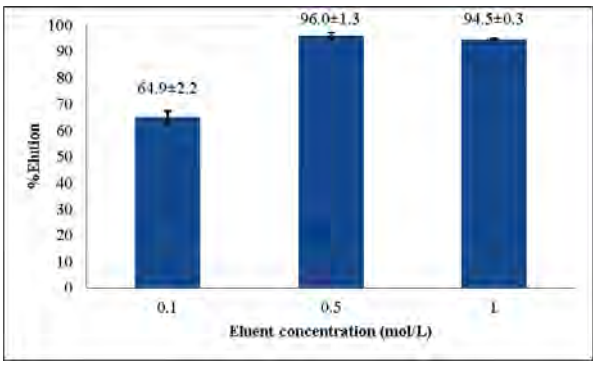

Figure 6. Effect of eluent concentration on extraction efficiency (n=3); extraction condition: 1 mL of creatinine standard solution (60 mg/L, pH 3), 50 mg of adsorbent and an hour of extraction and elution time.

3.3 Determination of creatinine in human urine sample

The possibility of creatinine determination in real sample using synthesized adsorbent was investigated by spiked method. The analysis was performed following the described extraction and analysis procedure under optimum condition. Standard solutions containing creatinine in the concentration range of 8-60 mg/L were extracted. The eluted solution was analyzed and then obtained results were used for calibration curve construction (Figure 7). Fresh urine sample from a healthy female with no kidney disease was diluted 50 times and the solution pH was adjusted to the value of 3 with HNO_3 solution. The obtained solution was employed as urine blank sample. The creatinine standard solution was added into the urine blank sample at various concentrations. The obtained solution was employed as urine spiked samples. The recoveries in the range of 97.3-98.7 were observed (Table 2). The results show that the synthesized adsorbent can be applied for analysis of creatinine in human urine samples.

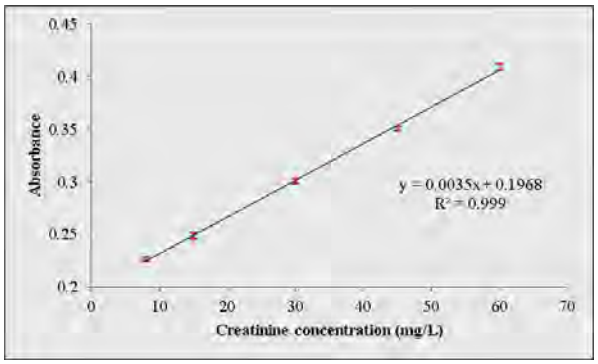

Figure 7. Calibration curve of creatinine constructed through extraction process (n=3).

Table 2. Determination of the creatinine in human urine sample (n=3).

Creatinine (mg/L) added	Creatinine (mg/L) found	%Recovery	%RSD
0	472.2	-	-
500	959.7	97.5	1.4
1000	1445	97.3	1.1
1500	1952	98.7	0.5

4. Conclusions

In this work, sulfonic acid functionalized MCM-41-coated magnetic nanoparticles (Fe_3O_4/MCM-41/SO_3H) was synthesized and used for extraction and isolation of creatinine from matrix interferences prior to the determination by conventional Jaffé method. The obtained adsorbent has high surface area and can be removed easily from sample matrix by external magnetic force. The parameters optimization was performed to achieve the effective extraction. By employing the proposed method under optimum condition, the adsorbent was used for the extraction and determination of creatinine in human urine sample with satisfactory results.

Acknowledgements

This work is financial supported by Department of Chemistry and Environmental Analysis Research Unit, Faculty of Science, Chulalongkorn University.

References

[1] H.D. Hoberman, E.A.H. Sims and J.H. Peters, *J. Biol. Chem.* **172** (1948) 45–58.
[2] M. Wyss, R. Kaddurah-Daouk, *Physiol. Rev.* **80** (2000) 1107–1213.
[3] D. Jacobi, C. Lavigne, J. Halimi, H. Fierrard, C. Andres, C. Couet and F. Maillot, *Diabetes Res. Clin. Pract.* **80** (2008) 102–107.
[4] T. Smith-Palmer, *J. Chromatogr. B.* **781** (2002) 93–106.
[5] T. Yao and K. Kotegawa, *Anal. Chim. Acta.* **462** (2002) 283–291.
[6] A. Radomska, E. Bodenszac, S. Glab and R. Koncki, *Talanta* **462** (2002) 283–291.
[7] J. Ruiz-Jiménez, J.M. Mata-Granados and J.M. Laque de Castro, *Electrophoresis* **28** (2007) 789–798.
[8] D. Tsikas, A. Wolf and J.C. Frolich, *Clin. Chem.* **50** (2004) 201–203.
[9] H. Husdam and A. Rapoport, *Clin. Chem.* **14** (1968) 222–238.
[10] S. Viraraghavan and K.G. Blass, *J. Clin. Chem. Clin. Bio.* **28** (1990) 95–105.
[11] M.H. Krooll, N.A. Roach, B. Poe and R.J. Elin, *Clin. Chem.* **33** (1987) 1129–1132.
[12] H.L. Pardue, B.L. Bacon, M.G. Nevius and J.W. Skoug, *Clin. Chem.* **33** (1987) 278–285.
[13] W. Jiahong, Z. Shourong, S. Yun, L. Jingliang, X. Zhaoyi and Z. Dongqiang, *J. Colloid. Interf. Sci.* **349** (2010) 293–299.

DETERMINATION OF ANTI-OBESITY DRUGS IN DIETARY SUPPLEMENTS FOR WEIGHT CONTROL BY CAPILLARY ELECTROPHORESIS

Natthaphong Chomvana, Natchanun Leepipatpiboon, Thumnoon Nhujak*

Chromatography and Separation Research Unit, Department of Chemistry, Faculty of Science, Chulalongkorn University, Pathumwan, Bangkok 10330, ThailandAffiliation

Abstract: Capillary zone electrophoresis (CZE) was optimized and validated for the determination of five contraband anti-obesity drugs in supplements for weight control: fenfluramine, ephedrine, pseudoephedrine, phentermine and sibutramine, within 10 min using a 100-mM Tris/phosphate buffer (pH 2.5) containing 20% acetonitrile in a fused-silica capillary under applied voltage of 25 kV and temperature of 25 ºC. This method allows the reliable detection of these adulterated drugs down to lower than 1 ppm with limits of detection (LOD) and limits of quantitation (LOQ) in ranges of 0.10-0.20 and 0.45-1.00 ppm, respectively, along with acceptable intraday and interday precision in migration time (t_m) and corrected peak area (A'_{corr}) shown by relative standard deviation of < 1.0% for tm and < 5.0% for A'_{corr}. A high linearity was obtained for calibration plots between peak area and concentration for all substances in levels of LOQ to 50 ppm, with correlation coefficients in the range of 0.9993–0.9997. Using this validated method for analysis of real samples extracted by 1:10 ethanol:water with proper dilution, sibutramine was found to be adulterated in four out of eight capsule sample of weight control, up to 5216.60 ppm (2.2% wt/wt).

1. Introduction

Supplements with slimming properties are a popular alternative for weight loss because they are simpler and more effective than exercise or diet. However, weight loss supplement may be adulterated with anti-obesity drugs especially some addictive, controlled or revoked substance. The mostly preferred anti-obesity drugs adulterated in supplement include sibrutramine (S), phentermine (P), ephedrine (E), pseudoephedrine (PE), fentermine (F), as shown in Figure 1. These drugs cause reducing hungriness and increasing metabolism, leading to weight loss. If consumers take these drugs consecutively for a long time without any control, they may be dangerous from side effects to the various systems of the body and to death. Adulterated anti-obesity drugs in the supplements for weight control are prohibited by the Food and Drug Administration [1-3]. However, the smuggling people still distribute in both general and online market. Therefore the analysis of these anti-obesity drugs is necessary for safety of consumers.

Analytical separation approaches developed for determination of the anti-obesity drugs include gas chromatography (GC), high-performance liquid chromatography (HPLC) and capillary electrophoresis (CE). Previous works on GC are for example, F in the blood [4] and S in urine [5]. In HPLC, the following works have been reported for determination of these drugs in a variety of samples; E/PE in blood [6] and urine [7], F/P/E/other in blood [8], E/PE in herbs [9], S/F/other in supplement tablets [10] and teas [11], E/other in supplement tablets [12], S/other in supplement powders [13], E/PE in herbal medicine powders [14], S/F/other in supplement powders [15] and S/F/E in supplement powders [16].

CE [17] is a separation technique in a capillary containing an electrolyte solution under the influence of applied electric field. CE separation mechanism is based on the difference in electrophoretic mobility of analytes. The simplest and most common type is capillary zone electrophoresis (CZE) which the capillary consists of a typical buffer such as borate, phosphate and acetate. Detector commonly used in CE is UV-Vis. Previous CZE works on determination of these drugs are for example; F/P/other substances in herbal powder and capsules for weight loss [18], E/other in herbal medicine powder [19] and supplement capsules [20]. Therefore, the aim of this work is to optimize and validate a CZE method for simultaneous determination of S, F, P, E and PE adulterated in dietary supplements for weight loss control.

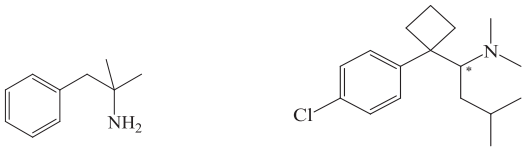

Phentermine, P (pK_a = 10.1) Sibutramine, S (pK_a = 8.5)

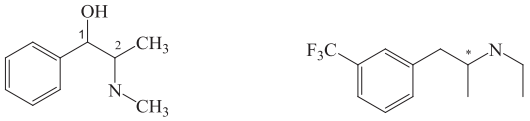

1R,2S- or *1S,2R*-Ephedrine, E (pK_a = 9.6) *R*- or *S*-Fenfluramine, F (pK_a = 10.1)

1R,2R- or *1S,2S*-Pseudoephedrine, PE (pK_a = 9.8)

Figure 1. Structures of five anti-obesity drugs.

2. Materials and Methods

2.1 Chemicals

Standards: Sibutramine (S), phentermine (P), fenfluramine (F), ephedrine (E), pseudoephedrine (PE)

were purchased from Sigma-Aldrich (Steinheim, Germany). Methanol (MeOH), phosphoric acid and hydrochloric acid were obtained from Merck (Darmstadt, Germany); acetonitrile (ACN) and tris-(hydroxymethyl) aminomethan form Sigma-Aldrich (Steinheim, Germany); sodium hydroxide form Labscan Asia (Thailand) Co, LTD. Internal stadrad (IS) is a p-toluidrine, was obtained from Sigma-Aldrich (Steinheim, Germany) The real samples were purchased from an online market (Thailand) and their brand names cannot be disclosed.

2.2 Preparation of buffer and standard solutions

A pH 2.5 tris-phosphate buffer is prepared by titrating a 500-mM phosphoric acid solution with a 5.0-M tris-(hydroxymethyl) aminomethane solution. Then the buffer was diluted five-fold with Milli-Q water and ACN or MeOH to give a 100-mM phosphate buffer containing an organic solvent at 0-40% (v/v). All running buffers were filtered through 0.45 μm filters, and then sonicated in a water bath for 10 min prior to use for CE analysis.

Stock standard solutions at 1000 ppm each in 4:6 MeOH:Milli-Q water were separately prepared by dissolving solid standards with MeOH and then diluting these with Milli-Q water. Working standard solutions containing five standards were prepared by pipetting an appropriate amonut of each stock standard solution and then diluting these with Milli-Q water.

2.3 Sample Preparation

Each representative powder sample was obtained from 12 capsules and its average weight per capsule was determined. An appropriate amount of homogeneous powder sample was weighted, and then extracted with a 1.0 ml of 10:1 Milli-Q water:EtOH by sonicating this in a water bath for 10 min, and then 12,000 ppm centifugting for 10 min at room temperature. Prior to CE analysis, each aliqout was filtered through a 0.45 μm filter, and appropriately diluted with 10% buffer.

2.4 CE conditions

All CE experiments were performed on an MDQ Beckman CE Instrument (Beckman Coulter, Inc., CA). An uncoated fused silica capillary used was 50 μm i.d. × 60.2 cm (50 cm to detector). The temperature was maintained at 25 ^{o}C. The following conditions were used for CE analysis; voltage of +25 kV, 0.5 psi pressure injection for 10 s, and Photo diode array-UV detection by scanning in a range of 200-400 nm and monitoring at 214 nm. Prior to analysis each day, the capillary was rinsed with 0.1-M phosphoric acid for 10 min followed by the running buffer for 10 min. Between each injection, the capillary was rinsed with 0.1-M phosphoric acid and a running buffer for 3 min.

3. Results and Discussion

3.1 Optimization conditions

A pH 2.5 100-mM tris-phosphate buffer was chosen in order that five weak base analytes of interest, with their pKa in a range of 8-10 [21], carry a fully positive charge (pH < pKa at least 2 units). Phosphate anions do not disturb the measurement with UV detector (range 200-300 nm). A tris-H^+ co-ion was used to obtain electrophoretic mobility matching between the co-ion and analyte ions in order to reduce peak distortion caused by electromigration dispersion [17]. Adding organic solvent in the buffer affects a change in electrophoretic mobilities of the analytes [17], and therefore, may lead to improve simultaneous separation of the several analytes. In comparison of ACN and MeOH added into the buffer at the same level in a range of 0-40%, ACN provided less migration time (t_m) and better separation of five test analytes. Figure 2 shows CZE electropherograms of five analytes using 0-40% ACN in the buffer. In order to compromise between fast analysis time, achieve base line resolution (R_s > 2.0 for quantitative analysis) and current stability, 20% ACN in a 100-mM phosphate buffer at pH 2.5 was chosen for validation of the method and application to real samples.

3.2 Validation of the method

Limit of detection (LOD) and limit of quantitative (LOQ) are defined as the concentrations of analyte giving a signal-to-noise ratios of 3 and 10, respectively. As shown in Table 1, instrumental LOD and LOQ for five analytes were obtained in a range of 0.1-0.2 ppm and 0.45-1.0 ppm, respectively, Using LOQ, it can be implied to quantitatively determine 1.1-2.5 mg/kg of five analytes in a solid sample, estimated that a final sample solution was prepared by weighting 0.40 g of a solid sample and then dissolving these with 1.0 ml of a solvent (1:10 EtOH:water). This sufficiently allows to measure the five analytes intently adulterated with the sample.

Internal calibration plots were established by plotting A'corr against the concentrations of each standard at seven levels in a range of LOQ to 50 ppm, where A'corr is the ratio of corrected peak area, peak area divided by migration time, of the standard to that of the internal standard. Highly linear relationship was obtained with correlation coefficient r2 ranging from 0.9994 to 0.9997.

Accuracy and precision for quantitative analysis were assessed at three levels of LOQ, 5 and 30 ppm. Intraday precision in t_m and A'_{corr} was evaluated from five consecutive runs, while interday precision from five consecutive days and each day for five runs. For overall five analytes at these three concentrations levels abovementioned, accepted intraday and interday precition were obtained with relative standard deviation (RSD) of <1% for t_m and <5.0% for A'_{corr}, respectively. Satisfactory accuracy was also obtained with recoveries of 81-110% at LOQ (except 76-81% for S), 88-102% at 5 ppm and 86-106% at 30 ppm, with 96% of the recovery data being within the acceptable range of 80-110% for the concentration in a range of 0.1-10 ppm and 90-100% at 100 ppm [22].

3.3 Application to real samples

Eight samples of capsule dietary supplements from different suppliers were determined for five adulterants. Using a spiking technique and comparing the UV spectra of standard peaks with the peaks of the sample at comparable t_m, only sibutramine was found in four out of these eight samples as an example in Figure 3, with the amount levels of 1.4 to 2.2% w/w.

Table 1 Calibration plots, LOD, LOQ

Analyte	Concentration range (ppm)	Calibration plots			LOD (ppm)	LOQ (ppm)
		Slope	Intercept	r^2		
Phentermine (p)	0.45-50.00	0.1651	0.0155	0.9997	0.15	0.45
Pseudoephedrine (PE)	0.50-50.00	0.1245	0.0058	0.9995	0.15	0.50
Ephedrine (E)	0.50-50.00	0.1153	0.0125	0.9994	0.15	0.50
Fenfluramine (F)	0.55-50.00	0.1057	0.0355	0.9994	0.10	0.55
Sibutramine (S)	1.00-50.00	0.1299	0.0375	0.9994	0.20	1.00

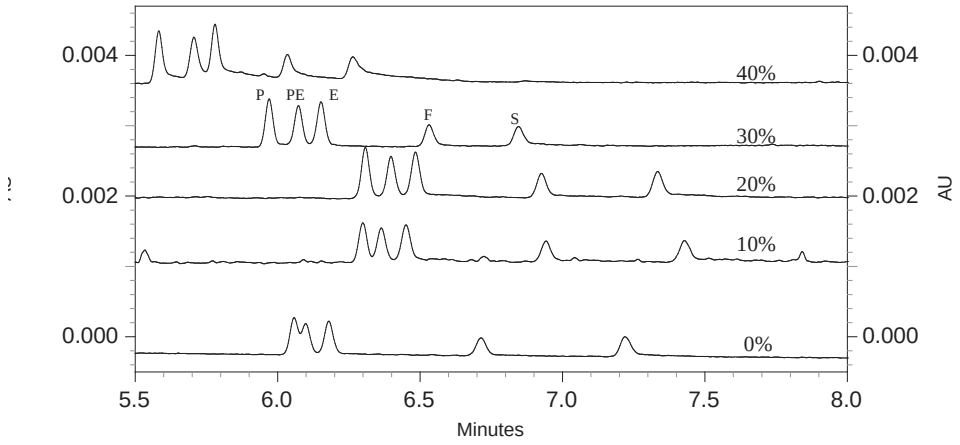

Figure 2. CZE electropherogram of five analytes using 0-40% ACN added into a 100-mM tris-phosphate buffer at pH 2.5. CE conditions: uncoated fused silica capillary 50µm i.d.× 60.2 cm (50 cm to detector), temperature 25 ^{o}C, voltage +25 kV, 0.5 psi pressure injection for 10 s and UV detection at 214 nm.

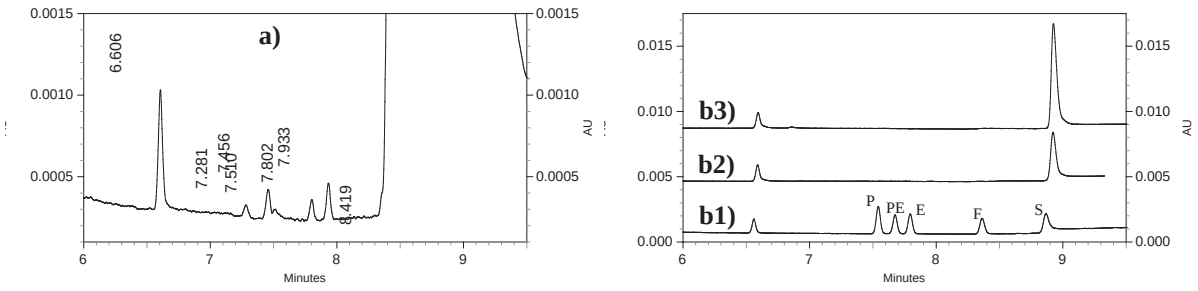

Figure 3. An example of CZE electropherograms for analysis of anti-obesity drugs adulterated in dietary suppreme. a) sample solution, b1) standard solution with internal standard, b2) 150 folds-diluted sample solution, b3) 150 folds-diluted sample solution spiked with S. CZE conditions as shown in Figure 2.

4. Conclusions

Advantages of our developed CZE method for determination of five contraband anti-obesity drugs adulterated in supplements for weight control include fast analysis time within 10 min, good resolution and simpler sample preparation, LOD down to less than 1 ppm, high linearity and satisfactory accuracy and precision. Thus, our developed CZE method can be used as an alternative for determination of anti-obesity drug in dietary supplements.

Acknowledgements

The authors gratefully acknowledge the financial support provided by the Nation Research University Project of CHE and the Rachadaphiseksomphot Endowment Fund (FW648I) and also the Thai Government Stimulus Package 2 (TKK25), under the Project for Establishment of Comprehensive Center for Innovative Food, Health Products and Agriculture (PERFECTA), for CE instrument support.

References

[1] C. Hanotin, F. Thomas, S.P. Jones, E. Leutenegger, P, *Int. J. Obes.* **22** (1998) 32–38.

[2] J.G. Jollis, C.K. Landolfo, J. Kisslo, G.D. Constantine, K.D. Davis, T. Ryan, *Circulation* **101** (2000) 2071-2077.

[3] F.L. Greenway, L.D. Jonge, D. Blanchard, M. Frisard, S.R. Smith, *Obesity* **12** (2004) 1152-1157.

[4] N.R. Srinivas, J.W. Hubbard, J.K. Cooper, K.K. Midha, *J. Chromatogr.* **433** (1988) 105-117.

[5] V.F. Sardela, M.T.R. Motta, *J. Chromatogr. B* **877** (2009) 3003–3011.

[6] G. Gmeiner, T. Geisendorfer, J. Kainzbauer, M. Nikolajevic, H. Tausch, *J. Chromatogr. B* **768** (2002) 215-221.

[7] A. Kaddoumi, M.N. Nakashima, M. Wada, N. Kuroda, Y. Nakahara, K. Nakashima, *J. Liq. Chromatogr. Relat. Technol.* **24** (2001) 57-67.

[8] M. Ichikawa, M. Udayama, K. Imamura, S. Shiraishi, H. Matsuura, *Chem. Pharm. Bull*. **51** (2003) 635-639.

[9] J. Ouyang, X. Gao, W.R.G. Baeyens, J.R. Delanghe Biomed. *Chromatogr*. **19** (2005) 266-271.

[10] A.I. Segall, E.A. Collado, R.A. Ricci, M.T. Pizzorno, *J. Liq. Chromatogr. Relat. Technol*. **26** (2003) 977-986.

[11] J. Wang, B. Chen, S. Yao, *Food Addit. Contam. Part A-Chem*. **25** (2008) 822-830.

[12] S. Martello, M. Felli, M. Chiarotti, *Food Addit. Contam. Part A-Chem.* **24** (2007) 258-265.

[13] Z. Yu, Q. Wei, Q. Fan, C. Wan, *J. Liq. Chromatogr. Relat. Technol.* **33** (2010) 452-461.

[14] J. Ouyang, X. Gao, W.R.G. baeyens, J.R. Delanghe, *Biomed. Chromatogr*. **19** (2005) 266-271.

[15] S. Inoue, S. Miyamoto, M. Ogasawara, O. Endo, G. Suzuki, *J. Health Sci.* **55** (2009) 183-191.

[16] S.H. Kim, J. Lee, T. Yoon, J. Choi, D. Choi, D. Kim, S.W. Kwon, *Biomed. Chromatogr*. **23** (2009) 1259-1265.

[17] M.G. Khaledi, High Performance Capillary Electrophoresis; Theory Techniques and Applications, *John Wliey & Sons, Inc., New York*, (1998) pp.25-73.

[18] Y.R. Ku, Y.S. Chang, K.C. Wen, L.K., *J. Chromatogr. A* **848** (1999) 537-543.

[19] V. Piette, F. Parmentier, *J. Chromatogr. A* **979** (2002) 345-352.

[20] V. Cianchino, G. Acosta, C. Ortega, L.D. Martinez, M.R., *Food Chem.* **108** (2008) 1075-1081.

[21] H. Fang, M. Liu, Z. Zeng, *Talanta* **68** (2006) 979-986.

[22] A.G. Gonzalez, M.A. Herrador, Trends Anal. Chem., 26 (2007) 227-238.

THE DETERMINATION OF PROTEIN AND CERTAIN ESSENTIAL ELEMENTS IN EARTHWORM *EUDRILUS EUGENIAE* FED WITH DIFERENT KINDS OF ORGANIC WASTE

Malliga Thongkheaw[1] and Tritaporn Choosri[2]*

[1,2]School of Chemistry, Institute of science, Suranaree University of Technology, Muang, Nakhonratchasima, Thailand 30000

* Correspondence; E-mail: tritapor@sut.ac.th, Tel: +66-44-22-4318

Abstract: **The objectives of this study were to determine the protein and certain essential elements contents in earthworms fed with different kinds of organic waste. *Eudrilus eugeniae* is one particular species of earthworms that has high rate of reproduction, grows extremely fast and is good in decomposing organic wastes. The protein and certain essential elements contents in earthworms fed with different kinds of organic wastes: soybean waste, neem leaves, ripe banana, and carton, were compared with the control group which was fed with nothing. The protein content was analyzed by the Kjeldahl method. The essential elements Ca, K, Mg, Fe, Cu, Mn, Zn and Co were analyzed by flame atomic absorption spectroscopy (FAAS). Na was analyzed by atomic emission spectroscopy (AES) and CHNS autoanalyzer was used with S. Phosphorus and chloride were determined using the molybdovanadate and Volhard method respectively. The protein contents in earthworm were found to be in the range 55.37-64.59% dried weight. The results for the analyses of major essential elements contents of the earthworm in percentages based on dried weight were: Ca 0.52-0.65, Cl 0.75-0.97, K 1.24-1.42, Mg 0.24-0.42, Na 0.44-0.50, P 0.24-0.27, and S 0.21-0.27. The trace essential elements in mg/kg dried weight were: Fe 2,116-3,231, Cu 46.3-52.5, Zn 180.2-192.7, Mn 35.4-94.7, and Co 1.16-4.96. The results showed that earthworms could be the protein source for animal feeds since the protein contents were moderately high, and the essential elements contents were quite comparable or better than the other feeds.**

1. Introduction

The African night crawler is excellent in vermi-composting, which is an effective natural form of recycling food and garden waste, turning them into nutrient-rich compost or worm castings. They are perfect for home vermicomposting bins and for vermicomposting more fibrous materials such as leaves [1]. African night crawlers are excellent as live fishing bait and also are used in exotic pet markets as food for birds, fishes, turtles and other reptilians. In this study, The African night crawlers were supplied by the earthworm farm owner in Uttaradit Province, who plans to formulate fish and frog feeds using earthworms in the future. Four different organic wastes, easily found in the farm area, were chosen as the earthworm feeds in the experiments. They were soybean waste, neem leaves, banana and cartons. Soybean waste is the waste from the process of making soya milk and can be found in household wastes. It contains high amount of nitrogen and protein. Neem is a large evergreen hardy tree, growing easily on dry, nutrient-lean soil [2, 3]. There are a lot of neem trees in the Uttaradit farm. Banana is food for human and animals but it is rancid and easily decomposed. Carton is a waste material from many processes and used carton can be found everywhere. It absorbs water and decomposes easily. Earthworm can consume this material as food [4]. Thus, these were materials chosen as earthworm feeds. The results of this study may help support the hypothesis that earthworm could be a source of essential elements and protein in animal feed. In addition, the results will provide more data concerning African night crawler earthworm in Thailand. The information will be transferred to the earthworm farm owner in Uttaradit Province who will use it as data base in the production of fish and frog formulations.

2. Materials and Methods

Feed preparation: Organic litters which were soybean waste, neem leaves, ripe banana, and small pieces of carton had been used in the experiment. Soybean waste was used as it was. Neem leaves were chopped to small pieces and fermented by soaking in water for 1 week until the substrate decayed. Ripe banana was chopped to small pieces and let stand for 1 day before used. Carton was soaking in water for 1 day to make it softer before used.

Earthworm growth condition: Earthworm breeding materials were composed of soil, cow manure and rice straw in a ratio of 3:1:1, mixed and put in slotted plastic containers. The breeding material was moisted with water. Placed 68 worms in each of the plastic containers. Each group of the earthworms were fed with different kinds of organic wastes; soybean waste (Sample 1), neem leaves (Sample 2), banana (Sample 3), and carton (Sample 4). The control Sample 5 was the earthworm in breeding material with no supplement organic litter.

Earthworm sample preparation: The adult earthworms were collected after 3 months for proteins and minerals analyses. After rinsing with distilled water, the worms were put on one Whatman No. 42 filter paper in a beaker, added a few drops of distilled water to maintain moisture. Kept the samples at room temperature for 2 days, changing the filter paper daily to allow complete evacuation of the gut contents.

Killed the earthworms by frozen them in -4 ^{o}C freezer for 1 day. The earthworms were then oven dried at 70 ^{o}C for 48 h to constant weights which were measured after cooling them to room temperature in a desiccators [5]. Earthworm samples were crushed using the agate mortar and sieved through a standard 0.18 mm sieve and kept in sealed plastic bags for further analysis.

Determination of protein content: Kjeldahl method was used to determine the protein contents of the earthworms. Weighed 0.5000-1.0000 g sieved sample and transferred to a digestion tube, added 4-5 glass beads, 15 ml conc. H_2SO_4, and slowly added 3 ml of 30-35% H_2O_2. Let the reaction subside then placed the tubes in a block digester. Samples were digested at 410 ^{o}C until the mixture was clear, then removed the digestion tubes from the block digester and let them cool to room temperature. Carefully added 50-75 ml H_2O. Dispensed 50-75 ml of 40 % NaOH solution from alkali tank before starting the distillation. Placed 250 ml receiving flask containing 25 ml of 4% H_3BO_3 solution with mixed indicator on receiving platform, with tube from condenser extending below the surface of absorbing solution. Steam distilled until 100-125 ml was collected and the color of indicator changed from pink to green. Removed the digestion tubes and receiving flask from the unit. The collected solution was titrated with 0.2000 N HCl to pink color end point, recorded the volume of the acid used, and titrated the reagent blank similarly.

Determination of essential elements content: The elements (Ca, Co, Cu, Fe, K, Mg, Mn, and Zn) were analyzed by atomic absorption spectrophotometer and Na was determined by using the technique of emission spectroscopy. Weighed 0.5000 g of each sieved samples into digestion tube. Added 30 ml of mixed acid (2:1 ratio of conc. HNO_3: conc. HCl) and digested at 50 ^{o}C for 2 h. The temperature was increased progressively to 150 ^{o}C for 2 h, and then to 200 ^{o}C for 1 h. The solution was cooled to room temperature and made up to 250 ml with deionized water, kept in polypropylene bottles and stored in a refrigerator until analysis. Phosphorus contents of the samples were determined using the molybdovanadate method. Weighed 2.0000 g of sieved sample into a crucible and heated at 600 ^{o}C for 4 h in the furnace and cooled down to room temperature before the analysis. Weighed 0.2000 g ashed sample into the digestion tube, added 12 ml of mixed acid (2:1 ratio of conc. HNO_3: conc. HCl) and digested at 150 ^{o}C for 1 h. The solution was cooled to room temperature, adjusted the color of the solution to yellow by adding vanadomolybdate reagent, then made up to 100 ml with deionized water. Measured the absorbance by using spectrophotometer at 400 nm against blank solution. Chloride content was determined by Volhard method. Weighed 0.5000 g sieved sample into 250 ml Erlenmeyer flask, added 10.00 ml of standard 0.1000 N $AgNO_3$ solutions to precipitate all chloride as AgCl, then added 20 ml conc. HNO_3. The solution was boiled on hot plate until all solid except AgCl dissolved. After the solution was cooled down, added 50 ml H_2O and 5 ml indicator before titrated a solution with a standard 0.1000 N NH_4SCN solution to a permanent light brown end point [6]. Sulfur content was obtained by using CHNS analyzer with appropriate standard reference material. The analysis was based on the combustion of sample into volatile gases and measured the amount of SO_2 using the conductivity detector. Weighed 0.2000 g sieved samples, put them in the tin capsules, and furled the capsules tightly. Prepared the standard reference material and the blank (empty tin capsule) in the same way. The CHNS analyzer was run and the results were obtained as percentages of sulfur in the sample.

3. Results and Discussion

Protein analyses: Protein contents were calculated from the amount of nitrogen found in Kjeldahl analysis by multiplying the %N obtained with 6.25, the conversion factor for meat sample. The percentages were based on dry weight. Even though earthworm can use a wide variety of organic materials for food, protein and carbohydrate rich wastes seem to be preferred to wastes with lower protein content. Sample 1 had the highest amount of protein (64.59%) as the soybean wastes had the highest amount of protein (29.60%) as well. Considered the protein contents in other organic wastes used as feeds and in earthworm shown in **Table 1** and **Table 2**. The protein content of neem leaves (11.14%) was higher than the protein contents of banana (3.20%) and carton (1.03%). But the protein contents in the earthworms fed with these litters were not in the same order as the order of protein contents in organic feeds. Sample 4 had higher protein content (59.63%) than Sample 3 (58.70%) and Sample 2 (56.06%). Sample 2 had the lowest amount of protein, even though the protein content in neem leaves was not the lowest. In this case, palatability might be the explanation since neem leaves had bitter taste. It is known that neem leaves contain certain biopesticide against various insects. Most of its parts contain azadirachtin, which has the most insecticidal activity among other limonoids, or tetranortriterpenoids present in neem trees [7, 8]. These properties of neem leaves might affect the palatability to the earthworm. But since the earthworm was all in the same breeding materials, they also consumed these materials for food. The control material or the breeding material itself contained 4.66% protein. This was the reason why the protein contents of sample 2 and sample 4 were not that low. It was also clear that the protein contents of the earthworms fed with organic litters as supplement to the breeding materials contained higher amount of protein than the earthworm fed with only breeding materials. The results were confirmed using one-way ANOVA test, (n=3), $P \leq 0.05$. This study might conclude that any organic wastes could contribute to higher protein production of earthworms.

Table 1 Protein and certain essential elements content in Earthworm fed with different kinds of organic wastes.

Sample	Nutrition concentrations												
	Protein*	Ca*	Cl*	K*	Mg*	Na*	P*	S*	Co**	Cu**	Fe**	Mn**	Zn**
Sample 1	64.59	0.53	0.97	1.33	0.24	0.45	0.27	0.27	4.96	50.30	2517.00	35.40	180.90
Sample 2	56.06	0.63	0.83	1.37	0.42	0.48	0.26	0.25	1.16	50.70	2497.00	85.40	187.40
Sample 3	58.70	0.52	0.82	1.42	0.29	0.50	0.26	0.24	2.91	46.30	2116.00	54.90	180.20
Sample 4	59.63	0.65	0.80	1.24	0.36	0.44	0.24	0.21	1.28	46.40	3231.00	43.10	180.70
Sample 5	55.37	0.60	0.75	1.39	0.30	0.46	0.27	0.22	2.48	52.50	3129.00	94.70	192.70

* Reported in % dried weight, ** Reported in mg/kg dried weight

Table 2 Protein and certain essential elements content in breeding material.

Sample	Nutrition concentrations												
	Protein*	Ca*	Cl*	K*	Mg*	Na*	P*	S*	Co**	Cu**	Fe**	Mn**	Zn**
Soybean waste	29.60	0.53	0.17	1.54	0.68	0.01	0.09	0.10	35.90	53.40	3573.00	42.80	38.60
Neem leaves	11.14	3.57	0.82	1.59	0.67	ND	0.06	0.04	8.57	39.20	4252.00	64.50	24.60
Banana	3.20	0.26	0.23	2.14	0.45	ND	0.02	ND	26.70	42.60	801.00	132.00	17.90
Carton	1.03	1.57	0.15	0.09	0.42	0.01	0.00	0.03	7.61	50.80	5439.00	54.80	36.20
Breeding material	4.66	1.37	0.40	0.98	0.74	0.05	0.14	0.04	14.10	67.90	33983.00	677.00	253.00

* Reported in % dried weight, ** Reported in mg/kg dried weight, ND = not detected

Major essential elements: It is well established that many inorganic elements are required for vital processes in human and animals, and are considered as essential elements. The results of the analyses of seven major essential elements in the earthworms fed with different kinds of organic wastes and in organic wastes used as feeds are displayed in **Table 1** and **2**. The results showed that the concentrations of each element were about the same in each earthworm group. For example, chloride concentrations in earthworms were 0.97% in Sample 1, 0.83% in Sample 2, 0.82% in Sample 3, and 0.80% in Sample 4 as shown in Figure 3. Chloride is the major anion of the body involved in osmotic pressure, making more than 60% of the total anionic equivalents in the extracellular fluid. It seemed that the amount of chloride in organic litters did not affect the amount of chloride in earthworms. Carton contained only 0.15% chloride (the lowest amount) while neem leaves contained the highest amount of chloride (0.82%).
Another example was the concentrations of K found in the earthworms. Potassium is the third most abundant element in the animal body. It plays many vital roles in life processes. The concentrations of K in each earthworm group were 1.33% in Sample 1, 1.37% in Sample 2, 1.42% in Sample 3, and 1.24% in Sample 4 as shown in Figure 4. It was clear that the concentrations of both chloride and potassium in each earthworm group were relatively constant and not depended upon the concentrations of the elements presented in the organic feeds. The concentrations of each element were relatively constant because they were essential elements. The earthworms tried to keep those concentrations constant for their proper functions in life processes. Even though the organic feeds and the breeding media contained very small amount of some essential elements, for example, carton waste contained 0.09% K and the breeding materials contained only 0.048% Na, the earthworms could get supply of the elements they needed through the accumulation processes from their surroundings. The amounts of major essential elements found in earthworms were depended on many factors such as the chemical form of the element which would determine its biological availability to the earthworms. The absolute amount of the element in organic feed also affected the elemental uptake of the earthworms.

Trace essential elements: Trace essential elements are required by the living organism in a minute amounts usually less than 100 mg/kg. Although the living organism contained and required very small amount of these elements, deficiency of

some elements can lead to the malfunction of life processes. **Table 1** and **2** showed the data presentations of the concentrations of Co, Cu, Fe, Mn, and Zn in the earthworms fed with different kinds of organic wastes compared with the concentrations of Co, Cu, Fe, Mn, and Zn in organic wastes. The findings showed the same trends as what had been found for the major essential elements. The concentrations of each element in each group of earthworms were relatively constant except for Co which were quite varied. Considered Cu as an example. Copper is a component of many enzymes involved in electron transport during aerobic respiration. The copper concentrations were relatively constant in different earthworm groups, being 50.3 mg/kg in Sample 1, 50.7 mg/kg in Sample 2, 46.3 mg/kg in Sample 3, 46.4 mg/kg in Sample 4, and 52.5 mg/kg in Sample 5. Another example is zinc, a part of many metalloenzymes. It plays an important role in protein, carbohydrate, and lipid metabolism. The concentrations of Zn were quite constant in earthworms fed with different organic litters: 180.9 mg/kg in Sample 1, 187.4 mg/kg in Sample 2, 180.2 mg/kg in Sample 3, 180.7 mg/kg in Sample 4, and 192.7 mg/kg in Sample 5 or the breeding materials. Again, the concentrations of Zn found were not depended on the amount of Zn presented in organic feeds. All except Fe have been shown in other studies to accumulate in earthworm tissues to level above those of the surrounding media [9-12] Concerning the amount of trace essential elements found in earthworms, besides the absolute concentrations of the elements in organic litters and the chemical form of the elements which determines their biological availability to the earthworms, an antagonistic reaction may have arisen. For example, the antagonistic reactions of Fe and other elements in organic feeds. High intakes of Zn, Mn, Cu, Co, Cd have been reported to interfere with Fe uptake and metabolism [13]. Antagonism and interaction between trace essential elements will also vary from feed to feed as levels of the individual elements vary. The results from the study provided the conclusion that the concentrations of the trace elements found in earthworms fed with different organic litters might be effected from the feeds due to the antagonistic reaction and interactions between elements in different feeds.

4. Conclusions

The results showed that the earthworms contained moderately high amount of protein (55.37-64.59% dried weight), so it would be an ideal source for protein supplement in animal feeds in the future. The earthworms bred in breeding material supplemented with organic litters produced higher protein concentration than the earthworms bred in breeding material only. Many research papers confirmed that the earthworm meals could be partially replaced the fish meal for culture fishes diet, with no detrimental effect [12, 14, 15]. This might be very useful since the protein component of a diet was the single most expensive portion in the formulation. Concerning the essential elements, earthworms could be good source of essential elements. They contained moderately amount of many essential elements especially K and Fe. The amounts of essential elements were relatively constant and depended very little on the amounts of essential elements in organic feeds. The amount of essential elements in earthworms depended on many factors such as the regulations of elements in the body, the absolute concentration of the element in organic feeds, the chemical form of the element which would determine its biological availability to the earthworm, and the natural accumulation processes. So this meant that any organic wastes could be used in vermiculture. There should be more researches on relation between food ingested and the protein and element contents in earthworms. The approach should be multidisciplinary to produce a complete assessment of the earthworm behavior.

Acknowledgements

The authors are greatly appreciated to the earthworm farm owner in Uttaradit Province, the supplier of the earthworms used in this study. The authors also wish to thank the Suranaree University of Technology for providing part of research fund.

References

[1] S. Gajalakshmi, E.V. Ramasamy and S.A. Abbasi, *Bioresource Technol*, **96** (2005) 1057-1061.
[2] L. Pundt, (2000). *Neem based insecticides*. Home and Garden News. July/August, pp. 6.
[3] S. Gajalakshmi and S.A. Abbasi , *Bioresource Technol*, **92** (2004) 291-296.
[4] R. Sherman, (2003). *Raising earthworm successfully*. [Online]. Available: http://www.bae.ncsu.edu/topic /vermicomposting/pubs/earthworms.pdf.(Retrieved May 14, 2010)
[5] J. Dai, T. Becquer, J.H. Rouiller, G. Reversat, F. Bernhard-Reversat, J. Nahmani, and P. Lavelle, *Soil Biol. Biochem*, **36** (2004) 91-98.
[6] E.A. Burns and R.F. Muraca, *Anal. Chim. Acta*, **23** (1960) 136-144.
[7] M. Gopal, A. Gupta, V. Arunachalam, and S.P. Magu, *Bioresource Technol*, **98** (2007) 3154-3158.
[8] B. Singh, D.K. Sharma, R. Kumar, and A. Gupta, *J. Hazard. Mater*, **177** (2010) 290-299.
[9] C.O. Gish and R.E. Christensen, *Environ. Sci. Technol*, **7** (1973) 1060-1062.
[10] R.I. Van Hook, *Bull. Environ. Contam. Toxicol*, **12** (1974) 509-511.
[11] M.P. Ireland, *Oikos*, **26** (1975) 74-79.
[12] E.A. Stafford. and A.G.J. Tacon, *Agri. Wastes*, **9**(1984) 249-266.
[13] E. J. Underwood. (1977). *Trace elements in human and animal nutrition*. Academic Press, London and New York, pp. 545.
[14] T. Akiyama, T. Mural, Y. Hirasawa, and T. Nose, *Aquaculture*, **37**(1984) 217-222.
[15] I.A. Ibanez, C.A. Herrera, L.A. Velasquez, and P. Hebel, *Anim. Feed Sci. Tech.* **42** (1993) 165-172.

TRACE ELEMENTAL ANALYSIS IN BIODIESEL BY INDUCTIVELY COUPLED PLASMA ATOMIC EMISSION SPECTROMETRY USING EMULSIFICATION SAMPLE PREPARATION TECHNIQUE

Amonrat Phomchomcha[1], Narong Praphairaksit[1*]

[1] Department of Chemistry, Faculty of Science, Chulalongkorn University, Pathumwan, Bangkok 10330, Thailand

[*] Author for correspondence; E-Mail: narong.pr@chula.ac.th, Tel. +66 2187613 , Fax. +66 22187598

Abstract: The presence of elemental contaminants in biodiesel is a serious threat that can lead to its operational problems and therefore must be quantified and/or regulated. In such determination the sample is typically subjected to either extensive and laborious digestion, or preferably dilution with organic solvents prior to analysis using inductively coupled plasma atomic emission spectrometry (ICP-AES). Although being somewhat satisfactory this approach suffers from several drawbacks, among which are the highly viscous sample, handling of unfriendly organic solvents, inevitably high organic load to the plasma, and the needs for expensive and rarely available organometallic standards for calibration. In this work, a simple and rapid sample preparation technique for ICP-AES analysis of biodiesel was developed. The oil sample (10% v/v) was emulsified with surfactant, co-solvent and water in order to reduce its organic character and allow the calibration against inorganic aqueous standard solutions. Various parameters regarding the type and amount of surfactants (Tween 20, Triton X-100 and span 80 of 2.5-10% v/v) and 10% v/v n-butanol as co-solvent were optimized and simultaneous determination of several trace elements (eg. Mg, Ca, K, Cu, Mn, Zn) in biodiesel was investigated. The emulsified samples were found to be stable at least during the analysis with recoveries of 83.96-101.82% and relative standard deviation (% RSD) of less than 3%.

1. Introduction

In the recent year because the sources of fossil fuels are limited [1,2], many countries in the world have turned their attention to an alternative fuel. Biodiesel, defined as a mixture of mono-alkyl esters, is produced from a wide range of vegetable oils and animal fats, more commonly by a lipid transesterification process [3,4]. In the evaluation of quality control in biodiesel, apart from structural analysis, the determination of inorganic constituents is also important since they can cause environmental problems and engine damage [5]. Trace levels of metals, such as K in biodiesel is especially important because alkaline hydroxides are used as catalysts in the transesterification process, and they can appear as contaminants in the final product [6,7]. Metals such as Cu and Zn may catalyze oxidation in contact with biodiesel. While Ca and Mg concentrations are important metals to ensure biodiesel quality, these metals, normally come from the washing water can form insoluble soap, giving rise to incrustations that can impair the functioning of a biodiesel-fueled engine [9]. Moreover, excess metals can create residues (sediment) that may plug fuel filters [8]. However, the determination of trace elements in biodiesel is difficult due to their low concentration, viscosity and many matrix interferences. Sample pretreatments are very important and among these are wet or dry digestion, microwave digestion or dilution with organic solvents. These techniques are usually difficult to be automated, time consuming, laborious and prone to contamination and losses. Biodiesel samples may be prepared as emulsions or micro-emulsions due to the homogeneous dispersion and stabilization of the oil droplets or micro-droplets in the aqueous phase, which brings the viscosity closer to that of an aqueous solution and reduces the organic load into the system [10]. This technique could potentially allow the use of aqueous standards for calibration instead of expensive and instable organometallic standards. In previous studies, co-solvent was used as detergentless emulsion to dilute to the final volume. The oil sample, surfactants or not surfactants and water were stabilized by a common solvent (saturated alcohol containing 3 to 8 carbon atoms) [11]. In addition, ICP-AES has been employed for the determination of metals due to its multi-element capability, wide linear dynamic range, high accuracy and precision. Hence, the aim of this work is to develop a simple yet effective analytical method for determination of some key elements (Ca, K, Mg, Cu, Mn, Zn) in biodiesel using a emulsification technique with ICP-AES.

2. Material and Methods

2.1 Instrumentation

The inductively coupled plasma optical emission spectrometer used for this study was a Thermo Scientific model iCAP 6500 (SciSpec Co., Ltd, Thailand). The analytical emission lines(nm) chosen were: Ca(393.3); K(769.8); Mg(279.5); Cu(324.7); Mn(257.6); and Zn(213.8). Instrumental conditions are shown in Table 1.

Table 1 : Operating parameters for ICP-AES measurements.

Power	1150	W
Auxilary gas flow	0.5	L/min
Nebulizer gas flow	0.7	L/min

Coolant gas flow	12	L/min
Flush pump rate	100	rpm
Analysis pump rate	50	rpm
Pump stabilization time	5	s
Sample flush time	30	s

2.2 Reagents and sample

All reagents were of analytical grade. Deionized water used was purified from the Milli-Q system. Non-ionic surfactant Triton X-100 and Tween 20 were from sigma-Aldrich, USA and France, respectively. While Span 80 from Fluka, Spain. Pure 1-butanol 99.9% as a co-solvent from sigma-Aldrich, Germany. Nitric acid 65% from Merck (Darmstadt, Germany). 1-propanol as a co-solvent was from Carlo Erba (Milan, Italy). Analyte (Ca, K, Mg, Cu, Mn, Zn) standard solutions were prepared from 1000 mg L^{-1} stock solutions from Merck, Brazil. A multi-element metal-organic standard (conostan S-21 + K, Baie D'urfe', canada) was used to spike the sample. A biodiesel sample from PTT co., Ltd.

2.3 Sample preparation

Emulsified samples were prepared by measuring 1.0 ml of 10 ppm multielement oil standards into 10.0 ml polypropylene bottles, followed by 1.0 ml of concentrated HNO_3 and shaken for 3 minutes with mechanical agitation. After that, 1.0 ml of surfactant (Triton X-100, Tween 20, Span 80 and mixtures thereof) and 1.0 ml of co-solvent (ethanol, methanol, propanol and butanol) were pipetted into the bottles and the final volume was adjusted using deionized water (milli-Q). The analytical merits of this technique were evaluated by its accuracy via spike recovery experiments. A simple external calibration was employed using commercially available inorganic standards for all calibrations

3. Results and discussion

The surfactants used in this study were Tween 21, Triton X-100 and Span 80. All of these were non-ionic surfactants having the hydrophile-lipophile balance (HLB) values of 16.7, 13.5 and 8.3 respectively. The higher values have more hydrophilicity (water soluble, oil- in-water), while the lower values have more lipophilicity (oil soluble, water-in-oil). Normally without any modification, a simple oil-water mixture sample would yield a drastically low emission signal presumably as a result of the incomplete vaporization/ionization and the diminished transportation efficiency of the more viscous oil sample. However, as clearly seen in Figure 1, the emission intensities obtained from all of the emulsified samples studied improved significantly to the levels close to those of the aqueous standard of the same concentration indicating that a much more complete excitation was attained. Triton X-100 was the surfactant that yield the intensity closest to that of the aqueous standard overall and thus was chosen as a model surfactant for the preparation of oil-in-water (o/w) emulsion for the following studies.

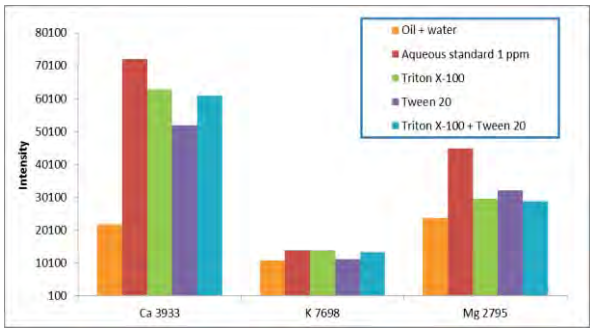

Figure 1. Intensity of the biodiesel samples obtained with different surfactants. (Span 80 was immiscible with the oil sample and thus no data was attained)

The amount of Triton X-100 was then varied between 2.5 and 10 % v/v and it was found that the optimum was established with 10% Triton X-100 as shown in Figure 2.

Figure 2. Effects of the amount of surfactant.

Next, the effect of co-solvent was investigated. 10% v/v of methanol, ethanol, propanol and butanol were added as co-solvent into the emulsified samples. Butanol was found to be the best co-solvent among these as it provided both the highest signal (Figure 3) and the longest stability time of the emulsion. The amount of butanol was also studied and as can be seen in Figure 4, the signals are not significantly different but 10% was selected as it not only provides higher signal but also the longest stabilized emulsion.

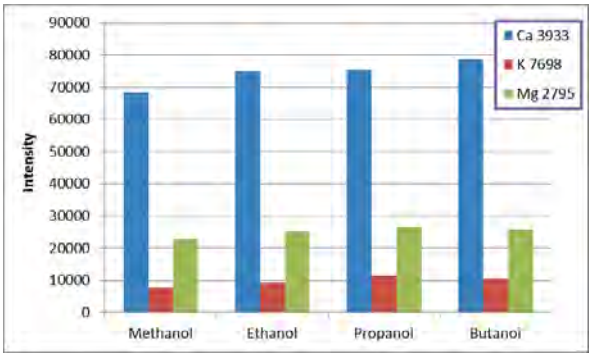

Figure 3. Intensities of the emulsified samples added with various co-solvents.

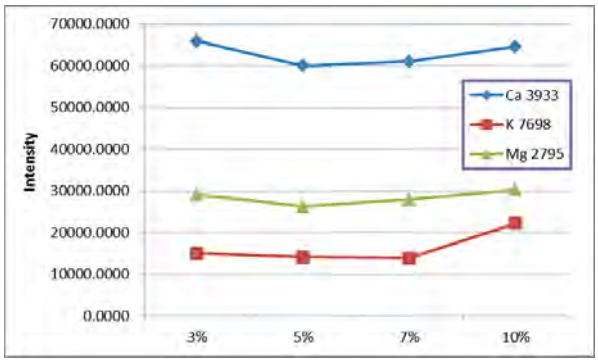

Figure 4. Effects of the amount of co-solvent (butanol).

In addition, the homogenisation method was also studied, especially, mixing an oil sample with nitric acid, which helps to digest the metals in oil to be dispersed and determined in aqueous phase. Figure 5 shows that mixing by mechanical agitation with the addition of butanol gives the highest recovery overall. The addition of a small volume of n-butanol not only reduces the viscosity but also helps maintaining the plasma and emulsion stability. Moreover, Cu, Mn and Zn were included with the common elements (Ca, K, and Mg) for checking the accuracy of the optimized conditions. It can be seen from figure 5 that the results obtained from Cu, Mn and Zn are as good as those obtained for the common elements. The emulsified sample is stable for up to 7 minutes. Good recoveries, ranging from 83.96 to 101.82%, were obtained (acceptable range, 80-120%) with relative standard deviation (%RSD) lower than 3%. The limit of detection (LOD) and limit of quantification (LOQ) for these elements were shown in table 2.

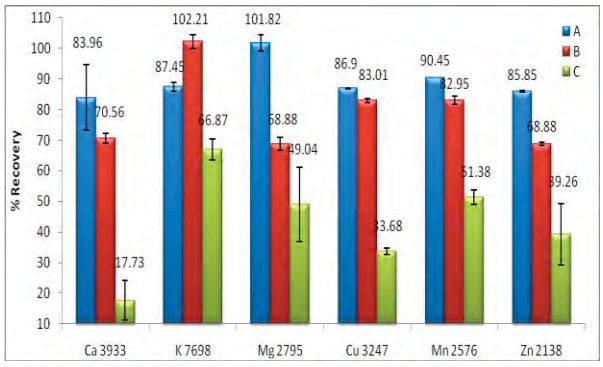

Figure 5. %Recovery of various elements in the emulsified samples prepared by: A (agitation with butanol added), B (agitation without butanol added) and C (untreated, oil+water sample)

Table 2 : Limit of detection (LOD) and limit of quantification (LOQ) from ICP-AES measurements.

Element	LOD (mg L^{-1})	LOQ (mg L^{-1})
Ca 393.3	0.0378	0.1262
K 769.8	0.1641	0.5470
Mg 279.5	0.0146	0.0489
Cu 324.7	0.0024	0.0081
Mn 257.6	0.0023	0.0075
Zn 213.8	0.0133	0.0444

4. Conclusions

It was demonstrated that Triton X-100 was a good surfactant for an oil-in-water emulsion system. Mixing of nitric acid and butanol helps to increase the emulsion stability time. Furthermore, good recoveries in the range of 83.96-101.82% were obtained for various elements. The emulsification technique developed has shown its potential to be a simple and easy sample preparation method for accurate determination of metals in biodiesel.

Acknowledgment

The authors would like to thank SciSpec Co., Ltd. for the support of ICP-AES instrument (iCAP 6500, Thermo Scientific) and PTT Chemical Public Company Limited (Thailand) for biodiesel samples. This work was supported by the Thailand Research Fund (RTA5380003) under Environmental Analysis Research Unit, Department of Chemistry, Faculty of Science, Chulalongkorn University.

References

[1] W. Xie, X. Huang , *Catal. Lett*. **107** (2006) 53-59.
[2] E.A. Faria, J.S. Marques, I.M. Dias, R.D.A. Andrade, P.A.Z. Suarez, A.G.S. Prado, *J. Braz. Chem. Soc*. **16** (2005) 1313.
[3] F. Ma, M.A. Hanna, *Bioresource Technol*. **70** (1999) 1-15.
[4] H. Fukuda, A. Kond, H. Noda, *J. Biosci. Bioeng.* **92** (2001) 405-416.
[5] M.A. Korn, D.C.M.B. Santos, M.A.B. Guida, I.S. Barbosa, M.L.C. Passos, M.L.M.F.S. Saraiva, J.L.F.C. Lima, *J. Braz. Chem. Soc*. **00** (2010) 1-7.
[6] K. Bozbas, *Sustain. Energ. Rev*. **12** (2008) 542–552.
[7] Knothe, G., Gerpen, J.V., and Krahl, J. (2005) *The Biodiesel Handbook. AOCS Books*: Cham-paign, IL.
[8] M. Mittelbach, S. Schober, *J. Am. Oil Chem. Soc.* **80** (2003) 817–823.
[9] A. de Jesus, A.V. Zmozinski, J.A. Barbar, M.G.R. Vale, M.M. Silva, *Energy Fuels* **24** (2010) 2109–2112**.**
[10] M.G.A Korn, D.C.M.B. Santos, M.A.B. Guida, I.S. Barbosa, M.L.C. Passos, M.L.M.F.S. Saraiva, J.L.F. C. Lima, *J. Braz. Chem. Soc*. **19** (2008) 856.
[11] H.M. Pessoa, F.H. Lyra, E.V.R. de Castro, R. de Campos, M.T.W. D. Carneiro and G.P. Brandão *J. Braz. Chem. Soc*. 23 (2012) 1421-1428.
[12] A. Montaser, D.W. Golightly (Eds.), *Inductively Coupled Plasmas in analytical atomic spectrometry, VCH Publishers*, New York, 1992.

A SIMPLE AND SENSITIVE FLOW INJECTION SPECTROPHOTOMETRIC PROCEDURE FOR DETERMINATION OF Ni(II) USING NITROSO-R SALT

Narabhats Rannurags[1], Urai Tengjaroenkul[1], Boonsom Liawruangrath[2], Saisunee Liawruangrath[3]*

[1] Department of Chemistry, Faculty of Science, Chiang Mai University, Chiang Mai 50200, Thailand
[2] Department of Pharmaceutical Science, Faculty of Pharmacy, Chiang Mai University, Chiang Mai, 50200, Thailand
[3] Department of Chemistry and Center of Excellence for Innovation in Chemistry; Material Science Research Center, Faculty of Science, Chiang Mai University, Chiang Mai 50200, Thailand

* Author for correspondence; E-Mail: E-mail:saisunee.l@cmu.ac.th

Abstract: A simple, sensitive and inexpensive spectrophotometric flow injection analysis (FIA) system were developed and fabricated for determination of nickel. The injection, propelling and detection system were exactly controlled and collected data by using the computer software programmed in our laboratory. This method is based on measurement of the absorbance of the Ni(II)-niroso-R salt complexes resulting in a orange color product at 490 nm in ammonium acetate buffer pH 8.5. The optimum condition for determination of Ni(II) were investigated with univariate method. The linear ranges of calibration were over the range of 0.25- 3.5 mg L^{-1} of Ni(II) with the correlation coefficients (r^2) of 0.9998. The relative standard deviation for 11-replicate injections was found to be 1.76% for 1.0 mg L^{-1} of Ni(II). The detection limit and quantification limit were 0.08 and 0.27 mg L^{-1}, respectively. The home-made FIA analyzer has been successfully applied to the determination of Ni(II) in water samples from electroplating industry. Results obtained by both proposed FIA and FAAS methods were in good agreement which verified by using student's t-test.

1. Introduction

Nickel and all compounds have not been displayed to be essential in human's body. Occupational exposure to human body arises in mining, refining, alloys and battery production, electroplating and welding. In addition, edible food containing nickel which is the major source of exposure for most people, but drinking water contains small amounts of nickel. It is commonly accepted that Ni(II) concentrations level of lower than 0.1 μg mL^{-1} in natural waters are innoxiously to aquatic organisms and irrigated plants [1]. Nickel and its compounds are toxic and cause environmental problem when they contaminate in surroundings. Excessive nickel to human can cause nose cancer, lung cancer and leukemia in the plentiful nickel area. In addition, the effect of nickel in patients who eat foods rich in nickel, such as oats, nuts, beans and chocolate show that illness incidence increased [2, 3]. Therefore, considering the low concentration level of Ni(II) ion in environmental, biological and food samples, sensitive analytical techniques are essential.

Several analytical techniques have been employed for analysis of Ni in various samples. Each of these proposed methods often propose advantages and disadvantages. The most commonly used method to detect trace nickel concentrations in water samples and foods is graphite furnace atomic absorption spectrometry (FAAS) [4], inductively coupled plasma mass spectrometry [5] and inductively coupled plasma atomic emission spectrometry [6, 7], which display fast elemental analysis, wide range of linearity and adequate detection limits for the determination of heavy elements present in environmental samples like river water, tap water, natural water and hair samples. These methods have good sensitivity and reproducibility, nevertheless they are unfortunately imperfect due to matrix interference in samples together with the high rate of analysis and the expensive maintenance of these instruments. Finally, flow injection analysis (FIA) methods for determination of nickel in various samples have been reported on flow based [8-10], reversed flow analysis [11] and stop flow analysis [12] with spectrophotometric measurement. Furthermore, FIA with FAAS system has been studied for determination of nickel [13]. FIA based on spectrophotometric detection displays some advantages such as instrumental simplicity, low cost of equipment, low running cost, high sensitivity and wide variety of organic reagents for nickel determinations. However, most of existing reagents have poor selectivity and then separation and preconcentration procedures may be essential to improve the determination of nickel. Conversely, a report of FIA for the determination of Ni(II) in waters using nitroso-R salt as the chromogenic agent has not been yet presented in the literature.

This work studies a rapid, sensitive and simple flow injection method for determination of Ni(II) based on the spectrophotometric detection of the soluble yellow complex formed by the reaction between Ni(II) and Nitroso-R salt. Result of this complex is examined at 490 nm. Under the optimum conditions, the proposed method was applied for determination of Ni(II) in water samples.

2. Materials and Methods

2.1 Chemicals and Reagents

A standard stock solution of Ni(II) 20 mg L^{-1} was prepared from a standard nickel solution (1000 mg L^{-1}, Fisher Scientific, England). Working standard solutions were freshly prepared from stock solutions of Ni(II) and diluted with the ammonium acetate buffer.

A stock nitroso-R salt 0.08 mol L^{-1} solution was prepared by dissolving 3.001 g of nitroso-R salt (Merck, Germany) in deionized water and adjusting the volume to 100 mL. The working solution of nitroso-R salt was daily prepared by appropriate dilution of stock nitroso-R salt solution in suitable buffer solution.

Ammonium acetate buffer solution of pH 6.5-9.5 were prepared by mixing an suitable ratio of 0.5 mol L^{-1} NH_4OH (Qrec, New Zealand) with 0.5 mol L^{-1} ammonium acetate (APS Finechem, Australia) which was prepared by dissolving 38.50 g of NH_4OAc in 1000 mL deionized water.

2.2 Manifold Design and Apparatus

The proposed two lines FI manifold for nickel determination is shown in Figure 1. The system consisted of a ten-port selection valve (V) controlled by a motor driver circuit board (M) and a peristaltic pump (P) with Tygon tubing (0.84 mm i.d. and 1.24 mm o.d.) which were controlled by computer software (C) programmed in our laboratory named "SIA" for injecting accurate volume of samples (S) and transporting appropriate flow rate of reagent (R), a PTFE tubing (0.84 mm i.d., 30 cm long) mixing coil was used as reactor (MC), a 10 mm path length with 120 µL flow through cell in the cell compartment of the UV-Vis spectrophotometer (Jenway 6305) as detector (D).

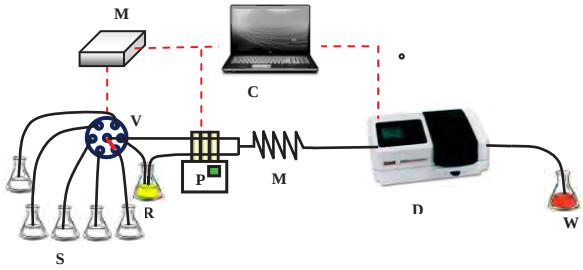

Figure 1. The proposed FIA system for nickel determination; S : sample/standard, R : reagent, V : selection valve, M : motor driver unit, P : peristaltic pump, MC : mixing coil, C : personal computer, D : spectrometer and W :waste

2.3 Recommended Procedure

Using the experimental setup with computer control as displayed in Figure 1. The method involved the injection of 80 µL standard Ni(II) or sample solution by switching the selection valve into a reagent stream of 0.104 mol L^{-1} nitroso-R salt mixed ammonium acetate buffer pH 8.5 with an appropriate flow rate of 2.5 mL min^{-1} using peristaltic pump (sample injection volume calculated from aspirating time and flow rate). Nitroso-R salt and Ni(II) solutions were reacted completely on the 30 cm mixing coil (MC) resulting in a yellow Ni(II)–nitoso-R complex then passed through the flow through cell of the spectrophotometer at 490 nm. The amount of Ni(II) content in water samples were calculated by reference to the calibration graph prepared under identical conditions by univariate method. A comparative determination of the Ni(II) in the sample solutions was carried out by FAAS method.

2.4 Water Samples Preparation

Water samples were collected with different time from electroplating industry and electronics industry in Northern Region Industrial Estate, Lam Phun Provinces, Thailand. The water samples were filtered over No.41 Whatman filter paper to remove suspended particulate matter at the selected sampling sites and stored at 4°C in the dark in polyethylene bottles. A 100 mL of water sample was transferred into 200 mL beaker using pipetted and then added 5.0 mL concentrated nitric acid to each sample and heated the samples on a hotplate until the volume has been reduced to the lowest volumes as possible (about 10 mL). Then set it to cool down at room temperature and transfer into 50 mL volumetric flasks, 5 mL deionized water was increased. Finally its volume was adjusted to 50 mL volumetric flask with deionized water and subsequently analyzed by the proposed FIA method.

3. Results and Discussion

The flow injection system was used as a basis for development of a simple, rapid and reproducible method with low reagent consumption (comparison with the bath-wise method) for analysis of trace nickel. Appropriate flow injection conditions for analysis of nickel were achieved. The method is based on the measurement of absorbance rising from Ni(II)-nitroso-R complex in an ammonium acetate buffer solution, formed by the reaction between Ni(II) and nitroso-R salt. The metal-to-ligand ratio was found to be 1:2 using mole ratio method.

The conditions for the determination of Ni(II) were optimized by studying the influences of the various parameters on the FIA gram, such as, pH concentration of nitroso-R salt, flow rate, reaction coil and sample loop, respectively. The optimum conditions obtained by means of the univariate optimization procedure. The optimum values were selected from the maximum sensitivity with low background and standard deviation (S.D.) The optimizations of the experimental conditions were carried out by using standard Ni(II) solution. In all experiments, five replicate measurements were performed for each studied parameter and the FIA manifold in Figure 1 was employed.

3.1 Effect of pH

The complexation of Ni(II)-nitroso-R salt was studied at different pH values in the range of 6.5-9.5. It was found that at the pH values below 8.5 or above 8.5 the sensitivity (slope of the calibration curve) decreased significantly because at pH 8.5 the complex of Ni(II)-nitroso-R salt might be formed more efficiently than the other pH. In addition, it can be seen that at pH lower and higher than 8.5 the sensitivity of Ni(II)-nitroso-R salt complex decreased due to at pH less than 8.5 the complex of Ni(II)-nitroso-R salt might not be formed effectively, and at pH greater than 8.5 the complex might be decomposed causing a decrease in sensitivity. Therefore, pH 8.5 was chosen because it provided the greatest sensitivity.

3.2 Effect of Nitroso-R Salt Concentrations

Effect of nitroso-R salt concentrations on the determination of Ni(II) (0.5-2.5 mg L^{-1}) was investigated over the range of 0.0026-0.021 mol L^{-1}. The absorbance increased with increasing concentrations of nitroso-R salt from 0.0026 to 0.010 mol L^{-1}, above which the absorbance slightly decreased Results show that nitroso-R salt concentration must be exceed that of Ni(II) ion concentration to reach effective complexation to achieve high sensitivity (slope of the calibration curve). As a result the optimum concentration of nitroso-R salt was 0.010 mol L^{-1}.

3.3 Effect of the Reaction Coil Tubing Length

The reaction coil are important for confirming complete reagent combining consequent in a time delay for development of a reaction between Ni(II) and nitroso-R salt. This condition was investigated by using PTFE tubing with diameter of 1.07 mm i.d. and length of reaction coil was varied from 10 to 50 cm. The sensitivity increased to a maximum at a reaction coil tubing length of 30 cm. It can be described that increasing the reaction coil length up to 30 cm give rise to an increase in the residence time permitting well mixing between Ni(II) and nitroso-R salt. Therefore, the reaction coil length 30 cm was chosen as optimum since it provided the greatest sensitivity.

3.4 Effect of Flow Rate

The effects of total flow rates on absorption signal of Ni(II)-nitroso-R complex in the FIA system were investigated for determining nickel, by injecting various concentration of standard nickel solution (0.5 - 2.5 mg L^{-1}) into the flow system. Flow rates were varied from 1.0 to 5.0 mL min^{-1}. It can be seen that the optimum flow rate was 2.5 ml min^{-1}. Moreover, the sensitivity of the calibration curve decreased, when the flow rate was lower than 2.5 ml min^{-1}. Due to the low flow rate increased in dispersion zone process and hence, peak broadening was observed. Furthermore, the sensitivity of the calibration curve was poorer when the flow rate was higher than 2.5 ml min^{-1}. This is due to the fact that the higher flow rate reduced the reaction time and so inadequate complex formation.

3.5 Effect of Sample Introduction Volume

The effect of sample volume on the determination of 0.5-2.5 mg L^{-1} Ni(II) that the influence on Ni(II)-nitroso-R complex absorption was studied by controlling pump flow rate and changing the switching time of the selection valve at sample line over the range of 50, 60, 70, 80, 90 and 100 µL. It was found that the sensitivity increases with rising sample volume up to 80 µL due to the enhancement in sample volume leading to the increment of the quantity of complex, that cause increases in peak height. Hereafter, the injection volume of 80 µL was considered to be optimum sample introduction volume for the proposed FIA system, which was used throughout the next experiments.

3.6 Analytical Characteristics

3.6.1 Calibration Curve and Detection Limit

A calibration curve was accomplished by injecting Ni(II) standard solutions into the proposed FIA system under the optimum conditions. All measurements were made in five replicate injections. The calibration curve (Figure 2) was linear over the range 0.25-3.5 mg L^{-1} and the linear regression equation of $y = 0.0458x + 0.0144$, (r^2=0.9998) where y is absorbance of Ni(II)-nitroso-R complex and x is the concentration of Ni(II) in mg L^{-1}. The detection limit and the quantification limit were calculated from the linear regression line of calibration curve and found to be 0.08 mg L^{-1} and 0.27 mg L^{-1}, respectively.

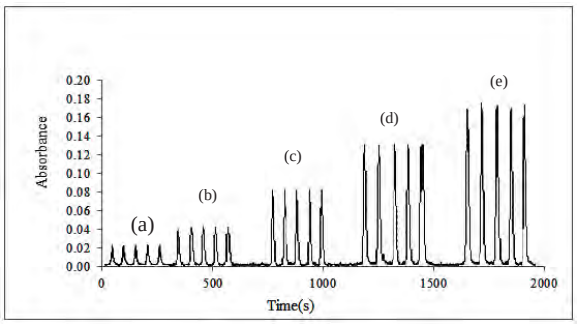

Figure 2. FIA-gram of standard Ni(II) solution at (a) 0.25 mg L^{-1}, (b) 0.5 mg L^{-1}, (c) 1.5 mg L^{-1}, (d) 2.5 mg L^{-1} and (e) 3.5 mg L^{-1},respectively

3.6.2 Reproducibility and Accuracy

The reproducibility of the proposed method was verified by 11 replicated determination of 1.0 mg L^{-1} standard Ni(II), underneath the optimum conditions. The relative standard deviation (RSD) was found to be 1.76%. Moreover, the percentage recoveries were studied by spiking 0.5 mg L^{-1} of Ni(II) standard solution into water samples for checking accuracy of this method. It was found that the range of percentage recovery was calculated to be 98.3-101.8 % (n=3). The sample throughput for the recommended procedure with a mean t_{base} of 45 s (n=7) was found to be 80 samples h^{-1}.

3.6.3 Interferences

The effect of various ions on the determination of 1.0 mg L^{-1} Ni(II) was considered according to the procedure described earlier. The tolerance limit of an ion was taken as the maximum amount (mg L^{-1}) causing an error not greater than 10% in the concentration of analytes [14]. It was seen that most ions studied did not interfere with the determination of Ni(II). The tolerance concentrations were studied species to 1.0 mg L^{-1} Ni(II) under the optimum conditions. It was found that Na^{+}, K^{+}, Ca^{2+}, Ba^{2+}, NO_3^{-}, NO_2^{-} and SO_4^{2-} did not interfere when present up to 200 mg L^{-1}. Al^{3+}, Cr^{3+}, Mg^{2+}, Cl^{-} and PO_4^{3-} did not have any effect up to 100 mg L^{-1}. Mn^{2+} was tolerated up to 80-fold excess. In addition, Pb^{2+}, Cd^{2+} and Zn^{2+} were permitted up to 30-fold excess. However, Fe^{3+}, Co^{2+} and Cu^{2+} were strongly interfered when they present more than 1-fold excess. Fe^{3+} were exist in the water samples in several μg mL^{-1} and need to be eliminated prior to analysis of Ni(II) by using 4.0% sodium fluoride as masking agent. Moreover, Co^{2+} can be eliminated by using 1.0% potassium oxalate solution as marking agent and Cu^{2+} was masked with 0.30% thiourea.

3.6.4 Determination of Nickel in Water Samples and Validation

Following the procedure described in the previous sections, the proposed method was applied to the determination of Ni(II) in water samples (E1-E7). The results obtained by the proposed FI spectrophotometric method compared favorably with those obtained by FAAS (Table 1) using the student *t*-test. It was seen that experimental *t*-value for Ni(II) assay, which was smaller than the theoretical *t*-value at a confidence interval of 95% (3.18) indicating that results obtained by both methods were in excellent agreement.

Table 1: Comparative determination of Ni(II) in water samples by proposed FIA and FAAS

Water sample	Concentrations (mg L^{-1})		D_i
	FIA*	FAAS*	
E1	0.281	0.273	0.008
E2	0.397	0.402	-0.005
E3	0.308	0.315	-0.007
E4	0.434	0.442	-0.008
E5	0.371	0.373	-0.002
E6	0.446	0.449	-0.003
E7	0.506	0.497	0.009
		$\bar{D}$ =	-0.0011
		S.D. =	0.0069
		t =	-0.28
	t-Distribution (95%) =		3.18

*average of triplicate results

4. Conclusions

The proposed FIA spectrophotometric method for determination of Ni(II) based on complexation between Ni(II) and nitroso-R salt has verified to be simple, sensitive and inexpensive. It was shown that the range of percentage recovery was calculated to be 98.3-101.8 % (n=3) and rapid with a sample throughput of 80 h^{-1}. This method has been successfully applied to the determination of Ni in water sample from electroplating and electronic industry and comparing to the FAAS. The results obtained by the proposed FIA are not significantly different from those obtained by FAAS method at a confidence interval of 95% (verified by student's t-test).

Acknowledgements

The authors gratefully acknowledge the Centre for Innovation in Chemistry: Postgraduate Education and Research Program in Chemistry (PERCH-CIC) for financial support. Special thanks are also expressed to Department of Chemistry, Faculty of Science and the Graduate School of Chiang Mai University for their partial funding.

References

1. R.E. Train, **Quality Criteria for Water**, Castle House Publications, 1979, pp. 105–106.
2. J. Kristiansen, J.M. Cristensen, B.S. Iversen and E. Sabbioni, *Sci. Total Environ*., **204** (1997) 147-160.
3. J.M. Cristensen, J. Kristiansen, N.H. Nielsen, T. Menne and K. Byrialsen, *Toxicol. Lett*., **108** (1999) 185-189.
4. H. Bag, M. Lale, A.R. Turker, *Talanta*, **47** (1998) 689-696.
5. A. Alimonti, F. Petrucci, B. Santucci, A. Cristaudo and S. Caroli, *Anal. Chim. Acta*, **306** (1995) 35-41.
6. K.S. Rao, T. Balaji, T.P. Rao, Y. Babu and G.R.K. Naidu, *Spectrochim. Acta B*, **57** (2002) 1333-1338.
7. K. Suvardhan, K. Suresh Kumar, L. Krishnaiah, S. Prabakhara Rao and P. Chiranjeevi, *J. Hazard Mater*., **B112** (2004) 233-238.
8. N. Chimpalee, D. Chimpalee, P. Keawpasert and D.T. Burns, *Anal. Chim. Acta*, **408** (2000) 123-127.
9. S. Vicente, N. Maniasso, Z.F. Queiroz and E.A.G. Zagatto, *Talanta*, **57** (2002) 475-480.
10. D. Vendramini, V. Grassi and E.A.G. Zagatto, *Anal. Chim. Acta*, **570** (2006) 124-128.
11. W. Peng, S. Shu-Jie and Z. Ding, *Microchem. J.*, **52** (1995) 146-154.
12. D.M. Magni, A.C. Olivieri and A.L. Bonivardi, *Anal. Chim. Acta*, **528** (2005) 275-284.
13. V.A. Lemos, C. G. Novaes, A. da Silva Lima and D. R. Vieira, *J. Hazard. Mater*., **155** (2008) 128-134.
14. S. Kruanetr, S. Liawruangrath and N. Youngvises, *Talanta*, **73** (2007) 46-53.

DEVELOPMENT OF DISPERSIVE LIQUID-LIQUID MICROEXTRACTION BASED ON ADJUSTMENT OF SOLVENT MIXTURE DENSITY FOR DETERMINATION OF ORGANOPHOSPHORUS RESIDUES IN WATER

Panida Khamnoon[1], Puttaruksa Varanusupakul[1*]

[1] Chulalongkorn University / Department of Chemistry, Chromatography and Separation Research Unit, Faculty of Science, Bangkok, Thailand

[*] Author for correspondence; E-Mail: puttaruksa.w@chula.ac.th, Tel. +66 22187612, Fax. +66 22541309

Abstract: Dispersive liquid-liquid microextraction (DLLME) was developed for the determination of organophosphorus pesticides (OPPs) in water sample. A high-density organic solvent as an auxiliary solvent was used for adjusting the density of a low-density organic solvent as an extraction solvent. As a result, the density of mixed solvent was higher than water and a phase separation by centrifugation and recovery of the extract were simplified. In this work, 20-50 µL of a mixture of the extraction solvent and the auxiliary solvent was mixed with 0.5-2.0 mL of a disperser solvent. Then, a mixed solution was injected into 5 mL of aqueous sample by syringe, rapidly. A cloudy solution was formed. After centrifugation, the sediment phase at the bottom was removed by microsyringe and directly analyzed by GC-FPD. The limits of detections for the method were range from 0.2 to 0.7 µg L^{-1}. The extraction recoveries for 2.0 µg L^{-1} of OPPs were in the range of 34 - 92 % and relative standard deviations were between 1.7 and 10.4% (n=3). The enrichment factors were about 300. The proposed method is simple, rapid, high enrichment factor and reduced the use of toxic solvent in conventional DLLME, which is environmental friendly.

1. Introduction

Organophosphorus pesticides (OPPs) are widely used in agriculture and considered very toxic to human and animals when absorbed by organism because of acetylcholinesterase deactivation [1]. The European Union established a maximum concentration of 0.1 mg L^{-1} for each individual pesticide and 0.5 mg L^{-1} for the total pesticides in drinking water and 1–5 mg L^{-1} for total pesticides in surface water for drinking purposes [2-4].

Dispersive liquid-liquid microextraction (DLLME) was developed by Razaee [5] from liquid phase micro-extraction, which used the extraction solvent in microliter level and high performance to pre-concentration. DLLME method is based on a ternary component solvent system in which the mixture of extraction solvent and disperser solvent is rapidly injected into aqueous sample. The extraction is enhanced by the formation of small droplets of extraction solvent in the aqueous sample. After centrifugation, the sediment phase at the bottom is removed by microsyringe and can directly analyse by chromatography technique. Nevertheless, the extraction solvents frequently used in DLLME, such as chloroform, dichloromethane, carbon tetrachloride, tetrachloroethylene and chlorobenzene, are extremely toxic and environmental unfriendly. Another DLLME method was then proposed by Leong [6], which based on a solidification of floating organic droplet (DLLME-SFO). This method used a lower density and toxicity organic solvent as an extraction solvent. However, the process of DLLME-SFO is more complicated than DLLME and a sediment phase is difficult to separate causing a loss of analytes.

This research is then interested in taking an advantage of the DLLME and DLLME-SFO technique. A high-density organic solvent was used as an auxiliary solvent for adjusting the density of a low-density organic solvent that acted as an extraction solvent. As a result, the density of mixed solvent was higher than water and a phase separation by centrifugation and recovery of the extract were simplified. It also reduces a toxic solvent consumption, which is environmental friendly. The proposed method was applied to analyze fifteen OPPs in the water sample by gas chromatography coupled with flame photometric detector (GC-FPD).

2. Materials and Methods

2.1 Reagents and solutions

A 100 mg L^{-1} standard solution of fifteen OPPs (ethoprophos, diazinon, disulfoton, etrimfos, pirimiphos-methyl, fenitrothion, triazophos, malathion, chlorpyrifos-ethyl, parathion-ethyl, pirimiphos-ethyl, chlorfenvinphos, methidathion, ethion and EPN) were purchased from Restek, USA. Mixed working standard solutions with concentration range of 0.10-0.25 mg L^{-1} were prepared in acetonitrile. All organic solvents were purchased from J.T. Baker (USA). River water sample was collected from Chao Phraya River in Bangkok, Thailand and stored at 4°C. The sample was filtered through a 0.45 µm membrane before analysis.

2.2 OPPs analysis by GC-FPD

Gas chromatography was performed on Agilent 6890 series (Agilent, USA) equipped with flame photometric detector (FPD). Separation was performed using a Rtx®-OP Pesticide 2 (proprietary Crossband® phase) capillary column with 30 m x 0.25 mm I.D. and 0.25 µm film thickness (Restek, USA). The carrier gas was helium (99.9995%) at constant flow rate of 1.0

mL/min. The injection port was set at 250 ºC in the pulsed splitless mode. The oven temperature was programmed as initially held at 80 ºC for 0.5 min, increased to 140 ºC at the rate of 20 ºC/min, then increased to 210 ºC at 4 ºC/min (held 1 min) and increased to 280 ºC at 30 ºC/min and held at 280 ºC for 10 min. The FPD was set as temperature at 250 ºC, hydrogen gas (99.9999%) at a flow of 80 mL/min and air zero (99.9999%) at a flow of 120 mL/min.

2.3 DLLME based on adjustment of solvent mixture density

A 5 mL water sample was put into a 10 mL centrifuge tube. Subsequently, a mixture of 10 µL toluene (extraction solvent) and 20 µL tetrachloroethylene, (auxiliary solvent) was mixed with 1.5 mL acetonitrile (disperser solvent). Then, a mixed solvent was injected into water sample by syringe, rapidly. A cloudy solution was formed. After centrifugation at 4500 rpm (Rotanta 460, Hettich, Germany) for 5 min, the sediment phase at the bottom was removed by microsyringe and directly analyzed by GC-FPD.

3. Results and Discussion

3.1 Selection of auxiliary solvent and extraction solvent ratio

A ratio of auxiliary solvent and extraction solvent can alter a density of mixed extraction solvent which affecting a sediment phase volume and an extraction efficiency. Therefore, 1:1, 2:1 and 3:1 ratio of tetrachloroethylene (auxiliary solvent) : toluene (extraction solvent) was studied. The extraction recovery and the enrichment factor of all OPPs using different ratio was shown in Table 1. Even through the ratio of 3:1 gave the highest extraction recovery but lower enrichment factor was obtained. Therefore, the ratio of 2:1 was selected for further studies as an acceptable extraction recovery and high enrichment factor.

3.2 Effect of auxiliary solvent and extraction solvent volume

The mixed extraction solvent volume of auxiliary solvent and extraction solvent is one of the important parameter that affected the extraction efficiency. The enrichment factor and extraction recovery of all OPPs at various volume of the mixed solvent of tetrachloroethylene : toluene (2:1) were shown in Table 2, respectively. High enrichment factor was achieved when lower the amount of the mixed solvent of auxiliary solvent and extraction solvent. In contrast, a low extraction recovery was obtained. Although 50 µL of the mixed solvent of the auxiliary solvent and the extraction solvent gave the highest extraction recovery, the lowest enrichment factor was attained. Therefore, 30 µL of tetrachloroethylene : toluene (2:1) was chosen which provided good in both enrichment factor and extraction recovery, and reducing the consumption of toxic organic solvent which is environmental friendly method.

3.3 Effect of disperser solvent volume

The disperser volume makes fine droplet formation of mixed extraction solvent dispersed in sample solution. In proposed method, the effect of disperser solvent volume was evaluated in the range of 0.5-2.0 mL of acetonitrile as shown in Figure 1. The suitable disperser volume was 1.5 mL as good extraction recovery and reproducibility were achieved.

3.4 Effect of salt addition

Usually, the salt addition in the extraction of organic solvents can enhance the extraction efficiency due to decreasing of the solubility of the analytes in aqueous phase by the salting-out effect. But on the other hand, this work was used the mixed extraction solvent between high-density solvent and low-density solvent for extraction. So, the salt addition may affect a separation between high and low-density solvent.

Table 1. Extraction recovery and enrichment factor (EF) of OPPs from spiked sample at concentration of 5 µg L^{-1} using different ratio of tetrachloroethylene and toluene. *Conditions:* sample volume, 5 mL; disperser solvent 1.0 mL of acetonitrile.

Pesticides	tetrachloroethylene : toluene							
	1:1		2:1		3:1		1:0	
	Recovery (%)	EF	Recovery (%)	EF	Recovery (%)	EF	Recovery (%)	EF
Ethoprophos	20 ± 1	247	23 ± 3	215	39 ± 2	144	35 ± 3	125
Diazinon	43 ± 2	539	50 ± 7	481	63 ± 6	235	72 ± 6	257
Disulfoton	39 ± 2	484	48 ± 6	457	64 ± 7	237	71 ± 7	253
Etrimfos	42 ± 3	526	48 ± 6	459	66 ± 5	244	72 ± 6	257
Pirimiphos-methyl	43 ± 4	538	52 ± 6	498	65 ± 8	241	73 ± 6	262
Fenitrothion	48 ± 3	600	54 ± 7	517	71 ± 5	264	74 ± 5	263
Malathion	46 ± 3	575	51 ± 6	484	68 ± 5	253	67 ± 4	240
Chlorpyrifos-ethyl	34 ± 5	421	54 ± 10	519	67 ± 8	251	69 ± 10	245
Parathion-ethyl	47 ± 3	586	56 ± 7	530	72 ± 7	267	79 ± 6	281
Pirimiphos-ethyl	37 ± 5	461	51 ± 5	480	65 ± 8	243	69 ± 7	248
Chlorfenvinphos	45 ± 3	559	50 ± 6	473	68 ± 6	251	69 ± 3	248
Methidathion	31 ± 3	392	37 ± 3	348	56 ± 4	208	49 ± 3	175
Ethion	31 ± 5	393	47 ± 4	448	66 ± 6	246	66 ± 6	234
Triazophos	45 ± 2	558	48 ± 6	451	67 ± 5	248	65 ± 4	231
EPN	46 ± 4	578	64 ± 7	609	89 ± 5	328	91 ± 7	324

Table 2. Extraction recovery and enrichment factor (EF) of OPPs from spiked sample at concentration of 2 µg L^{-1} at various volume of tetrachloroethylene : toluene (2:1). *Conditions:* sample volume, 5 mL; disperser solvent, 1.0 mL of acetonitrile.

	volume of tetrachloroethylene : toluene (2:1)									
	20 µL		25 µL		30 µL		40 µL		50 µL	
	Recovery (%)	EF	Recovery (%)	EF	Recovery (%)	EF	Recovery (%)	EF	Recovery (%)	EF
Ethoprophos	12 ± 10	132	23 ± 3	179	49 ± 15	212	51 ± 2	124	65 ± 4	101
Diazinon	28 ± 24	312	46 ± 6	354	74 ± 3	312	73 ± 3	180	92 ± 3	142
Disulfoton	18 ± 18	204	34 ± 3	259	53 ± 0	221	62 ± 4	151	72 ± 7	111
Etrimfos	26 ± 26	291	45 ± 6	344	69 ± 1	291	77 ± 5	189	90 ± 4	139
Pirimiphos-methyl	25 ± 26	284	48 ± 5	367	71 ± 1	299	78 ± 3	193	95 ± 7	147
Fenitrothion	27 ± 25	311	48 ± 5	369	74 ± 2	313	82 ± 5	200	101 ± 3	157
Malathion	24 ± 23	272	46 ± 5	357	74 ± 3	312	81 ± 2	199	103 ± 2	159
Chlorpyrifos-ethyl	17 ± 14	198	46 ± 5	350	95 ± 11	403	83 ± 2	204	108 ± 2	168
Parathion-ethyl	29 ± 29	327	52 ± 5	398	76 ± 1	319	89 ± 2	218	105 ± 9	163
Pirimiphos-ethyl	19 ± 20	213	45 ± 5	347	71 ± 3	296	85 ± 3	208	98 ± 5	152
Chlorfenvinphos	23 ± 24	261	48 ± 3	367	70 ± 3	294	78 ± 1	191	96 ± 6	149
Methidathion	16 ± 14	184	33 ± 1	251	52 ± 1	217	67 ± 2	164	88 ± 3	136
Ethion	16 ± 15	183	44 ± 6	335	71 ± 3	298	89 ± 4	218	106 ± 8	165
Triazophos	26 ± 25	293	51 ± 2	393	77 ± 2	321	90 ± 7	221	110 ±9	171
EPN	27 ± 29	301	54 ± 5	419	87 ± 3	364	101 ± 4	248	115 ± 8	179

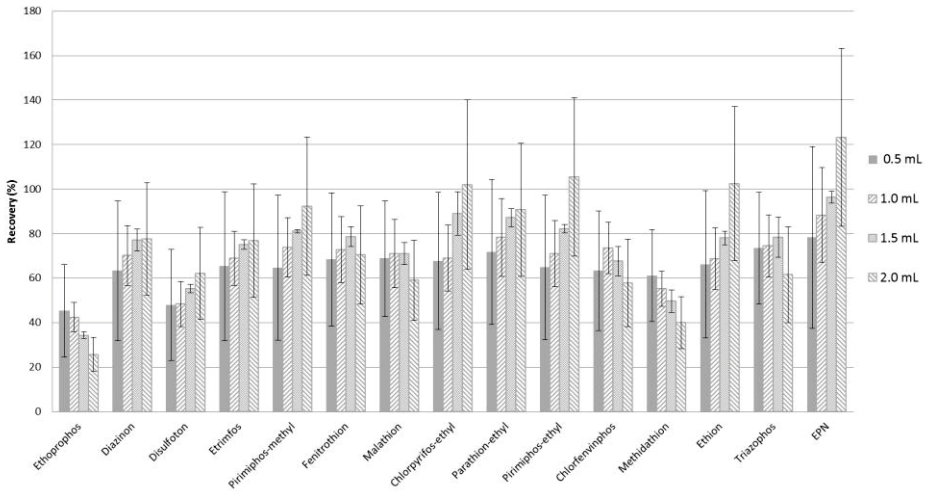

Figure 1. Extraction recovery of OPPs from spiked sample at concentration of 2 µg L^{-1} at various disperser solvent volume. *Conditions:* sample volume, 5 mL; tetrachloroethylene : toluene (2:1), 30 µL.

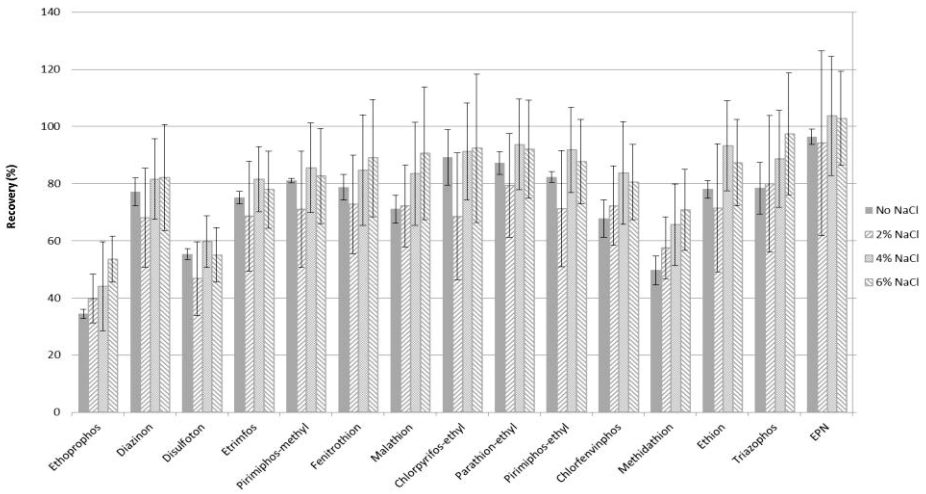

Figure 2. Extraction recovery of OPPs from spiked sample at concentration of 2 µg L^{-1} at different percentage of sodium chloride. *Conditions:* sample volume, 5 mL; tetrachloroethylene : toluene (2:1), 30 µL; disperser solvent 1.5 mL of acetonitrile.

which can observe some of analytes floating on top outside the sediment phase. As shown in Figure 2, the extraction recoveries of analytes for each percentage of sodium chloride was not different. Therefore, no addition of salt was chosen.

3.5 Extraction of OPPs in water by DLLME

To evaluate the proposed method, limit of detection (LOD), extraction recovery, relative standard deviations (%RSD) and enrichment factor (EF) were determined and summarized in Table 3. The limit of detection were ranged from 0.2 - 0.7 µg L^{-1}. The extraction recoveries for 2 µg L^{-1} of OPPs were in the range of 34 - 92 % and relative standard deviations were between 1.7 and 10.4% (n=3). The enrichment factors were ranged from 170-463.

Table 3. Limit of detection (LOD), extraction recovery, relative standard deviations (%RSD) and enrichment factor (EF) for the determination of OPPs in aqueous sample.

Pesticides	LOD (µg L^{-1})	Recovery (%)	%RSD	EF
	n=8	n=3		
Ethoprophos	0.2	34	1.7	170
Diazinon	0.3	78	7.1	392
Disulfoton	0.2	67	5.2	337
Etrimfos	0.3	77	6.2	387
Pirimiphos-methyl	0.4	85	10.4	426
Fenitrothion	0.4	84	5.6	422
Malathion	0.4	73	3.9	367
Chlorpyrifos-ethyl	0.5	75	5.6	375
Parathion-ethyl	0.4	92	7.6	463
Pirimiphos-ethyl	0.4	80	9.8	401
Chlorfenvinphos	0.4	75	3.7	374
Methidathion	0.4	52	8.1	260
Ethion	0.5	75	8.8	378
Triazophos	0.7	71	9.8	355
EPN	0.5	92	8.8	462

3.6 Real water analysis

The analysis of OPPs in real water sample using proposed method was performed. The river water sample was spiked with OPPs at concentration of 2 µg L^{-1}. The chromatogram was shown in Figure 3. and summarized in Table 4.

4. Conclusions

Dispersive liquid-liquid microextraction based on adjustment of solvent mixture density has been developed for determination of organophosphorus residues in water. The method provides simplicity, rapidly, ease to operate, and high enrichment factor. In comparison with conventional DLLME, this method was used lower consumption of toxic solvent, which is environmental friendly.

Table 4. Extraction recovery, relative standard deviations and enrichment factor for the determination of OPPs in real water sample.

Pesticides	Recovery (%)	%RSD	EF
	n=3		
Ethoprophos	46	6.1	181
Diazinon	84	11.2	329
Disulfoton	76	7.2	299
Etrimfos	84	13.6	331
Pirimiphos-methyl	89	9.5	351
Fenitrothion	86	14.4	339
Malathion	82	12.9	320
Chlorpyrifos-ethyl	89	13.9	350
Parathion-ethyl	93	10.5	366
Pirimiphos-ethyl	91	9.9	357
Chlorfenvinphos	84	10.1	328
Methidathion	64	9.1	252
Ethion	92	9.0	359
Triazophos	79	11.0	309
EPN	97	9.3	382

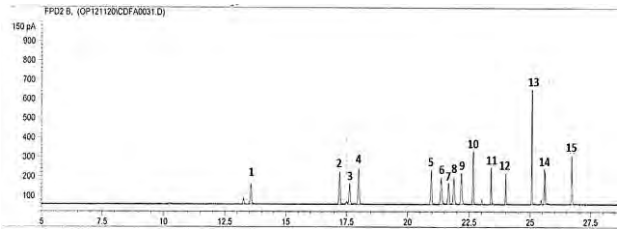

Figure 3. Chromatogram of river water sample with OPPs spiked at 2 µg L^{-1}.
Chromatogram : 1) Ethoprophos, 2) Diazinon, 3) Disulfoton, 4) Etrimfos, 5) Pirimiphos-methyl, 6) Fenitrothion, 7) Malathion, 8) Chlorpyrifos-ethyl, 9) Parathion-ethyl, 10) Pirimiphos-ethyl, 11) Chlorfen-vinphos, 12) Methidathion, 13) Ethion,14) Triazophos, 15) EPN

References

[1] L.M.L. Nollet, *Handbook of Water Analyis*, CRC Press, Boca Raton, FL (2007) 449–491.

[2] The Council of European Union (CEU), *Council Directive 2006/118/EC of 12 December 2006*, on Protection of Groundwater Contamination and Degradation 2006.

[3] World Health Organization (WHO), *Classification of Pesticides by Hazard and Guidelines to Classification*: 2009.

[4] The Council of European Union (CEU), *Council Directive 98/83/EC of 3 November 1998*, on the Quality of Water Intended for Human Consumption 1998.

[5] M. Rezaee, Y. Assadi, M.R. Milani Hosseini, E. Aghaee, F. Ahmadi, S. Berijani, *Journal of Chromatography A* **1116** (2006) 1-9.

[6] M.-I. Leong, S.-D. Huang, *Journal of Chromatography A*, **1216** (2009) 7645–7650.

DEVELOPMENT OF GLUTAMATE BIOSENSOR BASED ON IMMOBILIZED GLUTAMATE OXIDASE ON THE CHITOSAN CROSS LINKED WITH CARBON NANOTUBE MODIFIED GOLD NANOWIRE

Jiraporn Kitikul[1], Anchana Preechaworapun[2], Pusit Pookmanee[1,3], Sakchai Satienperakul[1,3], Tanin Tangkuaram[1,3*]

[1] Chemistry Program, Faculty of Science, Maejo University, Chiang Mai, 50290 Thailand
[2] Department of Chemistry, Faculty of Science and Technology, Pibulsongkram Rajabhat University, Phitsanulok 65000, Thailand
[3] Nanoscience and Nanotechnology Research Laboratory, Faculty of Science, Maejo University, Chiang Mai, 50290, Thailand
*E-mail: tanin@mju.ac.th

ABSTRACT

A glutamate oxidase (GlOx) immobilized on the chitosan (CHIT) cross linked with carbon nanotube (CNT) modified gold nanowire (AuNW) on the glassy carbon (GC) electrode was developed for the determination of glutamate in blood samples. The AuNW was produced using an alumina template membrane and characterized by scanning electron microscopy (SEM). The synthesized AuNW had a wire-like shape with diameter size around 200 nm. The CHIT cross linked CNT slurry was mixed with the AuNW and casted on the surface of GC electrode and followed by immobilizing with the glutamate oxidase (GlOx/AuNW/CHIT-CNT/GC). To optimize the response of the biosensor, the applied potential, GlOx loading, CHIT concentration and AuNW contents were investigated. This biosensor exhibited a rapid and linear response for glutamate concentration from 10 μM to 30 mM (R^2 = 0.9756) with the detection limit of 8.81 μM (S/N=3). The biosensor was successfully employed for the detection of glutamate in real blood samples.

1. Introduction

Glutamate is a non-essential of 20 proteinogenic amino acids. It is an important analyte in medical and food analysis due to its involvement in protein metabolism and neurotransmission which is also responsible in learning memory, neurodevelopment, biomaterial sensitivity and synaptic plasticity[1]. Glutamate is related to several neurological disorder's such as Stroke, Alzheimer's and Parkinson's disease and it's useful maker for the diagnosis of myocardial and hepatic disease[2].

More recently, several methods have been developed for glutamate measurements using different technique such as spectrophotometry[3], high performance liquid chromatography[4], gas chromatography[4], capillary electrophoresis[5], fluorescence[6], and mass spectrometry[7]. However, these methods are time consuming, expensive, laborious and requiring educated person and expensive. This work is wanted to use the biosensor that it was most popular and easy methods for detection of glutamate. These glutamate biosensors were designed based on glutamate dehydrogenase (GLDH)[8-10] and glutamate oxidases (GlOx)[11,12]. The glutamate biosensor based on GlOx was measured the concentration of glutamate by electrochemical monitoring the catalyzed hydrogen peroxide as described in chemical reaction (1) and (2) [13].

$$\text{Glutamate}+O_2+H_2O \xrightarrow{\text{GlOx}} \text{2-oxoglutarate}+NH_3+H_2O_2 \quad (1)$$

$$H_2O_2 \longrightarrow 2H^+ + O_2 + 2e \quad (2)$$

In this report we developed the glutamate biosensor based on AuNW, CHIT, CNT and GlOx to enhance the sensitivity, linearity and selectivity.

2. Materials and Methods

2.1 Chemical and reagent

Chitosan (CHIT, from crab shells, low molecular), multi-walled carbon nanotube (CNT), glutamate oxidase (GlOx, from Streptomyces sp., 1UN), glutaraldehyde (GA), $HAuCl_4 \cdot 4H_2O$, diethyl ether and NaH_2PO_4 were purchased from Sigma Aldrich. An anodic alumina membrane with the pore diameter of 200 nm was supplied by Whatman. A 0.1 M phosphate buffer solution (PBS) pH 7.4 was prepared and employed as a supporting electrolyte. Glutamate stock solution was prepared by dissolving in phosphate buffer solution. All solutions were dissolved in the ultrapure water which was obtained from Milli-Q-gradient system (Millipore, ≥ 18.2 MΩ cm^{-1}).

2.2 CHIT-CNT solution preparation

CHIT solution was prepared by adoption from Tangkuaram[14]. Briefly, 0.5 g CHIT flakes, as received, were added to water with stirring. The concentrated CH_3COOH was gradually added into the solution to maintain the pH near to 4-5 until its completed dissolution. The undissolved material was filtered while the clear and colorless filtrate's volume was adjusted to make up the volume to 100 mL of a 0.5% CHIT solution. The mole ratio of GA to CHIT was 200:1. The mix solution was extracted with diethyl ether for separation the unreacted GA. The

CHIT stock solution was stored in a refrigerator (4 ^{o}C) when not in use.

5 mg of CNT was dispersed in 1 ml of 0.5 % CHIT solution and ultrasonicated for 30 minutes. Then, 4 mg of AuNW was dispersed and followed by ultrasonicated for 30 minutes to receive a homogeneous dispersion.

2.3 Synthesized the AuNW

An alumina membrane was used as a template to synthesize the AuNW. The alumina membrane was gold sputtered at the current of 15 mA for 150 seconds prior used as a working electrode. A graphite carbon rod (5 mm of dia.) was used as counter while the Ag/AgCl (3 M KCl) was used as a reference electrode. The gold chloride solution was poured into the Teflon-made electrochemical cell. The deposition potential was operated at -0.9 V for 20,000 seconds. After that, the membrane was washed with 35% nitric acid to remove the sputtered-gold and followed by soaked with 3 M NaOH and centrifuged at 5,000 rpm for 15 minutes. The morphology of the AuNW was characterized by the scanning electron microscope (SEM).

2.4 Preparation of modified electrodes

The glassy carbon electrode (GC) was polished with fine emery paper and 0.05 μm alumina powder, rinsed thoroughly with ultrapure water prior to modify.

The GlOx/AuNW/CHIT-CNT/GC was prepared by drop casting of 20 μl of AuNW, CHIT and CNT mix solution, followed by 30 μl of GlOx was cast on to the electrode to obtain the GlOx/AuNW/CHIT-CNT/GC. For the GlOx/GC, GlOx/CNT/GC and GlOx/CHIT-CNT/GC were prepared in a same manner of GlOx/AuNW/CHIT-CNT/GC. All modified biosensors were rinsed with ultrapure water before used.

2.5 Experimental measurement

Electrochemical experiments were proceeded in an associated electrochemical cell comprising of a three electrodes, which is a modified electrode served as a working, GC (3 mm dia.) as a counter and Ag/AgCl (3 M KCl) as a reference electrodes. The glutamate biosensor was characterized by cyclic voltammetry. The amperometric measurements were performed in a 3 ml of PBS at room temperature with an applied potential of 0.7 V.

3. Results and Discussion

3.1Characterized AuNW

The typical SEM image of the AuNW was showed in figure 1. The size and shape of the synthesized AuNW had a wire-like shape with diameter size around 200 nm and with long about 1 mm.

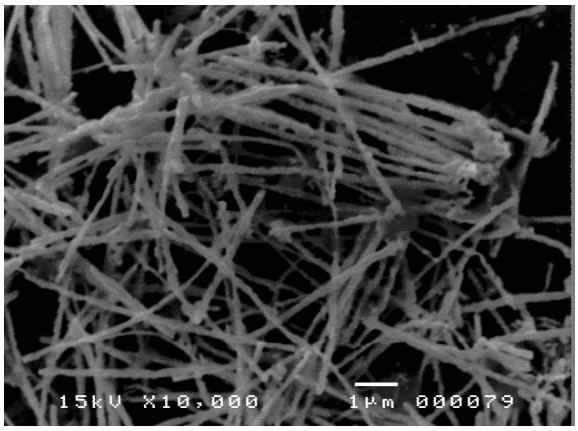

Figure 1. SEM image of AuNW

3.2 Cyclic Voltammetry characterization of modified electrode

The cyclic voltammograms for five types of electrodes; bare GC, GlOx/GC, GlOx/CHIT/GC, GlOx/CHIT-CNT/GC and GlOx/AuNw/CHIT-CNT/GC electrodes recorded at 50 mVs^{-1} in 0.1 PBS pH 7.4 in the absence (a) and presence (b) of 10 mM glutamate showed in figure 2. Upon the addition of glutamate, five electrodes showed typical catalytic cyclic voltammograms associated with increased anodic current. At the modified GlOx/AuNw/CHIT-CNT/GC (figure 2 e), the anodic current is the highest over all of electrodes at 0.7 V.

3.3 Optimization of the parameter

The next work addressed the optimization of the applied potential, GlOx loading, CHIT concentration and AuNW contents for the highest signal. figure 3A shows the applied potential on the amperometric response. The maximum response was reached at 0.7 V due to the oxidation of hydrogen peroxide to water. The higher applied potential more than 0.7 V is not only influence on the increasing of the current but also raising the background current. Therefore, the optimization applied potential is selected at 0.7 V.

Figure 3B shows the enzyme loading of the modified electrode. The response current rises obviously with the increasing of the loading content beyond 30 μl. The remarkable characteristic is the higher volume of GlOx (more than 30 μl) showed the smaller current, indicating there is due to a thickness of enzyme blocking the diffusion of hydrogen peroxide in to the glassy carbon surface. Thus, 30 μl of enzyme loading was selected for the further experiments.

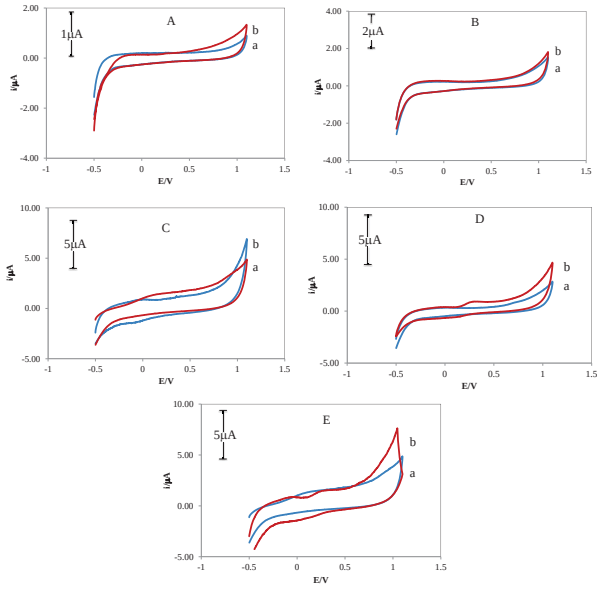

Figure 2. Cyclic voltammograms of A) bare GC, B) GlOx/GC, C)GlOx/CHIT/GC, D) GlOx/CHIT-CNT/GC and E) GlOx/AuNw/CHIT-CNT/GC electrodes at scan rate 50 mVs^{-1} in 0.1 PBS pH 7.4 in the absence (a) and presence (b) of 10 mM glutamate.

The effectiveness of the CHIT concentration was showed in figure 3C. The response currents reached the maximum at 0.5 % CHIT and decrease with increasing concentration of CHIT. This phenomenon was due to the thickness of CHIT act as the barrier of electron transfer.

To facilitate the electrochemical communication of the CNT and the electrode was examined on the CNT concentration. The result is shown in figure 3D. The response current was highest when 5 mg/ml of CNT used while the response current with 7 mg/ml of CNT is absent. This indicates that the over content of CNT plays a blocking barrier to the electron transfer.

The AuNW content provides an attached binding of GlOx. Figure 3E shows the effectiveness of the AuNW. The response currents reached the maximum at 4 mg/ml of AuNW. However the sensor response decreased at more than 5 mg/ml of AuNW, probably the large attachment amount of GlOx on the AuNW will blocked their active site.

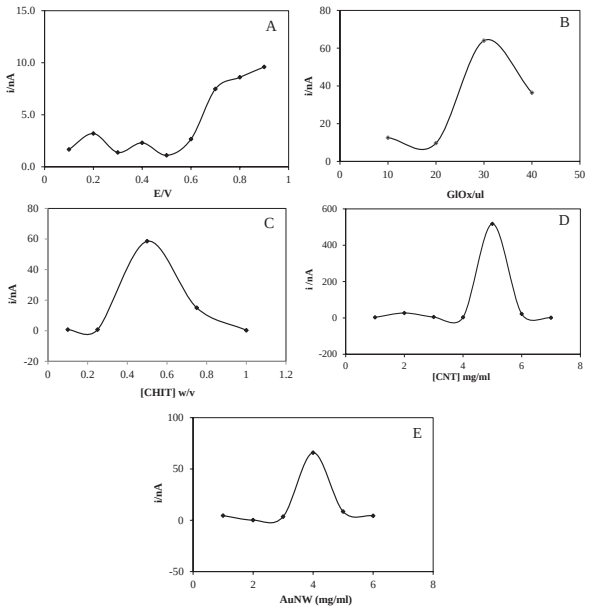

Figure 3. Optimization of the applied potential (A), enzyme loading (B), concentration of CHIT (C), concentration of CNT (D) and concentration of AuNW (E). Condition: Amperometric measurement in solution of 10 mM glutamate/0.1 M PBS pH 7.4, $E_{applied}$ 0.7 V.

3.4 Amperometric determination of glutamate with biosensor

The calibration plot using the GlOx/AuNW/CHIT-CNT/GC electrode under the optimized experimental condition was showed in figure 4. The biosensor exhibited the sensitive response corresponding to the glutamate concentration. The linear calibration range of this biosensor was from 10 µM to 30 mM (R^2 = 0.9756) with a sensitivity of 0.0016 $nA.\mu M^{-1}$. Inset of figure 4 also shows the linearity at lower concentration from 10 µM to 100 µM of glutamate. The limit of quantitation was 26.43 µM and the detection limit was 8.81 µM when the signal to noise ratio was 3.

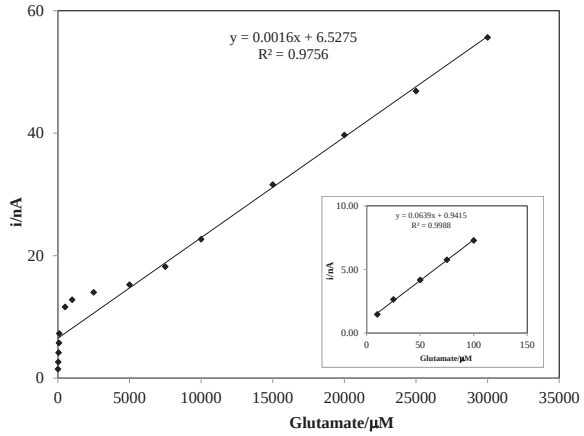

Figure 4. Calibration curve of the response of the GlOx/CHIT-CNT-AuNW/GC electrode at an applied potential was at 0.7 V versus Ag/AgCl in 0.1 M PBS

(pH7.4). Inset shows linearity in the low concentration of 10 – 100 μM.

3.6 Analytical application

The GlOx/AuNW/CHIT-CNT/GC electrode was applied to determine the glutamate content in human blood samples by using standard addition method. The results is comparative satisfactory with the results from a spectrophotometric method. All results are listed in Table 1. This biosensor was not significant different for both mean (T-test) and variance (F-test) from the spectrophotometer ($p>0.05$) at confident level of 95%.

Table 1. Determination of glutamte in human blood.

Sample	Biosensor (μM)	Spectro Photometer (μM)	T-test	F-test
1	315±8.19	319±8.89		
2	492±9.07	407±9.07	1.54	1.60
3	418±9.00	456±8.36		

4. Conclusions

A technique for fabricating glutamate biosensor have been developed which features an effective combination of CHIT, CNT, AuNW and GlOx. All of the composites can be used to construct a stable enzyme electrode. This biosensor was easy and reliable in glutamate determination. In addition, the biosensor exhibited the good characteristics such as low detection limit, high sensitivity and wide linear range.

Acknowledgements

The authors would like to acknowledge the financial support from the Research, Development and Engineering (RD&E) fund through The National Nanotechnology Center (NANOTEC), The National Science and Technology Development Agency (NSTDA), Thailand (P-12-01279) to Maejo University of Thailand.

Reference

[1] M. Jamal, J. Xu, K.M. Razeeb, *Biosens. Bioelectron.* **26** (2010) 1420-1424.
[2] M.M. Rahman, A. Umar, K. Sawada, *J. Phys. Chem. B* **113** (2009) 1511-1516.
[3] R. Maalouf, H. Chebib, Y. Saïkali, O. Vittori, M. Sigaud, N. Jaffrezic-Renault, *Biosens. Bioelectron.* **22** (2007) 2682-2688.
[4] R. Monosik, M. Stred' ansky, E. Sturdik, *Food Anal. Methods* (2012) 1-7.
[5] S. Tucci, C. Pinto, J. Goyo, P. Rada, L. Hernández, *Clin. Biochem.* **31** (1998) 143-150.
[6] J. Chapman, M. Zhou, *Anal. Chim. Acta* **402** (1999) 47-52.
[7] L.A. Dawson, J.M. Stow, A.M. Palmer, *J. Chromatogr. B. Biomed. Sci. App.* **694** (1997) 455-460.
[8] C. Jeffries, N. Pasco, K. Baronian, L. Gorton, *Biosens. Bioelectron.* **12** (1997) 225-232.
[9] Y. Cui, J.P. Barford, R. Renneberg, *Sens. Actuators, B* **127** (2007) 358-361.
[10] L. Tang, Y. Zhu, L. Xu, X. Yang, C. Li, *Talanta* **73** (2007) 438-443.
[11] S. Pan, M.A. Arnold, *Talanta* **43** (1996) 1157-1162.
[12] B.-C. Ye, Q.-S. Li, Y.-R. Li, X.-B. Li, J.-T. Yu, *J. Biotechnol.* **42** (1995) 45-52.
[13] J.M. Cooper, P.L. Foreman, A. Glidle, T.W. Ling, D.J. Pritchard, *J. Electronanal. Chem.* **388** (1995) 143-149.
[14] T. Tangkuaram, C. Ponchio, T. Kangkasomboon, P. Katikawong, W. Veerasai, *Biosens. Bioelectron.* **22** (2007) 2071-2078.

CHARACTERISATION OF BIO-OIL PRODUCT FROM PYROLYSIS OF JATROPHA CAKE

Saniporn Chanchaturaphan[1], Siriporn Larpkiatthaworn[2], Wasana Khongwong[2], Orapin Chienthavorn[1*]

[1]Department of Chemistry and the Center of Excellence for Innovation in Chemistry, Faculty of Science, Kasetsart University, P.O. Box 1011 Chatuchak, Bangkok 10903, Thailand.

[2] Thailand Institute of Scientific and Technological Research (TISTR), Technopolis, Klong 5, KlongLuang, Pathumthani 12120, Thailand

[*] Author for correspondence; E-Mail: fsciopc@ku.ac.th, Tel. +66 25625555, Fax. +66 25 793955

Abstract: To develop to be an efficient energy fuel the bio-oil was obtained from pyrolysis of jatropha residue with and without a palladium coated alumina (Pd/Al_2O_3) catalyst by using a quartz reactor. The pyrolysed bio-oil separated into three phase namely gas, light liquid and black liquid, which were mainly determined by gas chromatography-mass spectrometric detection (GC-MS). The gas composed of a mixture of hydrogen, carbon monoxide, carbon dioxide, methane, ethylene and ethane with different compositions, and carbon dioxide was the major product. The light liquid consisted of mostly acetic acid and other acids, alcohols, and a few nitrogen compounds. The black liquid is the key phase for using in the energy applications, consisting aromatic hydrocarbons, phenols, alcohols, ketones, ethers, aldehydes, alkanes, alkenes, acids, esters, N-heterocycles and N-nonheterocycles. The ratio of composition in both black and light liquid and in the gas phase were compared under conditions of pyrolysis with and without catalyst.

1. Introduction

While energy consumption is continuously increasing, conventional natural fuel sources are decreasing every day. The most important primary energy resource of the world is fossil fuel of which problem is that it is non-renewable. As an alternative biomass is one of renewable energy sources that can be converted into liquid fuels, since it comprises highly lignocelluloses, such as cellulose, hemicelluloses and lignin, obtained from crop or agriculture remains [1,2]. Burning biomass releases little of sulfur, nitrogen, and carbon dioxide that is a key factor affecting global warming and acid rain [2,4]. In a conversion of the biomass to liquid fuel pyrolysis is generally utilized by thermal depolymerisation occurring in absence of oxygen and at a temperature around 500°C. The decomposed biomass gives gases, char, and liquid that is called bio-oil. A typical bio-oil contains water, sugar, acids, esters, aldehydes, ketones, alcohols, ethers, aliphatic hydrocarbons, aromatic hydrocarbons, N-compounds, phenols and other derivatives, but the quantities of these compounds depend on type of raw materials and pyrolysis condition [5]. Such compounds are derived from fragmentation and polymerization of lignocelluloses in varied temperature ranges: hemicelluloses decompose at 250-400°C; celluloses degrade at 310-430°C; and lignin decomposes at 300-530°C [1,2,10]. Gases from biomass, such as carbon dioxide, carbon monoxide, methane, and shorted chain carbon, are released during pyrolysis process [6-8,10-12]. The compounds and product yields of biomass are varied, depending on biomass species, temperature, heating rate, moisture, feedstock, transportation and others [2,13,15]. Because the oil from biomass is an unstable mixture with high acidity, high water and oxygen content, and high viscosity, improving in the oil quality is therefore needed for a qualified transportation bio-fuel [2,3].

Biomass for the bio-oil production in this study was jatropha cake, which is a by-product from processes to remove oil from jatropha seeds. From literature review the main characteristic of jatropha oil residue analyzed by proximate analysis are 8.71% moisture, 4.30% ash, 70.92% volatile matter, 16.06% fixed carbon and 0.01% sulfur. In addition, an ultimate analysis declared 59.17% carbon, 6.52% hydrogen, 33.93% oxygen and 0.38% nitrogen [13]. To achieve high energy efficiency fuel generally contains optimal quantities of oxygen and nitrogen. In this study the bio-oil from jatropha residue was characterised, and compositions of the oil produced from pyrolysis process with and without Pd/Al_2O_3 catalyst were compared.

2. Materials and Methods

2.1 Sample preparation

Bio-oil was produced from jatropha residue by a pyrolysis system. The residue was crushed into powder of which particle size ranging between 75-850 μm. A 25 g of the powder in a 20 cm long x 2.5 cm i.d. quartz cylindrical tube was pyrolysed at 500°C for 30 min in the system to give bio-oil liquid passing through a condenser into a receiving flask of which sidearm outlet was for gas release or collection by using a gas sampling bag for further component analysis. Either 0, 5, 10, 20 and 100% of the catalyst was put on the top of the jatropha residue powder, and 4-5 alumina balls were loaded on top of the catalyst to prevent blowing up during the pyrolysis.

2.2 Product Analysis

Jatropha bio-oil was determined by pyrolysis gas chromatography (Py-GC-MS) using a 2020iD Frontier Lab pyrolyser connected with an Agilent 7820A gas chromatograph equipped with an Agilent 5975 mass selective detector (MSD). Helium of ultra high purity was used as a carrier gas at a flow rate of 1.0 mL/min. The pyrolyser temperature was controlled at 350°C for 0.5 min. For black liquid bio-oil a separation was carried out on a 30 m × 0.32 mm × 0.5µm UA-5(MS/HT) capillary column that was programmed at 40°C for 2 min, then increased at a rate of 5°C/min to 200°C, further raised at 10°C/min to 350°C, and held for 2 min. The GC injector and interface temperature were held at 280°C, and the injector split ratio was 25:1. The mass spectrometer was operated in the electron impact (EI) mode at 70 eV with the mass scanning range of 50 to 600 m/z. The black liquid bio-oil sample was mixed with silica gel (Wakogel C-200, 75-150 µm, Wako) with a ratio of 1:1 for prevention of overheating of the oil and 0.0025 g of the mixture was weighed into the pyrolysis cup before analysis. For the light liquid the separation was performed on a 60 m × 0.32 mm × 0.25 µm Stabilwax®-DA capillary column. The temperature program was started at 120°C, then increased at 5°C/min to 180°C, further raised at 10°C/min to 230°C, and held for 18 min. The GC injector and interface temperature were at 230°C with splitless injection mode. Chromatographic peaks of bio-oil components were identified by NIST (National Institute of Standards and Technology) mass spectral library, and the peak area percentage was calculated, corresponding to the summation of total possible jatropha residue peaks. For the pyrolysis gas in the gas sampling bag the separation was achieved on a 30 m × 0.32 mm × 3 µm GS-CarbonPLOT capillary column of which temperature program was initially set at 50°C for 1 min, then increased at 5°C/min to 70°C, and held for 3 min. The GC injector and interface temperature were at 50°C and 70°C, respectively. The GC-MS was operated with a split ratio of 10: 1 and scanning mass range of 15 to 200 m/z.

3. Results and Discussion

At the beginning of the pyrolysis gas was highly produced from the chamber, and the gas volume was measured by water displacement. The gas components in the gas mixture were identified as hydrogen, carbon monoxide, carbon dioxide, methane, ethylene and ethane. Gas collection was performed along the pyrolysis, and it was noticed that the first 5-min collected gas was flammable. GC-MS analysis of the gas confirmed the ethylene and ethane content in the gaseous mixture. The fresh liquid product obtained from the pyrolysis was not homogeneous. With a long storage period of the bio-oil the separation occurred as two liquid phases, namely light and black liquid. The black compartment gave strong smoking odour. It was also observed that the catalysed liquid product was more homogenous than the non-catalysed one. The GC-MS identification of light liquid revealed that the major components were water, acidic compounds, and oxygenated compounds.

3.1 Characterisation of Pyrolysed Products

From the GC-MS identification the black liquid from the pyrolysis of jatropha cake mainly composed of aromatic hydrocarbons, phenolic compounds, oxygenation compounds, acids, esters, aliphatic hydrocarbons, N-heterocycles, N-nonheterocycles and multifunctional large molecules. The compounds were classified by functional groups and the area percentage of each group was combined to obtain different amount of catalysed fractions as shown in Figure 1.

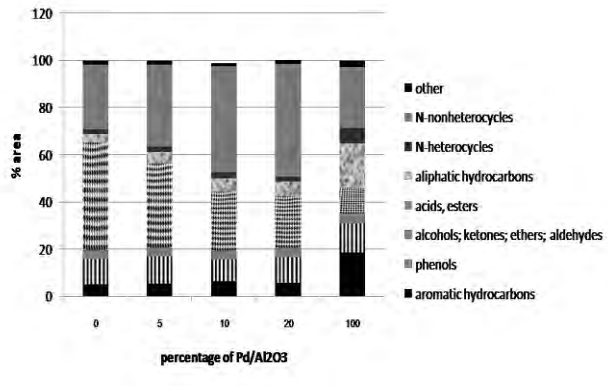

Figure 1. Area percentage of each component group of black liquid obtained from pyrolysis w/o Pd/Al_2O_3 catalyst

From the non-catalytic pyrolysis the chromatographic results indicated the content of each component group as follows. 4.24% of the aromatic hydrocarbon compounds consists of toluene, xylene, ethylbenzene, naphthalene, fluorine and alkyl-substituted benzene. The phenolic compounds of 14.70% contain phenol, n-alkylphenols and n-methoxyphenols, while 6.68% of the group of alcohols, ketones, ethers and aldehydes was propanol, 2-cyclopenten-1-one, 2-furanmethanol, 1-(2-furanyl)ethanone, E,E-10,12-hexadecadienal. The acids and esters content comprising acetic acid, cis-vaccenic acid, hexadecanoic acid (palmitic acid), octadecenoic acid (oleic acid) and octadecanoic acid (steric acid) were of 33.64%. The alkanes and alkenes compounds were 3.26% consisting 1-hexen-3-yne, alkyl-cyclopentene, alkyl-cyclohexane, pentadecane, heptadecane and 17-pentatriacontene. The N-heterocycles of 2.87% contain pyridine, alkyl-pyridine, pyrrole, alkyl-pyrrole, indole and alkyl-indole, whereas 30.80% of the N-nonheterocycles was propanenitrile, hexanenitrile, benzonitrile, benzylnitrile, oleanitrile and octadecanamide. A comparison of black liquids obtained from pyrolysis without the catalyst and with 5%, 10% and 20% catalyst revealed the alteration of the acidic and the N-nonheterocycle contents in the mixture. Increasing the weight ratio of catalyst to sample the acid and ester content decreased, on the other hand the N-nonheterocycle yields raised, while no change in the

amount was found for the aromatic or aliphatic hydrocarbon.

In the catalyst pyrolysis using (1:1) Pd/Al_2O_3 mixed with the cake (or 100% catalyst) the content of aromatic hydrocarbon significantly increased up to 18.62% and that of aliphatic hydrocarbon also improved to 18.82%. Phenols; alcohols, ketones, ethers and aldehydes; acids and esters; N-heterocycles; and N-nonheterocycles content in the mixture were 12.26%, 4.32%, 10.66%, 6.55% and 25.88%, respectively. The light bio-oil liquid was characterised as a mixture of acetic acid, propanoic acid, 2-furanmethanol, butanoic acid, hexanoic acid, 2-methyl-2-propen-1-ol, hydroxydecanoic acid, imidazole, glycerine, 3-pyridinol and isosorbine. From chromatographic results of one with and without the catalyst the components are similar in terms of both kind and number, except that with 100% catalyst no peaks were found for glycerine and isosorbine. The amount of each component however varied, depending on the amount of added catalyst. With 100% catalyst 3-pyridinol amount increased up to 11.8%, while with 5-20% catalyst the components did not much change in the amount. The acetic acid was 21-33% of total composition of the liquid.

The gaseous product collected from 5 g of the jatropha cakes and gave 0.5 L of volume. The gaseous mainly composed of hydrogen, carbon monoxide, carbon dioxide, methane, ethylene, and ethane which were different in the amounts, depending on the ratio of catalyst. Less percentage of each gas component was detected from the non-catalytic pyrolysis. For higher ratio of catalyst carbon dioxide was largely produced, while carbon monoxide and short chain hydrocarbons, namely methane, ethane, ethylene amount were also increased, confirming the cracking by the catalyst and oxygen removal.

A possible reaction occurred during the pyrolysis was postulated to be hydrodeoxygenation that removed oxygen containing compounds in the oil [1,3,4,9,14]. The Pd/Al_2O_3 catalyst supported the cracking of carbon-carbon, carbon-oxygen, and carbon-nitrogen bonds which corresponds to hydrogenation [8,9]. It was observed that the percentage of phenolic compounds was 12.26% similar to that of non-catalytic pyrolysis, but the number of detected components was smaller. This implied that the large phenolic molecules were cracked at carbon-oxygen bonds to give highly alkyl-substituted benzene products of which possible reactions were given elsewhere [3].

4. Conclusions

Pyrolysis GC-MS method facilitated the characterisation of bio-oil obtained with and without catalyst. Palladium supported on alumina (Pd/Al_2O_3) catalyst allowed highly oxygen-containing compounds removal from the oil, and supported the reaction to give aromatic hydrocarbons, which mostly were alkyl-substituted benzene and aliphatic hydrocarbons, and also decreased acidic compounds. On the other hand the nitrogen was not sufficiently removed. The catalyst did not have enough efficiency to improve the quality of bio-oil, it is therefore not recommended for bio-oil upgrading process.

Acknowledgements

The Center of Excellence for Innovation in Chemistry (PERCH-CIC), Office of the Higher Education Commission, Ministry of Education and the Thailand Institute of Scientific and Technological Research (TISTR) are acknowledged for financial support and studentship for S. Chanchaturaphan. We would like to express our appreciation to Dr. Makoto Toba and Dr. Kazuhisa Murata, AIST for his guidance on GC analysis. We are also grateful to Dr. Thanes Utistham from Energy Technology department, TISTR for laboratory facilities. The GC/MS equipment supported by the Japan International Cooperation Agency (JICA) was also acknowledged.

References

[1] D. A. Bulushev and J. R. H. Ross, *Catal. Today*. **171** (2011) 1-13.

[2] D. Mohan, C. U. Pittman, Jr. and P. H. Steele, *Energ. Fuel*. **20** (2006) 848-889.

[3] C. A. Fisk, T. Morgan, Y. Ji, M. Crocker, C. Crofcheck and S.A. Lewis, *Appl. Catal. A-Gen*. **358** (2009) 150-156.

[4] Z. Qi, C. Jie, W. Tiejun and X. Ying, *Energ. Convers. Manage*. **48** (2007) 87-92.

[5] K. Murata, P. Somwongsa, S. Larpkiattaworn, Y. Liu, M. Inaba and I. Takahara, *Energ. Fuel*. **25** (2011) 5429-5437.

[6] D. C. Elliott, *Energ. Fuel.* **21** (2007) 1792-1815.

[7] S. A. Raja, Z. R. Kennedy, B. C. Pillai and C. L. R. Lee, *Energy*. **35** (2010) 2819-2823.

[8] L. Devetta, A. Giovanzana, P. Canu, A. Bertucco and B. J. Minder, *Catal. Today*. **48** (1999) 337-345.

[9] C. Zhao, J. He, A. A. Lemonidou, X. Li and J. A. Lercher *J. Catal*. **280** (2011) 8-16.

[10] T. Qu, W. Guo, L. Shen, J. Xiao and K. Zhao, *Ind. Eng. Chem. Res*. **50** (2011) 10424-10433.

[11] E. Ranzi, A. Cuoci, T. Faravelli, A. Frassoldati, G. Migliavacca, S. Pierucci and S. Sommariva, *Energ. Fuel.* **22** (2008) 4292-4300.

[12] S.A. Raja, Z.R. Kennedy, B.C. Pillai and C.L.R. Lee, *Energy*. **35** (2010) 2819-2823.

[13] S.A. Raja, Z.R. Kennedy and B.C. Pillai, *IJCEA*. **2** (2010) 1-12.

[14] K. C. Kwon, H. Mayfield, T. Marolla, B. Nichols and M. Mashburn, *Renew. Energ.* **36** (2011) 907-915.

[15] S. T. Gopakumar, S. Adhikari, H. Ravindran, R. B. Gupta, O. Fasina, M. Tu and S.D. Fernando, *Bioresource Technol*. **101** (2010) 8389-8395.

Biological / Biophysical Chemistry and Chemical Biology

THE GAMMA-ORYZANOL CONTENT IN RICE BRAN EXTRACTED AND DETERMINED BY USING THE ADSORPTION COEFFICIENT (K)

Anakhaorn Srisaipet*, Khemtong Yoohom

Department of Chemistry, Faculty of Science, Maejo University, Sansai, Chiang Mai, Thailand

* Author for correspondence; E-Mail: anakhaorn@mju.ac.th, Tel. +66 53873529, Fax. +66 53873548

The major objectives of this study are extraction development and determination of Gamma-oryzanol in rice bran by using the adsorption coefficient (K) in equilibrium condition. The quantitative analysis of gamma-oryzanol in rice bran using adsorption coefficient has been affected by different types of organic solvents. Hexane and petroleum ether can extract gamma-oryzanol for 3.52 and 3.67 mg/g rice bran (dry basis) with the K value of 1.01 and 1.26, respectively. For ethyl acetate and isopropanol extraction, gamma-oryzanol yields are of 3.75 and 4.33 mg/g rice bran (dry basis) with the K value of 1.12 and 1.49, respectively. Results are well agreement with classical extraction method that used isopropanol as a solvent which yields 3.95 mg/g rice bran (dry basis). The composition of Gamma-oryzanol in crude rice-bran oil was analyzed by high performance liquid chromatography.

1. Introduction

Rice (*Oryza sativa*) production is a consequential food crop in Thailand. Rice bran (RB), a valuable by-product in the rice processing industry, contains 12-23% rice bran oil (RBO)[1]. It shows 95.6 % saponified matter, e.g. glycolipid and phospholipid and 4.2% unsponified matter, e.g. tocopherols, tocotrienols and γ-oryzanol [2]. γ-oryzanol is an important component in crude RBO varied in range of 0.10 - 2.9% depending on genetic and environmental factors [3,4]. It is a complex mixture of ferulate that is esterified with triterpene alcohols or sterol. γ-oryzanol shows the reduction of cholesterol in blood, appropriative in the anti-inflammatory, and anti-aging effect greater than tocopherols about 13 – 20 times [3, 5]. In addition, it demonstrated potential antioxidant for food, pharmaceutical and cosmetic industries.

Quantification of γ-oryzanol in RB can be determined by the analysis of the amount of γ-oryzanol in RBO.

Recently, the reputedly extraction techniques used to extract γ-oryzanol in RBO are supercritical fluid extraction (SFE) and direct solvent extraction (DSE) [4,5]. The requirement for special devices is drawback for SFE but not for (DSE). DSE method provides more advantages such as less time-consuming. However if the solvents being used for extraction have low potency, a large volume of solvents must be exploited. Solid-liquid extraction is an alternative extraction which uses the rapid equilibrium extraction principle or to be defined as solid – liquid equilibrium (SLE). SLE is described by the distribution or adsorption coefficient (K) of a solute between solid and solvent phase. The K value is the proportion of solute concentration in liquid and solid phase at equilibrium [4] as shown in equation (1), where C_m is concentration of solute in solvent phase and A_s is amount of solute adsorbed by one gram of the adsorbent (rice bran).

$$K = \frac{C_m}{A_s} \qquad (1)$$

C_m values can be determined as a ratio of the amount of solute in solvent phase (M_m) and solvent volume (V_m) while a ratio of the amount of solute in solid phase (M_s) and weight of rice bran (G_s) is defined for A_s, as shown in equation (2).

$$K = \left(\frac{M_m}{V_m}\right)\left(\frac{G_s}{M_s}\right) \qquad (2)$$

In this work, we attempt to use the SLE method to determine total lipid and γ-oryzanol in rice brans using the K value as described by equation (1) and (2), respectively. The qualitative analysis of γ-oryzanol has been accomplished by HPLC.via by solving two simultaneous equations was used

2. Materials and Methods

2.1 Materials

Gamma oryzanol were supplied by the Vegetable Oil Refinery (Bangkok, Thailand). Petroleum ether, 2-propanol, 2-butanol, *n*-hexane and ethyl acetate (analytical grade) were purchased from LabScan (Bangkok, Thailand). Acetronitrile and Methanol HPLC grade) were purchased from Fisher Chemicals (UK).

Rice brans were obtained from the local rice mills at Singburi, Thailand. The moisture content of bran was determined by hot-air drying at 105 °C until the

weight is constant. All samples were analyzed in duplicate.

2.2 Extraction of total lipid via Soxhlet extraction

The extraction of rice bran oil was applied from the Association Official Chemists (AOAC). Ten grams of dried rice bran is used for Soxhlet extraction by petroleum ether for 4 h. Solvent was evaporated and dried by rotary evaporator, then cooled and weighed. The extract method with other solvents; hexane, ethyl acetate and 2-propanol, was performed accordingly.

2.3 Determination of total lipid and γ-oryzanol by solid - liquid extraction via the adsorption coefficient (K)

1.0 gram of dried bran was weighed into two screw cap test tubes. 4 and 8 milliliters of petroleum ether or hexane or ethyl acetate or 2-propanol were added into the first and the second tubes, respectively. Extraction was performed by vortex mixing for 5 min at ambient temperature. The mixture was then centrifuged for 10 min at 4,000 rpm to separate the bran from miscella. Supernatants obtained from both samples were collected and reccorded for absorpion spectra by using a U-100 UV-VIS spectrophotometer (HITACHI, Japan). Quantifications of lipid and γ-oryzanol in the extracts were determined by standard curve. The total lipid and γ-oryzanol were calculated by the adsorption coefficient as described by equations (3),

$$K = \left(\frac{x}{V}\right)\left(\frac{w}{y-x}\right) \qquad (3)$$

where x is the amount (g) of lipid or γ-oryzanol in the extract, y is the total amount (g) of lipid or γ-oryzanol in the bran, V is the volume (ml) of solvent, and w is the weight of bran. K and y in equation (3) are unknown and can be determined by derivations as described in equation (4) and (5), where V_2 is twice volume of V_1 and x_1 and x_2 are the amounts of solute in the two extractions.

$$K_1 = \left(\frac{X_1}{V_1}\right)\left(\frac{w}{y-x_1}\right) \qquad (4)$$

$$K_2 = \left(\frac{X_2}{V_2}\right)\left(\frac{w}{y-x_2}\right) \qquad (5)$$

K_1 and K_2 is equal under assumption that the different amount of extraction solvent did not affect the K value, thus resulting in (equation (6) and (7), respectively.

$$\left(\frac{x_1}{V_1(y-x_1)}\right) = \left(\frac{x_2}{V_2(y-x_2)}\right) \qquad (6)$$

$$y = \frac{x_1 x_2}{2x_1 - x_2} \qquad (7)$$

Total amount of lipid and/or γ-oryzanol in the bran can be calculated according to equation (7) and the K value is determined by substituting the y value in equation (4) and (5).

2.4 HPLC analysis

The composition of γ-oryzanol was determined by HPLC using acetronitrile/methanol (10:9) solvent system as a mobile phase and C18 (Hewlett Packard) HPLC column (125 mm x 4.0 mm i.d.).

3. Results and Discussion

The total lipids and γ-oryzanol obtained from extraction of RB (% dried weight basis) were quantified by UV spectrophotometric method using external standard calibration. The maximum wavelengths (λ_{max}) and standard calibration of γ-oryzanol analysis were displayed in table 1 which is similar to a previous study [6]. Therefore, the wavelengths and linear Regression will be used in the next study.

Table1. Maximum wavelengths (λ_{max}) and standard calibration for γ-oryzanol analysis

Organic solvent	γ-oryzanol			
	λ_{max} (nm)		Calibration curve	
	Ref.	Experimental	Regression equation*	R^2
petroleum ether	314	314	Y=51.71x	0.999
hexane	315	314	Y=50.01x	0.999
ethyl acetate	320	317	Y=37.53x	0.999
2-propanol	326	328	Y=30.64x	0.999

*y = absorbance, x= concentration (mg/ml)

The percentage of total extracted lipid was determined by triplicate extraction of the dried bran by using an organic solvent (the average moisture content of rice bran was 10.59%). The total lipids and γ-oryzanol content (% dry weight basis) which extracted by Soxhlet extraction and adsorption coefficient method are shown in table 2.

Table 2. Total lipid and γ-oryzanol (% dry weight basis)

Organic solvent	Total lipid (Soxhlet)	γ-oryzanol				Adsorption coefficient (K)
		in lipid (%w/w)		in 1 g. of dried bran (mg)		
		Soxhlet	Adsorption coefficient	Soxhlet	Adsorption coefficient	
petroleum ether	28.83	0.944	1.69	1.69	3.52	1.01
hexane	20.75	1.332	1.76	3.84	3.76	1.26
ethyl acetate	34.35	0.733	1.80	2.52	3.75	1.12
2-propanol	34.69	1.140	2.33	3.95	4.33	1.49

As a results shown in table 2, it was suggested that the amount of γ-oryzanol determined by adsorption coefficient method was higher than Soxhlet extraction method. The γ-oryzanol level is not always depended on total extracted lipid level. Isopropanol could extract the highest yield of γ-oryzanol comparing to the other solvent extraction systems such as hexane, ethyl acetate and petroleum ether. This is because the hydroxyl groups on the benzene ring of ferulate esters might be interacted with alcohol functional group of isopropanol, rendering more liberations of γ-oryzanol during extraction [7]. Thus, isopropanol is suitable for extraction and determination of γ-oryzanol in the RB at ambient temperature (30°C). Moreover, the highest K value of solvent, the most solute is extracted from rice bran.

The compositions of the standard commercial γ-oryzanol in crude RBO extract were investigated by HPLC method. The chromatograms obtained are shown in Figure 1. The compositions given in table 3 show cycloartenyl ferulate, 24-methylene cycloartenyl ferulate, campestenyl ferulate, and sitostenyl ferulate. The patterns of chromatogram were in good agreement with previous reports [3, 8, 9].

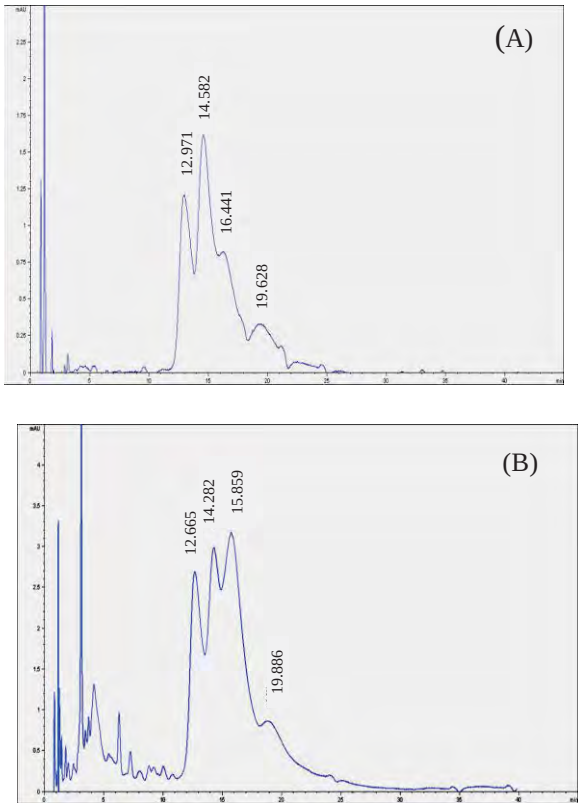

Fig. 1: HPLC chromatograms of the commercial γ-oryzanol mixture (A). γ-oryzanol from crude rice bran oil extract (B).

Table 3. Identification of γ-oryzanol component

Retention time (min)		Component
standard commercial γ-oryzanol	crude RBO extracted	
12.971	12.665	cycloartenyl ferulate
14.582	14.282	24-methylene Cycloartenyl ferulate
16.441	15.859	Campestenyl ferulate
19.628	19.886	Sitostenyl ferulate

4. Conclusions

The solid – liquid extraction by adsorption coefficient method can be used for determination of total lipid and γ-oryzanol in rice bran. The method is simple, less time- and cost-consuming and can be used for evaluating the quantity of solute in the solid.

Acknowledgements

The authors wish to thanks the Vegetable Oil Refinery (Bangkok, Thailand) for Gamma oryzanol standard. Thanks also Department of Chemistry, Faculty Science, Maejo University, Thailand for Financial supports.

References

[1] B.M.W.P.K. Amarasinghe, M.P.M. Kumarasiri and N.C. Gangodavilage, *Food and Bioproducts Processing*. 87 (2009) 108–114.

[2] C.R. Chen, L.Y. Wang, C.H. Wang, W.J. Ho and C.M.J. Chang, *Separation and Pirification Technology*. **61** (2008) 358–365.

[3] A.G.G. Krishna, S. Khatoon, P.M. Shiela, C.V. Sarmandal, T.N. Indira and A. Mishra, *Journal of the American Oil Chemists' Socity*. **78** (2001) 127–131.

[4] M.J.L. Garcia, J.M.H. Martinez, E.F.S. Alfonso, C.R.B. Mendonca and G.R. Ramaos, *Food Chemistry*. **115** (2009) 389–404.

[5] S. Lilitchan, C. Tangprawat, K. Ayusuk, S. Krisnakgkura, S. Chokmoh and K. Krisnangkura , *Food Chemistry*. **106** (2008) 752–759.

[6] P. Khuwijitjaru, N. Taengtieng and S. Changprasit , *Silpakorn University International JournalFood Chemistry*. **4** (2004) 154–165.

[7] M.H. Chen and C.J. Bergman, *Journal of Food Composition and Analysis*. **18** (2005) 319–331.

[8] J.Y. Cho, H.J. Lee, G.A. Kim, G.D. Kim, Y.S. Lee, S.C. Shin, K.H. Park and J.H. Moon, *Journal of cereal Science*. **55** (2012) 337–373.

[9] V.R. Pestana, R. C. Zambiazi, C.R.B. Mendonca, M.H. Bruscatto, M.J.Lerma-Garcia and G. Ramis-Ramos, *Journal of the American Oil Chemists' Socity*. **85** (2008) 1013–1019.

HYDROLYSIS REACTION OF CARBOHYDRATE FROM MICROALGAE TO SHORT CHAIN PRODUCT

Sudarat Phuklang[1], Nawin Viriya-empikul[2], Prasert Pavasant[1]*

[1]Chemical Engineering Research Unit for Value Adding of Bioresources, Department of Chemical Engineering, Faculty of Engineering, Chulalongkorn University, Phayathai Rd., Patumwan, Bangkok 10330
[2]National Nanotechnology Center (NANOTEC) National Science and Technology Development Agency 130 Thailand Science Park, Paholyothin Rd., Klong Luang Pathumthani 12120

* Author for correspondence; E-Mail: prasert.p@chula.ac.th, Tel. +66 22186870, Fax. +66 2 2186877

Abstract: Microalgae have earned their interest as renewable sources of various industrial compounds such as oil, lipid, protein, and carbohydrate. There are several attempts in the production and extraction of lipid intermediates from the microalgae but the economics of such technology still is doubtful unless it can be use in other applications. In this work, the carbohydrate in microalgae was converted to sugar using hydrolysis under hydrothermal condition in small batch autoclave. After that the residual of hydrolyzed sugar microalgae was employed as a raw material with aim to extract oil. The hydrolysis conditions were varied in terms of sulfuric (H_2SO_4) concentration (0-2%, v/v), reaction time (0.5-2 h) and incubation temperature (160 – 220 ^oC). The yield of reducing sugar (such glucose, fructose etc.) depends on the conditions applied in the hydrolysis method.

1. Introduction

Microalgae have received numerous attentions because of their many advantages. They have the potential to consume carbon dioxide which, in many instances, has been associated with the reduction of greenhouse gas emissions. In addition, they can remove nitrogen and phosphorus in polluted water [1]. Microalgae contain several high value components such as carbohydrate, protein and vitamin as well as antioxidants, and therefore algae extract can be used in versatile applications such as fertilization, animal feed and high-cost supplementary food. Nowadays, microalgae culture is mainly focused on biodiesel production due to their high lipid content, growth rate and requirement of smaller cultivation area [2-4].

However, microalgae can suffer from harvesting and drying costs especially applications that need to use dry biomass. Recent development therefore concentrates much on reducing costs. However, adding value to microalgae can also pose as an alternative solution for this economical restriction. The efficient conversion technique for carbohydrate from biomass is hydrolysis. There are various hydrolyzed techniques such as enzymatic hydrolysis [5], catalytic hydrolysis [6-7] and hydrothermal hydrolysis. Although the use of acid or enzyme can help improve hydrolysis yield [8-10], they require additional chemicals, and in some cases, this necessitated an additional washing step. The hydrothermal technique has the advantage of being a more environmental friendly choice (no chemical additives), but has to pay a price of high energy consumption. It becomes the objectives of this work to optimize the hydrothermal hydrolysis of carbohydrate in the algae and to examine the effect of acid in enhancing yield of sugar from carbohydrate.

2. Materials and Methods

2.1. Raw material

Fresh paste of *Scenedesmus Sp*. was obtained from centrifugation (4500 rpm, 10min) of the culture stock. The wet algae was frozen and then dried in a freeze-drier for 3 days. All of samples were stored at 25^oC until use. The total lipid and sugar content in biomass as determined according to the method of Mirón [11] were 12.76% and 11.77% of dry biomass weight, respectively.

2.2. Hydrothermal hydrolysis

The subcritical water hydrolysis was carried out in 30 cm^3 of a batch reactor made of stainless steel. 0.25g of freeze dried sample was suspended separately in 25 cm^3 of distilled water and charged into reactor. The reactor was then closed and heated by furnace to the desired temperature. In the hydrothermal reaction, reaction temperatures ranged from 160 to 220^oC. Reactions were carried out from 0.5 to 2 hours. After rapid cooling, the hydrolyzed samples from reactor were collected and filtered.

2.3 Dilute-acid catalyzed hydrolysis

In this experiment, water was replaced with 0.5-2% dilute sulfuric acid. The temperature of the hydrolysis was controlled at 180^oC for 2 h.

2.4 Lipid extraction

Soxhlet extraction, was treated here as a method that yields 100% of the lipid extract from microalgae. The hydrolyzed microalgae from 2.3 were filtrated through cellulose thimble, assembled to a 250 round bottom flask containing 180 ml of chloroform and methanol (MeOH) with ratio of 2:1 (v/v). The solvent was heated to vaporize with the cycle rate of approximately 12 min/round and the extraction was carried out for 2 h or until the colorless extract was observed. To recover the lipid extracted, the solvent was subsequently evaporated using a rotary evaporator and the remaining lipid in the vessel was measured gravimetrically.

2.5 Total sugar analysis

The anthrone–sulfuric acid method was applied to quantify the amount of total sugar [12]. 1 mL of microalgae solution from 2.2 was mixed with 5 ml of freshly prepared anthrone reagent. The resulting mixture was brought to 100 ◦C over a period of 12 min. A green color developed because of the formation of a glucose–anthrone complex. The mixture was cooled in ice bath and the optical density was read at a wavelength of 630 nm against a blank of 5 ml of the anthrone reagent mixed with 1 ml of distilled water. The anthrone reagent had been prepared by dissolving 10 mg of anthrone in 100 ml of sulfuric acid (72% w/w). A calibration curve was prepared for each experiment, using D+ glucose dissolved in distilled water. The glucose concentration (*C*g, mgml−1) and the optical density had the following relationship:

$$C_g = 0.327OD_{630} \ (R^2 = 0.999, P < 0.01)$$

2.6 Glucose concentration analysis

The filtrates obtained from Experiment 2.3 were determined glucose by HPLC with a refractometer detector (Shimadzu, Japan). The columns used for analysis was Aminex-HPX 87H column (300 mm, Bio-Rad Lab, CA, USA) under the following conditions: a temperature of 65°C, mobile phase 5 mM of H_2SO_4 and a flow rate of 0.57 ml min^{-1} [13].

3. Results and Discussion

3.1 Effect of temperature and time of hydrolysis reaction

The effects of reaction time and temperature on total sugar yield were shown in Fig.1. Increasing the reaction time from 0.5-2 h resulted in an almost linear increase the total sugar yield from 27.4 to 37.9% at 200°C. For the effect of temperature, they were in range 160-220°C. At the constant time, increased temperature could be increase total sugar yield from 33 to 37.5% at reaction time of 2 h. The raised temperature could not be affected to the total sugar yield because this temperature range could broken down starch bonding but could not cleaved all of cellulose. From the literature, starch was decomposed in a batch reactor at 180°C in the absence of catalyst [14] and cellulose hydrolysis drastically increased above 240°C [15].

3.2 Effect of acid concentration on hydrolysis reaction

Diluted acid catalyzed hydrolysis was reacted at temperature 180°C for 2 h to investigate the effect of acid in hydrolyzed carbohydrate. Fig. 2 shows the total sugar yield of hydrolyzed microalgae at different H_2SO_4 concentrations. . The highest total sugar yield (43.6-46.7%) was obtained under 0.5% of H_2SO_4. The maximum glucose concentration from this experiment was 0.19 g/l (0.9% of dry algae) at 2% of H_2SO_4. With an increase in acid concentration, the total sugar yield was nearly constant but the glucose concentration became higher. The total sugar yield and glucose concentration obtained under H_2SO_4 hydrolysis was higher than that under non acid hydrolysis, implying that H_2SO_4 could break starch and cellulose in microalgae to be short chain product.

Literature Gupta et al. (2009) [16] reported that the release in sugar increased with increase in acid concentration and it declined thereafter. They explained that any further increase in acid concentration caused the increase in releasing inhibitors (e.g. furfural, acetic acid) resulting in a decrease of sugar concentration.

3.3 Lipid extraction after hydrolysis

The extraction of lipid from the hydrolyzed microalgae was carried out at 180°C for 2 h. From Fig. 3, the mean total lipid was around 15.2, 15.3, 14.5, and 13.57%, after diluted acid hydrolysis using sulfuric acid at the concentrations of 0, 0.5, 1.0 and 1.5%, respectively. Besides, the extraction of 15.2% was higher than 11.7% extracted from the unhydrolyzed microalgae. After hydrolysis, the lipid could be obtained more easily and the extraction time decreased from 8 h to less than 3 h because cell wall structure became looser. Similar result was seen in the enzymatic hydrolysis and lipid extraction of soya beans [17] and *Chlorella sp*. [5].

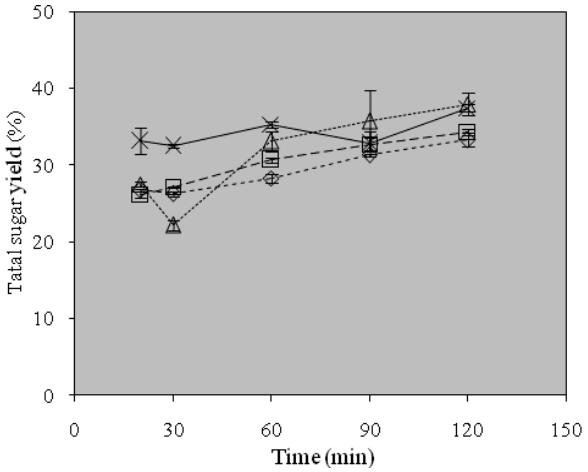

Figure 1. Effect of temperature and time on hydrolysis reaction of microalgae under conditions of microalgal concentration: 10 g/l. (Temperature: (◇) 160°C (□) 180°C (△) 200°C (×) 220°C)

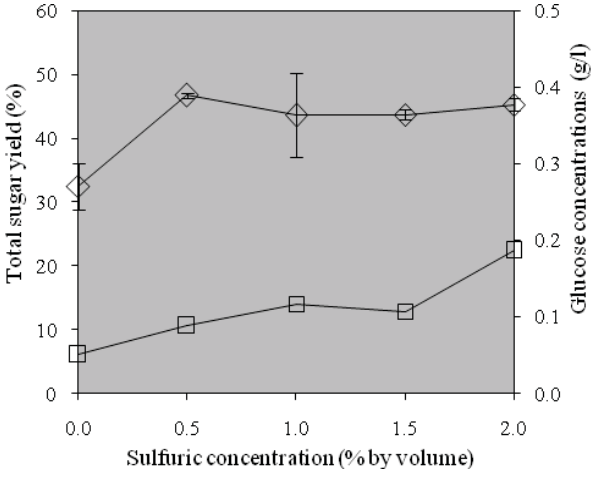

Figure 2. Effect of acid concentration on hydrolysis reaction of microalgae under conditions of reaction temperature: 180°C, time: 2h and microalgal concentration: 10 g/l. (Total sugar yield: (◇) and Glucose concentration: (□))

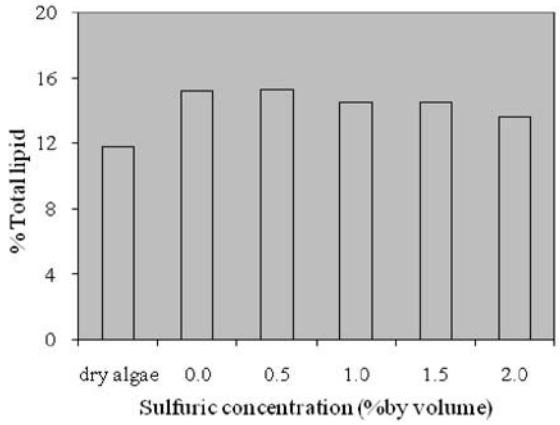

Figure 3. Effect of acid concentration from hydrolysis reaction on total lipid of hydrolyzed microalgal residue under condition of reaction Temperature: 180 °C, time: 2 h and microalgae concentration: 10 g/l.

4. Conclusions

Microalgae could be hydrolyzed under hydrothermal condition (200°C for 2h) and added dilute acid to enhance yield of total sugar (0.5% H_2SO_4). From dilute acid hydrolysis glucose (0.19 g/l) is a one of short chain product that grew up when increased acid concentration. Besides, the hydrolysis process delivered higher total lipid extraction efficiency of 15.2% was higher than 11.7% extracted from the unhydrolyzed microalgae. The results present the potentiality and efficacy of the hydrolysis of microalgae following with total lipid extraction.

Acknowledgements

The authors would like to acknowledge the financial supports from Engineering Research Unit for Value Adding of Bioresources, Department of Chemical Engineering, Faculty of Engineering, Chulalongkorn University.

References

[1] L.E. de-Bashan, J.P. Hernandez, T. Morey and Y. Bashan, *Water Resource* **38** (2004) 466-74.
[2] W. Becker, *Handbook of Microalgal Culture: Biotechnology and Applied Phycology*, Backwell Science Ltd, UK (2007), pp. 312–351.
[3] Y. Chisti, *Biotechnology Advances* **25** (2007) 294–306.
[4] I. Douskova, J. Doucha, K. Livansky, J. Machat, P. Novak, D. Umysova, V. Zachleder and M. Vitova, *Applied Microbiology and Biotechnology* **82** (2009) 179-185.
[5] F. Chun-Chong, H. Tien-Chieh, C. Jing-Yi, S. Chia-Hung and W. Wen-Teng, *Bioresource Technology* **101** (2010) 8750–8754.
[6] Z. Na, Z. Yimin, W. Xiaobin, G. Xiaowu and W. Qinhong, *Bioresource Technology* **102** (2011) 10158–10161.
[7] L. Pattana, T. Arthit, L. Vichean and L. Lakkana, *Bioresource Technology* **101** (2010) 1036–1043.
[8] P.S. Pushp and D.A.S. Marleny, *Food Research International* **44** (2011) 2452–2458.
[9] J.T. Su, C.C. Ho, L.J. Ye and O.K. Keun, *Bioresource Technology* **116** (2012) 435-440.
[10] G. Ying, W. Xian-Hua, Y. Hai-Ping and Chen Han-Ping, *Energy* **42** (2012) 1-9.
[11] A.S. Mirón, M.C. García, F.G. Camacho, E.M. Grima and Y. Chisti, *Enzyme and Microbial Technology* **31** (2002) 1015-1023.
[12] RT. Lorenz and GR. Cysewski, *Trends Biotechnol* **18** (2000) 160–167.
[13] P. Jung-Nam, S. Tai-Sun, L. Joo-Hee and C. Byung-Soo, *APCBEE Procedia* 2 (2012) 17-21.
[14] N. Makiko and F. Toshitaka, *Journal of Chemical Technology and Biotechnology* **79** (2004) 229–233.
[15] K. Eiji, S. Hisayoshi, T. Susumu, N. Hidehiko, F. Chouji and O.Takanari, *Journal of Materials Science* **43** (2008) 2179-2188.
[16] R. Gupta, K.K. Sharma and R.C. Kuhad, *Bioresource Technology* **100** (2009) 1214–1220.
[17] J.M. Dominguez, C. Acebal, J. Jimenez, I. Delamata, R. Macarron, and M.P. Castillon, *Biochemical Journal* **287** (1992) 583–588.

SCALEUP OF A NATURAL-INDUCED FLOW FLAT PANEL AIRLIFT PHOTOBIOREACTOR FOR CULTIVATION OF *ANKISTRODESMUS* SP.

Eakkachai Khongkasem[1], Kunn Kangvansaichol[2], Prasert Pavasant[1*]

[1] Chemical Engineering Research Unit for Value Adding of Bioresources,
Department of Chemical Engineering, Faculty of Engineering,
Chulalongkorn University, Phayathai Rd., Patumwan, Bangkok 10330.
[2]Department of Petroleum Products and Alternative Fuels Research, PTT Research
and Technology Institute 71 Moo 2, Phaholyothin Rd., Km.78,
Sanubtueb, Wangnoi, Ayutthaya 13170

[*] Author for correspondence; E-Mail: prasert.p@chula.ac.th

Abstract: This work aims to study the growth behavior of *Ankistrodesmus* sp. in natural-induced flow flat panel airlift photobioreactor under outdoor condition. The effect of the reactor size was examined using the reactors of various widths, i.e. 20, 30, 40 and 50 cm which corresponded to the working volumes of 67, 100, 122 and 118 L, respectively. The height of culture was maintained at 40 cm to eliminate the effect of hydrostatic pressure. The culture was subject to the day time light intensity of 100-268,000 Lux, with an average temperature of approximately 30°C. At 8 days of cultivation, the maximum cell concentrations of $5.88x10^6$, $6.11x10^6$, $6.15x10^6$ and $7.38x10^6$ cell ml^{-1} were obtained from the reactors with the widths of 20, 30, 40 and 50 cm, respectively. It was shown that the airlift of various sizes had virtually no significant effects on the growth and the properties of the obtained algae, i.e. lipid, carbohydate and protein. This proves that the flat panel airlift photobioreactors could be scaled up along the width to the required size without imposing serious growth and hydrodynamic effects on algal growth.

1. Introduction

Algal biomass has versatile applications as they contain several useful natural compounds such as carbohydrates, proteins, vitamins, minerals, and antioxidants [2]. Some species can accumulate a large quantity of oil which makes it significant as a source of future energy and some have other properties for other applications. For instance, *Ankistrodesmus* sp. is unicellular green microalgae, which can accumulate the total lipid content up to 24% [3]. *Scenedesmus* sp., on the other hand, effectively produces useful substances like proteins, lipid and carbohydrates [4].

Commercial microalgal culture is mostly carried out outdoors in order to utilize solar energy instead of expensive artificial light [1]. During outdoor culture, the growth rate and productivity are strongly affected by environmental factors such as light intensity temperature and air quality.

Airlift systems have been proven as an effective algal cultivating system as they provide adequate mixing and circulation with a reasonably low energy input. In our previous work, a flat panel airlift photobioreactor was proven to perform well without the need to install the separator plate between riser and downcomer [5]. In this study, this type of airlift photobioreactor was further employed to cultivate *Ankistrodesmus* sp. under outdoor condition using solar energy as the light source and no control of temperature. The effect of the reactor width was determined using the reactors of various widths, i.e. 20, 30, 40 and 50 centimeters. The properties of the obtained algae from each system were then analyzed.

2. Materials and Methods

2.1 Microorganisms and inoculum preparation

The initial inoculum of algal cell was cultivated in the standard sterilized BG11 medium [6] for one week.

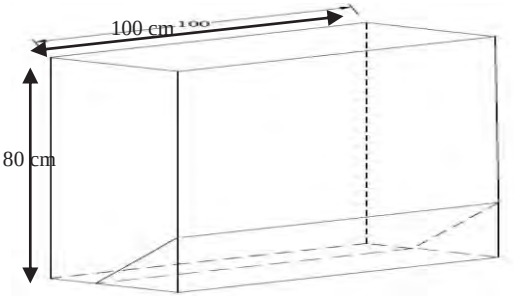

Fig. 1 Schematic diagram of flat panel airlift photobioreactor (FP-ALPBR)

The composition of the medium was (g l^{-1}): 1.5 $NaNO_3$0.040 $K_2HPO_4{\cdot}3H_2O$, 0.075 $MgSO_4{\cdot}7H_2O$, 0.036 $CaCl_2{\cdot}2H_2O$, 0.006 $C_6H_8O_7$, 0.006 $C_6H_8O_7{\cdot}n$Fe$\cdot n$$NH_3$, 0.001 EDTA$Na_2$, 0.020 Na_2CO_3 and trace metal (mg l^{-1}) 2.860 H_3BO_3, 0.220 $ZnSO_4{\cdot}7H_2O$, 0.390 $Na_2MoO_4{\cdot}2H_2O$, 0.080 $CuSO_4{\cdot}5H_2O$ and 0.050 $Co(NO_3)_2{\cdot}6H_2O$. This culture was then up-scaled to 1 L and 10 L autoclavable glass

bottles before being transferred to the flat plate airlift photobioreactor.

2.2 bioreactor set-up

The flat panel airlift photobioreactor (FP-ALPBR) was made of fiber glass with thickness of 3 mm. A schematic diagram of the FP-ALPBR is displayed in Fig. 1, with dimensions listed in Table 1. The width of FP-ALPBR was varied from 20 to 50 cm whilst the level of culture was maintained constant at 40 cm. The liquid culture in the system was agitated by injecting air through the long porous sparger at the column bottom at the flowrate of 0.3 vvm. The air was sterilized with 0.22 µm Gelman filter, before entering a flowmeter. The culture was placed under outdoor condition using solar energy as the light source and no temperature control.

2.3 Determination of suitable operating conditions

Experiments were carried out to determine the effect on cell growth of varying column widths. In batch operation, the culture was started with the initial cell concentration of approx. $1.5x10^6$ cells ml^{-1}. The culture was grown in the FP-ALPBR until stationary phase was reached. The algal cell density was daily measured microscopically using an improved Neubauer hemocytometer. From the cell density, the specific growth rate (µ; day^{-1}) was calculated using the following equation:

$$\mu = \frac{lnx_2 - lnx_1}{t_2 - t_1} \quad (1)$$

where X_1 and X_2 (cell ml^{-1}) are cell density at t_1 and t_2 (days).

The cell productivity (P; cell ml^{-1} day^{-1}) was calculated from:

$$P = \frac{N_2 - N_1}{t_2 - t_1} \quad (2)$$

where N_1 and N_2 (cell ml^{-1}) are cell density at time t_1 and t_2 (days).

Table 1 Dimensions of the flat panel airlift photobioreactors (FP-ALPBR) used in this work

Reactor type	Liquid level (cm)	Length (cm)	width (cm)	Volume (l)
F20	40	100	20	67
F30	40	100	30	100
F40	40	100	40	122
F50	40	100	50	118

The algal biomass was analyzed for its compositions, i.e. carbohydrate, lipid and protein.

3. Results and Discussion

3.1 Batch culture

The growth of *Ankistrodesmus* sp. in the flat panel airlift photobioreactor started with a 1 day lag phase, after which *Ankistrodesmus* sp. entered its exponential growth period where the cell concentration rapidly increased before reaching the stationary phase where the maximum cell densities were approx. 5.88×10^6, 6.11×10^6, 6.15×10^6 and 7.38×10^6 cell ml^{-1} from the reactors with the widths of 20, 30, 40 and 50 cm, respectively. The productivity and specific growth rate are shown in Table 2. The reason for this could be due to the behavior of concavity of liquid at the top level and the level of liquid nearly the slope line at the bottom of the reactor. Thus the airlift with 50 cm width exhibited the highest growth. In addition, F50 could obtain a higher energy transfer from gas bubbles which might affect the level of mixing in the reactor. In other works, low liquid velocity condition in the airlift with small width did not seem to support a proper circulation and the sedimentation of the *Ankistrodesmus* sp. However, this effect was not significant and the growth rate was not significantly affected.

There existed a diurnal pH variation in the reactor which could indicate the growth of *Ankistrodesmus* sp. as shown in Fig 3. pH was altered due to the changing in the amount of soluble carbon dioxide in the water, e.g. a reduction in soluble CO_2 resulted in an increase in the pH level of the solution.

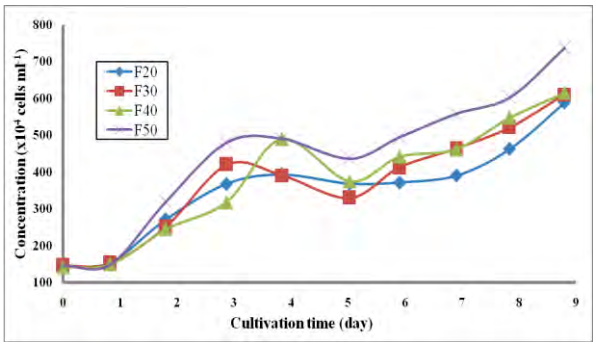

Fig. 2 Comparison between growth behavior of *Ankistrodesmus* sp. in the various reactors

Table 2 Comparison between cell concentration, productivity and specific growth rate in flat panel airlift photobioreactor for *Ankistrodesmus* sp.

Reactor type	Maximum cell density (cell ml^{-1})	Specific growth rate (µ; day^{-1})	Productivity (cells ml^{-1} day^{-1})
F20	5.88×10^6	0.161	50.67
F30	6.11×10^6	0.163	52.85
F40	6.15×10^6	0.167	53.76
F50	7.37×10^6	0.184	67.23

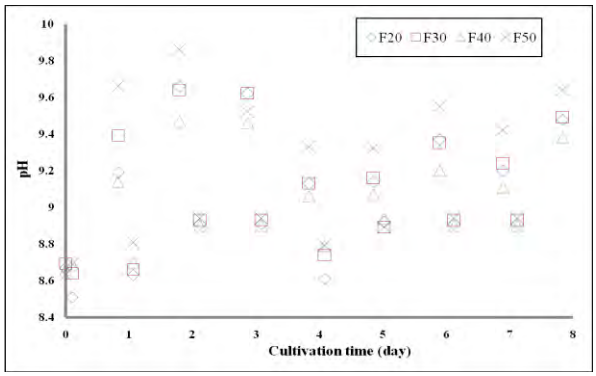

Fig. 3 Comparison pH effect of *Ankistrodesmus* sp. for the widths of 20, 30, 40 and 50 cm

At night, there was no light reaction and therefore CO_2 could not be uptaken, and a decrease in the solution pH can be observed.

3.2 Properties of the obtained algae

All algae contained protein, carbohydrate, lipid, nucleic acid, vitamin including antioxidants while the proportions varied from species to species. Many microalgal species can accumulate substantial amount of compositions [7]. Chemical composition of *Ankistrodesmus* sp can be variable, however, Table 3 indicates that that properties of the obtained algae from the various reactors did not vary significantly from each other.

3.3 Nutrient consumption

The primary nutrients, i.e. nitrogen (N), phosphorus (P), and potassium (K) consumed by the algae were analyzed as demonstrated in Fig. 4. It can be seen that nitrogen and potassium were not consumed greatly from the cultivation of *Ankistrodesmus* sp. as there was still a significant amount remaining after the cultivation. However, phosphorus seemed to be totally consumed within one harvesting cycle and this could pose a significant limiting nutrient for such cultivation.

Table 3 Comparison between protein carbohydrate and lipid in flat plate airlift photobioreactor for *Ankistrodesmus* sp.

Reactor type	%Protein	%Carbohydrate	%Lipid	Lipid Productivity ($mgL^{-1}day^{-1}$)
F20	29.43	33.14	23.43	3.38
F30	27.79	33.01	24.07	3.47
F40	28.86	29.14	25.96	4.29
F50	29.04	30.52	24.17	4.09

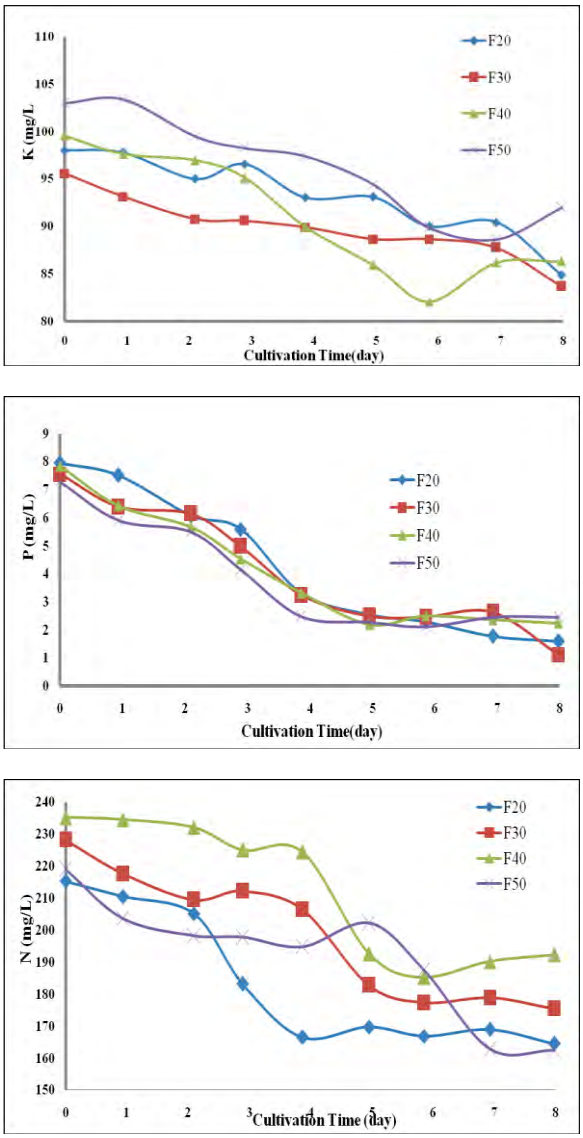

Fig. 4. Comparison amount of nutrient (K, P, N) *Ankistrodesmus* sp. for the widths of 20, 30, 40 and 50 cm

4. Conclusions

This investigation described the achievement in the cultivation of *Ankistrodesmus* sp. using a flat panel airlift photobioreactors operating at outdoor condition. It was found that the width of the reactor, i.e. 20, 30, 40 and 50 centimeters did not seem to have significant effect on the algal growth and the composition of the algae.

Acknowledgements

The authors would like to acknowledge the financial supports from Engineering Research Unit for Value Adding of Bioresources, Department of Chemical Engineering, Faculty of Engineering, Chulalongkorn University.

References

[1] M. Borowitzka, *J Mar Biotechnol*. **4** (1996) 185-191.
[2] C.U. Ugwu, H. Aoyagi and H. Uchiyama, Bioresourcen Technology. 99 (2008) 4021-4028.
[3] T.M. Mata, A.A. Martins and Caetano, *Renewable and Sustainable Energy Reviews*. **14** (2010) 217-232.
[4] A. Singh, P.S. Nigam and J.D. Murphy, *Biosource Technology*. **102** (2011) 26-34
[5] K. Issarapayup, S. Powtongsook and P. Pavasant, *J. Biotechnology*. **142** (2009) 227-232.
[6] R.Y. Stanier, R. Kunisawa, M. Mandel and G. Cohen-Bazire, *Bacteriol Rev*. **35** (1971) 171-205
[7] A. Demirbas and M.F. Demirbas, *Energy Conversation and Management* **52** (2011) 163-170.

CHARACTERISTICS OF MICROSPHERES PREPARED FROM GELATIN BLENDED WITH SILK FIBROIN

Sawanya Sinthop, Sorada Kanokpanont*

Chemical Engineering Research Unit for Value Adding of Bioresources, Department of Chemical Engineering, Faculty of Engineering, Chulalongkorn University, Phayathai Road,Patumwan, Bangkok 10330, Thailand

* Author for correspondence; E-Mail: *sorada.k@chula.ac.th*, Tel. +66-02-2186867

Abstract: Gelatin (G), a denatured collagen, is a biocompatible protein ; however, its uses in biomedical engineering might be limited by its rapid biodegradation. We proposed the blending with silk fibroin (SF), a fibrous protein derived from *Bombyx mori* silkworm which has high mechanical properties and slow biodegradation rate comparing to other natural materials. In this study, microspheres were fabricated from gelatin and Thai silk fibroin using water-in-oil (w/o) emulsion and glutaraldehyde crosslinking. The weight blending ratios of G/SF were varied from 100/0, 90/10, 70/30, and 50/50. Their physico-chemical properties, including morphology, crosslinking degree, water absorption, and in vitro biodegradation were evaluated. Average size of microspheres obtained were at 858.42±41.93, 832.97± 9.44 , 785.24±17.66 and 735.83 ±13.19 µm, respectively. Crosslinking degree and water absorption of G/SF microspheres increased with the increasing contents of SF. Blending of SF reduced average size and water absorption ability but increased the crosslinking degree. It also reduced degradation rate of the microspheres, comparing to those of the gelatin microspheres.

1. Introduction

Microsphere scaffold can be used for supporting 3-D tissue formation if high mass transfer of nutrient and oxygen is needed. It is essential that the microspheres must be made from the materials, which are biocompatibility, biodegradability, with sufficient mechanical property [1]. Gelatin is a collagen derived protein which has been extensively used for medical, pharmaceutical, and cosmetic applications. Its biosafety has been proven through long-term practical usage [2]. Gelatin microspheres are widely accepted as an efficient drug carrier for various administration routes, including nasal, gastrointestinal, and rectal delivery systems [3]. For example, carboplatin, an anti-tumor drug encapsulated in gelatin microspheres, has been successfully delivered via the nasal route with high lung targeting efficiency [4].

Silk fibroin is a fibrous protein derived from *Bombyx mori* silkworm which has the advantages in terms of high mechanical properties, biocompatibility and biodegradability. Thai silk fibroin was interested in tissue engineering researches. Wadbua *et.al.* prepared electrospun scaffolds derived from separated light-chain fibroin and heavy-chain fibroin, two major protein of silk fibroin. From *in vitro* biodegradation studies during, 30 days of incubation, light-chain fibroin scaffold were degraded to 100%wt., while mixed fibroin and heavy-chain fibroin scaffold were degraded only about 50%wt. [5]. Okhawilai *et.al.* prepared electrospun fiber mats from Thai silk fibroin (SF) and type B gelatine (GB) for controlled release. The results show that SF/GB fiber mats with higher SF contents degraded slower than the ones with lower SF contents [6].

In this work, we fabricated microspheres from gelatin and Thai silk fibroin using water-in-oil (w/o) emulsion and glutaraldehyde crosslinking at the different weight blending ratios. Their physico-chemical properties, including morphology, crosslinking degree, water absorption, and *in vitro* biodegradation were evaluated.

2. Materials and Methods

2.1 Materials

Cocoons of Thai silkworm “Nangnoi Srisaket 1” were kindly gifted from the Queen Sirikit Sericulture Center, Nakhonratchasima, Thailand. Type A gelatine with isoelectric point of 9 and average molecular weight of 100,616 dalton was kindly provided by Nitta Gelatin Co., Osaka, Japan. All chemicals used in this study were of analytical grade.

2.2 Preparation of silk fibroin

Silk fibroin solution was prepared using the method by Kim *et al.* [7]. In brief, Thai silk cocoons were boiled for 20 min in a solution of 0.02 M Na_2CO_3 and were rinsed thoroughly with deionized water to remove watersoluble proteins and other components. The fibroin fiber was dissolved in 9.3 M LiBr solution at 60 ºC for 4 h. Solution was dialyzed against deionized water for 2 days and followed by centrifugation at 9,000 rpm at 4 ºC for 20 min to remove insoluble debris. The final concentration of the fibroin was about 7-8 %wt. and then kept at 4 ºC until used.